PROJECT HYPO

PROJECT HYPO

AN INTENSIVE STUDY OF THE LAKE ERIE CENTRAL BASIN HYPOLIMNION AND RELATED SURFACE WATER PHENOMENA

Noel M. Burns, Ph.D
Canada Centre for Inland Waters
Burlington, Ontario

Curtis Ross
United States Environmental Protection Agency
Fairview Park, Ohio

Canada Centre for Inland Waters, Paper No. 6.
United States Environmental Protection Agency,
Technical Report, TS-05-71-208-24.

February 1972

Contents

FOREWORD vii

GLOSSARY ix

CONVERSION TABLE xii

1. PROJECT HYPO – AN INTRODUCTION 1
N.M. Burns and C. Ross

2. OXYGEN DEPLETION IN THE HYPOLIMNION OF THE CENTRAL BASIN OF LAKE ERIE, 1929 TO 1970 3
H.H. Dobson and M. Gilbertson
ABSTRACT 3
INTRODUCTION 3
DATA 3
RESULTS 6
DISCUSSION 6

3. PHYSICAL PROCESSES AFFECTING THE HYPOLIMNION OF THE CENTRAL BASIN OF LAKE ERIE 9
J.O. Blanton and R.A. Winklhofer
ABSTRACT 9
INTRODUCTION 9
METHODS 10
Location of Instrumentation 10
Description of Instrumentation 10
Data Handling 13
AREA DESCRIPTION AND CLIMATOLOGY 13
Area Description 13
Air Temperature 15
Water Temperature 15
Precipitation 16
Percent of Possible Sunshine 16
Winds 16
PRINCIPAL FEATURES OF THE TEMPERATURE STRUCTURE 17
Areal Temperature Distribution 20
Hypolimnion Temperature Regressions 22
Thermocline Fluctuations 22
TIME VARIABILITY OF HYPOLIMNION DISSOLVED OXYGEN 23
Dissolved Oxygen Regressions 24
Dissolved Oxygen – Current Correlations 27
Suspended Algae and Dissolved Oxygen Observations 28
Sediment Oxygen Demand 28
CURRENT PATTERNS 31
DISCUSSION 34
Hypolimnion Volume Variations 34
Northwest Movement of Hypolimnion Water 35
CONCLUSIONS 37

Contents (cont'd)

4. AN INVESTIGATION OF DIFFUSION CHARACTERISTICS OF THE HYPOLIMNION OF LAKE ERIE 39
C.R. Murthy
ABSTRACT 39
INTRODUCTION 39
EXPERIMENT 40
SAMPLING 42
RESULTS 44
CONCLUSIONS 44

5. SEDIMENT OXYGEN DEMAND IN LAKE ERIE'S CENTRAL BASIN, 1970. 45
A.M. Lucas and N.A. Thomas
ABSTRACT 45
INTRODUCTION 45
METHOD 46
RESULTS AND DISCUSSION 48

6. BIOLOGICAL STUDIES RELATED TO OXYGEN DEPLETION AND NUTRIENT REGENERATION PROCESSES IN THE LAKE ERIE CENTRAL BASIN. 51
T. Braidech, P. Gehring, and C. Kleveno
ABSTRACT 51
INTRODUCTION 51
METHODS 52
Phytoplankton 52
Sedimented Algae 54
Sedimentation Traps 54
Underwater Observations and Photographs 55
RESULTS 55
Phytoplankton 55
Sedimentation Traps 59
Sedimented Algae 61
Underwater Observations and Photographs 64
DISCUSSION 65
SUMMARY AND CONCLUSIONS 68
APPENDIX 146

7. MICROBIOLOGICAL STUDIES RELATED TO OXYGEN DEPLETION AND NUTRIENT REGENERATION PROCESSES IN THE LAKE ERIE CENTRAL BASIN 71
A.S. Menon, C.V. Marion, and A.N. Miller
ABSTRACT 71
INTRODUCTION 71
MATERIALS AND METHODS 72
Sample Collection 72
Laboratory Procedures 72
RESULTS AND DISCUSSION 73
Vertical Distribution of Bacterial Populations 73
Aerobic and Anaerobic Heterotrophic Bacteria 75
Sulfur oxidizing and sulphate reducing bacteria 79
Fall overturn 79
Deoxygenation Calculations 80
CONCLUSIONS 82
APPENDIX 164

Contents (cont'd)

8. OXYGEN-NUTRIENT RELATIONSHIPS WITHIN THE CENTRAL BASIN OF LAKE ERIE. 85
N.M. Burns and C. Ross
ABSTRACT 85
INTRODUCTION 85
METHODS AND PROCEDURES 85
ANALYTICAL PROCEDURES 87
RESULTS AND DISCUSSION 89
General 89
Heat Budget Model 90
Mesolimnion or Thermocline 95
Budget Calculations 99
External Influences 100
Oxygen Depletion Pattern 104
Oxygen Budget 105
Oxic Regeneration 110
Anoxic Regeneration 112
Fate of Regenerated Quantities 115
Internal Loading vs External Loading 116
SUMMARY 116
CONCLUSIONS 117

9. PROJECT HYPO – DISCUSSION OF FINDINGS. 120
N.M. Burns and C. Ross
ABSTRACT 120
EFFECTS OF ALGAE 120
CAUSES & SITE OF OXYGEN DEPLETION 121
SEDIMENT OXYGEN DEMAND 121
BUDGET CALCULATIONS 122
HYPOLIMNION VOLUME INCREASE 122
UPWELLING OF WATER MASSES 123
PROXIMITY OF A PROCESS OF CONTINUAL SELF-FERTILIZATION 123
PHOSPHORUS AND NITROGEN ELIMINATION FROM THE LAKE SYSTEM 123
MAJOR FINDINGS OF 'PROJECT HYPO' 124
ESTIMATES BASED ON FINDINGS 124
CONCLUSION FROM PROJECT HYPO 125

APPENDIX I – AN AUTOMATIC UNDERWATER CAMERA SYSTEM 127
R.J. Jirberg
ABSTRACT 127
INTRODUCTION 127
SYSTEM DESIGN 127
The Camera 127
Control Circuitry 128
Flash Unit 129
Underwater Housing 130
In-Situ Mounting 131
OPERATIONAL CONSIDERATIONS 131
CONCLUDING REMARKS 131

Contents (cont'd)

APPENDIX II – A SUBMERSIBLE AUTOMATIC DISSOLVED OXYGEN-TEMPERATURE MONITORING SYSTEM **133**
C.J. Beier
INTRODUCTION 133
DESCRIPTION OF EQUIPMENT 133
Dissolved Oxygen Parametric System 134
Temperature Parametric System 135
Power Supply 136
Mooring 136
INSTRUMENT IN OPERATION 137
Calibration and Servicing 137
DISCUSSION OF RESULTS 138
Performance 138
General Findings 139
CONCLUSIONS 140
RECOMMENDATIONS 140

APPENDIX III – PHOSPHORUS AND HYPOLIMNIAL DISSOLVED OXYGEN IN LAKE ERIE. . . . **141**
M. Gilbertson, H.H. Dobson and T.R. Lee
INTRODUCTION 141
PHOSPHORUS CONTRIBUTIONS 141
OXYGEN DEPLETION 144
CONCLUSIONS 144

APPENDIX IV – BIOLOGICAL DATA **146**
TABLES 146

APPENDIX V – BACTERIOLOGICAL DATA **164**
METHODS 164
TABLES 164
GRAPHS 175

APPENDIX VI – DATA AND PUBLICATION INFORMATION **178**
DATA INFORMATION 178
PUBLICATION INFORMATION 178
INDEX 181

Foreword

The work reported in this volume is unique in several ways. One was the close co-operation achieved between the scientists of the Canada Centre for Inland Waters, Department of Environment, and those of the U.S. Environmental Protection Agency's Cleveland office. This high degree of co-operation was achieved in a very informal way rather than through establishment of formal committees and other structures. Perhaps this was the key to its success. A second unique feature of the project was the range of disciplines brought to bear on questions of the reasons for, the extent of, and the effects of oxygen depletion in the bottom waters of Lake Erie. In this volume you will find reports by bacteriologists, biologists, chemists, physicists, engineers, and other specialists.

We also included in the volume, an appendix which indicates the implications of the "Project Hypo" findings for public policies to control eutrophication and the extent of oxygen depletion in Lake Erie. This appendix (Appendix III) involves input from economists and economic geographers from the social science group at the Canada Centre for Inland Waters as well as work by the natural scientists.

Finally, most of the credit for the success of this whole project rests with Dr. Noel M. Burns, the Canadian co-ordinator for the project and the overall project leader, and Mr. Curtis Ross, the U.S. project co-ordinator. It is hoped its success will lead to more frequent international co-operation in in scientific projects on the Great Lakes in future years.

J.P. Bruce
Director
Canada Centre for Inland Waters

George L. Harlow
Director
Ohio District Basin Office
U.S. Environmental Protection Agency

Glossary

ABIOLOGICAL: A type of process which does not involve any biological action; it is purely physical or chemical in nature.

AEROBIC HETEROTROPHIC BACTERIA: Bacteria capable of living only in the presence of free oxygen.

ALGAL RAIN: The precipitation of algae down the water column of the lake following an algal bloom.

ANAEROBIC HETEROTROPHIC BACTERIA: Bacteria that will grow only in the absence of free oxygen.

ANAEROBIC: The condition of water which contains no dissolved air (often used interchangeably with anoxic).

ANAEROBIC BACTERIAL RESPIRATION: Energy deriving process by bacteria in which the final hydrogen acceptor is an inorganic compound other than oxygen (nitrate, sulfate, carbonate).

ANOXIC: The condition of water which contains no dissolved oxygen.

AUTOTROPHIC: Bacteria that are able to obtain energy from inorganic sources, e.g., nitrogen, carbon dioxide, hydrogen and sulfur.

BACTERIAL BIOMASS: The total quality of bacteria present per unit surface area or volume in a body of water. Usually, it is an expression dealing with the total weight of a bacteria population.

BACTERIAL RESPIRATION: Energy deriving process by bacteria in which molecular oxygen is the final hydrogen acceptor.

BIOTYPE: A group of individuals occurring in nature, all with essentially the same genetic constitution; a species usually consists of many biotypes.

CHEMOAUTOTROPHIC BACTERIA: Microorganisms capable of living in a strictly inorganic environment, utilizing carbon dioxide as the sole source of carbon, and obtaining their energy by the oxidation of an inorganic substrate (ammonia, iron, sulfur, nitrite), the nature of which is specific for that particular bacterial type.

CHEMOCLINE: A zone in a lake where the concentrations of certain chemical species vary in the vertical direction; this zone is usually found in the region of the thermocline some time after thermal stratification has occurred.

DESULFOVIBRIO SP: A genus of the family *Sprillaceae.* Gram negative vibrio, usually occurring singly but sometimes in short chains looking like spirilla; motile by single polar flagellum; straight anaerobes which reduce sulfates to hydrogen sulfide.

DROGUES: Current following devices useful to determine mean currents.

EDDY DIFFUSIVITY: A parameter to quantify diffusion due to turbulence.

ENTRAINMENT: The erosion by turbulent motion of a less-turbulent fluid into the more-turbulent fluid.

EPILIMNION: The turbulent superficial layer of a lake lying above the thermocline; in summer the epilimnion is warmer than the hypolimnion.

Glossary (cont'd)

EUTROPHIC: A term applied to lakes that have abundant plant life and high biological productivity. Quantification can be in terms of algal abundance or nutrient levels. (Mesotrophic and oligotrophic mean mediumly productive and unproductive respectively.)

EXTERNAL LOADING: This term signifies the quantity of materials being added to the lake by rivers, outfalls and from the air.

FACULTATIVE ANAEROBES: Organisms capable of growth under both aerobic and anaerobic conditions.

FLUOROMETRIC SAMPLING: An optical technique to detect concentrations of fluorescent dye in water.

GRADIENT: The change in a property such as pressure, velocity or dissolved oxygen concentration per unit of distance.

HETEROTROPHIC: A type of bacteria that depend upon organic substances for food.

HYPOLIMNION: The region of a body of water that extends from the thermocline to the bottom of a lake which is colder than the surface water during the summer.

INTERNAL LOADING: This term is used here to signify the quantity of materials returning to the water from the lake sediments.

MICROAEROPHILES: Organisms which grow best at low oxygen tensions, high tensions being inhibitory.

MESOLIMNION: See thermocline as this zone is also called the thermocline.

NITRIFICATION: The transformation of ammonia by bacteria of *Nitrosomonas* and *Nitrosococcus* genera to nitrites, and of the nitrites by bacteria of the genus *Nitrobacter* to nitrates.

NITRIFYING BACTERIA: Bacteria that utilize ammonia and ammonium compounds to yield nitrates.

OVERTURN (TURNOVER): The period of mixing, by vertical circulation, of previously stratified water masses. This phenomenon may occur in spring and/or fall; the result is a uniformity of physical and chemical properties of the water at all depths.

OXIC: The condition of water which contains dissolved oxygen.

PEAK CONCENTRATION: Maximum concentration generally observed at the centre of the diffusing dye plume/patch.

PHOSPHORUS, PARTICULATE: Represents the quantity of phosphorus in the water which will *not* pass through a 0.45 micron membrane filter.

PHOSPHORUS, SOLUBLE: Represents the quantity of phosphorus which will pass through a 0.45 micron filter.

PHOSPHORUS, SOLUBLE REACTIVE: This measures the phosphorus which is primarily in the orthophosphate form together with some of the easily hydrolysable forms of organic phosphorus; this term is sometimes used interchangeably with phosphate.

Glossary (cont'd)

PHOSPHORUS, SOLUBLE ORGANIC: This form of phosphorus is considered to be the soluble phosphorus content of the water minus the soluble reactive phosphorus.

PHOTOPERIOD: Relative lengths of alternating periods of lightness and darkness as they affect the growth and maturity of an organism.

POTENTIAL ENERGY: Energy available due to the displacement of a fluid parcel from its equilibrium position.

PROGRESSIVE VECTOR DIAGRAM: A diagram which describes the path of a water or air parcel through which it would have moved if the velocities recorded by the instrument are added together. The addition is done by computing the vector sum of displacement at fixed time intervals.

REGENERATION: This term is used here in the sense of particulate materials returning to the soluble form within the lake.

SEMI-PERMANENT: An adjective specifying permanence in an average sense. There may be significant deviations from the average.

SEDIMENT-OXYGEN DEMAND (SOD): The rate at which oxygen is removed from the overlying water by oxygen consuming processes occurring at the sediment-water interface and within the sediment.

SUBMARINE OUTFALLS: Outlet pipes located 1-2 km offshore at the lake floor (or ocean floor) for discharge of waste effluents.

RESPIRATORY QUOTIENT: $= \dfrac{\text{Volume of } CO_2 \text{ produced (at standard temperature and pressure)}}{\text{Volume of } O_2 \text{ consumed (at standard temperature and pressure)}}$

THERMOCLINE: The transition zone between the warm epilimnion and cold hypolimnion of stratified bodies of water in which the temperature exhibits the greatest difference in a vertical direction. This zone is also called the mesolimnion.

THIOBACILLUS SP: A genus of the family *Thiobacteriaceae* – small gram-negative rod-shaped cells – motile or non-motile – energy derived from the oxidation of incompletely oxidized sulfur compounds – sulfate is the main product of oxidation – grow under acid or alkaline conditions and derive carbon from carbon dioxide or from bicarbonates in solution – autotrophic and facultatively autotrophic.

UPWELLING (NEARSHORE): Vertical upward motion resulting from horizontal flow of water away from the shore.

VOLATILE SOLIDS: This quantity represents the weight lost from a dry sample when the sample is ignited at 650°C for one half-hour.

Conversion Table

	1 m.mole = 1 millimole = 1 mole x 10^{-3} 1 μmole = 1 micromole = 1 mole x 10^{-6} p.p.m. = parts per million = mg/liter p.p.b. = parts per billion = micrograms/1
Alkalinity	1 m.mole $CaCO_3$ alk/1 = 1000 μmoles $CaCO_3$ Alk/1 = 100.1 mgm $CaCO_3$ Alk/1
Carbon dioxide	1 m. mole CO_2/1 = 44 mgm CO_2/1 = 44 p.p.m. CO_2
Iron	1 μmole Fe/1 = 55.8 μgm Fe/1 = 55.8 p.p.b.
km^3	1 km^3 = 10^{12} litres = 10^{15} ml 1 km^2 = 10^6 m^2 = 10^{10} cm^2 = 0.39 sq. mile
Manganese	1 μmole Mn/1 = 54.9 μgm Mn/1 = 54.9 p.p.b. Mn
Nitrogen	1 μmole N/1 = 14 μgm N/1 = 14 p.p.b. N/1
Oxygen	1 m.mole O_2/1 = 32 mgm O_2/1 = 2 m. gm. at O_2/1 1 mgm O_2/1 = 31 μmoles O_2/1 = 62 μgm at O_2/1
Phosphorus	1 μmole P/1 = 31 μgm P/1 = 31 p.p.b. P = 95 μgm PO_4/1 = 95 p.p.b. PO_4 1 metric ton P = 1.12 short tons P = 32.2 x 10^3 moles P
Silica	1 μmole SiO_2/1 = 60 μgm SiO_2/1 = 60 p.p.b.
Sulphate	1 μmole SO_4/1 = 96 μgm SO_4/1 = 96 p.p.b. SO_4

1. *Project Hypo - An Introduction*

N.M. Burns, Ph.D.
Canada Centre for Inland Waters,
Burlington, Ontario, Canada

C. Ross
U.S. Environmental Protection Agency
Region V, Fairview Park, Ohio, U.S.A.

In December of 1969, communication between Mr. J.P. Bruce, Director of the Canada Centre for Inland Waters, Burlington, Ont. and Mr. G.H. Harlow, Director of the Water Quality Office, United States Environmental Protection Agency, Fairview Park, Ohio, established the fact that both organizations were very interested in discovering the degree and causes of the depletion of oxygen during the summer in the Central Basin of Lake Erie. Some oxygen deficiency was first observed in the Central Basin in 1929 by Fish *et al.* (1960). Since that time the literature has been populated with studies indicating increased oxygen deficiencies throughout the Central Basin. Carr (1962) indicated that oxygen depletion in Central Basin hypolimnion had gradually increased in area over the last three decades. FWPCA (1968) estimated the Central Basin bottom water to be oxygen deficient (2 mg/1 or less) over an area of approximately 2600 square miles. Davis (1966) has indicated that phytoplankton increased between 1927 and 1964 at a rate of 44.3 cells/ml/year; however, the increase rate between 1956 and 1964 was 122.0 cells/ml/yr. In addition Davis observed that important changes of dominant algal genera had occurred during the same time interval.

There are three main reasons for concern over the increasing area of oxygen depletion in the Central Basin. Naturally, oxygen depletion leads to the death of fish and many other favored life forms replacing them with undesirable species. Also anoxic water is odorous and unpalatable, making the lake unsuitable as a municipal water source; Cleveland is already experiencing difficulties associated with the occasional occurrence of anaerobic water at the city water intake. Finally, while anoxic conditions are usually the result of profuse productivity resulting from excessive nutrient supply, of far greater concern is the fact that anoxic conditions cause a release of nutrients from the sediments to the water (Mortimer, 1941 and 1942), raising the frightening possibility of the initiation of a cyclic process of self-fertilization in the lake. For these reasons, a meeting was held by interested Canadian and American personnel to formulate an approach to investigate the problem. It was immediately obvious to all attending that a much more thorough investigation of the entire situation could be undertaken if both organizations pooled resources. A joint Canadian-United States project was set up with the organization and the implementation of the project left to the scientists involved. Since biology, bacteriology, physics, and chemistry are all interrelated in the problem of oxygen depletion, it was decided to investigate changes in each of these four disciplinary areas. Each Government provided major manpower and equipment inputs. The main laboratory ship was Canadian, the various moorings together with the ship which laid and retrieved them were American. Both Canadian and American launches were used in carrying out subprojects. Similarly, both American and Canadian mobile bacterial laboratories were used and shore analyses were done at both Cleveland and Burlington. This equitable situation arose without any bargaining; each organization just donated as much as it could towards the project. The results achieved have been far in excess of those which would have been obtained if each group had worked independently of the other.

Field work for the study was conducted from June through August with the intensive phase lasting from July 27 through August 25. In addition data from all 1970 CCIW (Canada Centre for Inland

Waters) Lake Erie Monitor Cruises have been utilized.

Topographically, the Central Basin is separated from the deep eastern basin by a low, wide submerged sand and gravel ridge, north of Erie, Pennsylvania and the rocky island chain north of Marblehead separates the Central Basin from the shallow Western Basin. The Central Basin depth averages 18.3 m with a maximum depth of 25 m existing near the center of the basin. The bottom is generally flat, reaching the average depth soon after leaving the shoreline. The total basin area extends about 6,300 square miles being approximately 50 miles wide and 130 miles long. Cultural and industrial development are much more pronounced along the south shoreline than the north shoreline.

Twenty-five water sampling stations were set up across the basin with an additional sixteen stations set up where bathythermograph records of the water column were taken. Five of the twenty-five stations were termed "major stations" and were sampled intensively for chemical, biological, bacteriological, and physical variables. It was hoped that findings at these five stations would help uncover some of the interrelationships which operate in limnology between the four scientific disciplines involved in this study. This has been an interesting and rewarding but difficult task.

Project Hypo has proved to be an arduous undertaking for most of the people who were involved in it, but the reports will almost certainly show that the output of time and energy has been worth the results obtained.

REFERENCES

CARR, JOHN F. 1962. Dissolved Oxygen in Lake Erie, Past and Present. Reprinted from Publication No. 9, Great Lakes Research Division, Institute of Science and Technology, The University of Michigan, 1962, pp. 3-11.

DAVIS, CHARLES C. 1966. Biological Research in the Central Basin of Lake Erie, Publication No. 15, Great Lakes Research Division, The University of Michigan, 1966, pp. 22.

FISH, CHARLES J. and ASSOCIATES. 1960. Limnological Survey of Eastern and Central Lake Erie, 1928–1929. U.S. Fish & Wildlife Service, Spec. Science Rep. Fish, No. 334, 198 p.

FEDERAL WATER POLLUTION CONTROL ADMINISTRATION. 1968. Lake Erie environmental summary: 1963-1964. U.S. Department of the Interior, Great Lakes Region Publication, 170 p.

MORTIMER, C.H. 1941-42. The Exchange of Dissolved Substances between Mud and Water. J. Ecol. *29*, 280 (1941); *30*, 147 (1942).

2. *Oxygen Depletion in the Hypolimnion of the Central Basin of Lake Erie, 1929 to 1970*

H.H. Dobson and M. Gilbertson
Canada Centre for Inland Waters
Box 5050, Burlington, Ontario.

Evidence is provided for the progressive eutrophication of Lake Erie. Historic records of dissolved oxygen in the hypolimnion were collected and an average depletion rate was established for each year. The present depletion rate (3.6 mg. $l.^{-1}$ $month^{-1}$) is more than double the rate estimated for 1929. The rate of deoxygenation has increased at the approximate annual rate of .075 mg. $l.^{-1}$ $month^{-1}$ $year^{-1}$ in large part due to increases in phytoplankton production caused by increased nutrient inputs.

INTRODUCTION

Lake Erie is undergoing widespread environmental modification due to human influences around the lake shore. Several chemical and biological analyses are being performed to document the present rate of change but relatively little information has been published concerning the recent history of this environment. Davis (1964) reported quantitative and qualitative changes in the daily phytoplankton counts in water samples from the Cleveland, Ohio water supply between 1919 and 1963. These changes were thought to be caused by the increasingly rapid eutrophication of the Lake Erie water. Carr (1962) reviewed the published literature on dissolved oxygen in Lake Erie and noted that there were indications of increased oxygen consumption in the bottom waters. We have used information concerning oxygen values in the hypolimnion as an index of the rate of environmental change. Our study was confined to the Central Basin which lies between Port Burwell and Erie in the east and Pelee Point and Sandusky in the west. The deepest part of this basin is 25 metres. During the summer the thermocline occurs at about 17 metres, thus the greatest thickness of the hypolimnion is only about 8 metres (see Figure 1).

DATA

Information was obtained from published and preliminary reports concerning oxygen concentrations in the hypolimnion of this basin (Carr 1962, Powers *et al.* 1960, Fish *et al.* 1960, Beeton 1963, Great Lakes Institute 1964, 1965, Rogers 1962, 1963, Unpublished data, Canada Centre for Inland Waters 1967-1970). Since mixing of stratified layers of water can occur at the periphery of the thermocline, it was necessary to be selective about the reported data. Unmixed water of the hypolimnion, here termed bottom water, was characterized in this study by temperatures within 3°C of the minimum temperature observed during a sampling survey (see Figure 2).

The oxygen concentration was determined by the Winkler method (A.P.H.A.). The sodium azide modification was used in 1960 and the modification of Pomeroy and Kirschman was used between 1967 and 1970. Sample sites were selected on a grid system in the years since 1960. However, sites before that year were not so rigorously selected, though they generally achieved a representative distribution through use of several line transects. An arithmetic mean value was obtained for the oxygen concentration in the bottom water for each series of samples.

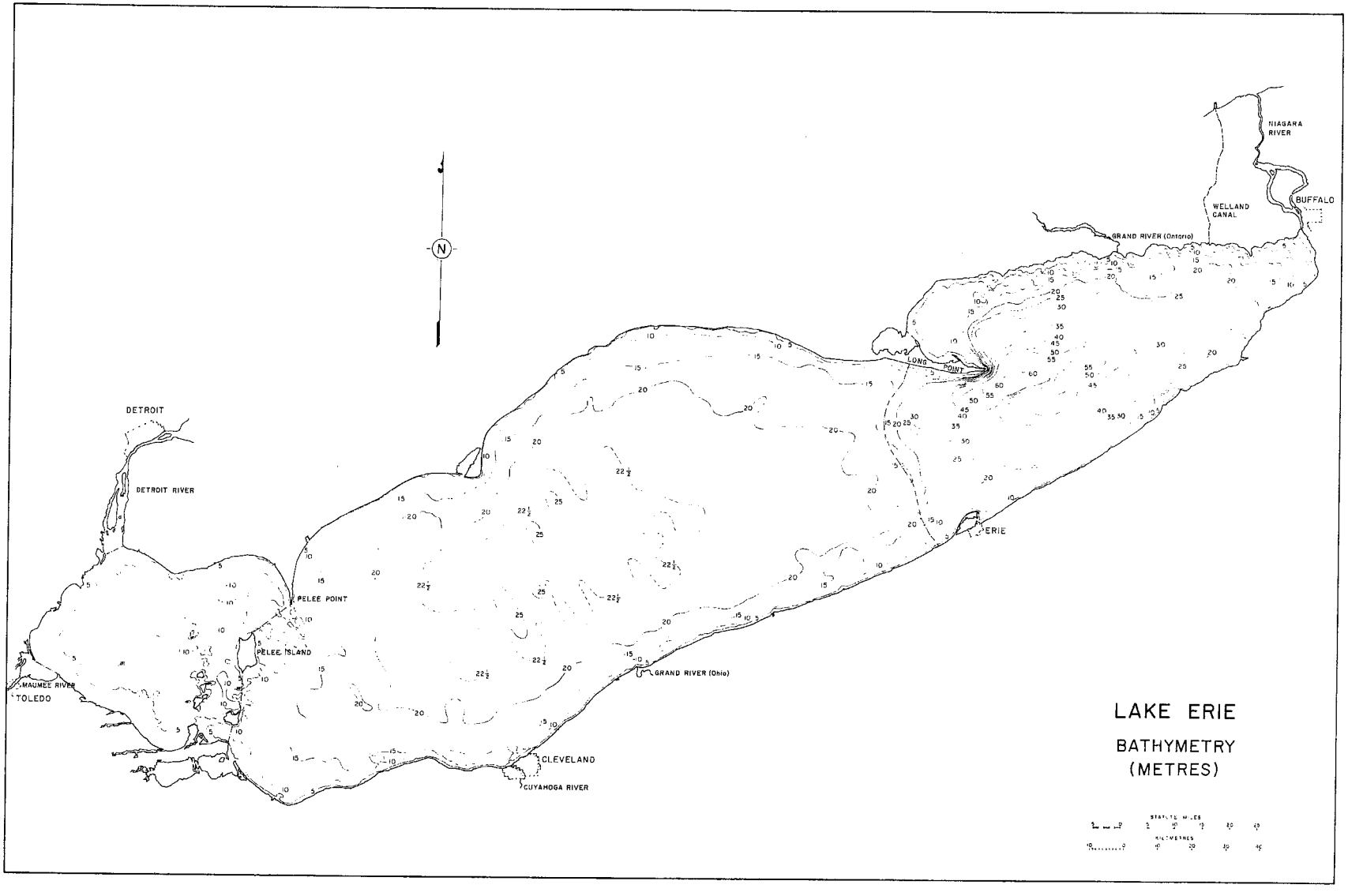

Figure 1. Lake Erie showing the major bathymetric features.

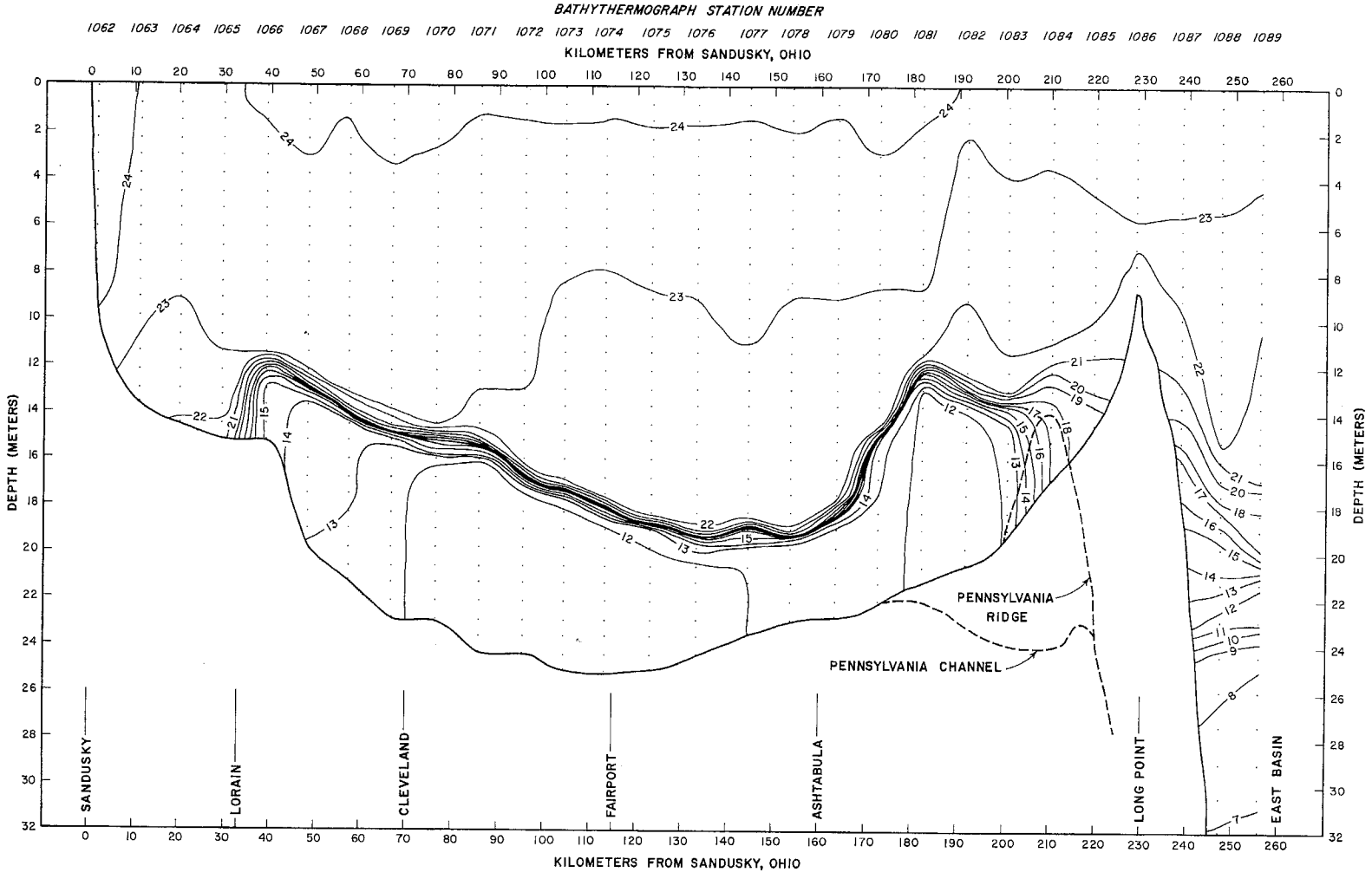

Figure 2. An example of the temperature structures which can exist in the Central Basin of Lake Erie along the major axis of the lake. (Lake Erie, temperature (°C) in a vertical section from Sandusky-Long Point – The Eastern Basin, August 13 & 14, 1953, Vertical exaggeration X 5,000 (data from Herdendorf, 1967)).

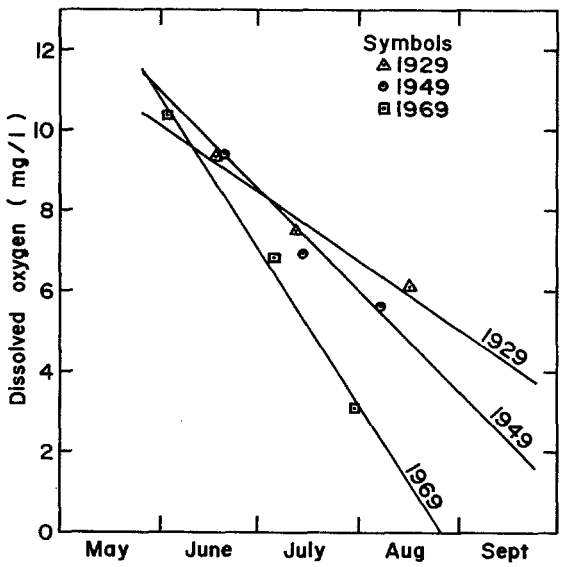

Figure 3. Dissolved oxygen in the bottom-water of central Lake Erie during 1929, 1949, and 1960: mean values for each cruise, and the inferred straight-line trends for each year.

RESULTS

In Figure 3 the mean oxygen concentrations in the bottom water are shown for the years 1929, 1949, and 1969 during the period of summer stratification. The oxygen concentration at the beginning of the stratified period has not changed in four decades. However the rate of oxygen depletion has markedly increased and the onset of deoxygenated conditions in the bottom water has become earlier.

The mean depletion rates for dissolved oxygen are shown in Figure 4 for the years for which information is available. The long term trend represents a line through the arithmetic means of the 3 groups of estimates and through the value for the year 1929. The trend indicates that the rate of deoxygenation of the bottom water has increased in the last two decades at the approximate annual rate of .075 mg.litre^{-1} month^{-1} year^{-1} (2.2 μmoles litre^{-1} month^{-1} year^{-1}).

DISCUSSION

Since the duration of the period of stratification in the lake is about 110 days, a critical depletion rate of 3.0 mg. litre^{-1} month^{-1} (94 μmoles litre^{-1} month^{-1}) determines whether much of the basin will become deoxygenated before the autumnal overturn. It appears that this critical value occurred about 1960 and this is consistent with the observed increased incidence of zero values for dissolved oxygen in samples analysed since that year.

Two similar trophic classifications of lakes have been discussed using arbitrary values of oxygen depletion in the hypolimnion (Hutchinson 1957). In one of these classifications, a value of .025 mg.cm.$^{-2}$ day^{-1} (7.8 millimoles O_2 m.$^{-2}$ day^{-1}) delimited the transition from an oligotrophic to a mesotrophic state, and a value of .055 mg.cm^{-2} day^{-1} (17.2 millimoles m.$^{-2}$ day^{-1}) delimited the transition from a mesotrophic to an eutrophic state. Lake Erie has a hypolimnion depth which varies with season, location and between years. Assuming a negligible amount of oxygen entered the bottom water after stratification and an average hypolimnion depth of about 4 metres, Central Lake Erie became mesotrophic around 1940 and is presently becoming eutrophic.

The details of the mechanism of the observed oxygen depletion were part of the subject of "Project Hypo". Burns and Ross (pg 107) have indicated that biological processes are more important in

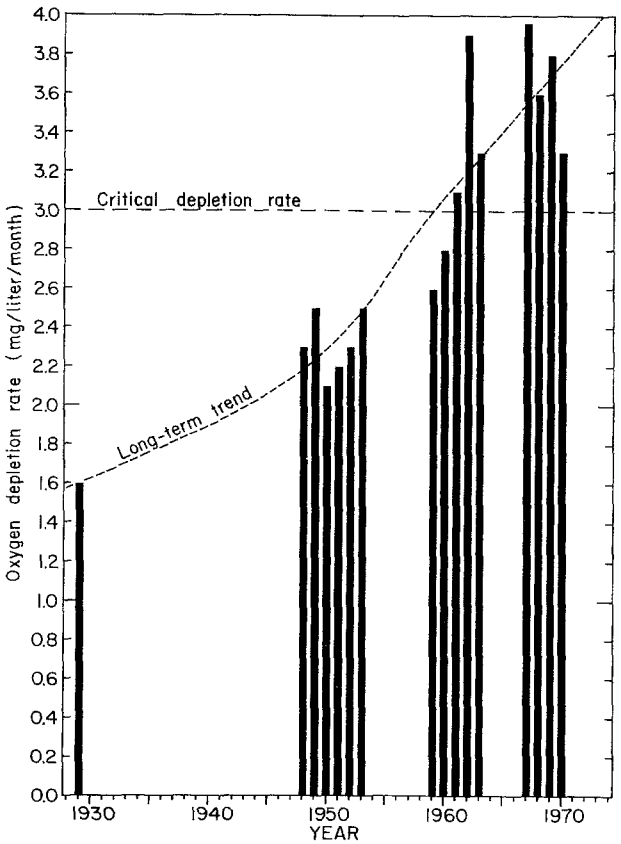

Figure 4. Mean depletion rates for dissolved oxygen during summer in the bottom-water of central Lake Erie. Note that the critical rate of 3.0 mg/liter/month, reached in 1961, produces zero oxygen levels before the end of summer stratification.

consuming oxygen than are inorganic chemical processes. Deoxygenation of the bottom water by organic wastes of direct human origin is relatively unimportant. The main source of organic matter is detrital phytoplankton material which has sedimented to the lake bottom where it is subsequently decomposed by bacteria. Increased phytoplankton production, and thus increased oxygen depletion, has been caused by increased nutrient enrichment from the large cities on the lake, particularly Detroit and Cleveland.

The distribution of hypolimnetic oxygen has been plotted for each of the years. The maps reveal that there is a large area of the offshore region with uniform oxygen concentrations. Oxygen depletion is more pronounced near the south shore and along the western edge of the hypolimnion. This effect is due to high phytoplankton production associated with high nutrient concentrations in the epilimnion and to the relative thinness of the hypolimnion in these areas. Higher oxygen values are found in the eastern end of the Central Basin. This is associated with influxes of water, which are less depleted of oxygen, from the Eastern Basin and with lower phytoplankton production.

This analysis has used the rate of oxygen consumption in the bottom waters of the Central Basin of Lake Erie as an index of the degree of modification of this environment. The International Joint Commission (1969) has recommended the removal of phosphate from detergents, reduction of phosphorus from municipal and industrial effluents and the control of phosphorus from agricultural activities. The implementation of these recommendations should lead to improvement of the oxygen conditions in the bottom waters (Gilbertson, Dobson and Lee, pg. 143).

We are grateful for the encouragement we have received from Mr. J. P. Bruce and Dr. R.A. Vollenweider in this work.

REFERENCES

AMERICAN PUBLIC HEALTH ASSOCIATION. Standard Methods for the Examination of Water and Wastewater. (Various editions).

BEETON, A.M. 1963. Limnological survey of Lake Erie, 1959 and 1960. Great Lakes Fishery Commission, Technical Report No. 6. 32 p.

CARR, J.F. 1962. Dissolved oxygen in Lake Erie, past and present. Pub. No. 9, Great Lakes Res. Div., Univ. of Michigan, pp. 1-14.

DAVIS, C.C. 1964. Evidence for the eutrophication of Lake Erie from phytoplankton records. Limnol. Oceanog. 9 (3): 275-283.

FISH, C.J. and ASSOCIATES. 1960. Limnological survey of eastern and central Lake Erie, 1928 – 1929. U.S. Fish and Wildlife Service, Special Scientific Report – Fisheries No. 334. 198 p.

GREAT LAKES INSTITUTE, UNIV. OF TORONTO. 1964. Great Lakes Institute Data Record, 1962 Surveys, Part 1, Lake Ontario and Lake Erie. Report PR 16, 97 p.

GREAT LAKES INSTITUTE, UNIV. OF TORONTO. 1965. Great Lakes Institute Data Record, 1963 Surveys, Part 1: Lake Ontario, Lake Erie, and Lake St. Clair. Report PR 23. 195 p.

HERDENDORF, C.E. 1967. Lake Erie Bathythermograph Recordings, 1952-1966. Ohio Dept. of Natural Resources, Geological Survey, Information Circular No. 34. 36 p. & 1 map.

HUTCHINSON, G.E. 1957. A treatise on Limnology, Vol. 1. J. Wiley and Sons, Inc., New York. 1015 p.

INTERNATIONAL LAKE ERIE WATER POLLUTION BOARD AND INTERNATIONAL LAKE ONTARIO – ST. LAWRENCE RIVER WATER POLLUTION BOARD. 1969. Report to the International Joint Commission on the Pollution of Lake Erie, Lake Ontario, and the International Section of the St. Lawrence River. Vol. 1. 150 p.

POWERS, C.F., D.L. JONES, P.C. MUNDINGER, AND J.C. AYERS. 1960. Applications of data collected along shore to conditions in Lake Erie. Pub. No. 5, Great Lakes Res. Div., Univ. of Michigan. 78 p.

RODGERS, G.K. 1962. Lake Erie Data Report, 1961. Great Lakes Institute, Univ. of Toronto, Prelim. Rept. No. 3. 141 p.

RODGERS, G.K. 1963. Lake Erie Data Report, 1960. Great Lakes Institute, Univ. of Toronto, Prelim. Rept. No. 11. 138 p.

3. *Physical Processes Affecting the Hypolimnion of the Central Basin of Lake Erie*

J.O. Blanton, Ph.D.
Canada Centre for Inland Waters
Burlington, Ontario, Canada

A.R. Winklhofer
U.S. Environmental Protection Agency
Region V, Ohio District Office
Fairview Park, Ohio, U.S.A.

Central Basin water temperature, currents, wind, and hypolimnion dissolved oxygen were monitored in situ as part of "Project Hypo". A semi-permanent tilt of the thermocline was clearly associated with the dominant southwest winds. The thermocline was shallowest along the Canadian shore. Fluctuations in the southwest wind component correlated with fluctuations in thermocline position and with maximum current speeds in the hypolimnion. Peak southwest winds caused increased flow of hypolimnion water toward the Canadian coast. Eastern Basin inflow to the Central Basin and hypolimnion outflow in upwelling zones cannot account entirely for the measured hypolimnion volume fluctuations that were attributed to vertical entrainment. Periods of low wind energy, followed by brief periods of high wind energy coincided with hypolimnion volume increases.

The average hypolimnion dissolved oxygen depletion rate, from four in situ monitors, was 3.3 mg.l.$^{-1}$month^{-1}. The measured dissolved oxygen fluctuations were related to water movements, and fluctuations solely attributable to the presence of algae were not detected.

INTRODUCTION

Lake Erie is unique among the Great Lakes in several of its natural characteristics, each of which has a direct bearing on its condition. Furthermore, the physical processes affecting the lake are influenced by the climatology peculiar to this portion of the northern hemisphere. The purpose of this report is to summarize the pertinent physical processes affecting the hypolimnion of the Central Basin of Lake Erie and to interpret the observed phenomena in terms of the "Project Hypo" objectives.

Currents and temperatures in Lake Erie have been studied from time-to-time since before the turn of the century. Past efforts to obtain current measurements in the hypolimnion of the Central Basin have largely proven unsuccessful due to its thinness. Wind driven currents in Lake Erie are most variable in direction and are the fastest of the large scale water movements. Large volumes of water can be moved in a very short time.

A variety of *in situ* instrumentation was deployed in Lake Erie during "Project Hypo" to measure the physical processes governing the principal movements of hypolimnion water and to document the hypolimnion dissolved oxygen content changes in detail. The data were analyzed to determine the relationship between the dominant winds, dominant motions in the hypolimnion and the response of the thermocline to these motions. As a result of this work, the general circulation pattern and magnitudes of the currents in the hypolimnion were determined as was also the ultimate state of much of the hypolimnion

water transport in the Central Basin. The data were further analyzed to determine the relationship between wind energy, measured hypolimnion volume changes, and oxygen entrainment.

METHODS

Data contained in this report were obtained from existing land monitoring stations, from *in situ* automatic monitoring devices operated during the study and from cruise sampling data.

Most climatological data were obtained from the U.S. Environmental Science Services Administration and the Canadian Department of Transport. Lake level data were obtained from the U.S. National Ocean Survey, Lake Survey Center. Lake water temperatures at Put-in-Bay, Ohio, were obtained from the Ohio Division of Wildlife.

Twenty-five locations were selected for monitoring of pertinent data. These sampling locations are shown in Figure 1. Sample collection and instrument servicing were performed using the Canadian ship CSS *Limnos* and launch *Agile* and the U.S. Coast Guard Cutter *Bramble* and the U.S. launch *Blue Water*. Additional data were obtained from the monthly monitor cruises of the Canadian ship M/V *Martin Karlsen*.

LOCATION OF INSTRUMENTATION

Lake Erie Central Basin water temperature, epilimnion and hypolimnion currents, over-the-lake wind and dissolved oxygen phenomena were automatically monitored *in situ* at selected locations (Fig. 1). Table 1 lists the stations, the depth of each instrument, the time of station occupancy and the type of record.

DESCRIPTION OF INSTRUMENTATION

Twenty-six Geodyne Model No. A-119 temperature recorders were used to automatically monitor *in situ* water temperature and thermocline movements. The temperature recorders were a bourdon-tube-driven stylus scribing on a carbon-backed chart paper advancing at the rate of 3 mm (1/8 inch) every 20 minutes. The overall accuracy of the instrument was ± 0.3°C.

Lake currents were monitored *in situ* using 20 Geodyne Model No. A-100 current meters. A magnetically coupled vane was mounted on top of the instrument to sense current direction. Current speed was measured with a magnetically coupled Savonius rotor positioned at the bottom of the instrument. Data were stored internally on 16 mm photographic film, using a binary coding system. The current meters were preset to record every 20 minutes. The Savonius rotor was sensitive to approximately 0.9 cm/sec as shown by towtank tests conducted by the U.S. Army Corps of Engineers. Other tests (Gaul, *et al.*, 1963) show that the rotor is very reliable between 0.8 and 212 cm/sec. The vane was sensitive within 10° at 2.57 cm/sec, 2° at 1.29 cm/sec, and had a resolution of 2.8 degrees.

Over-the-lake winds were measured using five Geodyne Model No. A-140 wind recorders, each mounted on a toroidal-shaped buoy. Wind direction and velocity were measured at approximately 1.8 meters (6 feet) and 3.7 meters (12 feet) above the lake surface, respectively. The data were recorded every twenty minutes on 16 mm photographic film using a binary coding system. The wind recorders were accurate to ± 5% for wind direction (referenced to magnetic north).

Six automatic submersible Weston and Stack monitors were employed to continuously and simultaneously monitor temperature and dissolved oxygen (Beier, pg 133). One monitor was moored approximately 1.5 meters (5 feet) above the lake bottom at each of five stations from July 13 through September 3. A monitor was used aboard ship for obtaining vertical profile data and for use in *in situ* experiments.

Current meters and temperature recorders were moored using a basic taut-line mooring configuration (Fig. 2). With the able assistance of the U.S. Coast Guard Cutter *Bramble*, instrumentation

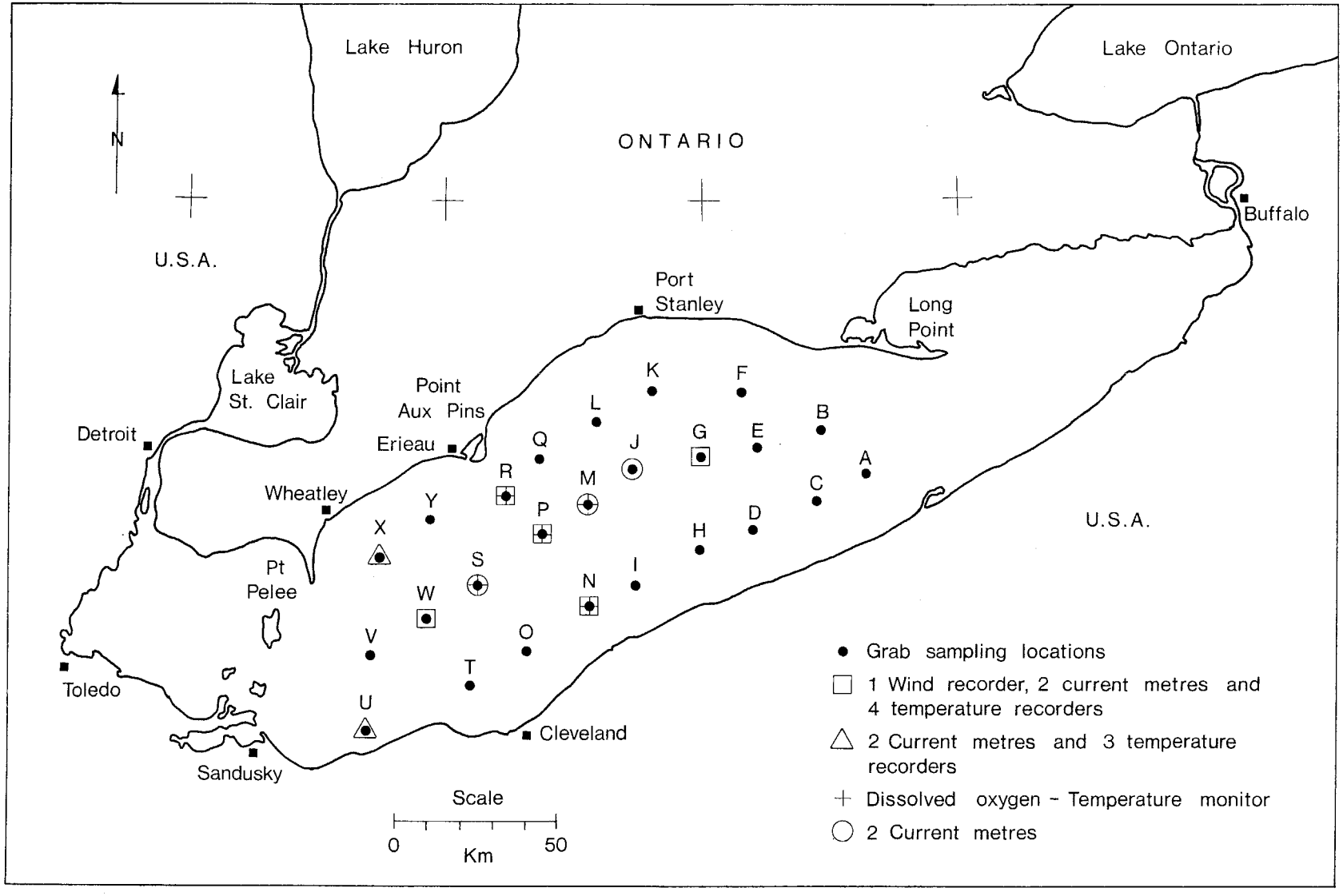

Figure 1. Lake Erie "Project Hypo" monitoring locations, 1970.

TABLE 1. Instrumented station descriptive data. (Station locations on Figure 1)

Station	Instrument	Depth (meters)	Time of Station Occupancy-1970	Type of Record
U	Current Meter	9.8	7/13-9/1	No record after Aug. 18
	Temperature Recorder	11.9	7/13-9/1	None
	Current Meter	12.8	7/13-9/1	Complete
	Temperature Recorder	13.0	7/13-9/1	Complete
	Temperature Recorder	14.0	7/13-9/1	Complete
	Total Depth	14.6		
X	Current Meter	10.4	7/13-8/31	None
	Temperature Recorder	14.3	7/13-8/31	Complete
	Temperature Recorder	16.2	7/13-8/31	Complete
	Current Meter	16.5	7/13-8/31	None
	Temperature Recorder	17.7	7/13-8/31	Complete
	Total Depth	18.3		
W	Wind Recorder		7/13-9/1	No speed
	Current Meter	10.7	7/13-9/1	Complete
	Temperature Recorder	14.0	7/13-9/1	Complete
	Temperature Recorder	16.0	7/13-9/1	Complete
	Temperature Recorder	18.0	7/13-9/1	Complete
	Temperature Recorder	19.8	7/13-9/1	Complete
	Current Meter	20.7	7/13-9/1	Complete
	Total Depth	22.6		
S	Current Meter	10.0	7/12-9/3	No speed after Aug. 19
	Current Meter	21.0	7/12-9/3	Periodic interval without speed
	Dissolved Oxygen-Temperature Monitor	21.3		Complete
	Total Depth	23.0		
R	Wind Recorder		7/13-9/2	None
	Current Meter	8.8	7/13-9/2	No record after Aug. 7
	Temperature Recorder	12.8	7/13-9/2	None
	Temperature Recorder	15.5	7/13-9/2	Complete
	Temperature Recorder	18.0	7/13-9/2	Complete
	Temperature Recorder	21.0	7/13-9/2	Complete
	Current Meter	22.0	7/13-9/2	No speed
	Dissolved Oxygen-Temperature Monitor	22.2		Complete
	Total Depth	23.8		
P	Wind Recorder		7/12-9/2	Complete
	Current Meter	8.8	7/12-9/2	None
	Temperature Recorder	12.5	7/12-9/2	Complete
	Temperature Recorder	16.2	7/12-9/2	Complete
	Temperature Recorder	19.2	7/12-9/2	Complete
	Temperature Recorder	21.6	7/12-9/2	None
	Current Meter	23.2	7/12-9/2	None
	Dissolved Oxygen-Temperature Monitor	23.5		Complete
	Total Depth	25.0		
N	Wind Recorder		7/14-9/3	No speed
	Current Meter	9.4	7/14-9/3	Periodic intervals without speed
	Temperature Recorder	13.4	7/14-9/3	Complete
	Temperature Recorder	15.5	7/14-9/3	Complete
	Temperature Recorder	17.7	7/14-9/3	Complete
	Temperature Recorder	19.8	7/14-9/3	Complete
	Current Meter	21.0	7/14-9/3	Periodic intervals without speed
	Dissolved Oxygen-Temperature Monitor	21.3		Complete
	Total Depth	23.0		

TABLE 1. (cont'd)

Station	Instrument	Depth (meters)	Time of Station Occupancy-1970	Type of Record
M	Current Meter	9.5	7/13-9/2	Complete
	Current Meter	22.2	7/13-9/2	No speed
	Dissolved Oxygen-Temperature Monitor	22.6		Partial
	Total Depth	24.0		
J	Current Meter	9.0	7/13-9/2	No record after Aug. 17
	Current Meter	21.0	7/13-9/2	Complete
	Total Depth	23.0		
G	Wind Recorder		7/13-9/2	Complete
	Current Meter	9.0	7/13-9/2	Complete
	Temperature Recorder	12.8	7/13-9/2	Complete
	Temperature Recorder	15.0	7/13-9/2	Complete
	Temperature Recorder	17.0	7/13-9/2	Complete
	Temperature Recorder	19.5	7/13-9/2	None
	Current Meter	20.4	7/13-9/2	Complete
	Total Depth	22.2		

was set during the week beginning July 12 and retrieved during the week beginning August 30. The dissolved oxygen-temperature monitors were serviced from the Canadian launch *Agile* and U.S. launch *Blue Water*.

DATA HANDLING

Temperature recorder data on strip charts were manually read at 20-minute intervals and tabulated. Temperature calibration was checked and the data adjusted if necessary, based on pre- and post-operation calibration checks and by comparison with data obtained during the many basin surveys. In addition, the length of record was checked against the in-place time. Three records required time adjustment. The corrected data were then entered onto punch cards for computer analysis. The temperature-dissolved oxygen monitor data were processed in much the same manner, the major difference being that only hourly data were used.

Current meter and wind recorder data are on 16 mm film in a binary format. Under contract the films were developed and read using an automatic film reader. The film reader output consisted of an IBM compatible magnetic tape and a multiple-channel analog plot containing every bit of information on the digital film. The reader magnetic tape was further processed to produce a computed magnetic tape containing vectorily averaged current direction and speed data (converted into desired units) for each interval of record. The computed magnetic tapes were further processed through the computer facilities at CCIW and McMaster University.

AREA DESCRIPTION AND CLIMATOLOGY

Adequate understanding of the significance of the data obtained during the study requires a knowledge of the physical features and climate of the basin. Each of the three Lake Erie basins have unique physical features. The climate of the Lake Erie basin is characterized by rapidly changing weather. Weather to a large extent controls the lake's circulation and thermal structure. The basins have been described by various investigators in great detail (FWQA, 1968) therefore only a brief summary is presented.

AREA DESCRIPTION

Lake Erie is centered at 42°15′ north latitude and 81°15′ west longitude, with its long axis orientated at about N70°E. The lake is approximately 386 kilometers (240 miles) long and more than 80 kilometers (50 miles) wide near the midpoint of its long axis.

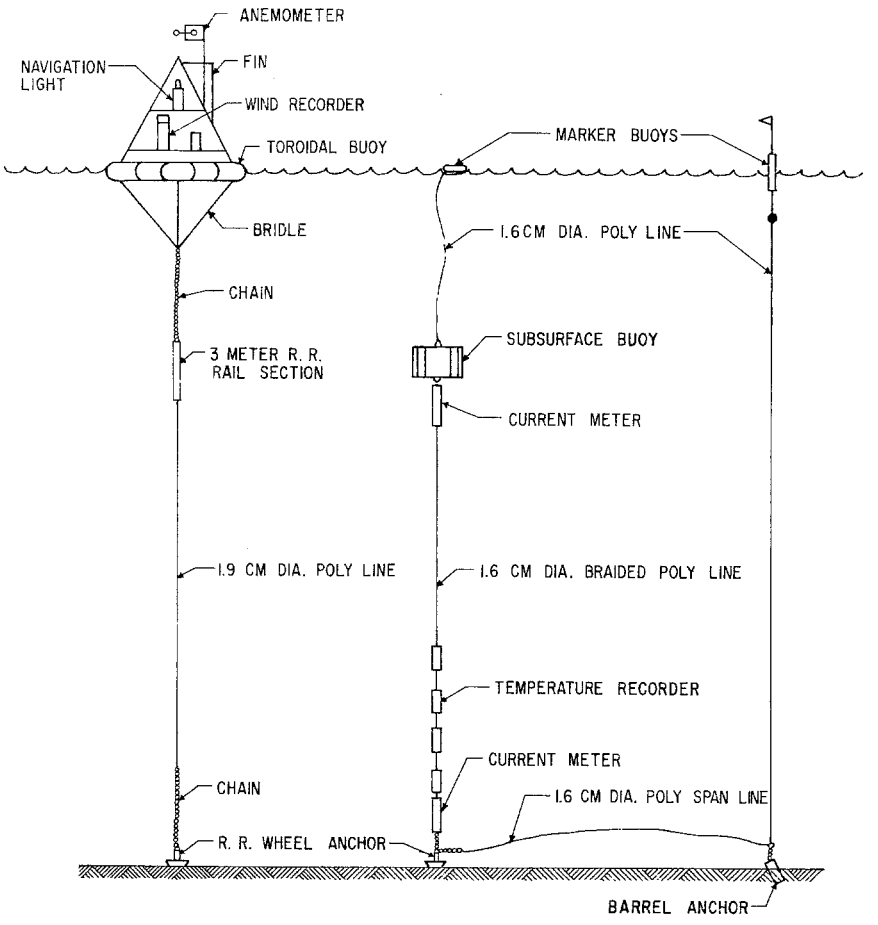

Figure 2. Typical taut-line instrument mooring system.

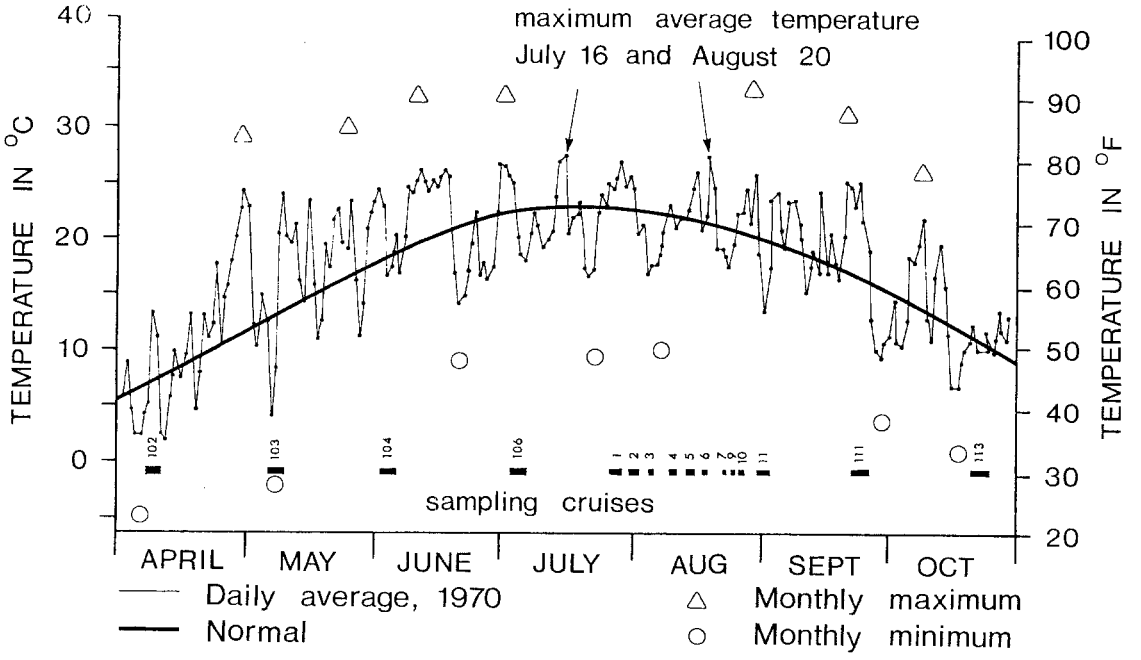

Figure 3. Daily air temperatures at Cleveland, Ohio – 1970.

The relatively flat-bottomed Central Basin is separated from the Western and Eastern Basins by a rocky island chain to the west and a low, wide, sand and gravel ridge to the east near Erie, Pennsylvania. The average depth of the Central Basin is 18.3 meters (60 feet) with a maximum depth of 25 meters (82 feet). The surface area of the Central Basin is approximately 14,873 square kilometers (5,650 square miles) or approximately 57 percent of the total lake area. The volume of the Central Basin is approximately 270 cubic kilometers or approximately 59 percent of the total volume of Lake Erie.

Lake Erie, due to its shallowness and orientation of its long axis parallel to predominant southwest and northeast winds, is particularly susceptible to short-term lake level changes. Water storage in Lake Erie has been above normal over the past three years.

AIR TEMPERATURE

Air temperatures in the Lake Erie Basin generally decrease northeastward from the southwestern end of the basin. Daily air temperatures at Cleveland Hopkins International Airport are shown in Figure 3 for April through October, 1970. Temperatures at Cleveland are not necessarily indicative of over-the-lake (Central Basin) temperatures; however the trends are considered representative of the area.

Average monthly temperatures at Cleveland for the first three months of 1970 were well below normal. Monthly average temperatures during April, May, and June were above normal. Near normal average monthly temperatures occurred during July, August, and September. The maximum average daily temperature was 27.2°C (81°F) on July 16 and August 20. The highest temperature recorded was 32.8°C (91°F) on August 30.

The longest duration (12 days) of above normal temperatures commenced on June 7. Conversely, the longest duration (9 days) of below normal temperatures commenced on September 27.

WATER TEMPERATURE

Daily (4 PM reading) water temperatures at Put-in-Bay, Ohio during the period April through October, 1970, and normal temperatures are shown in Figure 4. The maximum temperature was 26.7°C (80°F) on August 14. Warming and cooling trends are, in general, coincident with those for air temperature at Cleveland. Modifications to the trends are caused by the amount of sunshine, strength and duration of winds and by humidity. The above normal air temperatures during April, May, and June are reflected in the rapid warming of the lake water during the same period.

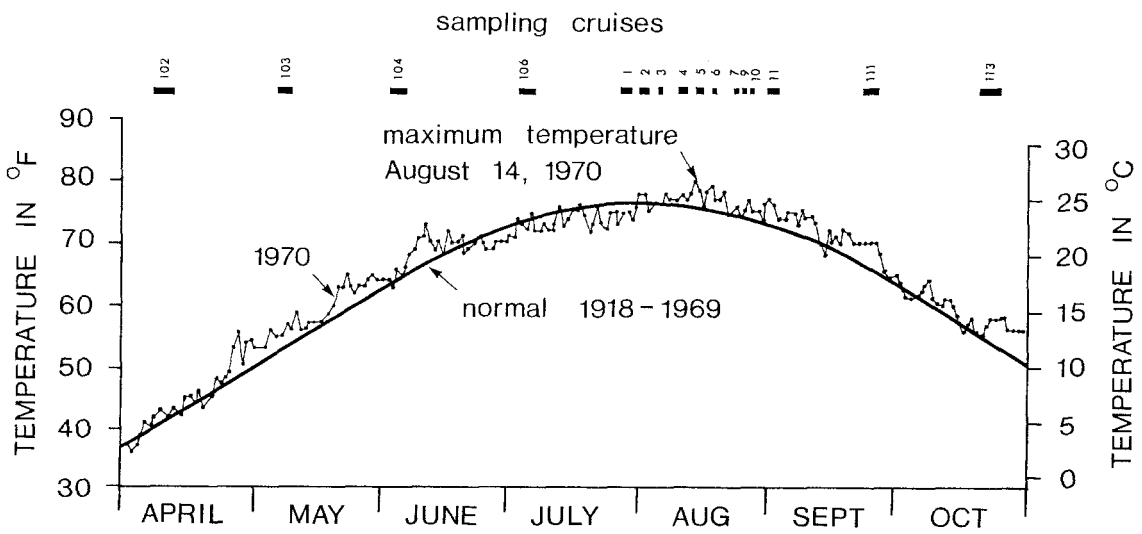

Figure 4. Daily water temperatures at Put-in-Bay, Ohio – 1970. (4 PM Readings)

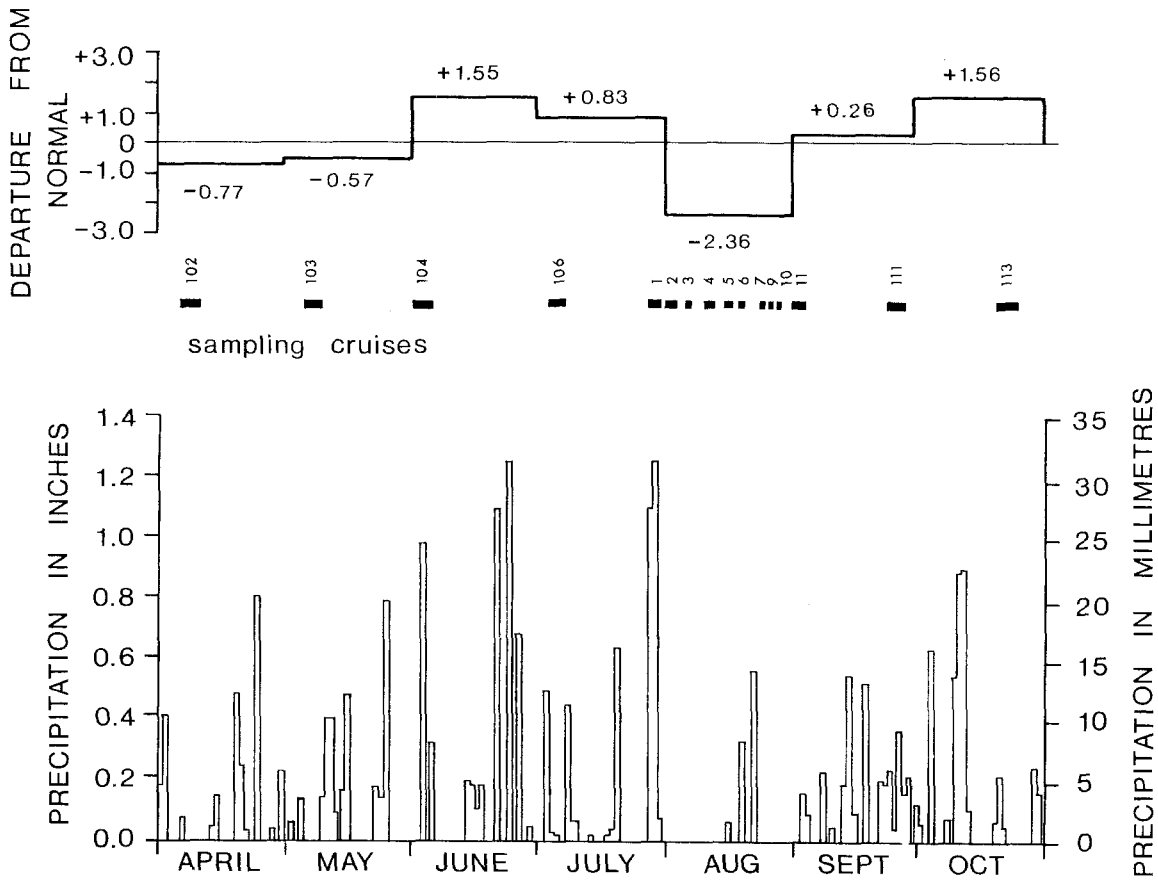

Figure 5. Daily precipitation at Cleveland, Ohio – 1970.

PRECIPITATION

Over-the-lake precipitation is not routinely monitored. Precipitation as measured at land stations is not necessarily indicative of that over the lake. Localized storms, particularly during the summer, significantly reduced the coherency of data between stations. Daily precipitation data at Cleveland Hopkins International Airport for the period April through October, 1970 (Fig. 5) are presented only to give a general indication of conditions during the study.

Precipitation at Cleveland during April, May, and August was below normal. Above normal precipitation occurred during June, July, September, and October. The most intensive phase of the study took place during August, the dryest month.

PERCENT OF POSSIBLE SUNSHINE

Percent of possible sunshine at Cleveland Hopkins International Airport for the period April through October, 1970 is shown in Figure 6. The highest monthly percent of possible sunshine occurred during June and lowest during October. During the period, April through October, only 5 days had 100 percent of possible sunshine, none of which was in June, July, or August. In the same period, 30 days had 30 percent or less of possible sunshine, October having 11 days and August one day.

WINDS

While there are several weather stations surrounding Lake Erie, it is extremely difficult to find a station with wind data that is truly representative of over-the-lake conditions. The influences of land topography are only too well known. The lighthouse at Long Point, Ontario serves as a weather station

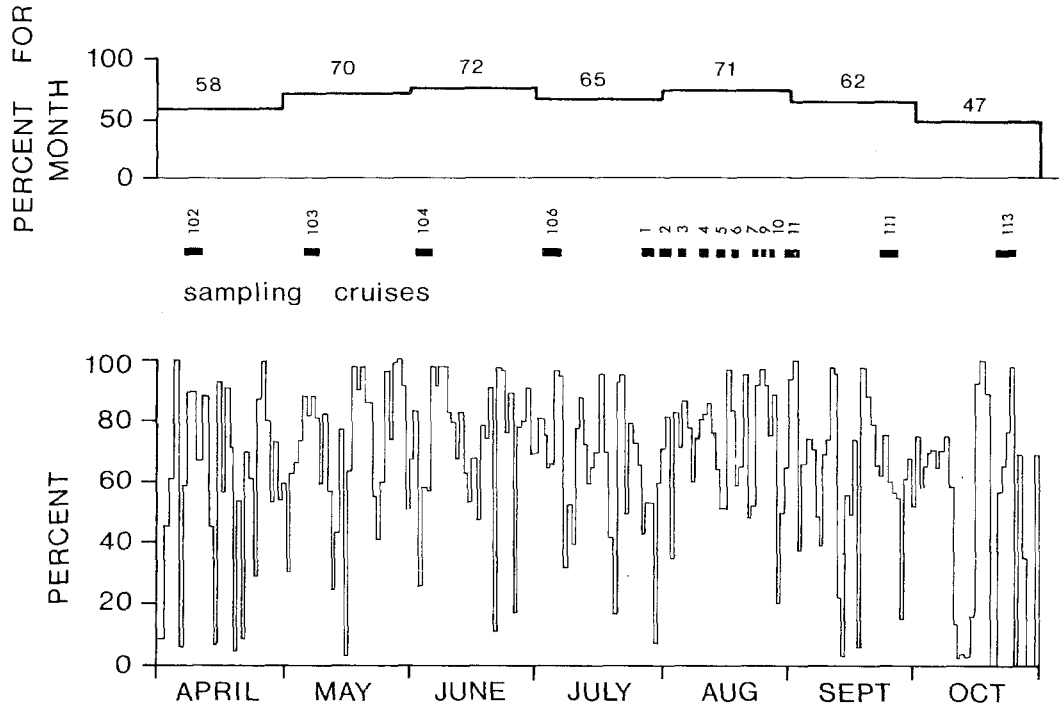

Figure 6. Percent of possible sunshine at Cleveland, Ohio – 1970.

operating only during the shipping season. Moreover its location offers a minimum of influence from the surrounding land. Ten-year averages (1960-1970, excluding 1965) of historical data from Long Point, Ontario are shown in Figure 7(A). Most noticeable are the prevailing southwest winds (from the southwest) during June, July, and August. A similar analysis of 1970 data (Fig. 7(B)) reveals that July, 1970 had a higher incidence of strong southwest winds. August, on the other hand, had less frequent southwest winds and a slightly more frequent occurrence of north to northeast winds.

To supplement the Long Point wind data, wind recorders were moored at five locations. Of these, only two gave data of sufficient quantity and quality to be of use. The wind frequency histograms (Fig. 8) for August, 1970 at stations P and G are compared with that of Long Point for the same period. (Resolution of direction was greater for the over-the-lake data than for the Long Point data.) The wind distribution at station G, closest to Long Point, closely resembled Long Point data. Station P, however, displayed a greater frequency of WNW to NW winds. Since Long Point is a part of the national network of meteorological stations, and thus has good quality control, the Long Point data were used almost exclusively in subsequent analysis of limnological data.

A progressive vector diagram of daily winds at Long Point (Fig. 9) was drawn for the period July 14 through August 31, 1970. Arrows point in the direction *toward which* the wind is blowing. The dominant incidence of southwest winds is clearly shown. It is interesting to note that most of the strong southwest winds occurred before and after the CSS *Limnos* cruises.

PRINCIPAL FEATURES OF THE TEMPERATURE STRUCTURE

Temperature data obtained from the *in situ* instrumentation and from the electronic bathythermograph casts from the CSS *Limnos* have yielded a rather detailed description of the distribution of temperature in the Central Basin. In general, the average hypolimnion temperature ranged from 10.1°C for *Limnos* Survey 1 to 11.9°C for *Limnos* Survey 7. In other words, heat was added more or less continuously to the hypolimnion. The manner in which the heat was distributed throughout the Central

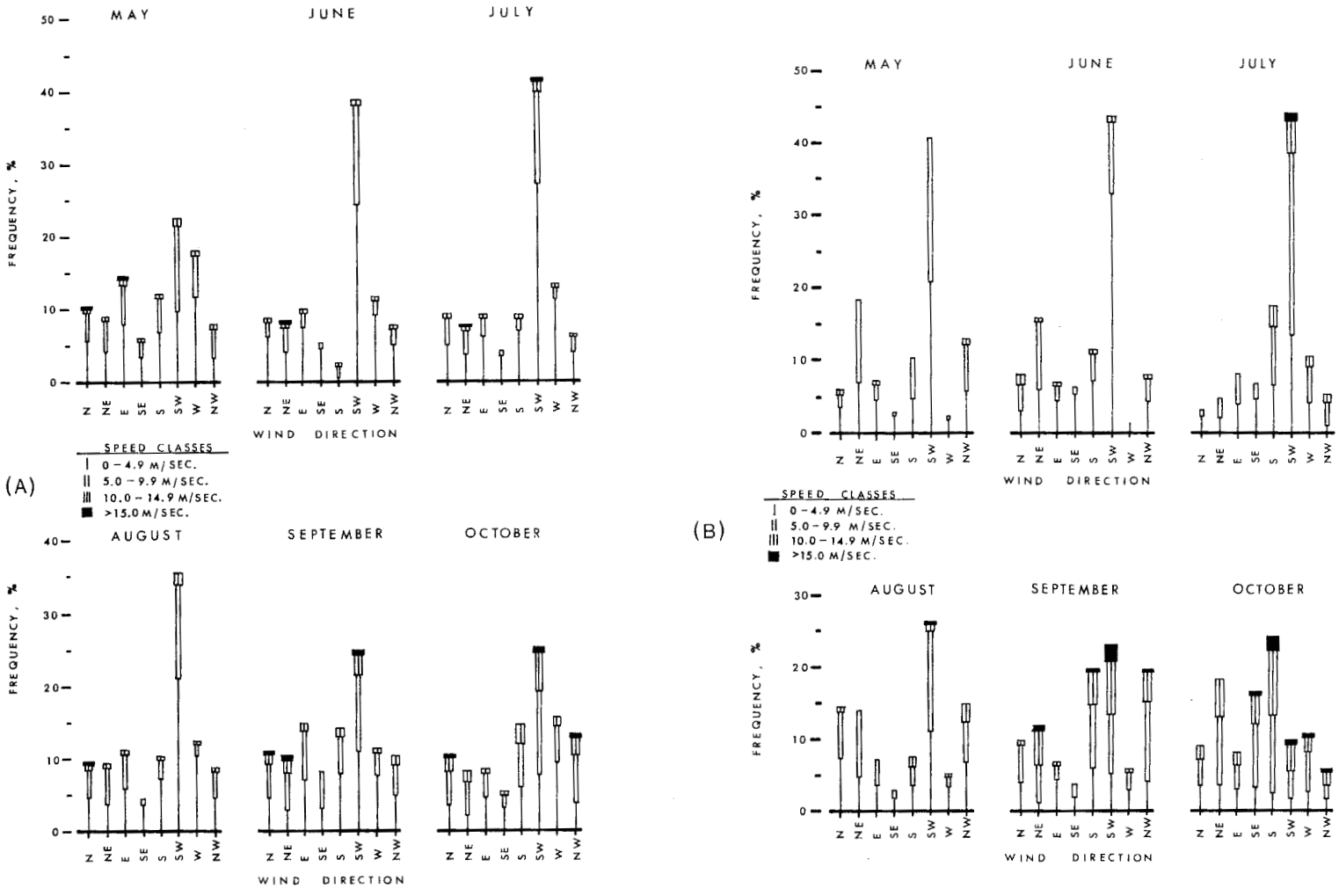

Figure 7. (A) Histograms of the monthly average winds at Long Point, Ontario: 1960-1970 excluding 1965. (B) Histograms of the monthly winds at Long Point, Ontario: May through October, 1970.

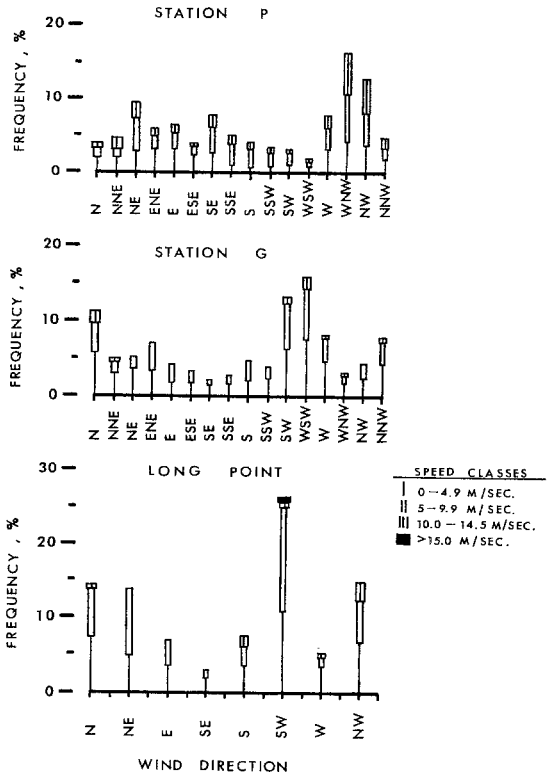

Figure 8. Comparison of over-the-lake and Long Point wind histograms for August, 1970.

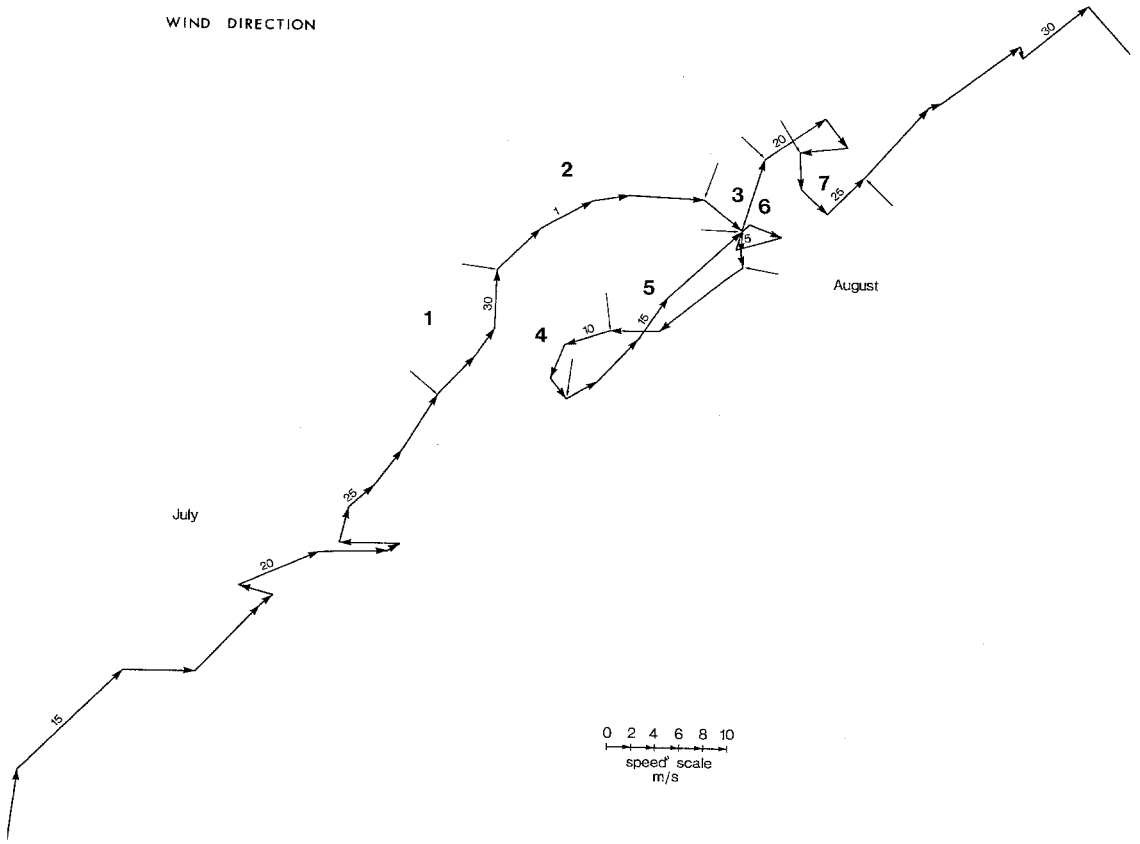

Figure 9. Progressive vector diagram of daily winds at Long Point for the period July 14 through August 31, 1970. Small numbers denote days of the month. Large bold-faced numbers between the small arrows denote the CSS *Limnos* cruise periods.

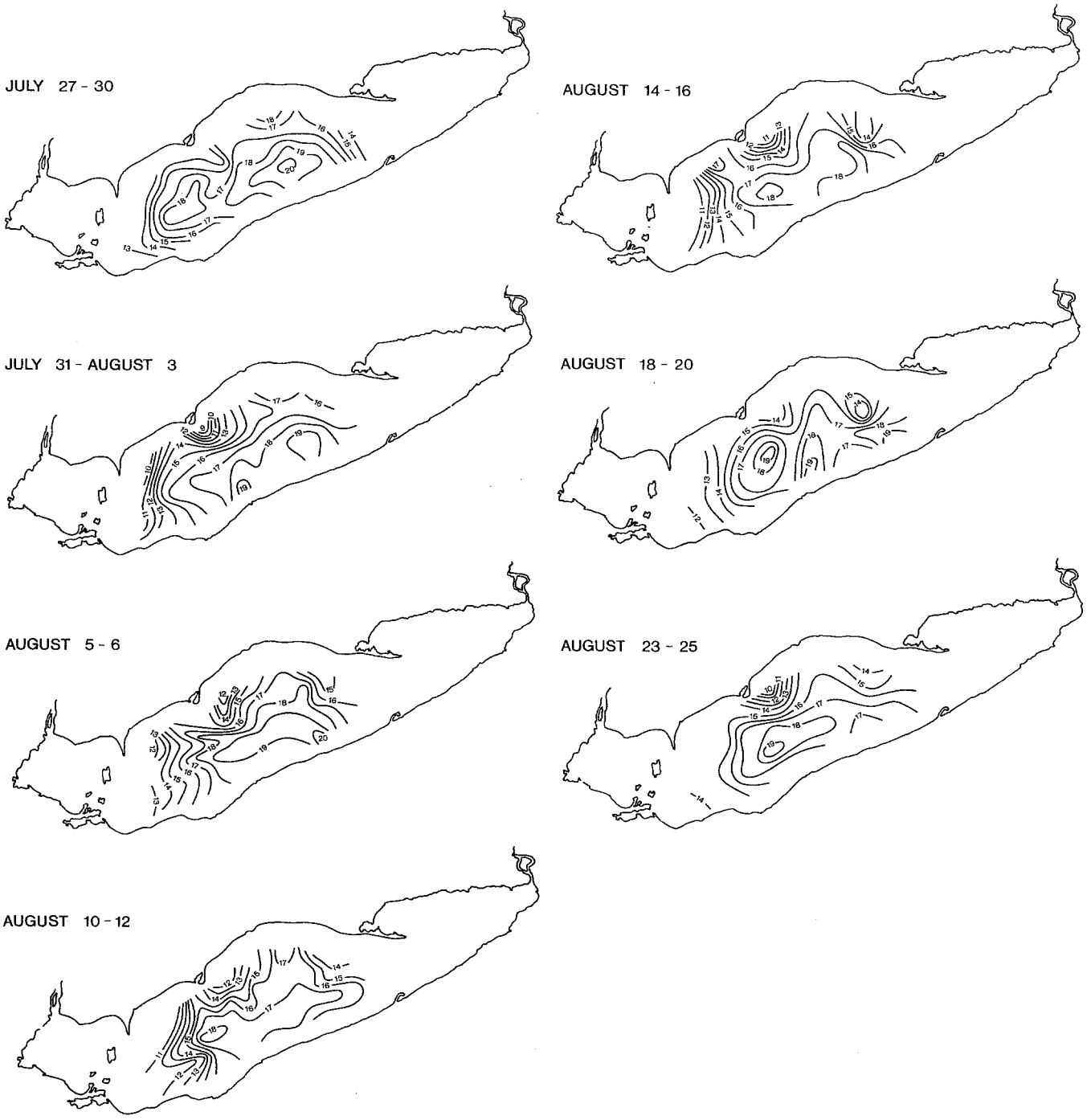

Figure 10. Topography of the Central Basin thermocline during the seven CSS LIMNOS cruises. (Depth of top of hypolimnion from surface shown in meters.)

Basin together with discussion of the principal features of the thermal structure are the subjects of this section.

AREAL TEMPERATURE DISTRIBUTION

For each of the cruises there are two maps describing the temperature structure (Figs. 10, 11). The first series of maps is essentially the topography of the main thermocline. A second series describes

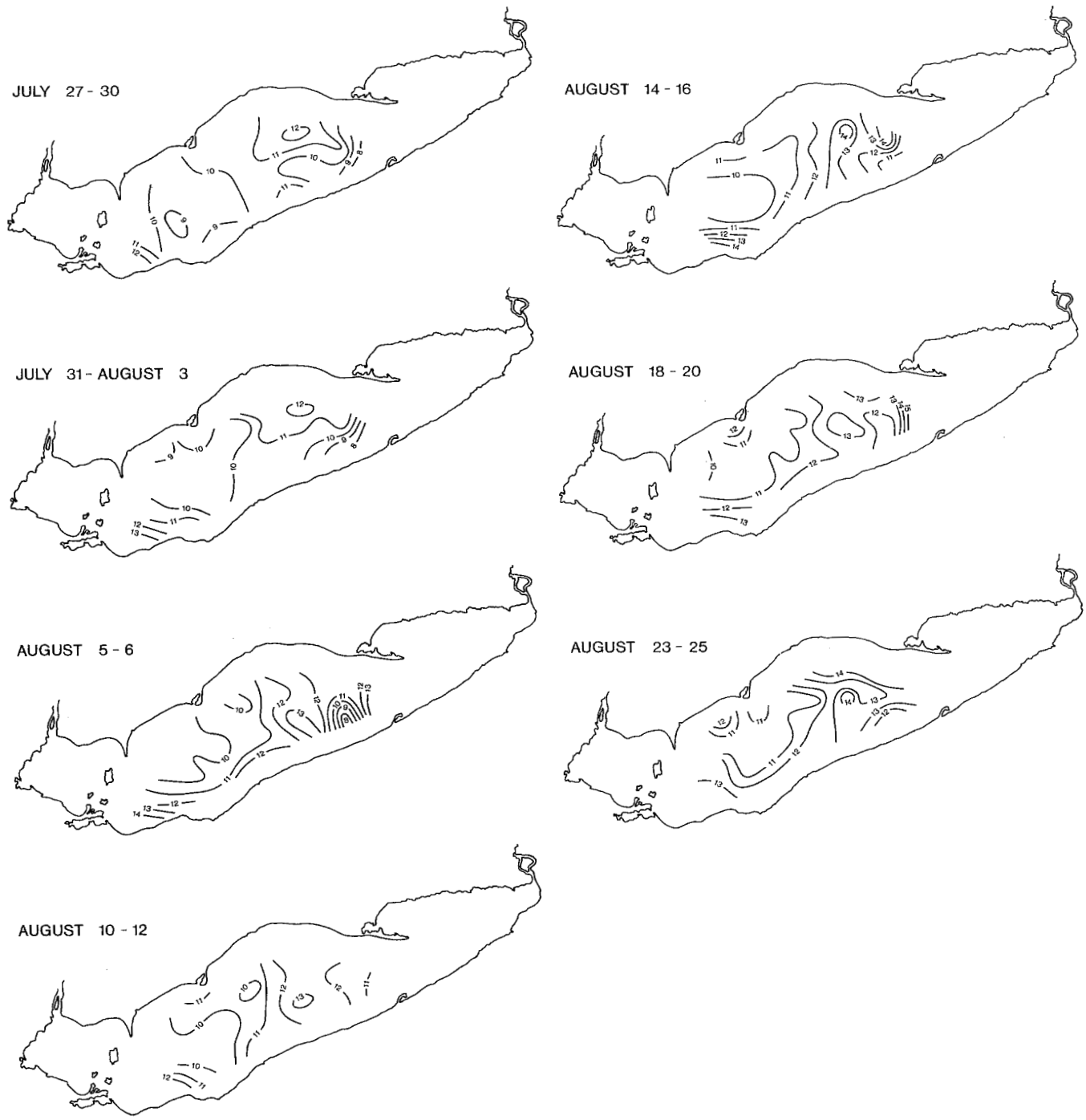

Figure 11. Hypolimnion temperature distribution in the Central Basin during the seven CSS LIMNOS cruises. (Temperatures in °C).

the temperature distribution in the hypolimnion. Several features on these maps are consistent from cruise to cruise.

There is a semi-permanent tilt to the thermocline with the deepest depressions generally located on the U.S. side of the International boundary. The thermocline is the shallowest along the Canadian shoreline east of Pointe Aux Pins and near the western end of the Central Basin. A quite remarkable feature is a valley in the thermocline topography generally located one-third of the way from

TABLE 2. Lake Erie Central Basin hypolimnion temperature regressions.

Station	Depth (meters)	Beginning Date	Beginning Temperature	Rate of Temperature Change, °C/month
Nearshore				
N	21.3	7/14	8.4	+1.7
R	21.0	7/14	8.4	+1.9
X	16.2	7/14	8.2	+1.3
	17.7	7/14	7.8	+1.2
Midbasin				
P	23.5	7/14	9.4	+0.5
S	21.3	7/14	9.8	+0.3
W	19.8	8/4	9.4	+0.7
M	22.6	7/28	10.2	+0.7

Pointe Aux Pins to Point Pelee. The difference in depth between the high, northeast of Pointe Aux Pins, and the low to the southwest is as great as six meters. This feature is presumably related to the wind-induced circulation of water around Pointe Aux Pins.

Colder water is generally found in the middle of the basin between Cleveland, Ohio and Erieau, Ontario. The temperature of the hypolimnion increases toward the east and toward the U.S. shore. Some of the maps show colder water near the channel connecting the Eastern and Central Basins.

HYPOLIMNION TEMPERATURE REGRESSIONS

From the preceding maps it is apparent that heat is distributed non-uniformly within the hypolimnion. The data from several of the *in situ* temperature recorders and temperature-dissolved oxygen monitors have been used to differentiate between rates of temperature increase in several areas of the hypolimnion. Nearshore areas are represented by stations N, R, and X. Areas in the middle part of the basin are represented by stations S, P, W, and M. A linear regression of the data from each of the stations was used to calculate the increase in hypolimnion temperatures (Table 2). The main result of these calculations is that the nearshore locations experienced temperature increases exceeding 1.2°C/month, while the increases at the midbasin locations were less than 0.7°C/month. The temperatures in the hypolimnion measured by the thermographs coincided closely with those measured by the CSS *Limnos* during Survey 1. That is, the midbasin areas were slightly colder than the nearshore areas. Particularly surprising, however, was that two weeks before Survey 1, this trend was reversed and the nearshore areas were colder compared with the midbasin areas (Table 2). The rates in Table 2 are less than the average rate of temperature increase of 1.8°C/month calculated from CSS *Limnos* data. This is not surprising since no thermographic data were obtained in the eastern portion of the hypolimnion.

THERMOCLINE FLUCTUATIONS

A thermograph array was moored at each of seven locations (Table 1). An excellent time series of thermal structure was obtained at four locations. Thermograph data for each array were contoured on a depth versus time plot. Temperatures between thermographs were determined by straight-line interpolation. The ability to define the thermal structure was principally a function of thermograph spacing.

The thermal structure at each of the four locations exhibited fluctuations ranging from time scales of hours up to time scales of several days. The thermal structure at the central location (station P) was dominated by short-term fluctuations having a period of approximately 17 hours, near the theoretical inertial period. The thermocline displacements varied from 1 to 3 meters during the 17-hour period. At station W, the thermocline displacements associated with the inertial period were noticeably less in magnitude and frequency of occurrence. At all stations there were significant periods of the order of several days duration where no significant fluctuations in thermocline elevation were measured. At stations N and R, the stations near the perimeter of the hypolimnion, the variability was noticeably more chaotic. During

several episodes lasting as long as one week, severe fluctuations caused distinct changes in the vertical displacement of the thermocline. The thermocline depth at station R could change by as much as 5 meters in 5 hours. Some of the high-amplitude, short-duration fluctuations occurred only at stations N and R near the perimeter of the hypolimnion, and they appear to be related with large amplitude fluctuations in lake level.

The semi-permanent tilt to the thermocline was also substantiated by the *in situ* thermographs. The thermocline at R was on the average approximately 2 meters higher than at N which is consistent with the maps of the thermocline topography (Fig. 10). This tilt is clearly consistent with the dominant southwest winds.

A portion of the thermal structure records at the four locations along with water level differences between Cleveland, and Buffalo, N.Y. are shown in Figure 12. For this particular portion the data show remarkable correlation with the wind (Fig. 9). The episode (July 29 through August 9, 1970) includes a relatively long and continuous period of SW to W winds beginning back as early as July 24 up to and including August 3. After August 3, wind speed diminished and winds changed to the north and east. During the period of southwest winds, the water level at Buffalo relative to that at Cleveland steadily increased into August 3. Coinciding with this period, the thermocline at N and W deepened while the thermocline at R became shallower. *Limnos* cruise data on August 2, 1800 EDT, showed that the thermocline approached to within 9 meters of the surface at station R. At N and W the hypolimnion was almost entirely replaced by epilimnion water during this period. After cessation of southwesterly winds, the wind shifted to north and northeast, and the water levels changed abruptly so that the elevation at Cleveland was higher than those at either Buffalo, New York or Port Stanley, Ontario. The thermocline at stations N and W returned more-or-less to its original depth. At N, the recovery took place approximately 2 hours after SW winds subsided. At R, however, the thermocline took about 2 days longer to return from 9 meters to a depth of about 17 meters. The shoaling of the thermocline on the leeward side of Pointe Aux Pins undoubtedly accounts for part of the delay. Internal waves near the inertial period began at P on July 31 during SW winds and continued through the entire period. These waves did not dampen out until the middle of August.

A leading conclusion from the episode described above is that the water level differences between Buffalo and Cleveland supply the pressure head required to shift the hypolimnion. When the head is a maximum (Buffalo relative to Cleveland), the hypolimnion is shifted to the northwestern end of the Central Basin. This causes a large amount of potential energy to be stored here and to the east of Pointe Aux Pins. Upon relaxation of the wind, this potential energy is suddenly released, causing the hypolimnion to return to equilibrium. The potential energy appears to be sufficient to overcome any tendency for a cross-lake pressure head (such as that established occasionally between Cleveland and Port Stanley) to depress the hypolimnion along the south shore. In other words, the relatively brief episodes of NE or E winds (Fig. 9) do not impart sufficient energy to overcome the enormous amount of potential energy stored during SW wind conditions.

TIME VARIABILITY OF HYPOLIMNION DISSOLVED OXYGEN

Investigations have been conducted to define the dissolved oxygen conditions in the Central Basin hypolimnion of Lake Erie during summer thermal stratification (Fish 1960, Carr 1962, Thomas 1963, for example). All too often these investigations were limited both in areal extent and frequency of data collection, therefore the time variability of hypolimnion dissolved oxygen has not been well defined. With this in mind, automatic submersible temperature-dissolved oxygen monitors were procured and operated in conjunction with frequent synoptic basin surveys.

A monitor was moored at each of five (Fig. 1) Central Basin locations, approximately one and one-half meters above the lake bottom. The monitors were in place for approximately 50 days beginning July 13 and 14, 1970. Complete records were obtained from four monitors. Only a partial record was obtained from one monitor due to leakage of an electrical connector.

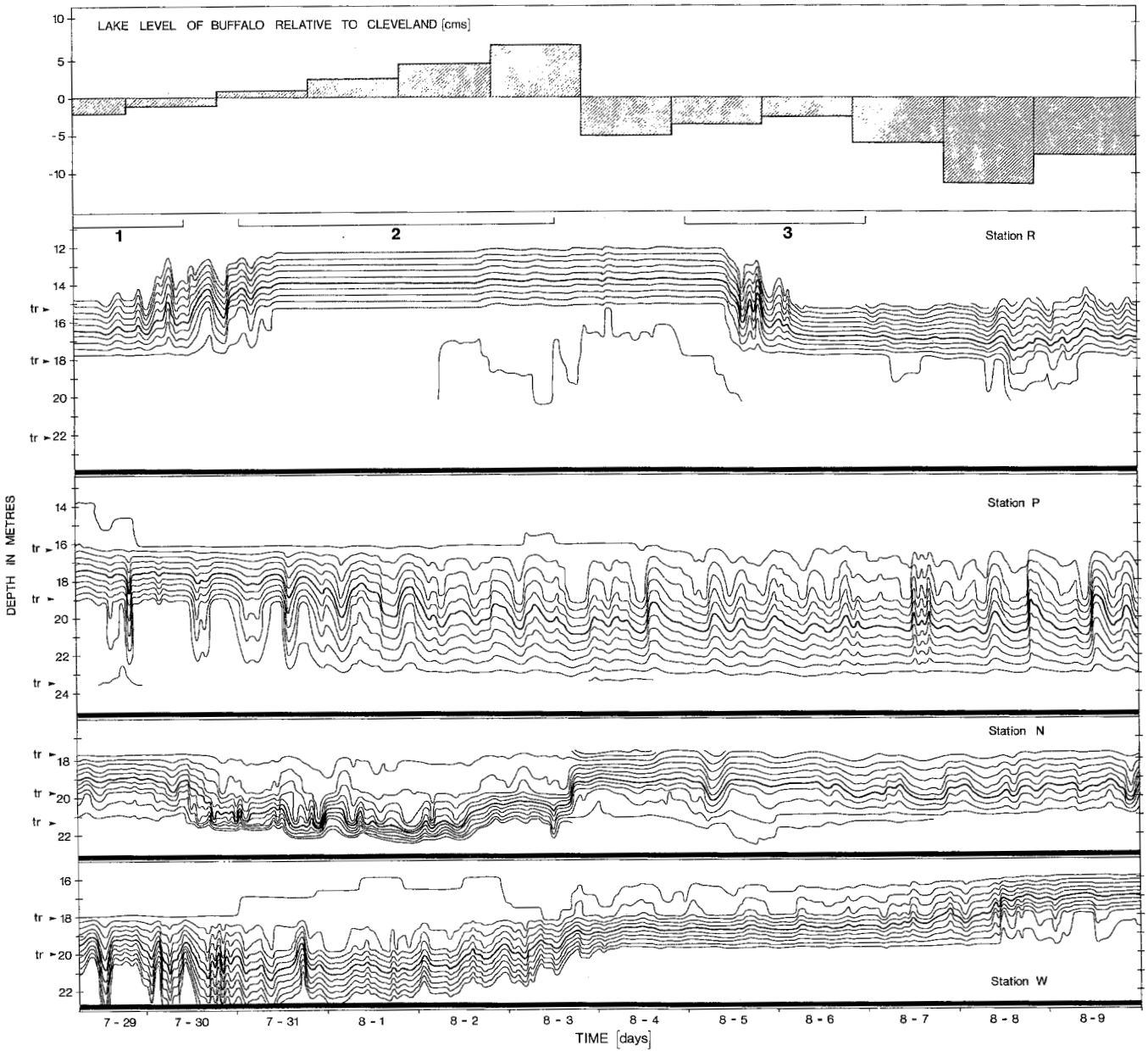

Figure 12. Time series of thermal structure at stations R, P, N, and W, and lake level differences between Buffalo and Cleveland for the period July 29 – August 9, 1970. The shaded areas represent estimated data when the thermocline passed above or below the last thermograph (tr) in the array. The CSS LIMNOS cruise periods are shown by the numbered brackets (station R). Isotherms are drawn at 1°C intervals. The 15°C isotherm is accented.

DISSOLVED OXYGEN REGRESSIONS

The hourly dissolved oxygen (D.O.) and temperature data for stations N, P, R, and S are shown in Figure 13. These data were analyzed by a least squares linear regression program. For comparative purposes, July 14 was selected as a common starting date for the analysis. The regression analysis did not consider data after the first occurrence of zero dissolved oxygen. The results are shown in Table 3.

Zero dissolved oxygen was first recorded at stations R and N (stations nearest the hypolimnion perimeter) on August 24 and 25. Approximately eight days later, zero dissolved oxygen was recorded at the midbasin stations P and S.

TABLE 3. Regression analysis of hourly dissolved oxygen data showing depletion rates for stations R, P, N, and S

Station	D.O. on July 14 mg/1	Date when D.O. became zero	Depletion Rate mg/1/month	Standard Deviation
R	5.2	Aug. 24	3.2	± 0.3
P	5.2	Sept. 1	3.2	± 0.2
N	7.6	Aug. 25	3.3	± 1.0
S	5.6	Sept. 1	3.5	± 0.3
		Average	3.3	

The dissolved oxygen depletion rates as calculated from the monitor data are somewhat lower than that reported by Burns and Ross (pg 118). They report a rate of 3.84 mg.$l.^{-1}$ $month^{-1}$ (40 μmoles O_2 $l.^{-1}$ day^{-1}), based on hypolimnion dissolved oxygen budget calculations from *Limnos* cruise data. The rate of depletion for the hypolimnion in 1970 reported by Dobson and Gilbertson (pg 7) was 3.3 mg.$l.^{-1}$ $month^{-1}$ which is the same as the average rate reported in the above table. It should be noted that the data

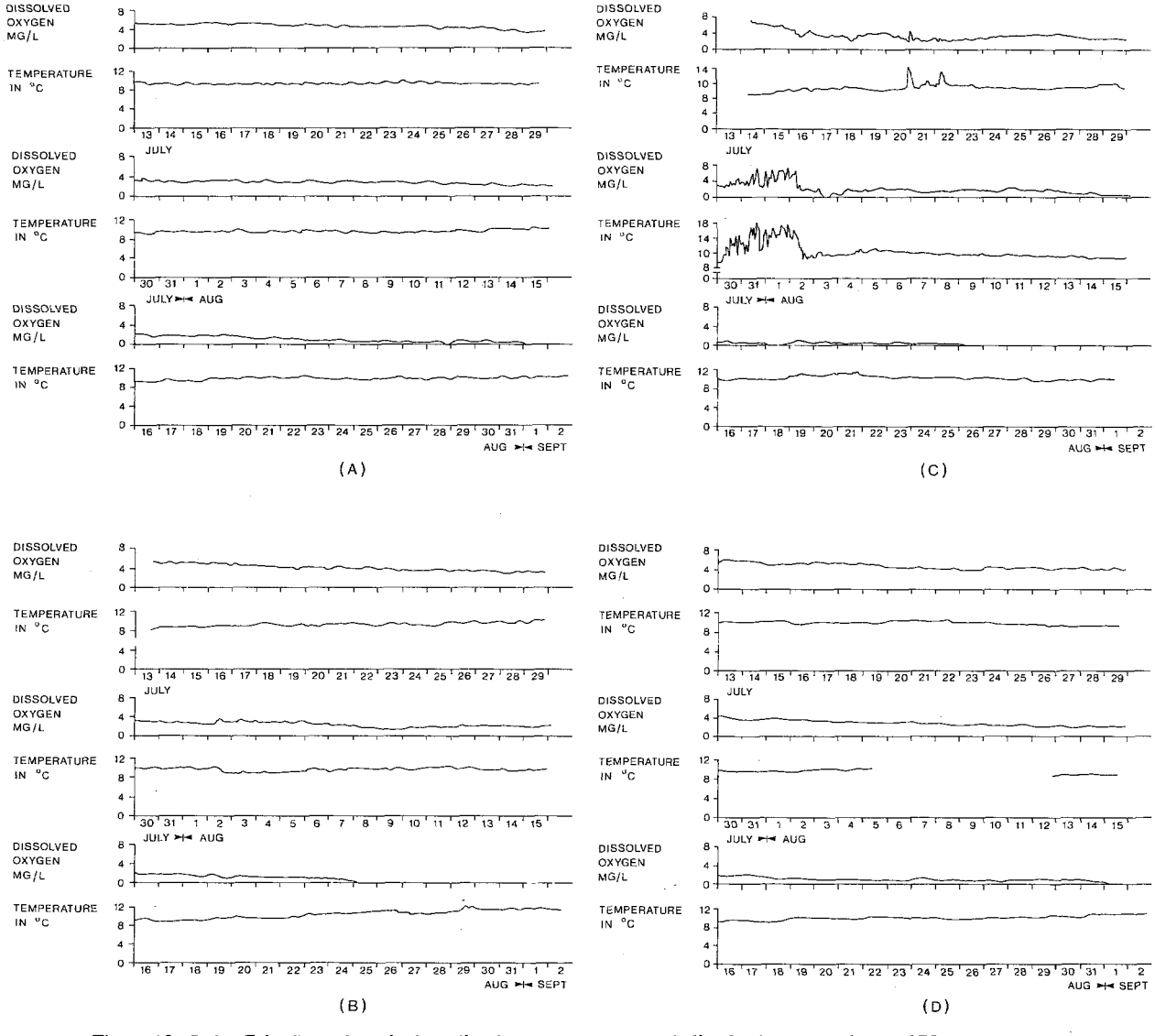

Figure 13. Lake Erie Central Basin hypolimnion temperature and dissolved oxygen data, 1970. (A): Station P, depth 23.5 meters. (B): Station R, depth 22.2 meters. (C): Station N, depth 21.3 meters. (D): Station S, depth 21.3 meters.

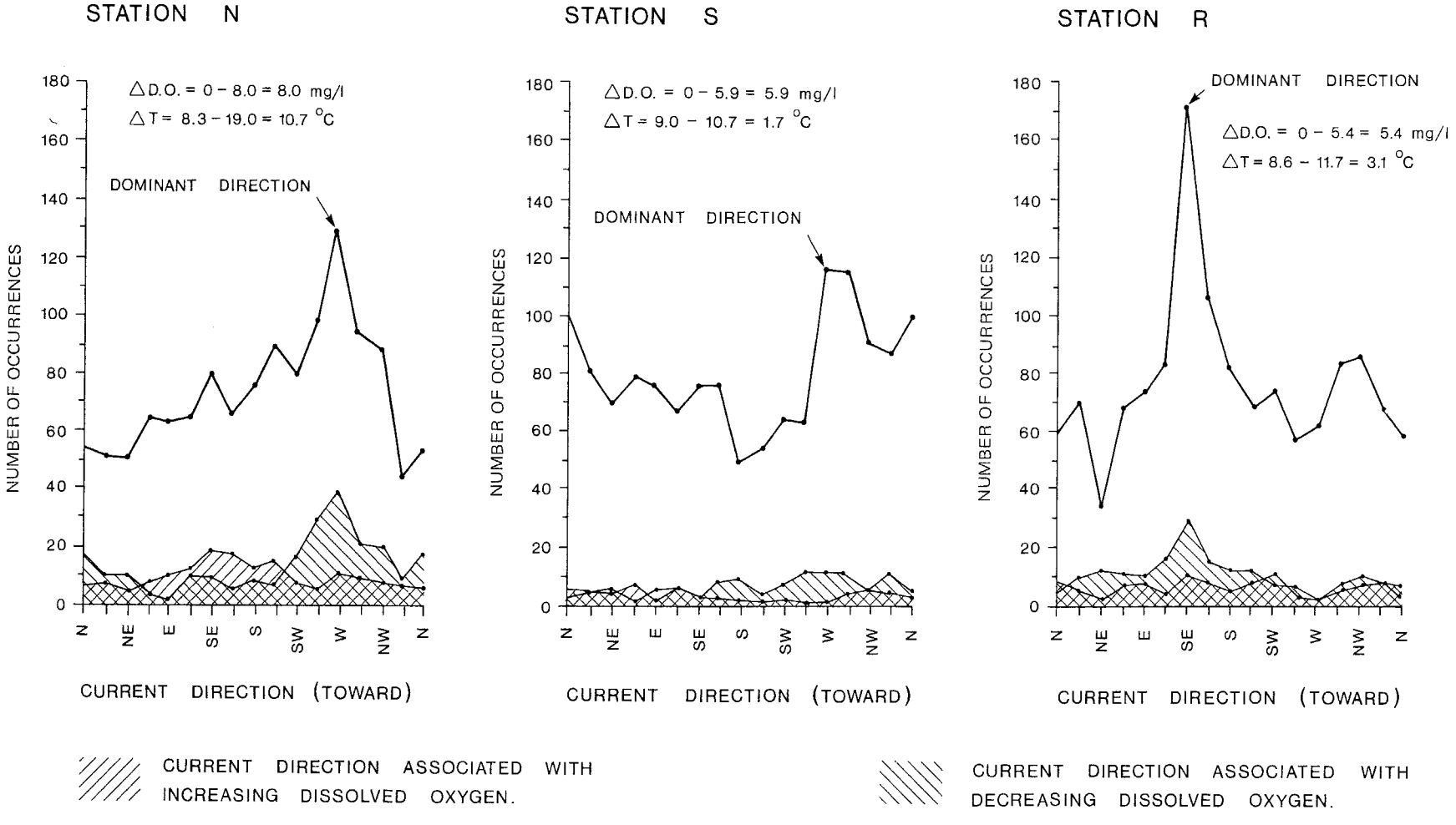

Figure 14. Hypolimnion current – dissolved oxygen correlations at Stations N, S, and R, based on hourly observations during the period July 13 through September 3, 1970. The deltas (△) represent absolute ranges of temperature and dissolved oxygen at each station.

used by Burns and Ross were obtained from a greater number of locations near the hypolimnion perimeter. Therefore, their rate may be more representative of an overall basin rate. These rates of depletion are consistent with the long-term trend of increasing rate of depletion in the past four decades reported by Dobson and Gilbertson (pg 6), and Thomas (1963).

Dissolved oxygen depletion rates as previously defined are indicative of general trends. Careful examination of the monitor data reveals dissolved oxygen fluctuations varying in amplitude and duration interspersed with episodes of no net change. The *in situ* data depict the net change of dissolved oxygen during a given time interval due to physical, chemical, and biological processes. It is impossible to identify and accurately assess the contribution of each process to a given dissolved oxygen change.

DISSOLVED OXYGEN – CURRENT CORRELATIONS

Dissolved oxygen data at stations N, S, and R measured approximately 1.5 meters above the lake bottom, and current direction measured approximately 2.5 meters above the lake bottom, were analyzed (Fig. 14) to determine if dissolved oxygen increases or decreases were associated with particular current directions. A dissolved oxygen change was considered to be 0.1 mg/1 or more. The analysis assumed that the measured current directions were representative of those at the depth of dissolved oxygen measurements.

The dominant current directions are west at stations N and S and southeast at station R (Fig. 14). Dissolved oxygen decreases at N are correlated with water moving away from shore and are coincident with the dominant current direction. Increases of dissolved oxygen at N are associated with water moving toward shore. No correlation was expected at S because no strong oxygen gradients were measured at that station (Fig. 13 (D)). Decreasing dissolved oxygen was associated with the dominant current direction at station R. The dominance of southeast currents appears to have precluded any dominant dissolved oxygen increases that might be associated with other directions.

The reader should recognize that the analysis does not differentiate between dissolved oxygen changes due to movement of dissolved oxygen gradients and changes due to other physical, chemical, and biological processes. The general decline of dissolved oxygen during the period of record may have, in fact, biased the analysis, associating the dominant direction with decreasing dissolved oxygen.

The most pronounced dissolved oxygen variations were recorded at station N. Two episodes were selected to demonstrate the impact of oxygen gradient movements on the measured data.

An episode of dissolved oxygen change is shown in Figure 15. Under the influence of southwest winds, maximum lake levels were attained at Buffalo, July 20 at 2100 EST. Approximately four hours later maximum thermocline depression was recorded. The thermocline depression was coincident with an accelerated decline in dissolved oxygen followed by an abrupt increase in dissolved oxygen and temperature as the monitor became enveloped in the thermocline. The sequence was reversed with the return of hypolimnion water. Hypolimnion currents were toward the westsouthwest prior to the thermocline depression, shifted toward the north as the thermocline depressed and reversed in direction as the thermocline returned to its normal elevation.

During another episode hypolimnion dissolved oxygen (Figure 16) gradually increased through July 26 then gradually decreased. Hypolimnion water temperature varied inversely with the dissolved oxygen. The gradual increase in dissolved oxygen was associated with hypolimnion water moving toward shore and down lake, and the gradual dissolved oxygen decrease was associated with water moving offshore and up lake.

These two episodes, one involving short-period fluctuation (order of 7 or 8 hours) and one involving a long-period fluctuation (order of 7 days) serve to emphasize the influence of oxygen gradients. Several episodes similar to these are contained in the 50-day record at N. The leading conclusion from the data is that when an oxygen gradient lies perpendicular to the shore, the onshore-offshore components of the currents account to a large degree for the *in situ* changes measured in dissolved oxygen.

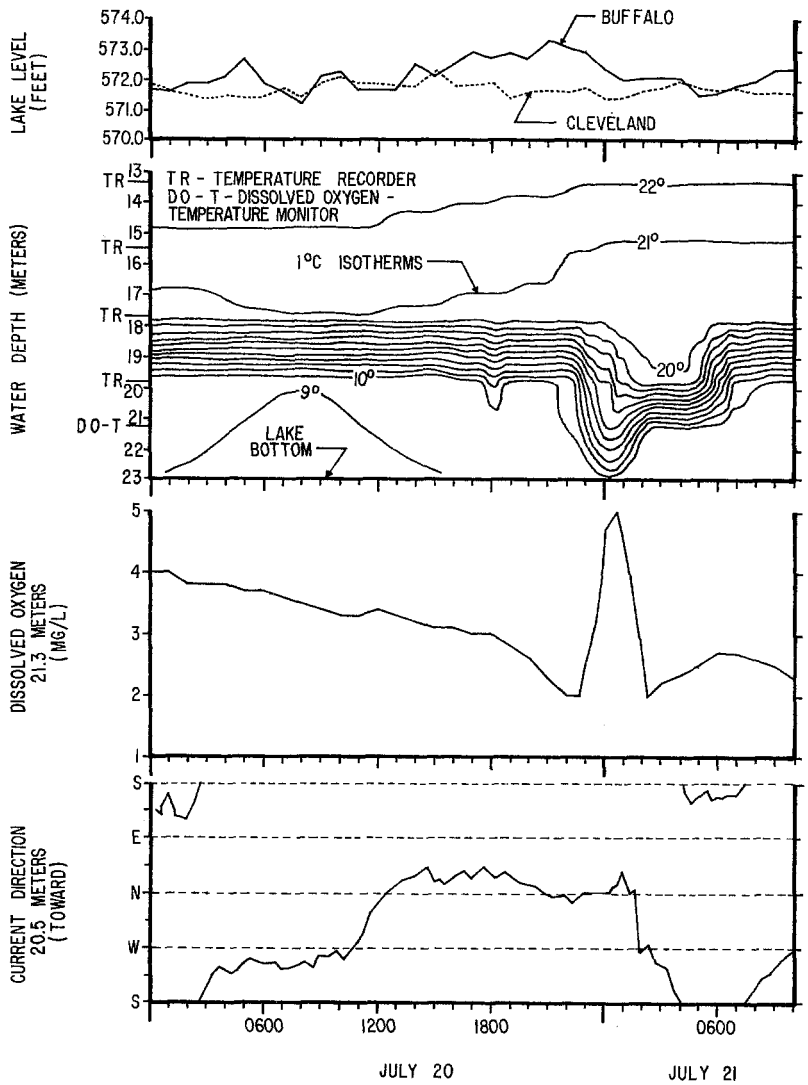

Figure 15. Lake level, thermal structure, hypolimnion dissolved oxygen and current regime at Station N for the period July, 20-21, 1970.

SUSPENDED ALGAE AND DISSOLVED OXYGEN OBSERVATIONS

An automatic underwater camera (Jirberg, pg 127), taking hourly photographs of the lake bottom, was operated at station P. In addition to photographing variations on the sediment surface, the camera documented the occurrence of suspended matter in the 1-meter water column between the camera and sediment. The suspended matter, appearing green in color (apparently algae), was noted during two camera settings. These observations are shown in Figure 17 along with temperature and dissolved oxygen measurements taken 1.5 meters above the bottom. The algae were observed during periods varying from one to twenty hours. Dissolved oxygen variations solely attributable to the presence of suspended algae were not noted. The longest periods when suspended algae were observed coincided with strong southwest winds and high-speed currents in the epilimnion and hypolimnion. However these data are insufficient to be conclusive. More importantly, diurnal dissolved oxygen variations were not observed at any of the five monitoring stations.

SEDIMENT OXYGEN DEMAND

In situ sediment oxygen demand (SOD) was measured at station P in the Central Basin of Lake Erie. Two experiments were performed in which 137 liters of hypolimnion were confined over 0.206

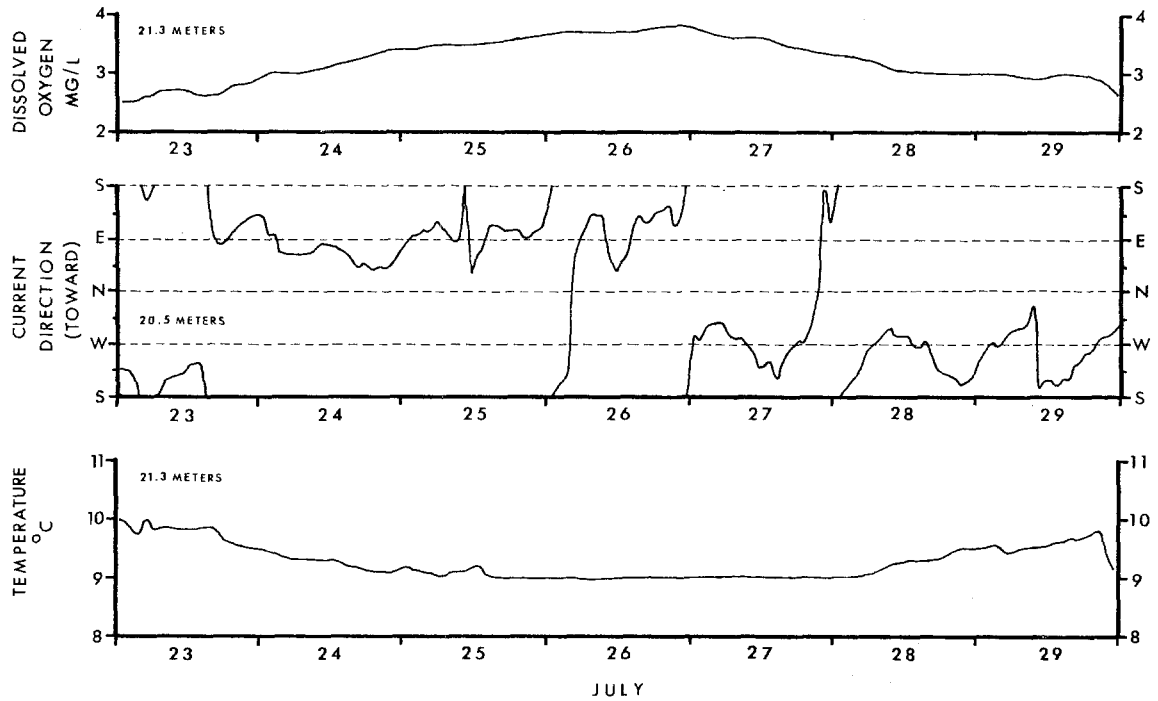

Figure 16. Hypolimnion dissolved oxygen, temperature and current direction at Station N for the period August 2-10, 1970.

m^2 of lake bottom. The temperature and dissolved oxygen concentrations of the confined water were continuously monitored over periods of from 5 to 7 days. A specially designed transparent box (Fig. 18) was pushed into the sediment to a depth of 53 cm. The top of the box, which contained the temperature and dissolved oxygen sensors, was not put into place until the following day to assure that quiescent conditions had been reestablished. The instrument module was moored at a depth of 10 meters to facilitate data retrieval without disturbing the box.

The first experiment (Fig. 19) was conducted over a period of 6.92 days. At the beginning of the experiment sunlight penetrated to the lake bottom, and the sediment was brown with small amounts of algae present. At the conclusion of the experiment sunlight was still present, and a layer of algae had appeared on the lake bottom surrounding the box. Temperature variations (Fig. 19) were small ranging from 8.6 to 9.4°C over the course of the experiment. The initial oxygen concentration of 4.6 mg/1 (143 μmoles O_2/1) decreased to 1.7 mg/1 (53 μmoles O_2/1) at the conclusion of the experiment. During the 6.92 days the dissolved oxygen decreased at a rate of 0.432 mg.$1.^{-1}$ day^{-1} (13.8 μmoles $O_2 \cdot 1.^{-1}$ $days^{-1}$) (by regression analysis) and exhibited a SOD of 0.28 gms O_2 $m.^{-2}$ day^{-1} (8.7 millimoles O_2 $m.^{-2}$ day^{-1}).

The second experiment (Fig. 19) covered a period of 5.58 days. The box was placed approximately 9 meters from the site of experiment #1. Sunlight penetrated to the sediment which was covered with small tufts of algae. As the experiment progressed, the amount of algae on the sediment next to the box increased until August 3, when layers 4 cm thick were noted. From August 4 up to the conclusion of the experiment, algae were abundant throughout the hypolimnion. The large number of falling algae had the following effects: they reduced the amount of sunlight reaching the lake bottom; they increased the layer of algae on the sediment; and, to varying degrees, covered the transparent box. Temperature variations were small ranging from 8.6 to 9.4°C over the course of the experiment. The dissolved oxygen concentration decreased from 4.0 to 1.2 mg/1 (125 to 39 μmoles O_2/1) or at a rate of 0.52 mg.$1.^{-1}$ day^{-1} (16 μmoles O_2 $1.^{-1}$ day^{-1}) (by regression analysis). The SOD was calculated to be 0.35 gm O_2 $m.^{-2}$ day^{-1} (10.9 millimoles O_2 $m.^{-2}$ day^{-1}). During both experiments no diurnal dissolved oxygen variations were detected.

The SOD values of 0.28 and 0.35 gms O_2 $m.^{-2}$ day^{-1} (8.7 and 10.9 mmoles O_2 $m.^{-2}$ day^{-1}) obtained during this study must be considered equivalent since there are insufficient data for establishing

the reproducibility of this test. The average SOD of these experiments (0.31 gms O_2 $m.^{-2}day^{-1}$; 9.7 mmoles O_2 $m.^{-2}day^{-1}$) compares favorably with the integrated daily rates for this station (0.4 gms O_2 $m.^{-2}day^{-1}$; 12.5 mmoles O_2 $m.^{-2}day^{-1}$) obtained by Lucas and Thomas (pg 49) from June through August

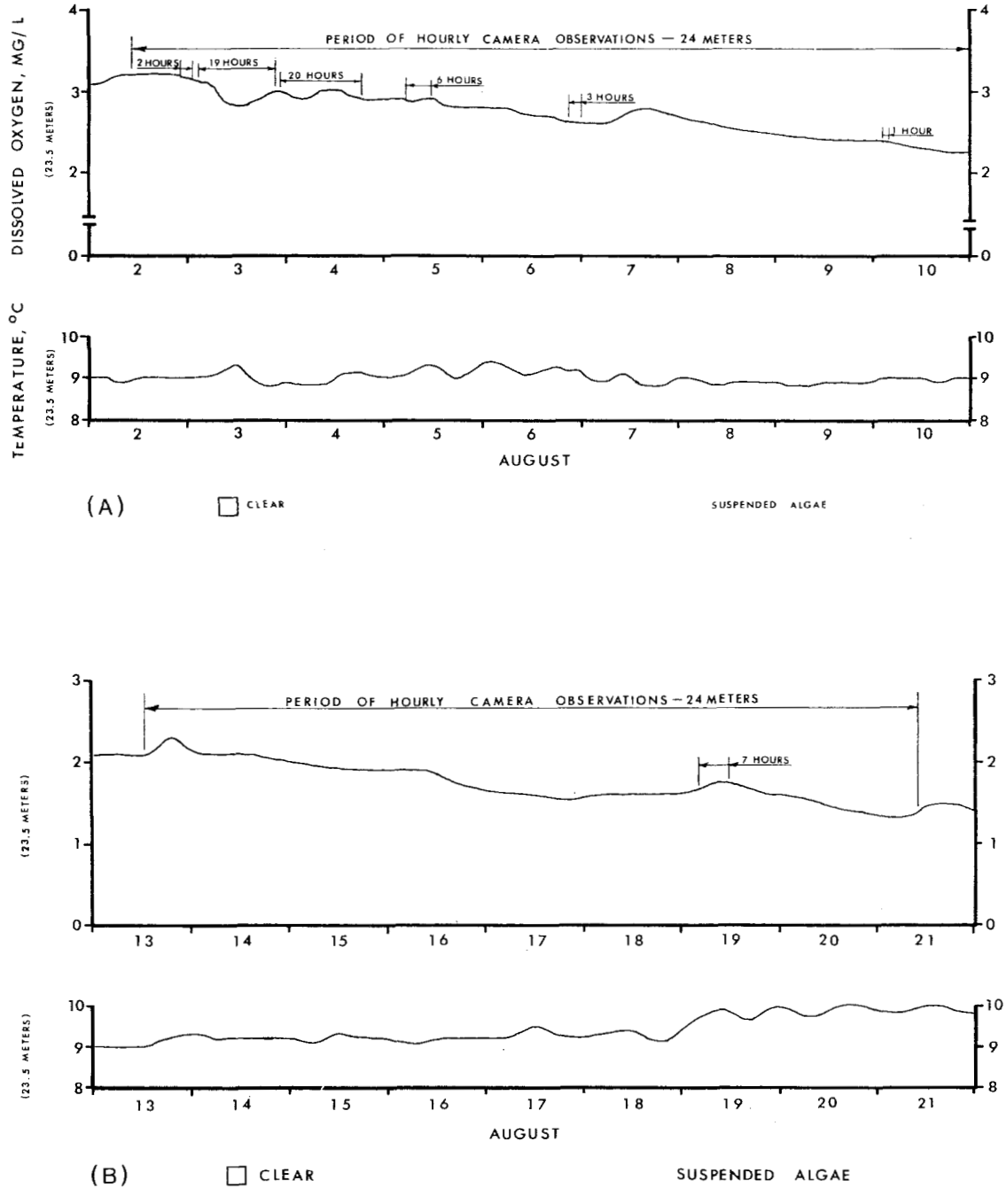

Figure 17. Hypolimnion dissolved oxygen and suspended algae observations at Station P. (A): August 2-10, 1970. (B): August 13-21, 1970.

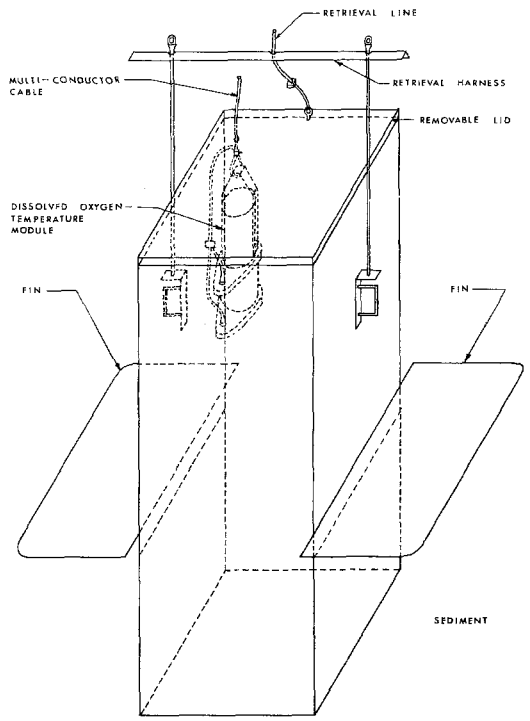

Figure 18. *In situ* **sediment oxygen demand box.**

1970. The correlation of the data is surprisingly good considering that the ratio of volume of water to sediment surface area was much smaller in the Lucas and Thomas experiments.

The depletion rate ($mg.l^{-1}day^{-1}$) in the box does not correspond to environmental depletion rates because the box is a closed system. However, the measured SOD ($gm.m.^{-2}day^{-1}$) obtained from this study should be applicable to the hypolimnion if it is assumed that the entire Central Basin sediment has a SOD approximately equal to that obtained in this experiment. The total SOD for the Central Basin would be $3.96X10^9$ gms/day ($12.3X10^7$ moles/day) based on a total sediment area of 12,697 km^2. Using the depletion rate of 0.39 gms O_2 $m.^{-2}day^{-1}$ (12.2 millimoles O_2 $m.^{-2}day^{-1}$) for the hypolimnion calculated by Burns and Ross (pg 118) an oxygen depletion rate of $4.96X10^9$ gms/day ($15.6X10^7$ moles O_2/day) is obtained.

While the agreement between the net depletion rate and the SOD uptake rate appears good, it cannot be concluded that the SOD is the depletion rate. The variety and complexity of a lake system precludes the assumption that a single parameter can define a situation.

CURRENT PATTERNS

The array of current meters set out for "Project Hypo" gave reasonably good return of data (Table 1). Current data were first converted to two-hour averages of speed and direction. Then these two-hour averages were converted to frequency histograms of speed and direction. When speed data were missing, only direction data were evaluated to compute the histograms. From each histogram (one per instrument), the dominant direction (i.e. that direction which had the highest frequency of occurrence in the data) was selected. Each frequency histogram represents data of approximately 1.5 month duration. These data are presented in Figure 20(A) for epilimnion currents and in Figure 20(B) for hypolimnion currents. The dominant current directions and range of average speeds for the direction classes are shown in Table 4.

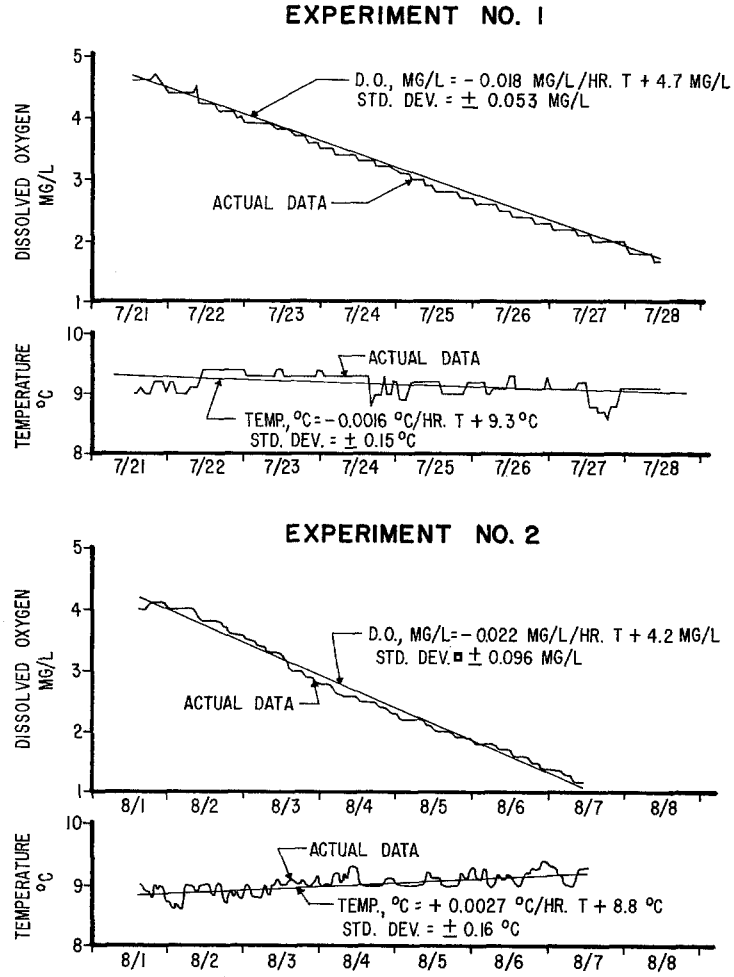

Figure 19. *In situ* **sediment oxygen demand data at Station P, 1970. Actual data were read to the nearest 0.1 mg/l and 0.1°C.**

The epilimnion circulation appears to fit the pattern of an anticyclonic (clockwise in northern hemisphere) gyre, insofar as direction is concerned. The gyre inferred here should not be confused with the nearshore currents moving easterly along the south shore (FWQA, 1968). The nearshore regime should be considered separately from the water motions associated with the deeper portions of the basin. Station U is probably within the nearshore regime described by the FWQA (1968) and would not be directly connected with the gyre. The strongest epilimnion currents occurred at station R, just off Pointe Aux Pins.

The epilimnion current meters deployed during "Project Hypo" were located in the "intermediate depth regime" defined by Hamblin (1971). The anticyclonic gyre shown in Figure 20(A) is also reflected in Hamblin's analysis of the circulation of the intermediate depth regime.

The hypolimnion circulation shows remarkable consistency with dominant flow toward the Canadian shore. This finding agrees with that of Hartley (1968). Hypolimnion currents at station R are possibly part of a return flow whose position is closely connected with Pointe Aux Pins. Unfortunately no speed data are available for the hypolimnion at station R to determine what portion of the northward hypolimnion flow is returned within the hypolimnion (as suggested by the data at station R) versus the portion that would be lost from the hypolimnion by vertical circulation at the northern boundary (i.e., upwelling).

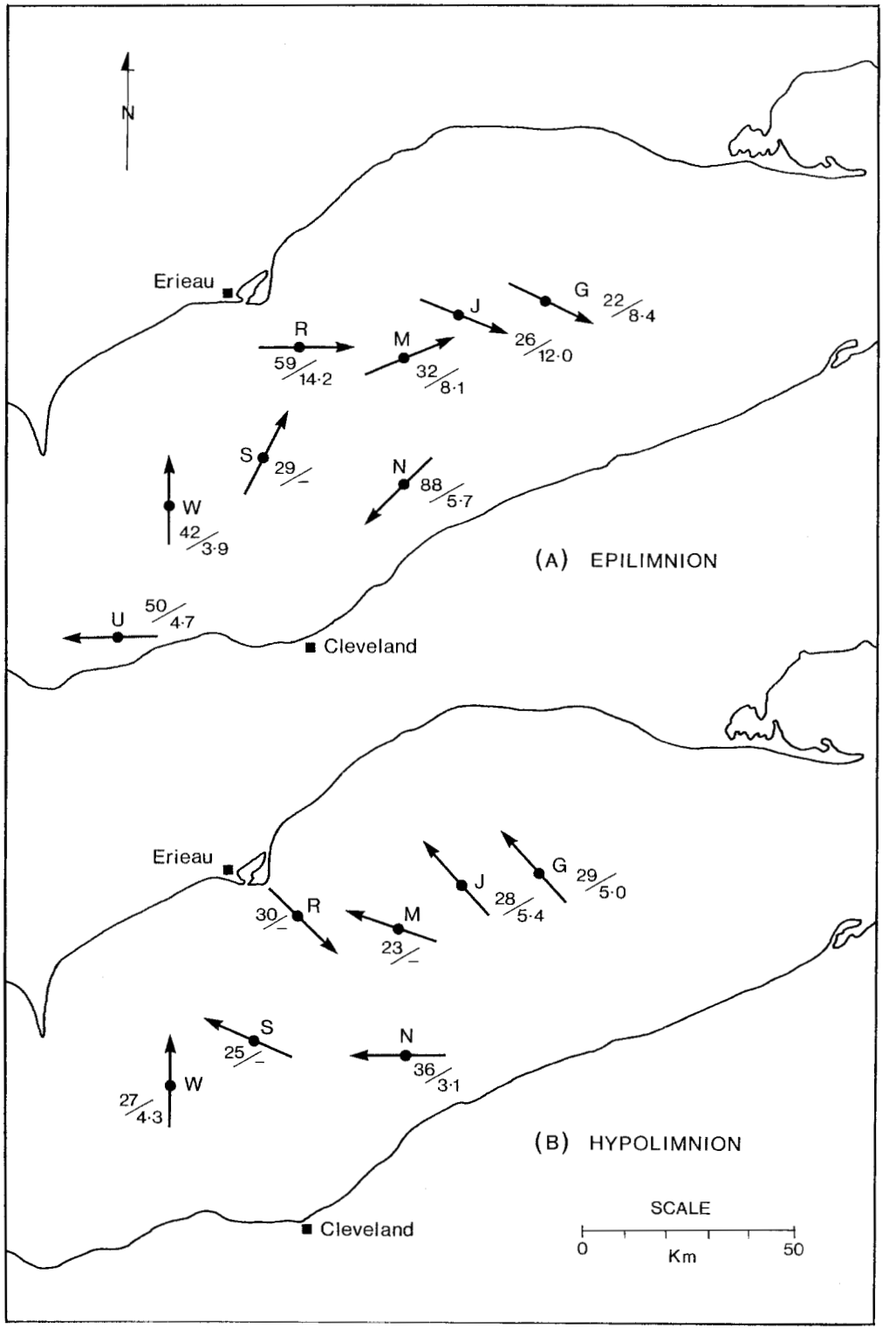

Figure 20. Lake Erie Central Basin currents during the period July 14 – September 3, 1970. (A) Epilimnion currents (B) Hypolimnion currents. The arrows represent the dominant direction toward which the currents were moving. The number to the left of the slash represents the percentage frequency of occurrence of all currents within 30° either side of the dominant direction. The number after the slash is the average speed in cm/sec. of the currents associated with the dominant direction.

TABLE 4. Summary of epilimnion and hypolimnion current (based on two-hour averages)

	Epilimnion			Hypolimnion		
	Depth (meters)	Dominant Direction	Speed Ranges** (cm/sec)	Depth (meters)	Dominant Direction	Speed Ranges** (cm/sec)
Station U						
	9.8*	W	5.6-13.4 (27.8)***			
	12.8	W	3.2- 4.8 (17.7)			
Station W						
	10.7	N	3.6- 6.0 (44.6)	20.7	N	2.7-4.7 (98.5)
Station S						
	10.0	NNE	2.9- 4.2 (19.8)	21.0	WNW	2.6-4.9 (49.5)
Station R						
	8.8*	E	5.3-17.6 (30.3)	22.0	SE	(No Speed)
Station N						
	9.4	SW	3.8- 7.4 (56.7)	21.0	W	2.2-3.3 (56.7)
Station J						
	9.0*	SSE	9.5-12.5 (29.4)	21.0	NW	3.5-5.6 (15.1)
Station G						
	9.0	SSE	5.4-10.3 (35.8)	20.4	NW	3.7-5.4 (17.7)
Station M						
	9.4	ENE	5.3- 9.7 (79.4)	22.2	WNW	(No Speed)

*Short Record, refer to Table 1
**Range in average speeds for all direction classes
***Numbers in parentheses represent maximum observed two-hour speeds.

In general, epilimnion current speeds are greater, by an order of magnitude, than hypolimnion current speeds. Fast epilimnion currents occur for a longer duration than hypolimnion currents. From two-hourly wind and current data, it is apparent that maximum wind speeds precede by less than four hours maximum current speeds in the epilimnion and hypolimnion. Hypolimnion current speeds as great as 98.5 cm/sec (Table 4) were noted. FWQA (1968) reported current speeds as great as 61 cm/sec.

DISCUSSION

The physical data obtained during "Project Hypo" emphasize the importance of the dominant southwest winds in determining the net circulation patterns observed in the Central Basin. The semi-permanent thermocline tilt, the anticyclonic epilimnion gyre, the transbasin movement of hypolimnion water and the thermocline topography are all a reflection of the dominant southwest winds and the basin topography.

HYPOLIMNION VOLUME VARIATIONS

From the data of the monthly monitor cruises of the M/V *Martin Karlsen* and the seven CSS *Limnos* surveys, reasonably good estimates of hypolimnion volume were obtained for the summer of 1970 (Fig. 21). These volumes were kindly supplied by N.M. Burns, Canada Centre for Inland Waters. On comparison of hypolimnion volume changes with the wind energy for Long Point, Ontario, periods of low wind energy followed by short bursts of high wind energy can account for the volume increases observed during the CSS *Limnos* cruises. Consider the actual volumes of water contained in the thermocline (Fig. 21). During periods of relatively low wind energy, there is insufficient energy in the epilimnion or hypolimnion to maintain a sharp thermocline. Under these conditions the thermocline thickens. If this episode is followed by a brief period of high wind energy, the turbulence induced in the epilimnion and hypolimnion erodes the top and bottom of the thermocline. This causes the thermocline to sharpen and the epilimnion and hypolimnion volumes to increase. However due to the large area to depth ratio of the Central Basin hypolimnion, a small change in thickness results in a relatively large change in volume, whereas in the epilimnion only a fractional volume change occurs. For example, from CSS *Limnos* Survey 5 to Survey 6, the thermocline volume decreased by approximately 5 cubic kilometers. This resulted in a one percent increase in epilimnion volume, whereas the hypolimnion volume increased by 10 percent.

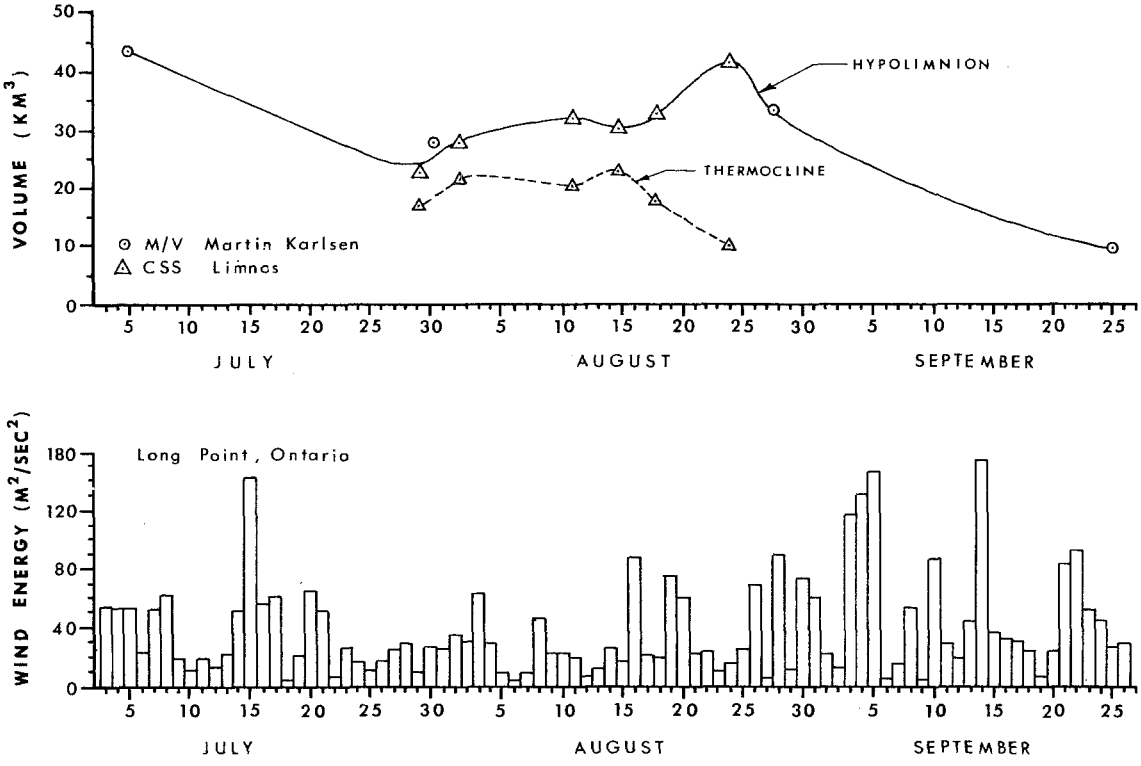

Figure 21. Correlation of wind energy at Long Point, Ontario with measured volumes of the Central Basin hypolimnion and thermocline region: summer, 1970. Wind energy data are derived from daily averages of squared speed of the mean square vector wind.

During periods of high wind energy such as those occurring in the two weeks prior to CSS *Limnos* Survey 1 and after Survey 7, the more turbulent epilimnion will entrain the less turbulent hypolimnion. This mechanism of entrainment whereby a more turbulent fluid entrains a less turbulent one has been demonstrated by theory and experiment (Phillips, 1966). Convection in late summer and early fall accelerates entrainment.

Burns and Ross (pg 122) have reported that the increase in hypolimnion volume in August effectively helped to reduce the measured depletion rate of the Central Basin hypolimnion. The beneficial consequences of downward entrainment cannot be depended upon as an annual occurrence. Given the condition of prolonged high energy winds there may not be sufficient opportunity for the thermocline to thicken. This thickening sets the stage for subsequent downward entrainment once the hypolimnion currents begin to erode the thermocline.

NORTHWEST MOVEMENT OF HYPOLIMNION WATER

Hypolimnion current measurements together with data reported by Hartley (1968) define a net northwest movement of hypolimnion water. The net movement seems clearly the result of the prevailing southwest winds. For the first time hypolimnion current speeds were actually measured.

When one compares the daily components of southwest wind at Long Point to the daily components of hypolimnion currents resolved along the dominant direction, there is fairly good correlation between the higher southwest wind speeds and the higher current speeds (Fig. 22). Since the southwest winds and the northwest hypolimnion water movement are dominant during stratification, it is important to consider what happens to this water when it reaches the Canadian shore. Three possibilities exist: (1) recirculation of the water within the hypolimnion as might be suggested by the dominant southeast direction at station R (Fig. 20(B)), (2) upwelling of the hypolimnion water near the shoreline and consequent vertical mixing with the epilimnion water, and (3) a combination of (1) and (2).

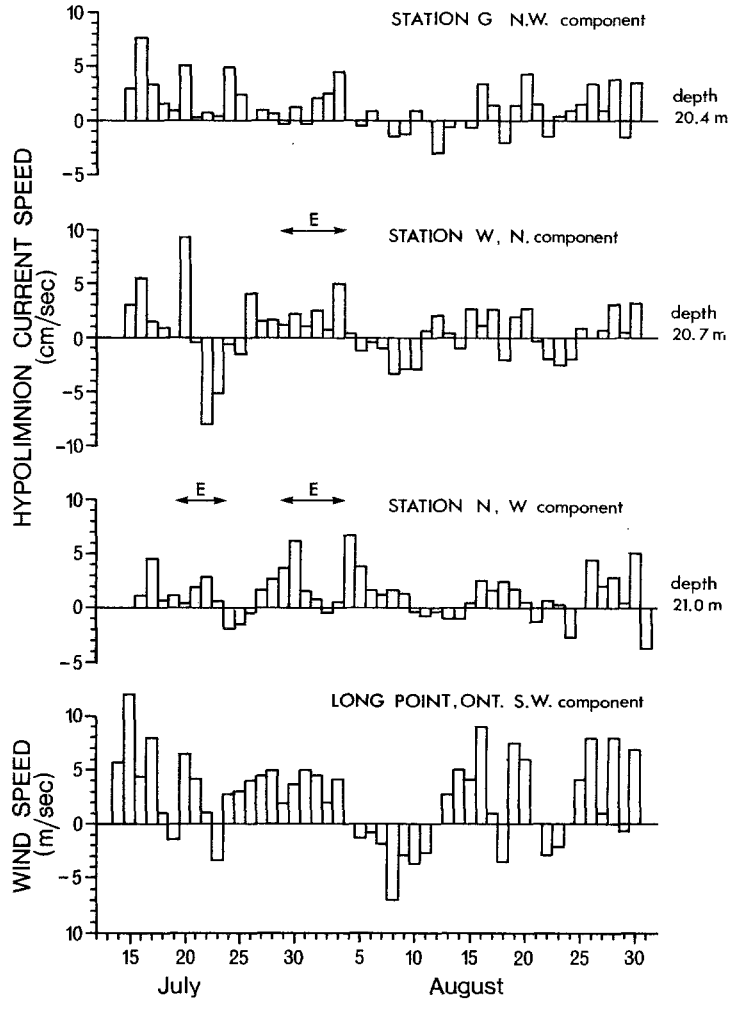

Figure 22. Correlation of daily averages of the dominant components of hypolimnion currents with the southwest wind component at Long Point, Ontario. Wind data are derived from daily means of the vector wind. E denotes periods of epilimnion intrusion.

The absence of speed data at station R precludes any accurate assessment of the first possibility. There are sufficient data concerning upwelling to estimate volumes of hypolimnion water that could be involved in upwelling episodes.

As discussed previously, from July 30 to August 3 (Fig. 12) the hypolimnion at station R moved from a depth of approximately 16 meters to within 9 meters of the surface. This represented a vertical movement of approximately 7 meters in 4.75 days, equivalent to $2X10^{-3}$ cm/sec. During this same period, the average hypolimnion currents were estimated to be approximately 2 cm/sec toward the Canadian shore. Assuming that the average hypolimnion dimensions throughout which this flow occurred were approximately 2 meters thick and 100 kilometers long, it is calculated that $4X10^3$ m^3 /sec could potentially upwell at the shore. Using the upwelling velocity calculated above, an area of approximately 200 km^2 would be required to accept the upwelled water. Areas of upwelling with dimensions comparable to this have been documented in aerial survey data reported by Richards *et al.* (1969). These relatively small areas are usually confined within several kilometers of the shore and often escape detection by monitoring cruises.

In actual upwelling zones, the hypolimnion is readily accessible to wind-induced mixing. In other words, the enriched anoxic hypolimnion water is mixed with epilimnion water and distributed in the basin. This probably accounts for many documented sightings by commercial pilots, fishermen, and scientists at EPA of profuse surface algal blooms between Pointe Aux Pins and Pelee Point, Ontario during August and early September. Also commercial fishermen consider the lake bottom in this area a repository for miscellaneous debris such as decaying algae and trash.

Simultaneous with the southwest wind induced upwelling, it is apparent that there is an intrusion of Eastern Basin water into the Central Basin via the channel near Erie, Pennsylvania. Current data obtained in the channel during the summer of 1970 were analyzed by Dr. H.S. Weiler of the Data Processing Section of CCIW. These data document episodes of intrusion of Eastern Basin water into the Central Basin during southwest winds. Using data from the same period (July 30 through August 3, 1970) when upwelling occurred along the Canadian shore, it was possible to estimate the volume of Eastern Basin inflow. Assuming the cross section of inflow to be 13 kilometers wide by 6 meters thick ($7.8 \times 10^4 m^2$) and estimating the average velocity during inflow to be 5 cm/sec, the volume transport was $4 \times 10^3 m^3$/sec. It is tempting to conclude that the two transports are equivalent, and that the upwelled water is replenished by inflow from the Eastern Basin. However, it could not be determined from these data what portion of the inflow went to the Central Basin hypolimnion and what portion went to the epilimnion. Nevertheless, it is apparent that the loss of water from the hypolimnion due to upwelling is overshadowed by an order of magnitude by the actual rate of volume changes of the hypolimnion (Fig. 21) during the same period. Therefore neither upwelling nor inflow from the Eastern Basin can apparently account for the measured volume changes.

A vertical entrainment model was used by Burns and Ross (pg 90) to predict hypolimnion temperatures. Their predictions agreed within 0.5°C of the observed hypolimnion temperatures. Based on this agreement and the fact that their model did not include advection into or out of the hypolimnion, it is concluded that advection did not have a significant role in the measured hypolimnion volume changes during the period of the intensive study.

CONCLUSIONS

1. Periods of low wind energy followed by brief periods of high wind energy can account for hypolimnion volume increases observed during "Project Hypo". This cycling of wind energy cannot be depended upon as an annual occurrence. Given conditions of long duration high energy winds with few intervening calm periods, hypolimnion oxygen entrainment from above would be minimal resulting in the hypolimnion becoming anoxic at an unprecedented rate.

2. The net hypolimnion water movement is the result of the dominant southwest winds. This situation causes the Canadian nearshore areas, east of Pointe Pelee, to be a potential staging area for profuse algal blooms caused by the accumulation of nutrient-rich anoxic water in upwelled areas.

3. Dissolved oxygen depletion rates as determined from *in situ* monitor data confirm the long-term trend of increasing rate of depletion.

4. Measured hypolimnion dissolved oxygen fluctuations solely attributable to the presence of algae were not detected.

5. The sediment oxygen demand could conceivably account for the measured hypolimnion oxygen depletion rate. However, due to the variety and complexity of the lake system, it cannot be assumed that this single parameter can define a situation.

ACKNOWLEDGEMENTS

The authors wish to thank the scientific and operational staffs of CCIW and U.S. EPA, Region V, Ohio District Office, Fairview Park, Ohio for their efforts in carrying out the field work and for

processing the overwhelming quantity of data. Particular appreciation is extended to N.M. Burns and C. Ross for exchanging with the authors their findings and conclusions. The authors also thank B.G. Constantelos for his contribution to the report concerning the sediment oxygen demand.

REFERENCES

CARR, J.F. 1962. Dissolved oxygen in Lake Erie, Past and Present. *In* Proc. 5th Conference on Great Lakes Research, Great Lakes Research Division, Pub. No. 9, University of Michigan, pp. 1 – 14.

FEDERAL WATER POLLUTION CONTROL ADMINISTRATION, 1968. Lake Erie environmental summary: 1963-1964. U.S. Department of the Interior, Great Lakes Region Publication, 170 p.

FISH, C.J. *et al.* 1960. Limnological survey of eastern and central Lake Erie. U.S. Fish and Wild. Serv. Spec. Sci. Rept. – Fish. No. 334, 198 p.

GAUL, R., J. SNODGRASS, and D. CRETZLER, 1963. Some dynamical properties of the Savonious rotor current meter. *In* Marine Sciences Instrumentation, Vol. 2, Instrumentation Society America, Plenum Press, New York.

HAMBLIN, P.F. 1971. Circulation and water movement in Lake Erie. Inland Waters Branch, Canadian Department of Energy, Mines and Resources, Scientific Series No. 7, 49 p.

HARTLEY, R.P. 1968. Bottom currents in Lake Erie. Proc. 11th Conf. on Great Lakes Res., Inter. Assoc. Great Lakes Res., pp. 398-405.

PHILLIPS, O.M. 1966. The Dynamics of the Upper Ocean. Cambridge University Press, Cambridge, Mass.

RICHARDS, T.L., J.G. IRBE and D.G. MASSEY, 1969. Aerial surveys of Great Lakes water temperature: April, 1966 to March, 1968. Meteorological Branch, Canadian Department of Transport Climatological Studies No. 14, 30 p.

THOMAS, N.A., 1963. Oxygen deficit rates for the central basin of Lake Erie. *In* Proc. 6th Conf. on Great Lakes Research, Great Lakes Res. Div. Pub. No. 10, Univ. of Michigan, p. 133. (Abstract only).

4. *An Investigation of Diffusion Characteristics of the Hypolimnion of Lake Erie*

C.R. Murthy
Canada Centre for Inland Waters
Burlington, Ontario, Canada

A dye patch diffusion experiment was carried out in early August to study large scale diffusion characteristics of hypolimnion waters in central Lake Erie. Experimental data were obtained by fluorometric sampling, to define the peak concentration, horizontal and vertical spread of the dye patch at different times. The vertical spread of the patch was restricted to the hypolimnion because of the strong thermocline. The horizontal spread was an order of magnitude less, corresponding eddy diffusivity two orders of magnitude less, and the observed peak concentration was two orders of magnitude greater compared to surface layer diffusion for comparable time scales of the order of 60 hours.

INTRODUCTION

Diffusion experiments in the past have been largely carried out in the surface layers of the oceans and lakes, and a fairly large amount of data has been collected from these experiments. In spite of the practice of discharging effluents at some distance offshore using submarine outfalls, very few diffusion experiments have been conducted in deep water or in the thermocline region. The reason for this lies in the practical difficulties of carrying out diffusion experiments in deep water. In this paper a practical method

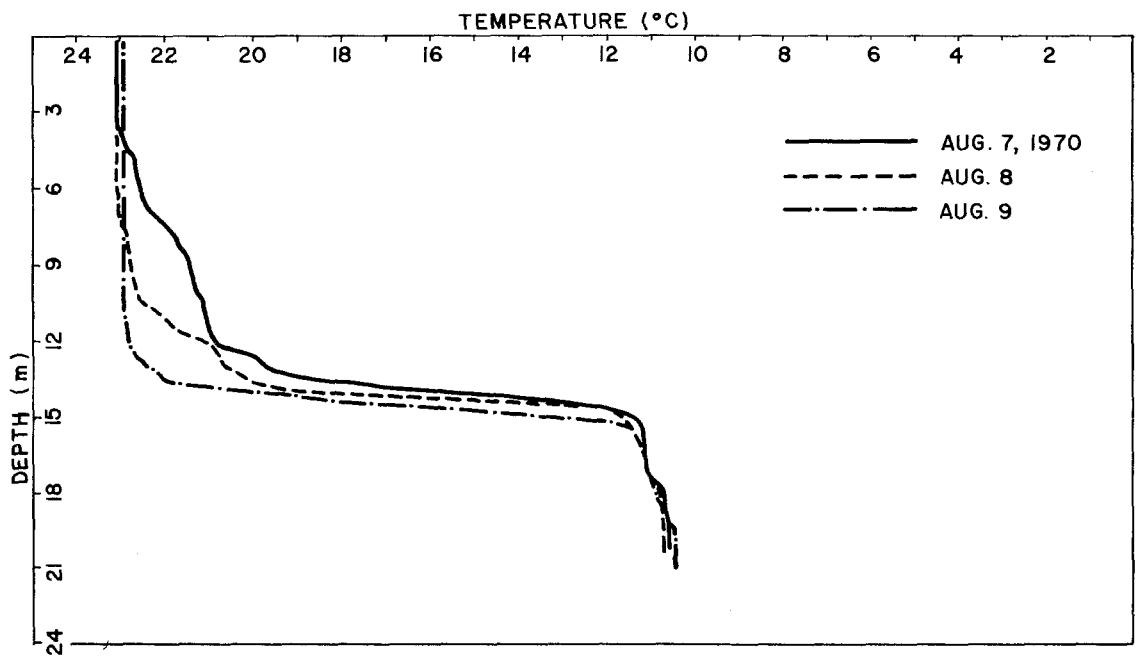

Figure 1. Temperature vs. depth profiles near Erieau, Lake Erie.

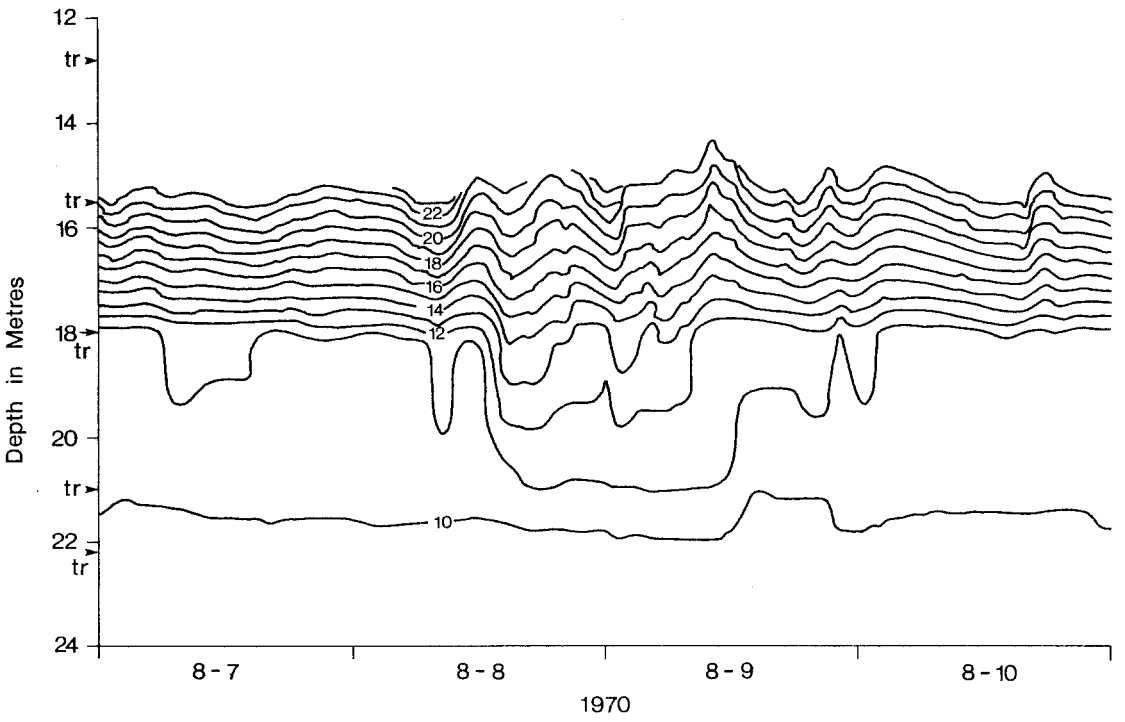

Figure 2. Thermal structure off Erieau, based on a time series from four temperature recorders.

to conduct dye diffusion experiments in deep water as well as some interesting results on the horizontal and vertical dispersion characteristics of hypolimnion waters of Lake Erie Central Basin are described.

EXPERIMENT

In mid-summer central Lake Erie has a well-mixed warm surface layer, a strong thermocline 2-3 m thick with a temperature drop of 8-10°C and a well-mixed hypolimnion of 4-6 m. Figure 1 shows typical temperature profiles taken in early August illustrating the above situation. This structure was also fairly stable during the experiment (Figure 2). A dye release experiment was designed to study the diffusion characteristics of the hypolimnion waters.

A slug of water soluble rhodamine B dye preadjusted to a specific gravity of 1.00 by mixing with methanol was released instantaneously in the hypolimnion waters, 10 km off Erieau, using a specially devised system. The sampling of the dye patch thus formed was accomplished by the continuous flow fluorometric technique.

The dye source was prepared on the day of the experiment using the facilities of the ship C.S.S. LIMNOS, which was also available for later sampling of the dye patch. Fifty gallons of dye was pumped into a plastic bag, the closed end of which was tied to a concrete block with a 2 m line. The plastic bag was held clear of the ship. On completion of the filling, the open end was tied together and an inflated car inner-tube with a 1 m long line was used to hold the plastic bag in position. The dye source so prepared was then towed by a small boat to the area of the dye release and lowered to the bottom of the lake by a long line tied to the concrete block. The configuration of the dye source *in situ* is shown in Figure 3. The dye source was placed mid-way in the hypolimnion, which extended from 14 m down to 20 m. A diver released the dye by carefully cutting the plastic bag with a sharp knife. Immediately after dye release, deep drogues set at 10, 15, 16 and 17 m were released in the vicinity to indicate the approximate location of dye patch at later times.

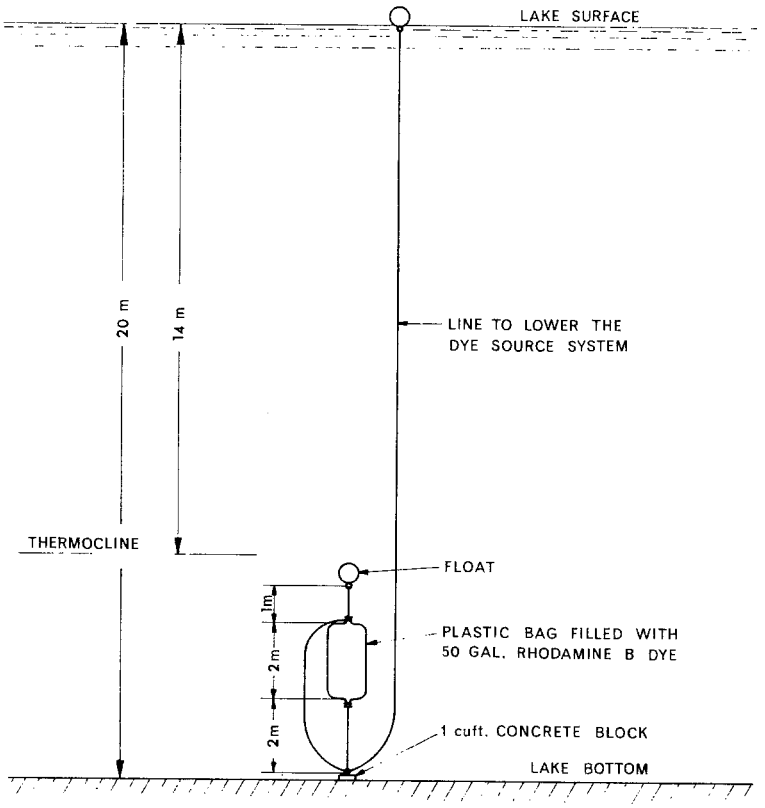

Figure 3. Dye source configuration.

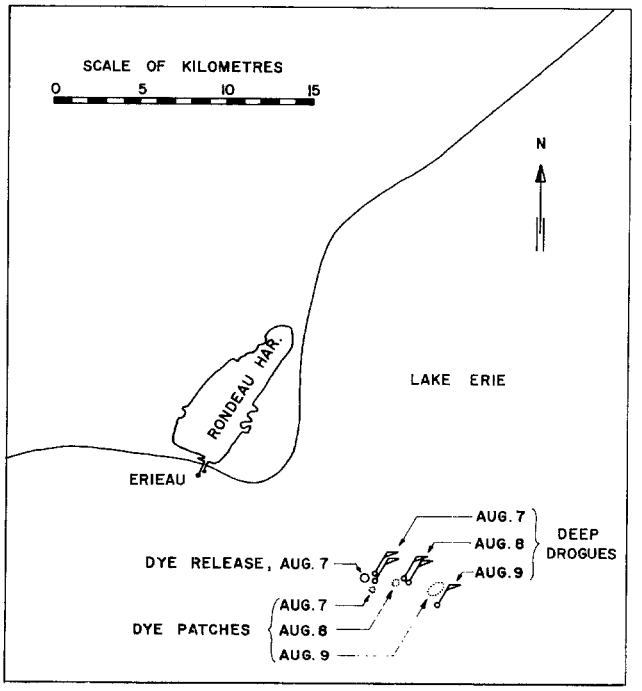

Figure 4. Movements of the dye patches and drogues.

The sampling system consisted of a "Jacuzzi" submersible pump which sampled through a 5/8-inch hose, an EBT (electronic bathythermograph) to control the depth of sampling and a support cable attached to a 400 lb. weight. The entire assembly was suspended from a pulley block and operated by a powered hose reel and winch arrangement. The sampling system had a lag time of 90 secs. and this was not considered serious since at each depth, samples were drawn over a period of 6 mins.

The experiment was conducted from August 7-9, 1970, as a coordinated program of "Project HYPO". Figure 4 shows some details of the experiment.

SAMPLING

Locating and sampling the submerged dye patch was considerably complicated and often frustrating, the only clue being the positions of the deep drogues released with the dye. A systematic procedure was adapted in order to achieve detailed sampling of the diffusing dye patch. In order to locate the dye patch precisely, the positions of the deep drogues were plotted on an enlarged map of the area. Then a grid large enough to include the drogues and possibly enclose the entire dye patch was established on this map. This grid, which was used for precise navigation of the ship during sampling consisted of north-south and east-west lines equally spaced 1/4 nautical mile (~463 m) apart. With the grid established, an attempt was made to contact the dye patch fluorometrically, first at the centre of the grid and then moving away from the centre following the grid lines. The sampling itself consisted of taking vertical concentration profiles at the intersection of grid lines. This procedure, although tedious and time consuming, was a practical and convenient way to locate and sample the submerged dye patch systematically.

Due to a number of unforeseen field problems including equipment failure, detailed sampling of the dye patch was not possible on August 7 and 8. However, on August 9 extensive sampling was carried out and the entire dye patch covered. A typical vertical concentration profile taken on August 7, 12 hours after dye release is shown in Figure 5. Further examples of vertical concentration profiles collected systematically on August 9, about 60 hours after dye release and a corresponding horizontal distribution of the observed peak concentration along the patch are contained in Figure 6. From a number

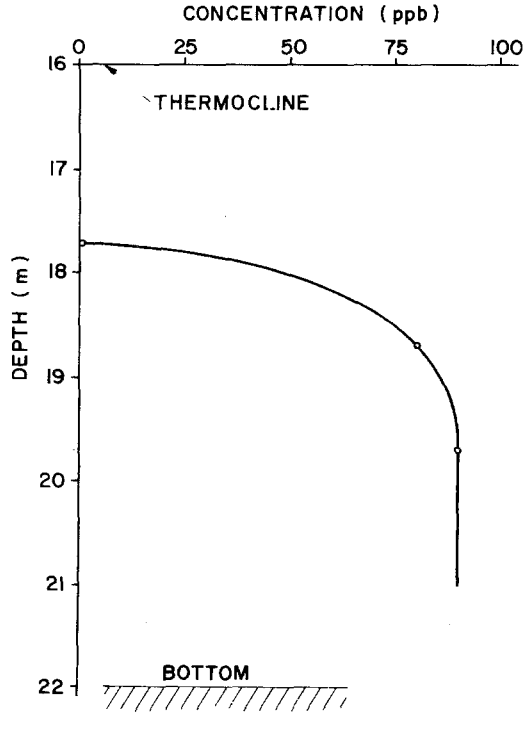

Figure 5. Typical vertical concentration profile.

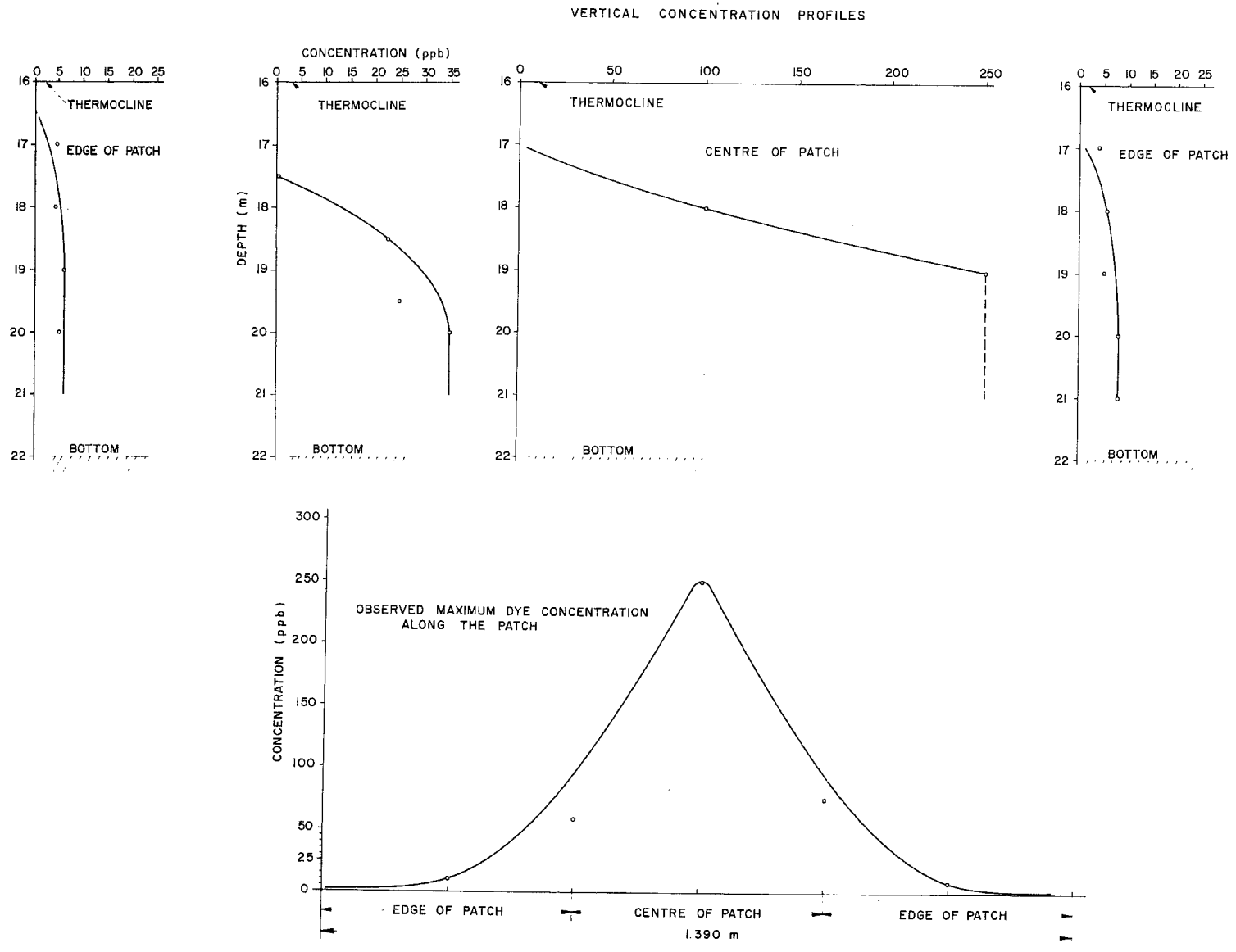

Figure 6. Four vertical concentration profiles (top) and the observed maximum dye concentration horizontally through the patch (bottom).

TABLE 1. Comparison of dispersal characteristics between the hypolimnion of Lake Erie and the surface layer of Lake Ontario.

	Project HYPO (L. Erie) (Hypolimnion)	Project MELON (L. Ontario) (surface layer)
Mean current (U)	2 cm/sec	10-15 cm/sec
Horizontal spread (S)	1.4 km	15 km
Eddy diffusivity (K_H)	10^3 cm^2/sec	10^5 cm^2/sec
Peak concentration (C_P)	250 ppb	6 ppb

of vertical concentration profiles collected systematically within the grid, it was possible to define the characteristics of the diffusing dye patch such as its horizontal and vertical spread, and the peak concentration.

RESULTS

A number of interesting results may be derived from the rather limited data available from the experiment.

(a) The dye patch drifted with the lake currents 3 km or so from its initial position during 60 hours of the experiment (see Figure 4). The bottom current estimated from the displacement of the dye patch and deep drogues was typically 2 cm/sec.

(b) The vertical spread was restricted to the hypolimnion waters since the strong thermocline acted as an almost impermeable barrier for upward vertical mixing. Consequently the measured vertical concentration profiles were regular (Figures 5 and 6).

(c) The horizontal spread of the dye patch was surprisingly small, 1400 m or so in 60 hours of experiment, at least an order of magnitude less compared to surface layer diffusion for comparable time scales and the corresponding eddy diffusivity was of the order of 10^3 cm^2/sec., two orders of magnitude smaller (Figure 5 and Table 1).

(d) As a consequence of restricted vertical mixing and poor horizontal dispersion, much higher peak concentration ($\sim$ 250 ppb) was observed. This peak was two orders of magnitude greater compared to those associated with surface layer diffusion for comparable time scales.

CONCLUSIONS

Considering that only one experiment was conducted and even in that, detailed data was not forthcoming, it is difficult to draw any firm conclusions. However, the results raise an important practical question in regard to the possibility of discharging effluents at lake bottom using offshore submarine outfalls.

By discharging the effluents through an offshore outfall placed at the lake bottom, at some distance say 2-3 km from shore, the entire water column is available for dispersing the effluents. But during summer the discharge is normally below the thermocline and the effluents are most probably trapped below the thermocline with very little transport and mixing. With shoreward transport of the concentrated submerged effluent field and the possibility of occasional upwellings, very high concentrations may be brought to the surface close to the shoreline. Doubtless such conditions are unfavourable although there is a good possibility of dispersing effluents effectively due to intensive vertical mixing associated with upwellings. Just how frequently such shoreward transport and upwellings occur in different locations of the shoreline and whether indeed the mixing is adequate under such conditions is difficult to say without some concrete experimental evidence.

5. Sediment Oxygen Demand in Lake Erie's Central Basin, 1970

A.M. Lucas and N.A. Thomas
Environmental Protection Agency
Division of Field Investigations, Cincinnati
Cincinnati, Ohio, U.S.A.

Sediment oxygen demand (SOD) rates were measured at five locations in Lake Erie's Central Basin in June, August and September, 1970. The rates were determined from changes in the dissolved oxygen concentration of water sealed and circulated within black and clear plexiglass chambers imbedded in the lake bottom. SOD rates recorded in June varied from 1.2 to 2.2 gm O_2 $m.^{-2}day^{-1}$ and were indicative of eutrophic conditions. In August, rates measured during the daylight hours with the clear chamber (0.0 – 0.4 gm $O_2 m.^{-2}day^{-1}$) were less than those measured at night with the clear chamber or during the day with the black chamber (0.7 – 1.0 gm O_2 $m.^{-2}day^{-1}$). Oxygen produced by the photosynthetic activity of algae on the lake bottom offset the SOD during part of the day resulting in daily SOD rates of 0.4 to 0.7 gm O_2 $m.^{-2}day^{-1}$. Rates measured in September with oxygenated surface water trapped and carried to the bottom in the chambers ranged from 1.0 to 2.4 gm O_2 $m.^{-2}day^{-1}$.

INTRODUCTION

The sediment oxygen demand (SOD) was measured at six locations in the Central Basin of Lake Erie (Figure 1) as part of "Project Hypo". To investigate the magnitude of the SOD and its relation to the accelerated late summer oxygen depletion of the hypolimnion of the Central Basin, measurements were made seasonally (May – September) and diurnally.

Sediment oxygen demands usually result from the decomposition of organic materials which accumulate over a period of time. The decomposition rate of these sediments is low during the winter because of low water temperatures and SOD rates are correspondingly low. In the spring and early summer when temperatures are increasing and dissolved oxygen (DO) is at its maximum, the SOD rates are usually at their maximum. Although decomposition rates increase as summer progresses and temperatures increase, SOD rates usually decrease because of the loss of oxidizable sediments from decomposition which occurred in spring and early summer. However, a renewal of the supply of benthic organic materials during the summer months could cause the SOD rates to remain at or exceed the level of the springtime SOD rates.

The loss of DO in the hypolimnion has been theorized to result from the settling of dead algae from the surface waters to the bottom of a lake, creating a sediment oxygen demand (Hutchinson, 1957). In stratified lakes the oxygen demand of bottom materials is usually extremely critical because there is no renewal of oxygen resources beneath the thermocline. Upon reaching the thermocline, organic materials rapidly settle to the bottom because of reduced water currents. There they decompose using dissolved oxygen. Depletion of DO in the hypolimnion is usually gradual over the period of stratification.

In Lake Erie's Central Basin however, DO depletion does not follow the expected pattern of a gradual DO withdrawal during the entire period of stratification. The SOD does not decrease but increases in late summer to deplete the DO resources of the hypolimnion. Other workers have theorized (Kleveno *et al.*, 1971) that this increased demand results from the resuspension of sediments (which can increase oxygen demand by a factor as high as ten) or from the death and decomposition of viable benthic algae.

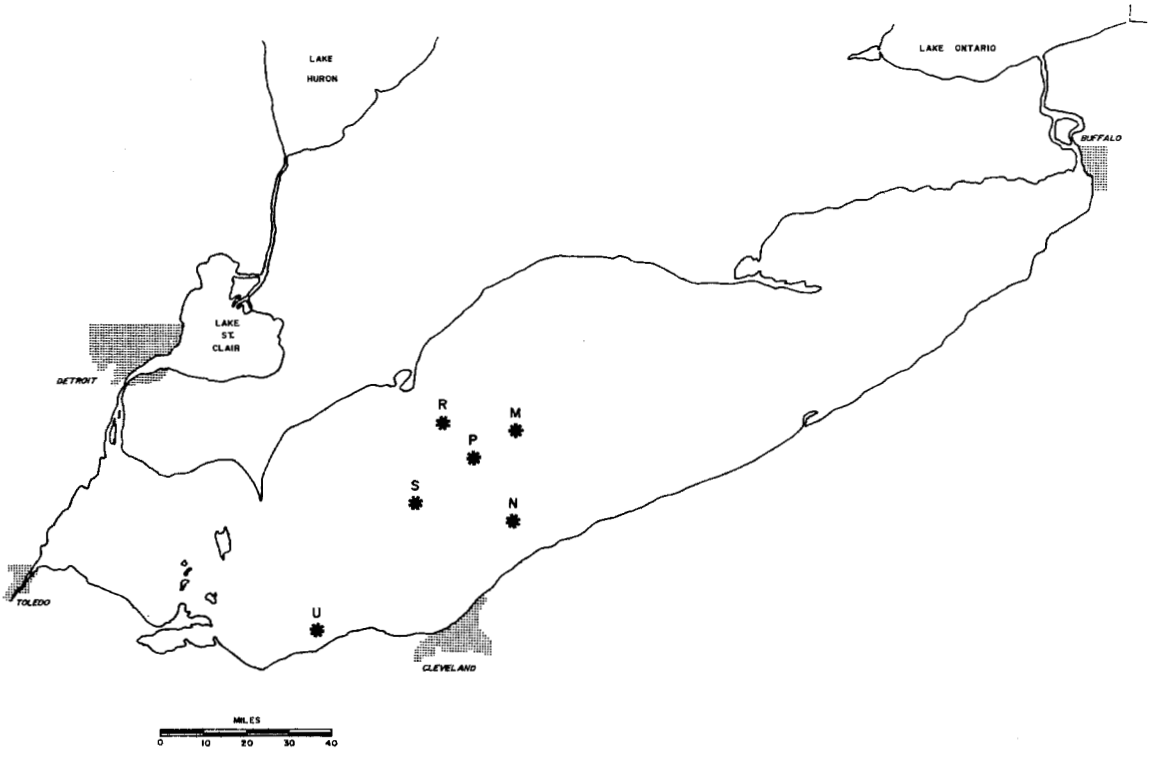

Figure 1. Sediment oxygen demand recording locations, Lake Erie, 1970.

METHOD

Sediment oxygen demand rates were estimated from changes in the DO concentration of water sealed in black and clear plexiglass chambers (Figure 2). Prism-shaped chambers were constructed to maximize the ratio of bottom area to volume and still have the circulating systems at a sufficient distance from the bottom to prevent riling of the bottom sediments. Each chamber was set on a bias to allow gases to collect at one corner and escape through a check valve. The chambers were bolted to stainless steel flanges and cutting edges which effectively sealed the water within the chambers when they were lowered onto soft bottom sediments. Because of the extremely soft bottom in Lake Erie, wider masonite flanges were added to prevent the chambers from sinking into the sediments. Each chamber covered 0.25 square meter of bottom and held 12 liters of water. Water in the chambers was cirulated with attached 12-volt submersible pumps. To determine the effectiveness of the seal, salt was introduced into the system to raise the specific conductance within the chamber above the ambient conductance. The increased conductivity was then monitored during the test run. Changes in DO were measured and recorded with a portable recording DO meter.

Dissolved oxygen concentration changes were sufficient in one-half to one hour to estimate the SOD. Test runs with both clear and black chambers extended from before sunrise to noon and from late afternoon to dark in August to estimate changes in SOD resulting from the response of the algae (see Fig. 3) to sunlight. To minimize riling of bottom sediments, the chambers were carefully lowered onto the bottom. An estimate of the amount of riling of the benthic materials was made by stopping the pumps before removing the chambers from the bottom and examining the water trapped in the chamber plumbing. Visual observations of the conditions within the clear chamber on the lake bottom were made by divers.

The SOD rate can be calculated on an areal basis from the following formula:

$$S.O.D. = \frac{(Ci - Cf)\,V}{t\,A}$$

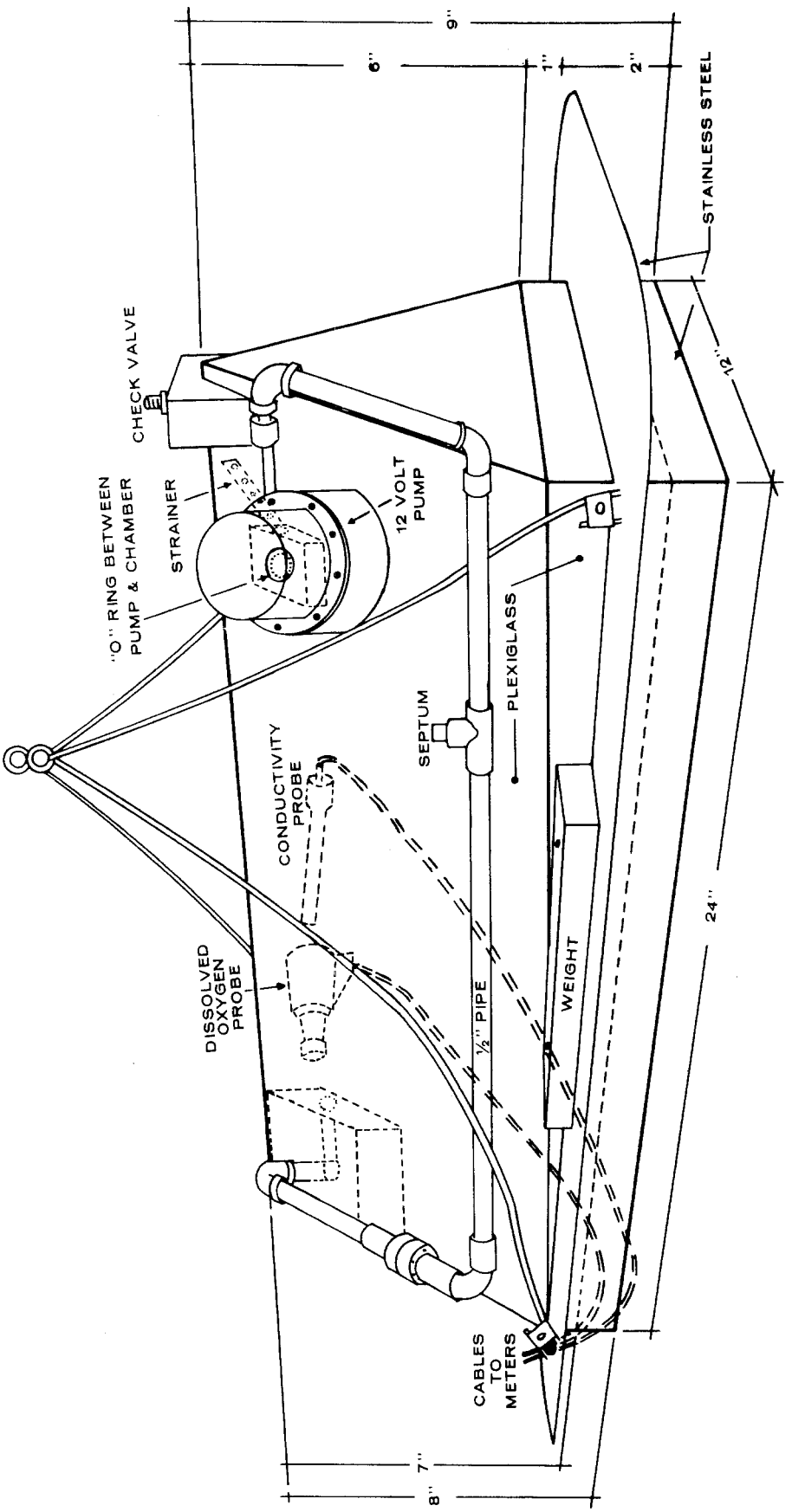

Figure 2. Sediment oxygen demand chamber.

where:

S.O.D. = sediment uptake rate in gm O_2 $m.^{-2}$ day^{-1}
V = volume of confined water in m^3 (.012)
A = bottom area within chamber in m^2 (.186)
t = test period in days
Ci = initial measured DO of chamber in mg/1
Cf = final measured DO of chamber in mg/1

This formula applies to situations where benthic sediment demands are not affected by photosynthesis. When photosynthesizing algae or rooted aquatic plants are present, an integrated rate incorporating the oxygen contribution by the plants must be calculated. Daily integrated rates in August were determined polarographically from a diurnal curve developed from rates obtained at Stations P and R (Figure 3). The daily integrated SOD rates take into account both the gross oxygen demand rates (measured with the dark chamber or with the clear chamber at night) and the reduced oxygen demand rates (measured with the clear chamber when oxygen produced by plants is partially satisfying the gross oxygen demand). At Station P, for example:

Dark chamber (gross) SOD rate = 0.8 mg O_2 $m.^{-2}$ day^{-1}
Clear chamber (reduced) SOD rate = 0
Daily integrated (net) SOD rate = 0.4 mg O_2 $m.^{-2}$ day^{-1}

In September, measurement of SOD rates was affected by the lack of DO in the hypolimnion. Surface water containing some DO was trapped within the chambers while they were lowered to the bottom.

RESULTS AND DISCUSSION

Depletion of DO from the hypolimnetic waters of Lake Erie's Central Basin was caused primarily by the oxygen demand of bottom sediments since the biochemical and chemical oxygen demand of these waters when separated from any interaction with the sediments was found to be too small to explain the observed oxygen depletion rates, i.e., the oxygen demand of the hypolimnion water* was too

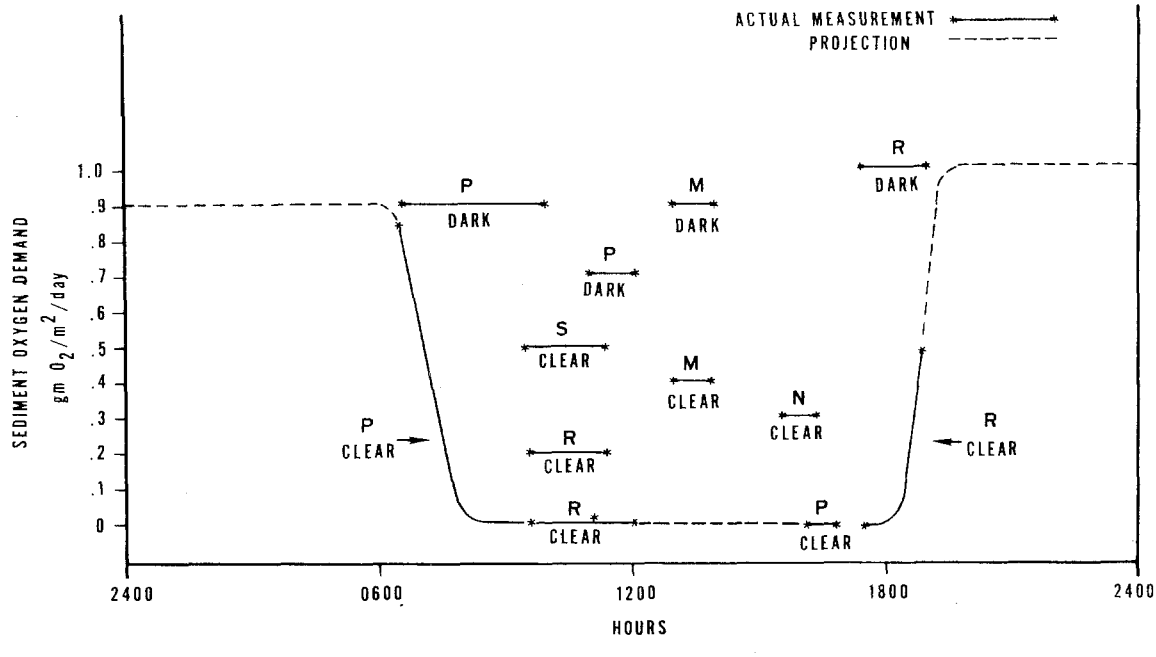

Figure 3. Sediment oxygen demand measurements, Central Basin, Lake Erie August 4-7, 1970.

*Unpublished data, U.S. Environmental Protection Agency, Region V, Fairview Park, Ohio.

Table 1

BENTHIC OXYGEN DEMAND STUDY

LAKE ERIE

1970

Station	Date	Times	Temperature in Hypolimnion	D.O. in Hypolimnion	D.O. in Chamber	Rate, gm O_2/m^2/day	Chamber and Bottom Conditions
			°C	mg/l	mg/l		
U	May 4	1040 – 1120	9.0	13.0	13.0	3.9	Black chamber; stirred condition not known
U	June 18	1000 – 1030	13.7	3.8	3.7	9.3-31	Clear chamber; stirred
S	June 15	1315 – 1650	9.0	8.0	8.5	1.2	Clear and black chambers; not stirred
S	Aug. 5	950 – 1130	11.0	2.8	3.0	0.5	Clear chamber; slightly stirred
S	Aug. 5	950 – 1100	11.0	2.8	3.0	5.6	Black chamber; stirred
S	Aug.		11.0	2.8	–	0.7	Integrated daily rate
S	Sept. 1	1350 – 1440	12.0	0	4.2	2.4	Black chamber; slightly stirred
R	June 16	1040 – 1135	9.0	8.7	8.2	1.4	Black chamber; not stirred
R	June 16	1040 – 1140	9.0	8.7	8.2	1.8	Clear chamber; not stirred
R	June 15	1900 – 2000	9.0	8.7	8.2	1.4	Black chamber; not stirred
R	Aug. 4	945 – 1100	9.5	2.8	2.4	0.0	Clear chamber; not stirred
R	Aug. 6	1730 – 1900	9.5	2.8	3.0	1.0	Black chamber; not stirred
R	Aug. 6	1730 – 1830	9.5	2.8	3.0	0	Clear chamber; not stirred
R	Aug. 6	1830 – 1900	9.5	2.8	3.0	0.5	Clear chamber; not stirred
R	Aug.		9.5	2.8	–	0.5	Integrated daily rate
R	Sept. 1	900 – 930	11.0	0.05	0.6	1.4	Black chamber; moderately stirred
P	June 16	1330 – 1430	8.0	7.4	7.0	1.2	Clear chamber; slightly stirred
P	June 16	1320 – 1420	8.0	7.4	7.0	1.7	Black chamber; slightly stirred
P	Aug. 4	1600 – 1700	9.1	3.0	3.0	0.0	Clear chamber; not stirred
P	Aug. 6	1100 – 1215	9.1	3.0	3.2	0.7	Black chamber; not stirred
P	Aug. 6	1100 – 1200	9.1	3.0	3.2	0.0	Clear chamber; not stirred
P	Aug. 7	620 – 800	9.1	3.0	3.0	0.9	Black chamber; not stirred
P	Aug. 7	620 – 700	9.1	3.0	3.0	0.9	Clear chamber; not stirred
P	Aug. 7	800 – 1045	9.1	3.0	2.6	0	Clear chamber; not stirred
P	Aug.		9.1	3.0	–	0.4	Integrated daily rate
P	Sept. 5	1100 – 1150	12.0	0.1	1.8	1.3	Black chamber; not stirred
N	June 16	1700 – 1815	8.5	8.7	8.8	2.2	Clear chamber; slightly stirred
N	Aug. 5	1550 – 1650	13.5	2.5	2.8	0.3	Clear chamber; not stirred
N	Aug.		13.5	2.5	–	0.6	Integrated daily rate
N	Sept. 2	1300 – 1400	13.9	0	0.5	1.0	Black chamber; slightly stirred
M	Aug. 6	1440 – 1600	9.7	3.0	3.2	0.9	Black chamber; not stirred
M	Aug. 6	1440 – 1600	9.7	3.0	3.2	0.4	Clear chamber; not stirred
M	Aug.		9.7	3.0	–	0.6	Integrated daily rate
M	Sept. 2	1600 – 1740	10.8	0.1	1.7	1.2	Black chamber; slightly stirred

low to account for the observed oxygen depletion rates. The average SOD rate for all stations in June was 1.6 gm O_2 $m.^{-2}$ day^{-1} (Table 1). This is a moderately high rate for lake sediments in that eutrophic lakes have oxygen demand rates in excess of 0.3 – 0.5 gm O_2 $m.^{-2}$ day^{-1} (Hutchinson, 1957). A rate of 2.2 gm O_2 $m.^{-2}$ day^{-1} measured at Station N indicates the presence of additional oxygen consuming materials which had accumulated in that area of the basin.

In early August, the SOD had a diurnal pattern. At Station P the rate was zero during part of the daylight hours while at night the rate was 0.8 gm O_2 $m.^{-2}$ day^{-1}. The diurnal fluctuation in the SOD could have only been caused by the photosynthetic activity of plant life. Either surface algae remained viable after they settled to the bottom or algae were growing on the lake bottom. At this time of the year, light penetration to the lake bottom was of greatest daily duration permitting any plant life on the bottom to photosynthesize and produce oxygen. These algae did not increase the DO concentration in the hypolimnion; however, they did partially offset the SOD.

An integrated SOD rate which incorporates diurnal fluctuations in oxygen uptake more nearly represents the actual daily SOD during early August. At Station P the integrated rate based on a diurnal curve (Figure 3) was 0.4 gm O_2 $m.^{-2}$ day^{-1}.

Tests conducted at Station P indicated that prior to sunrise on August 7 the SOD rates obtained with the clear and black chambers were similar. As the light intensity increased (0630 hours) the SOD in the clear chamber decreased, indicating a positive response of the algae to light. The SOD in the black chamber remained constant. Between 0800 and 1000 hours the clear chamber was reduced to zero. SOD measurements made with the clear chamber on August 4 from 1600-1700 hours showed that the SOD rate was zero. Results from these tests at Station P indicated that throughout most of the daylight hours the SOD rate was zero.

On August 6 at Station R the SOD rate was zero in the clear chamber from 1730-1830 hours. During the next 30 minutes, under approaching darkness, the SOD rate increased to 0.5 gm O_2 $m.^{-2}day^{-1}$. During the same period the black chamber had a rate of 1.0 gm O_2 $m.^{-2}day^{-1}$. A difference in the clear and black chamber rates was also observed at Station M. Measurements conducted on August 6 from 1440-1600 hours yielded SOD rates of 0.4 and 0.9 gm O_2 $m.^{-2}day^{-1}$ in the clear and black chambers, respectively.

Integrated daily SOD rates in August ranged from 0.4 to 0.7 gm $O_2 m.^{-2}day^{-1}$ at the five recording stations (Table 1). Because no meaningful dark chamber rates were obtained at Stations S and N, integrated daily SOD rates were calculated with the assumption that the gross SOD rates at these two stations were similar to those measured at the other stations (0.9 gm O_2 $m.^{-2}day^{-1}$).

The reduction of the SOD during daylight hours in August resulted from the production of oxygen by the algae in sufficient quantity to partially offset the oxygen demand of the sediments. At that time, part of the oxygen demand resulted from the respiration of viable algae. The combined respiration of the algae and bacteria on the lake bottom (gross SOD) was still less than the SOD in June. This would indicate either that some of the sediments had been oxidized during June and July thus reducing the oxygen demand, or that benthic algae which covered the sediment were inhibiting oxygen transfer across the mud-water interface. The reduction in the SOD was still insufficient to prevent the depletion of dissolved oxygen in the hypolimnion; however, it did extend the time to depletion to the end of August.

Although the DO in the hypolimnion was near zero in early September, measurements of SOD rates with oxygen-containing surface water trapped in the chambers did indicate that a high SOD may have occurred immediately prior to this period. In September the measured SOD rates (1.0 – 2.4 gm $O_2 m.^{-2}day^{-1}$) were similar to those in June. The lake bottom was observed by divers to be covered with dead algae in September (see pg 77) which would have had a greater oxygen demand than live algae. The higher measured SOD rates in September as compared to August resulted from the cessation of photosynthetic activity and the oxygen demand of decomposing algae.

The effect of stirred sediments on the SOD can be evaluated from the results obtained in May and June at Station U. Because the extremely soft sediments were riled when the chamber was lowered onto the bottom at this station, SOD rates at Station U in June were four to fourteen times higher than rates measured at the other four stations. Near this station, hydraulic dredges riled the lake bed sediments while sand was washed from the sediments. The DO in the hypolimnion in June at Station U was less than half of that at other stations. The low DO at this station resulted from a shallower hypolimnion, the oxygen demand of the resuspended materials, and an increase in the SOD when these materials settled to the bottom. The SOD rate measured in May (3.9 gm $O_2 m.^{-2}day^{-1}$) at Station U was twice as high as those which occurred in June at the four other stations.

REFERENCES

KLEVENO, C.O., T.E. BRAIDECH AND P.E. GEHRING. 1971. Hypothesis for dissolved oxygen depletion in the Central Basin hypolimnion of Lake Erie. Proc. 14th Conf. on Great Lakes Research, University of Michigan. In Press.

HUTCHINSON, G.E. 1957. A treatise on limnology. John Wiley and Sons, Inc., New York, 1014 p.

6. *Biological Studies Related to Oxygen Depletion and Nutrient Regeneration Processes in the Lake Erie Central Basin*

T. Braidech, P. Gehring, and C. Kleveno
Environmental Protection Agency
Fairview Park, Ohio, U.S.A.

Algae found on the sediment in the Central Basin of Lake Erie during the summer of 1970 were predominantly Tribonema and Oedogonium. The algae were of planktonic origin and exhibited growth on the bottom after light became limiting for other sedimented forms. A reduced sediment oxygen demand indicates sedimented algae contributed oxygen to the hypolimnion for a period of time. The reduction of incident light available to the algae on the sediment, the result of increased plankton in the epilimnion and the decreasing photoperiod with the approach of the autumnal equinox, increased the rate of oxygen consumption. Respiring bacteria utilized the remaining oxygen in the hypolimnion in the degradation of dead algae. Nutrients regenerated from the sediments as a result of oxygen depletion in the hypolimnion became available to algae as reflected by increased growths of Anacystis in and near the thermocline.

INTRODUCTION

In an attempt to define the mechanics of Lake Erie hypolimnion oxygen depletion, Kleveno *et al.* (1971) postulated that Lake Erie hypolimnetic deoxygenation was due to bacterial decomposition of profuse benthic growths of algae, *Tribonema utriculosum* and *Oedogonium sp.*, killed by the reduction of light penetrating to bottom waters. The reduction in light penetration was the result of increased plankton densities in overlying waters in late summer.

Based in part on this postulate, the biological program as designed for "Project Hypo" was to define comprehensively phytoplankton conditions throughout the water column and on the sediments. Special techniques – scuba diving, a National Aeronautics and Space Administration (NASA) designed time sequence camera, sedimentation traps, sedimented algae sampling, and an *in situ* sediment oxygen demand measuring device – were primarily employed to explain the presence, origin, and viability of heretofore unobserved, apparently metabolizing algae, especially the filimentous *Tribonema sp.* and *Oedogonium sp.* at the bottom of the Lake Erie Central Basin.

Five stations, designated P, M, S, N, and R, were selected for the biological parameters (Fig. 1). Most biological samples were collected by biologists operating from a launch. The phytoplankton samples were collected by scientific personnel aboard the Canadian Survey Ship "Limnos" and U.S. Coast Guard Cutter "Bramble".

Phytoplankton samples were collected and analyzed to determine if the major genera of the sedimented algae originated in the water column as opposed to being indigenous to the substrate, and also to measure changes in the standing crop. All organisms were analyzed quantitatively for numbers and volume and identified to genera when possible. The purpose of the sedimentation trap studies was twofold: (1) to substantiate phytoplankton analysis with respect to the origin of the sedimented algae, and (2) to

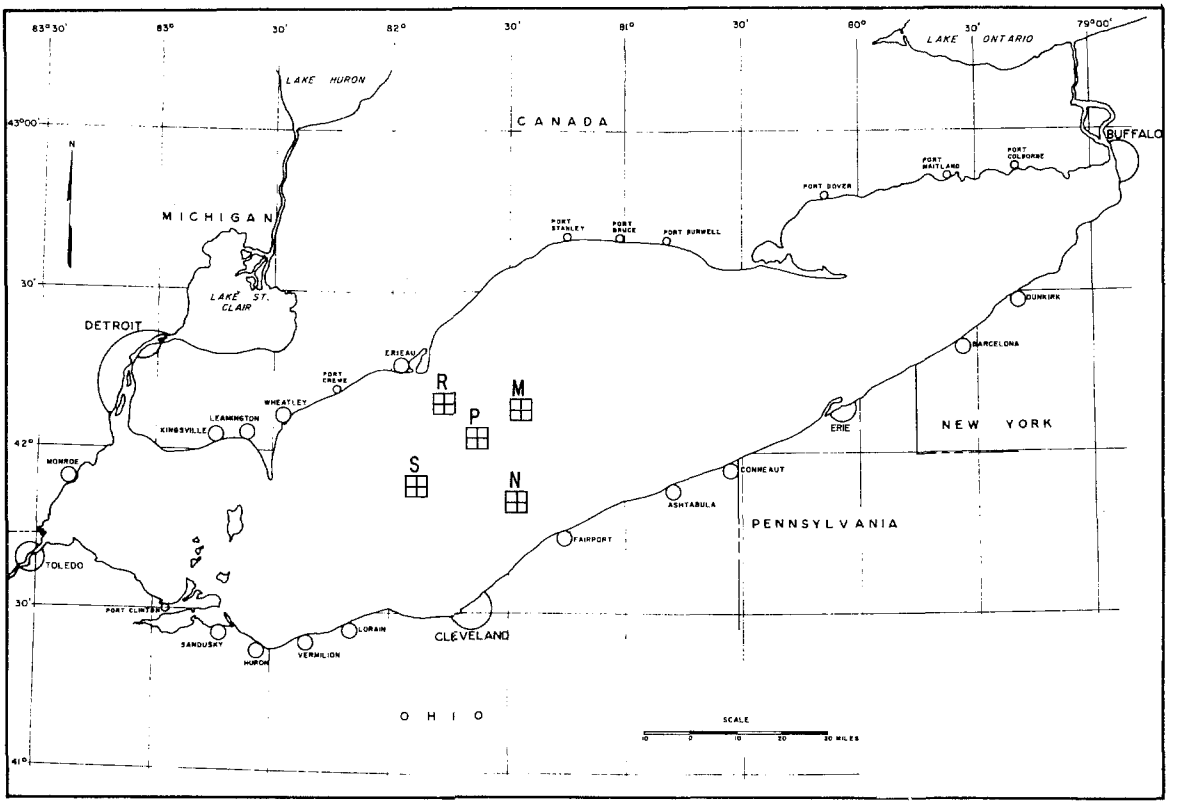

BRAIDECH, GEHRING & KLEVENO

Figure 1. Map of Lake Erie showing the five stations where biological studies were conducted.

quantitatively determine the amount of algae and other organic materials settling to the bottom in the hypolimnion. The trap samples collected over a period of 34 days were analyzed for volatile solids and phytoplankton numbers and volume. The sedimented algae grab samples were expected to show trends in the amount of algae and volatile solids in the sediment during the study. Sediment oxygen demand (SOD) studies were performed on three different occasions during the summer. The purpose of these tests was to illustrate the net effect of the algae on the SOD rate and also to relate the SOD to hypolimnetic oxygen depletion. These studies were performed by scientists from the Division of Field Investigations of the Environmental Protection Agency, Cincinnati, Ohio (Lucas & Thomas pg 48).

The biology program was divided into two segments. A period of background study extended from June 15, 1970 to July 25, 1970. During this period, biology samples were taken as often as possible, depending largely on the availability of vessels. During the intensive study period from July 26, 1970 to September 2, 1970, samples of sedimented algae from the bottom and from specially designed sedimentation traps were collected approximately once a week. Phytoplankton sample frequency was regulated by the number of cruises aboard the CSS "Limnos" and the USCG "Bramble". There were ten cruises by these vessels during the intensive study, and generally plankton samples were collected from the five stations on each of the cruises.

METHODS

All laboratory analyses were performed according to "Standard Methods for the Examination of Water and Wastewater" 12th Ed. unless otherwise described.

PHYTOPLANKTON

Four levels of the water column were sampled at each station. These locations were: (1) 1 meter below the surface, (2) approximately midway between the surface and the thermocline, (3) within

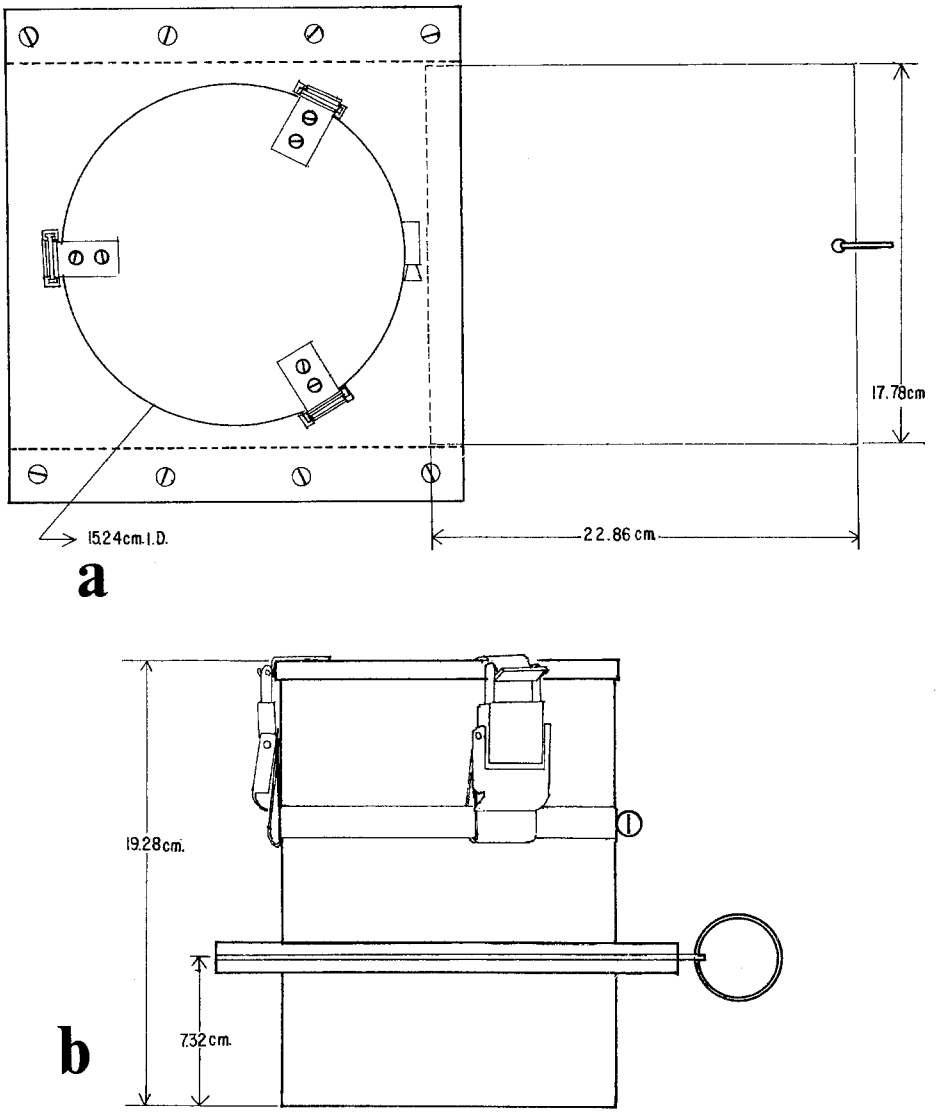

Figure 2. Sedimented Algae Sampler, (a) top view, showing sliding door in open position; (b) side view.

the thermocline, and (4) 1 meter above the bottom. Supplementary samples were taken at depths were dissolved oxygen or transparency measurements indicated the possibility of unique plankton activity.

All samples obtained during the background study and during the first seven cruises, July 26 to August 25, 1970, were collected by grab sampling with a Van Dorn bottle. A pump system for sample collection was used during the final three cruises, August 25 to September 2, 1970. Sample depth was measured by meter wheel. An approximate 1800 ml sample was collected for phytoplankton analysis. The sample was preserved with 60 ml of merthiolate and stored until analysis could be made.

The low numbers of phytoplankton required a tenfold concentration of the original sample for statistical validity. All samples were examined at 200x in a Sedgwick-Rafter counting cell and the algae enumerated using the clump count technique. Depending upon phytoplankton density, one to four strips across the cell were examined. Identification of the phytoplankton to generic level was made when possible, and the number per milliliter was computed for each genus. The average volume for each genus was determined and total volumes for each sample were computed.

SEDIMENTED ALGAE

To obtain samples of sedimented algae for analysis a sampler was constructed which would retrieve only the uppermost layers of lake sediment (Fig. 2). The diver-operated sampler, made from clear plexiglass, was cylindrical in shape, with a sliding aluminum door and removable lid. Samples were obtained by a diver taking the sampler with him to the bottom of the lake. At the bottom the diver would remove the upper cap and open the sliding door. The sampler was carefully placed on the sediment, and pushed into the lake bottom to a depth just above the level of the sliding door. The sampler top was then replaced, secured in position by the three snaps, and the sliding door closed, trapping the top thin layer of sediment and algae. The sample was brought aboard ship, immediately poured into a one gallon polyethylene bottle and 100 ml of methiolate added as preservative. Any residue left in the sampler was washed into the sample container with distilled water. The bottle was then labelled and sent back to laboratory.

The algae in the benthic samples were identified to genus when possible and enumerated. However, diatoms were not counted as part of the sedimented algae since most of the diatoms were silicic skeletal remains of the spring pulse and exerted no significant oxygen demand on the overlying waters.

SEDIMENTATION TRAPS

Sedimentation traps were placed at three levels, 2 m, 38 cm and 8 cm above the sediments in the hypolimnion. Two stations, P and S were arbitrarily chosen for placement of the traps. The traps were made from clear plastic in the shape of a cylinder (Fig. 3). A circular plastic base was fixed to the

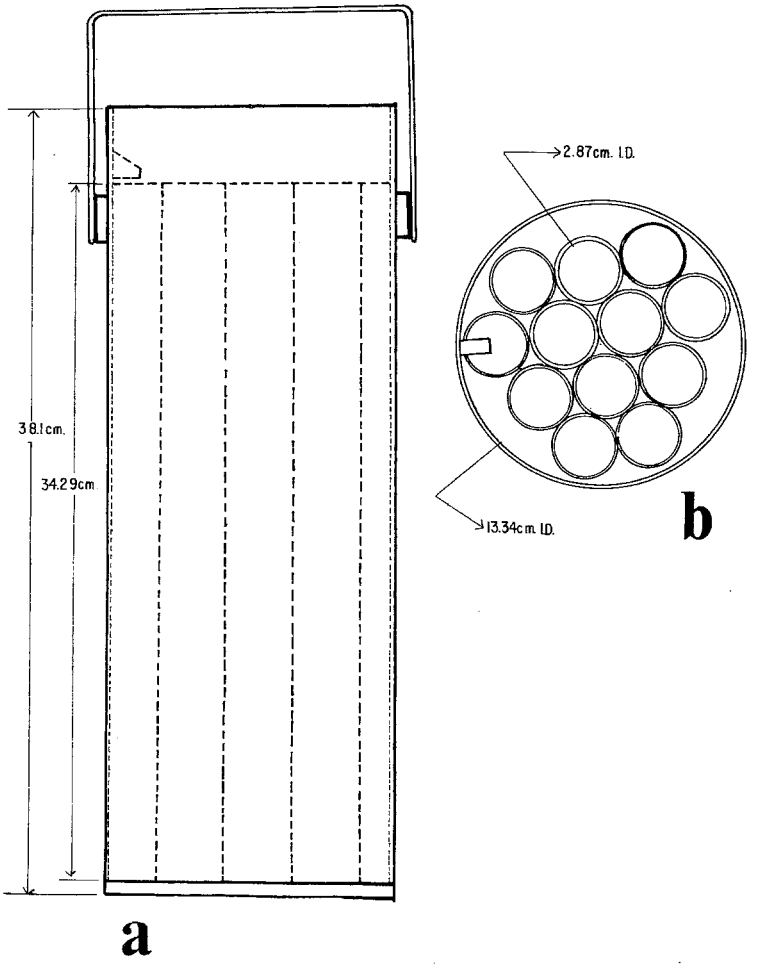

Figure 3. Sedimentation Trap, (a) side view; (b) top view, showing removable inner cylinders.

bottom of the cylinder while the top was left open. Inside the trap were twelve smaller removable cylinders. The removable cylinders, which were open at both ends, reduced turbulence in the trap and thus allowed for efficient settling and reduced the possibility of the algae being washed out of the trap. The fully assembled trap had a volume of 4,550 ml. A protective cap was placed on the open end during installation to prevent any diver caused resuspended sediment from entering the trap.

The traps were to be retrieved once every two weeks during the background study, and once a week during the intensive study. Unfortunately the buoy marking station P was never relocated during the study, so no trap data were obtained from this station prior to the intensive survey.

The procedure for retrieving the traps was rather simple. A diver descended to the trap and placed a cap over the open mouth. He then removed the trap from its mooring and returned it to the surface. On board ship the trap contents were distributed between three half-gallon polyethylene bottles, and seventy-five milliliters of merthiolate were added as preservative to each bottle. The samples were then returned to the laboratory for analysis.

In the laboratory the trap samples were concentrated by centrifugation. Volatile solids were determined on an aliquot of the sample. The average amount of volatile solids deposited in a trap per day was determined by dividing the weight of volatile solids by the number of days the trap was exposed, and converted to volatile solids per square centimeter per day by dividing by the cross sectional area of the trap.

To ascertain the quantity and kinds of algae settling to the lake bottom, a phytoplankton analysis was performed on the concentrated trap samples. The algal count in number per milliliter was converted to number per square centimeter of trap by the following formula:

$$\frac{PV}{A} = No/cm^2$$

where P is the number of algae per milliliter, V is the volume of the trap and A is the cross sectional area of the trap. This answer was divided by the number of days that the trap was exposed giving the average number of algae deposited per square centimeter of trap per day. The rate of algae deposition by volume ($\mu^3 x10^7 cm.^{-2} day^{-1}$) was also determined.

UNDERWATER OBSERVATIONS AND PHOTOGRAPHS

Many changes in color, algal cover of the sediments and turbidity in the hypolimnion of the Central Basin of Lake Erie were photographed and observed at the five stations from June to September, 1970 by biologists utilizing scuba diving techniques and underwater photographic equipment. In addition, an underwater time lapse camera installed at the centermost station P photographed the sediments once every hour (Jirberg pg 127). A directional indicator located in the camera's field was used to determine current direction at the sediment water interface. Attempts to photograph the lake bottom at each station were made at least once a week. However, during the earlier phase of the study, the weekly schedule was not realized.

RESULTS

PHYTOPLANKTON

Phytoplankton volumes and numbers are presented in Tables 1 and 2 (Appendix IV) for each depth and station. However, phytoplankton volumes are the basis for the following discussion. The trends in volume can be seen in Figures 4 to 9, and the dominant genera by volume are presented by station in Table 3 (Appendix IV). These tables and graphs include background data from June 16 to July 25 as well as the complete data from the intensive study, July 25 to September 2.

Results from June 16 to the 23, indicate very low phytoplankton volume at all stations except station N. Volumes at most stations were less than $75x10^4 \mu^3$/ml. At station N, pennate and centric diatoms contributed heavily to the larger volumes ($348.7x10^4 \mu^3$/ml and $567.4x10^4 \mu^3$/ml) found at 18 and

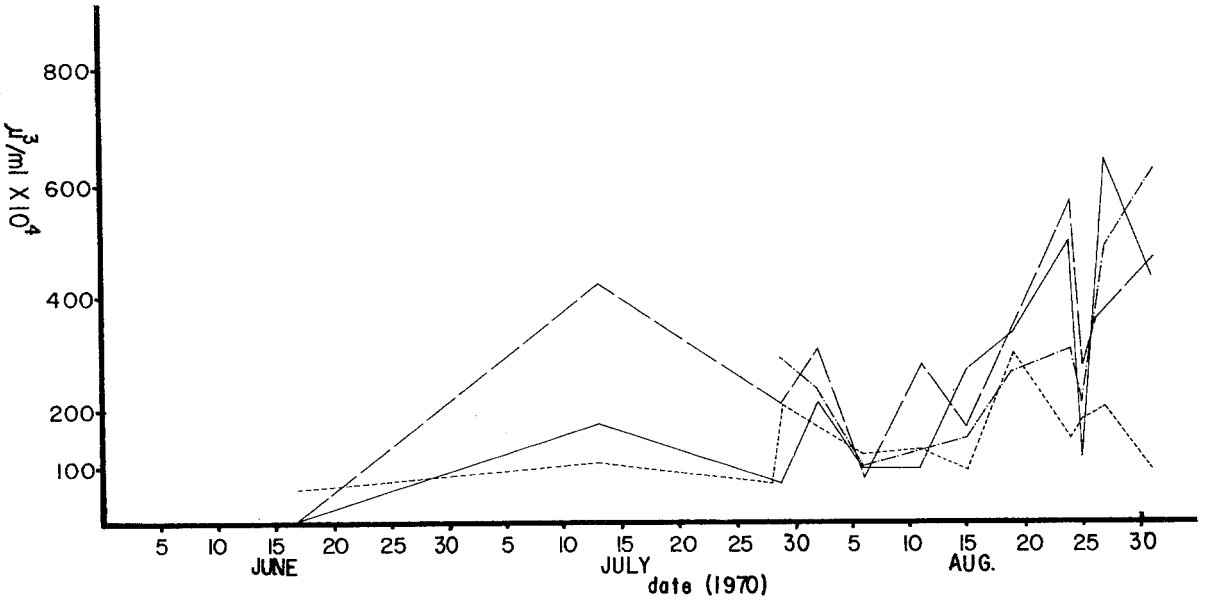

Figure 4. Station P, Total Phytoplankton Volume

The surface volumes are denoted by a solid line (————). The mid-epilimnion volumes are denoted by a long dashed line (— — —). The thermocline volumes are denoted by a dash-dot line (—.—.—). The hypolimnion volumes are denoted by a short dashed line (- - - - - -).

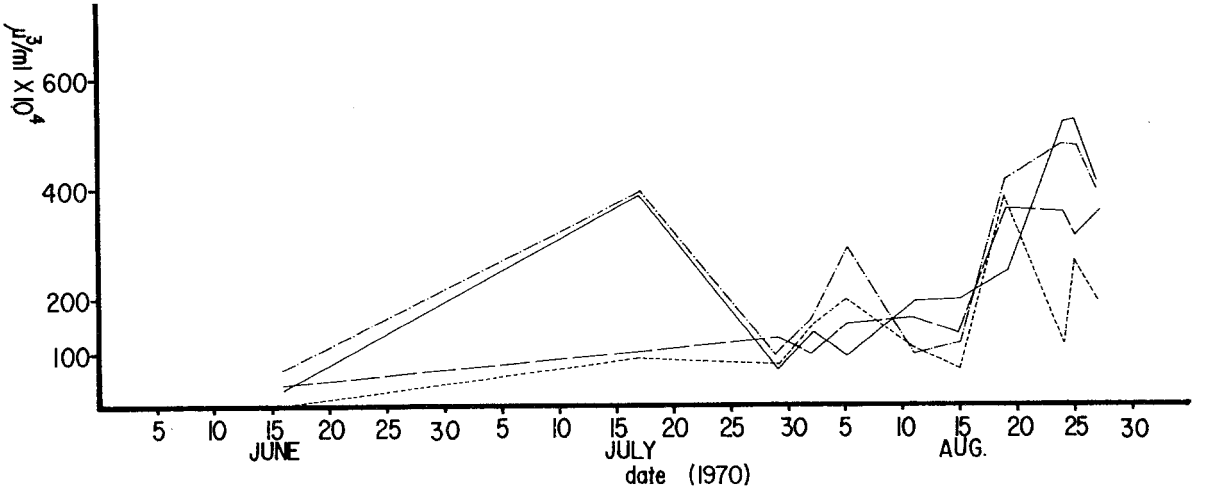

Figure 5. Station M, Total Phytoplankton Volume

The surface volumes are denoted by a solid line (————). The mid-epilimnion volumes are denoted by a long dashed line (— — —). The thermocline volumes are denoted by a dash-dot line (—.—.—). The hypolimnion volumes are denoted by a short dashed line (- - - - -).

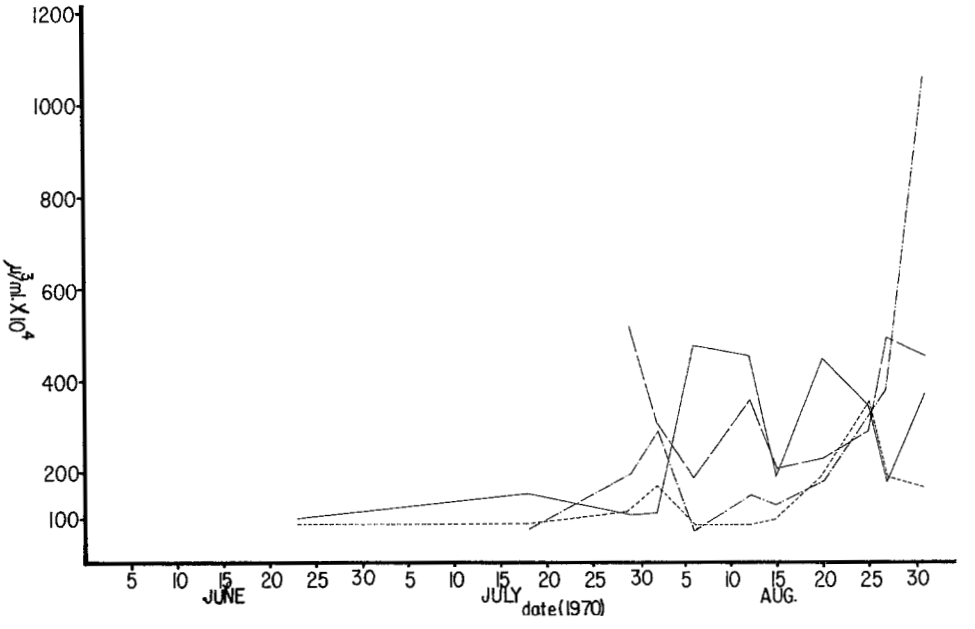

Figure 6. Station S, Total Phytoplankton Volume

The surface volumes are denoted by a solid line (————). The mid-epilimnion volumes are denoted by a long dashed line (— — —). The thermocline volumes are denoted by a dash-dot line (—·—·—·). The hypolimnion volumes are denoted by a short dashed line (– – – – –).

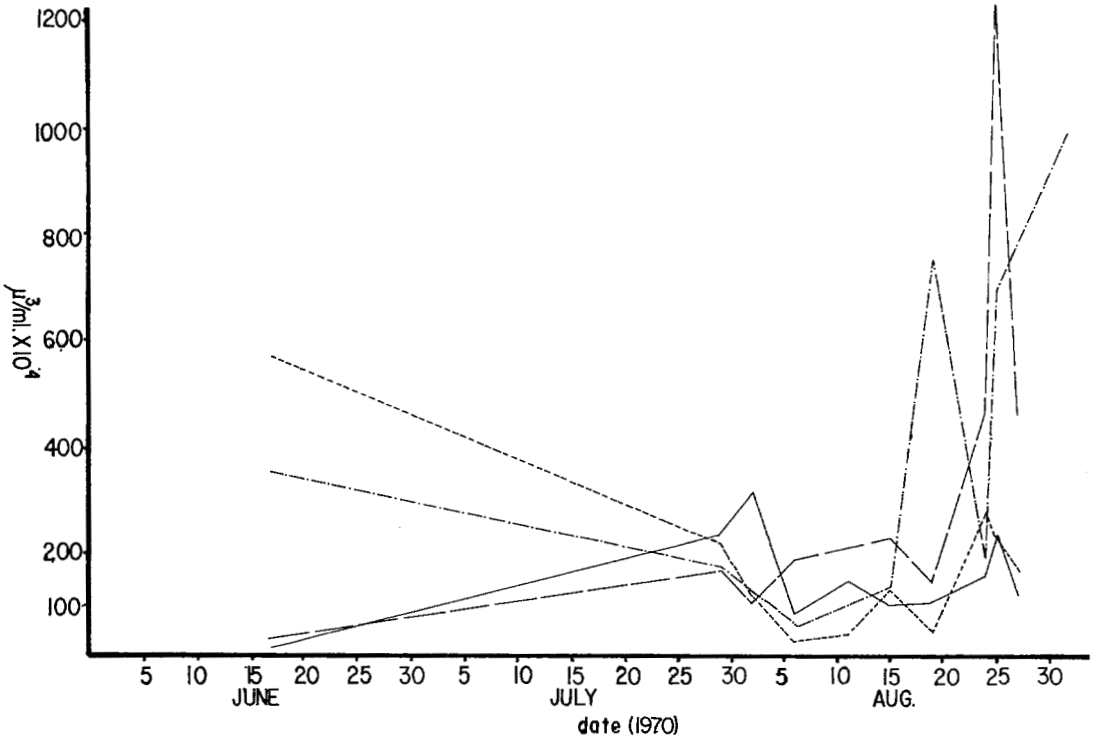

Figure 7. Station N, Total Phytoplankton Volume

The surface volumes are denoted by a solid line (————). The mid-epilimnion volumes are denoted by a long dashed line (— — —). The thermocline volumes are denoted by a dash-dot line (—·—·—·). The hypolimnion volumes are denoted by a short dashed line (– – – – –).

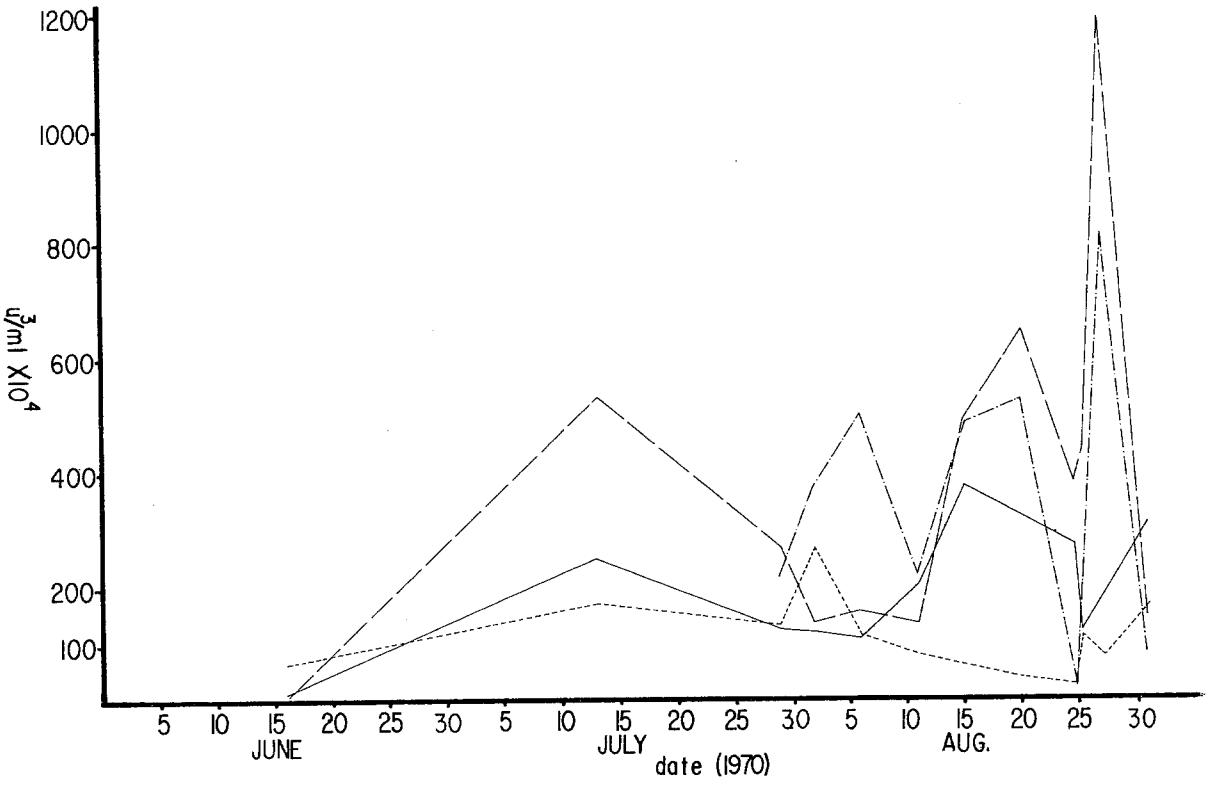

Figure 8. Station R, Total Phytoplankton Volume.

The surface volumes are denoted by a solid line (————). The mid-epilimnion volumes are denoted by a long dashed line (— — —). The thermocline volumes are denoted by a dash-dot line (— • —• —). The hypolimnion volumes are denoted by a short dashed line (– – – – –).

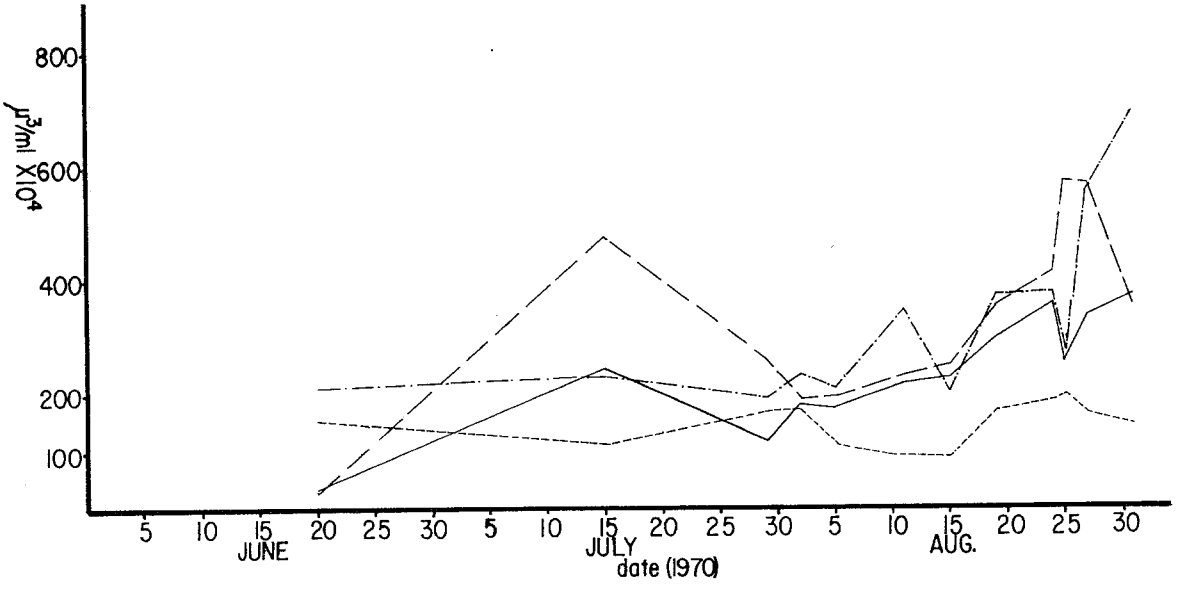

Figure 9. Average Phytoplankton Volume.

The surface volumes are denoted by a solid line (————). The mid-epilimnion volumes are denoted by a long dashed line (— — —). The thermocline volumes are denoted by a dash-dot line (— • —• —). The hypolimnion volumes are denoted by a short dashed line (– – – – –).

19 meters, respectively. In addition to diatoms, *Tribonema* was frequently found to be the dominant genus during this period. The lowest volume found during the entire "Hypo" study, $2.3 \times 10^4 \mu^3$/ml, occurred on June 16 at station M.

Oedogonium was the dominant algal form occurring from the surface to the thermocline between July 13 and July 18. The predominance of *Oedogonium* at the upper sampling levels was broken only once, by *Anacystis*, at station M. The highest *Oedogonium* volumes were measured at mid-epilimnion and thermocline depths. Centric diatoms, pennate diatoms and *Tribonema* were the most common forms in the hypolimnion. The highest total phytoplankton volume recorded during mid-July was $531.4 \times 10^4 \mu^3$/ml at the mid-epilimnion depth of station R. Samples were not taken at station N during this time.

Oedogonium was also the most prevalent genus during Survey 1 (July 29) of the intensive study, the greatest volumes occurring consistently at mid-epilimnion and thermocline. Diatoms dominated the hypolimnion at three stations, but these volumes were not significantly large. The highest phytoplankton volume recorded during Survey 1, $517.7 \times 10^4 \mu^3$/ml, occurred at the mid-epilimnion level of station S, bolstered in large part by an *Oedogonium* volume of $451.4 \times 10^4 \mu^3$/ml.

There was no one particular predominant genus found on August 2 during Survey 2. *Oedogonium, Ceratium, Anacystis* and pennate diatoms in order of frequency all prevailed during this cruise. *Ceratium* reached the highest volume measured for an individual genus and contributed largely to the highest total phytoplankton volume of $377.2 \times 10^4 \mu^3$/ml found at the thermocline of station R.

Phytoplankton assemblages on Survey 3, August 5 and 6, were similar to those of Survey 2. *Anacystis*, however, was most voluminous at the surface of all stations except station R where *Cosmarium* had a greater volume. The largest *Anacystis* volume, $410.0 \times 10^4 \mu^3$/ml, occurred at the surface level of station S. *Ceratium, Oedogonium* and pennate diatoms, in order of frequency, dominated the lower three sampling levels at all stations. The thermocline level at station R showed the highest total phytoplankton volume measured during Survey 3, $500.1 \times 10^4 \mu^3$/ml which was largely supported by a *Ceratium* volume of $427.1 \times 10^4 \mu^3$/ml.

Anacystis was the most frequent algal form found during Survey 4 (August 11 and 12) with a peak volume occurring at the surface of station S. However the highest phytoplankton volume of $884.4 \times 10^4 \mu^3$/ml occurred at station M just above the thermocline, largely the result of a *Ceratium* pulse which reached $800.1 \times 10^4 \mu^3$/ml. *Anacystis, Ceratium* and *Oocystis* were the most frequent genera found on August 15 (Survey 5). Phytoplankton volumes at station R were substantially higher than the other stations, with a peak of $491.5 \times 10^4 \mu^3$/ml at the mid-epilimnion level.

On August 19 and 20 during Survey 6, *Anacystis* prevailed at every level except the surface and bottom depths of station N which were dominated by *Oocystis* and *Ceratium*, respectively. The highest recorded value, $650.3 \times 10^4 \mu^3$/ml, occurred at station R just above the thermocline.

During Survey 7, August 24 and 25, *Anacystis* again was found to be the most frequent phytoplankton genus. The greatest total phytoplankton volume measured during Survey 7, $749.8 \times 10^4 \mu^3$/ml, occurred at station N in the thermocline.

During Survey 9 through 11, *Anacystis* consistently had the greatest volume with an occassional predominance recorded by *Oocystis* or *Cosmarium*. Maximum phytoplankton volumes of between $1000.0 \times 10^4 \mu^3$/ml and $1250.0 \times 10^4 \mu^3$/ml were recorded on each of these cruises.

SEDIMENTATION TRAPS

The sedimentation traps placed at station S yielded only one group of samples before the anchor rope to the surface marker became fouled in the set, destroying most of the traps. The remains of this set were subsequently installed at station P on July 28 and yielded data until August 21. Furthermore, only the upper trap (2 meters from bottom) of each setting was used for analysis, since the lower traps were biased by diver-induced resuspended sediment.

In all, the sedimentation traps were retrieved six times during the study. Exposure time varied from three to thirteen days. In general, and as expected, increases in the amounts of volatile solids were accompanied by increases in the amount of phytoplankton (Fig. 10). Results from the first setting (Table 4, Appendix IV) June 23 to July 6, show volatile solids of 0.118 $mg.cm.^{-2}day^{-1}$ and phytoplankton numbers of $0.96x10^4 cm.^{-2}day^{-1}$. During the second period, July 28 to August 1, a decrease in volatile solids to 0.061 $mg.cm^{-2}$ day^{-1} and an increase in phytoplankton to $2.17x10^4 cm.^{-2}day^{-1}$ was measured. A large increase in both volatile solids and phytoplankton occurred between August 1 and August 4 as measurements of 0.177 $mg.cm.^{-2}day^{-1}$ and $6.33x10^4$ organisms $cm.^{-2}day^{-1}$ respectively were recorded. During the period August 4-17, volatile solids and plankton numbers decreased to the study lows, 0.045 $mg.cm.^{-2}$ day and $0.79x10^4$ organisms $cm.^{-2}$ day^{-1}. Results from the last setting August 17 to August 21, show another increase to 0.168 $mg.cm.^{-2}day^{-1}$ of volatile solids and $2.84x10^4$ organisms $cm.^{-2}day^{-1}$ of phytoplankton.

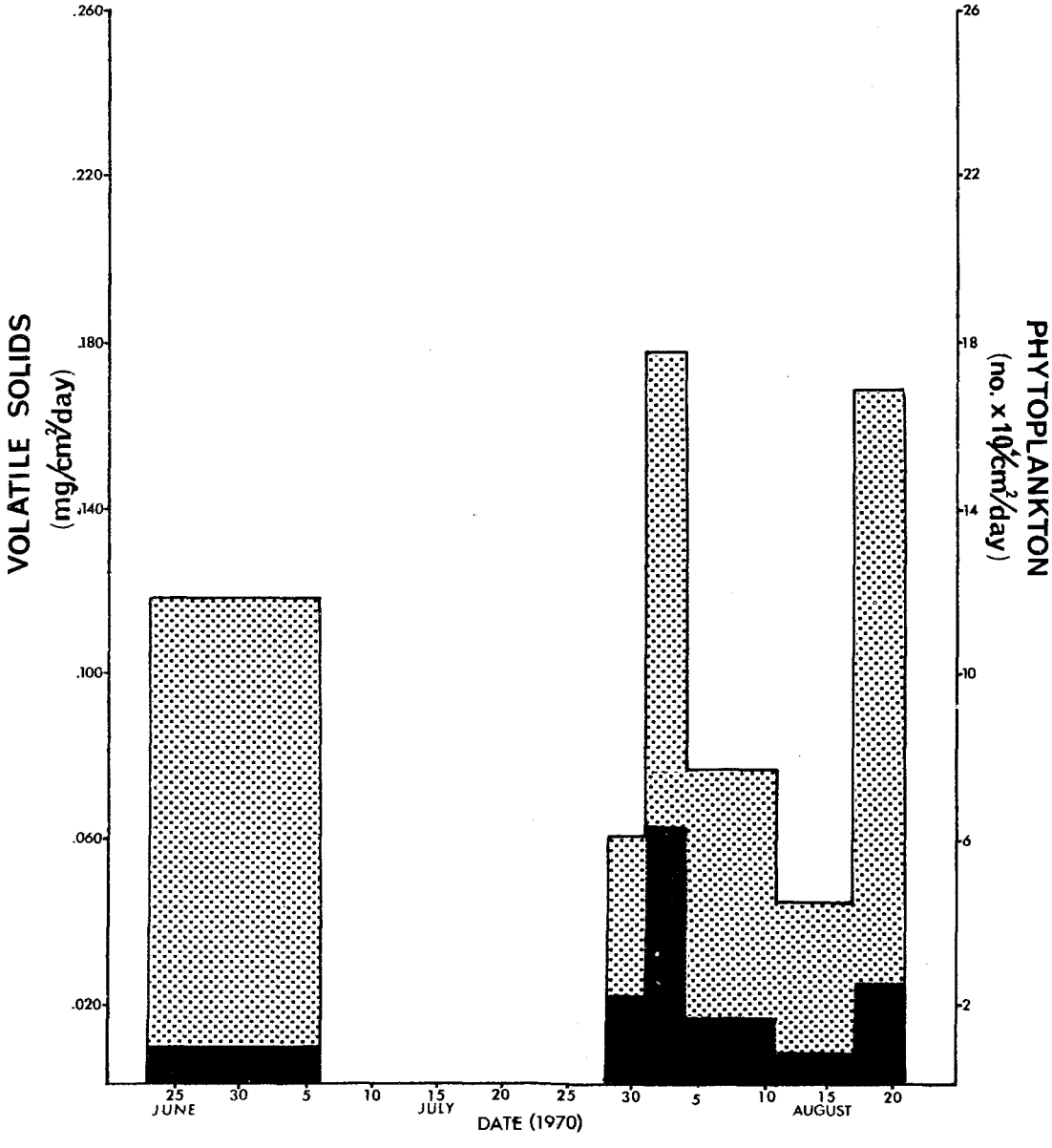

Figure 10. Sedimentation Trap Analysis. The graph shows phytoplankton numbers depicted by the dark shading and volatile solids depicted by the light shading.

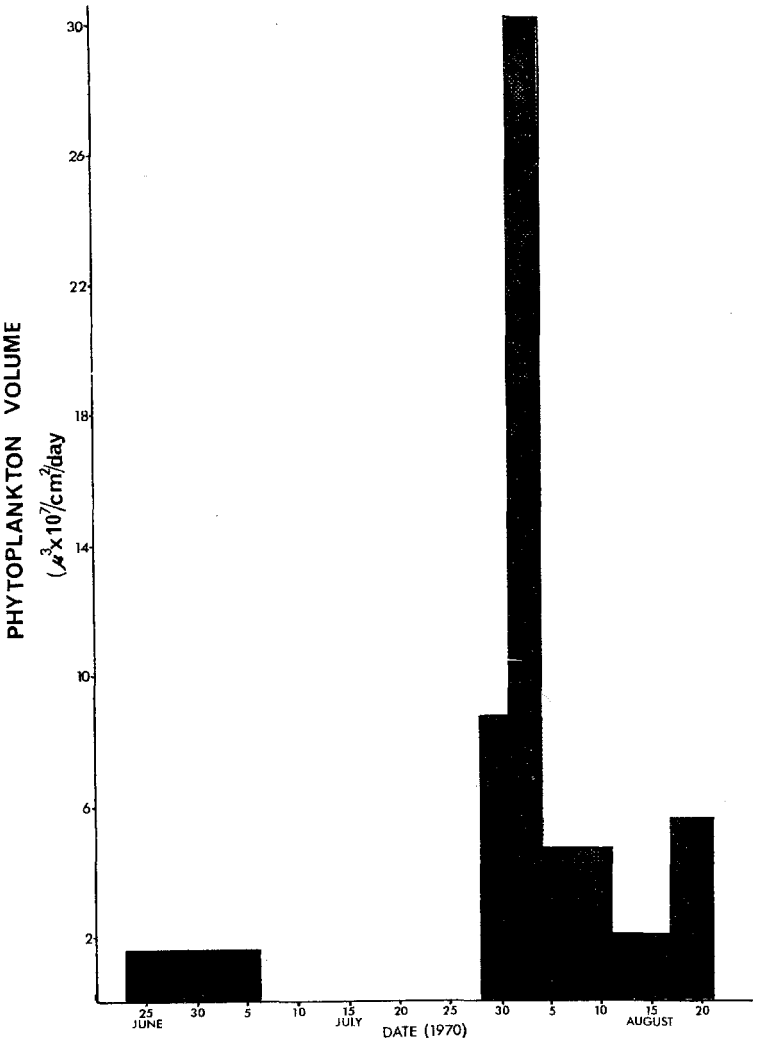

Figure 11. Sedimentation Trap Analysis. The graph shows the phytoplankton volume found in the sedimentation traps at different times during the summer.

Sedimentation trap phytoplankton volume analysis exhibits strikingly similar peaks to the phytoplankton counts (Fig. 11). However the peak between August 1 to August 4 is much greater by volume than by count. Dominance by volume (Table 5, Appendix IV) closely parallels that found in the water column at station P (Table 3, Appendix IV). Centric diatoms were the most common algal form at the start of the study. *Oedogonium* became dominant in late July, and was replaced by *Anacystis* towards the end of the study. The second and third most prevalent forms in the traps do not follow the water column dominance as closely, but do display volume peaks occurring in the same time sequence.

SEDIMENTED ALGAE

Station P was sampled a total of nine times during the study (Fig. 12) with the diver-operated bottom sampler. The algae on June 16, 1970 were found to be 428 organisms/cm^2. Most of the algae were of the coccoid green type although some *Tribonema* were present. On August 8 the numbers of algae, which had been slowly increasing, rose to 11,872 organisms/cm^2 with *Tribonema* being the most numerous form. From then until September 1, 1970, algae displayed large fluctuations ending at a peak of 13,700 organisms/cm^2 with *Tribonema* again most abundant.

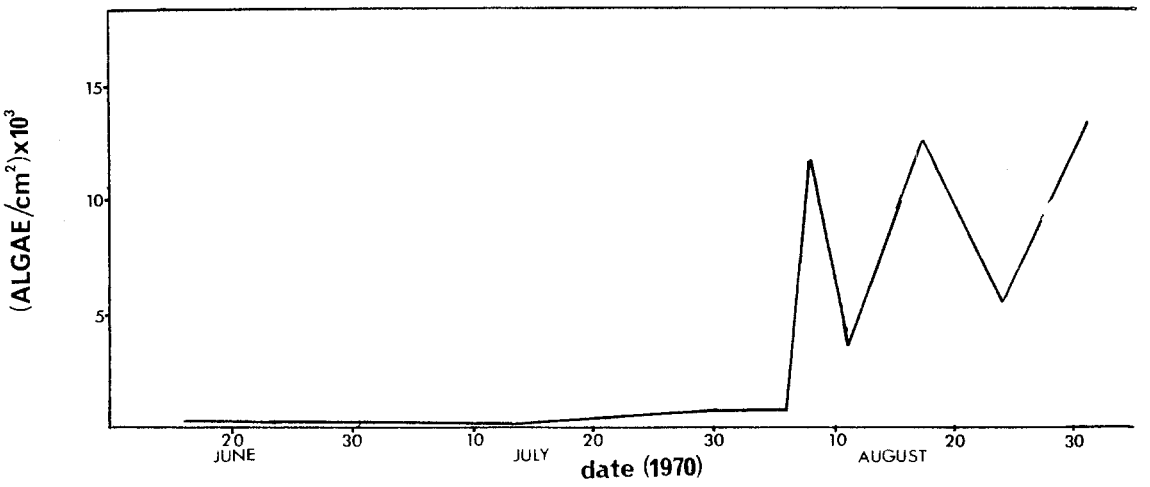

Figure 12. Sedimented Algae Station P. Graph of the results of analysis for sedimented algae.

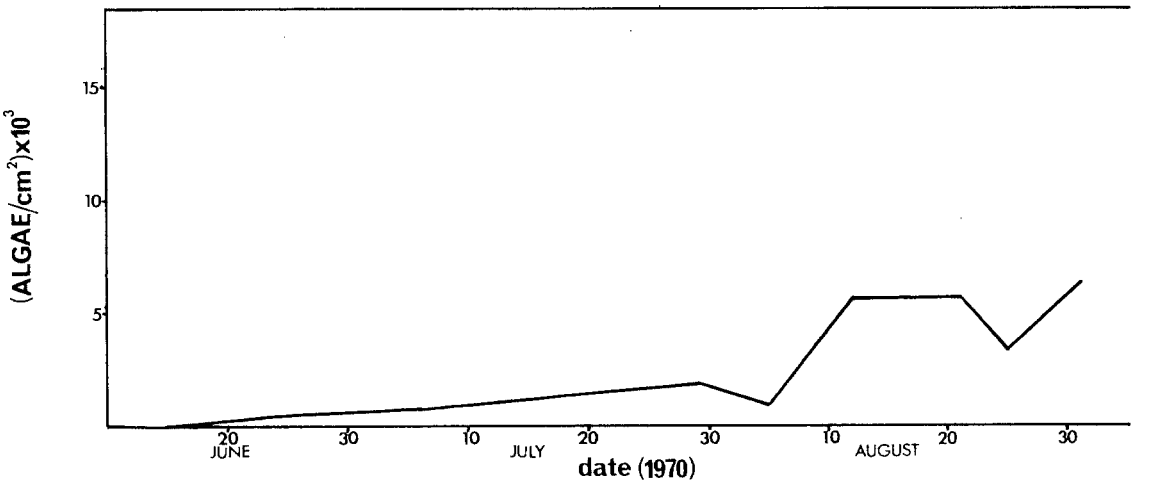

Figure 13. Sedimented Algae, Station S. Graph of the results of analysis for sedimented algae.

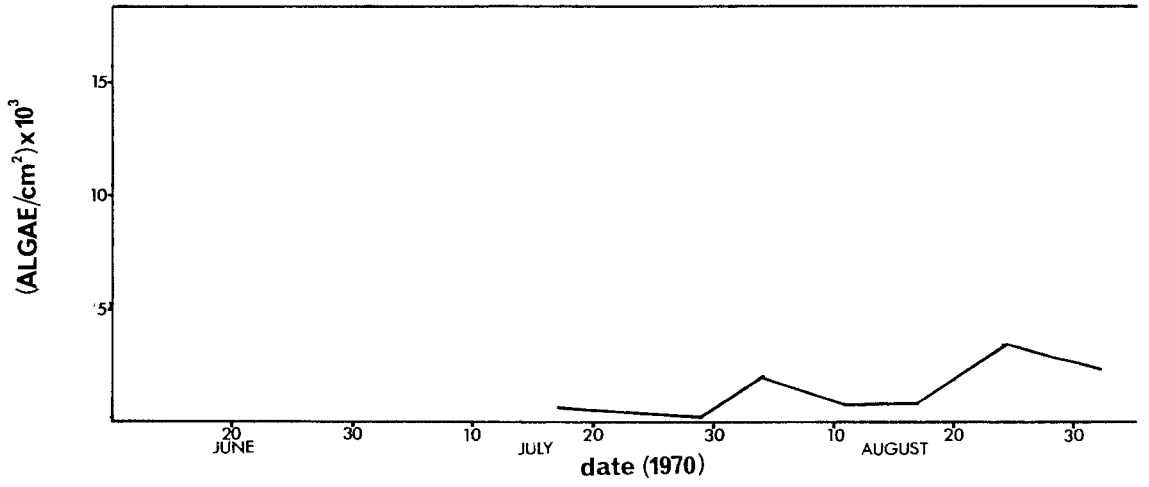

Figure 14. Sedimented Algae, Station M. Graph of the results of analysis for sedimented algae.

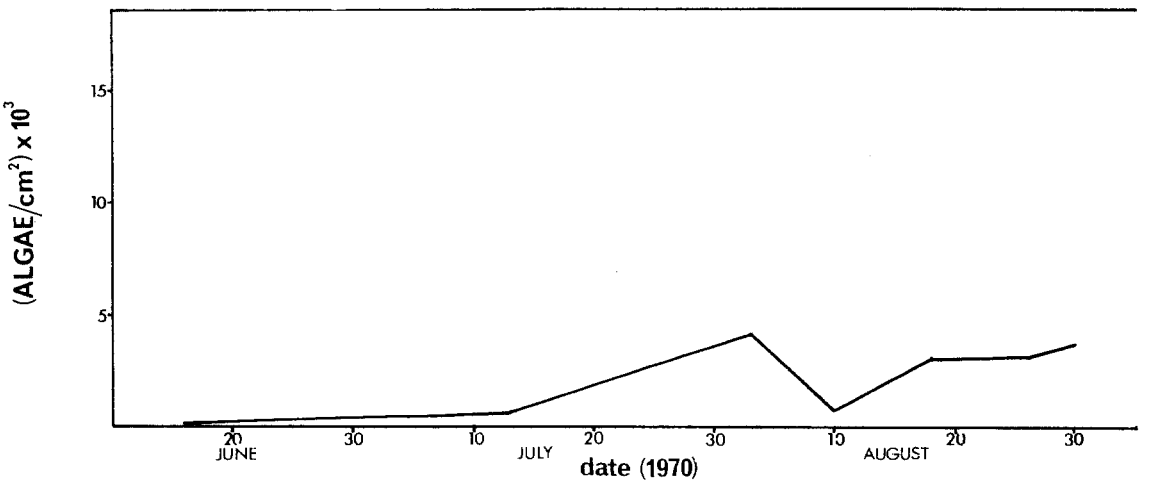

Figure 15. Sedimented Algae, Station R. Graph of the results of analysis for sedimented algae.

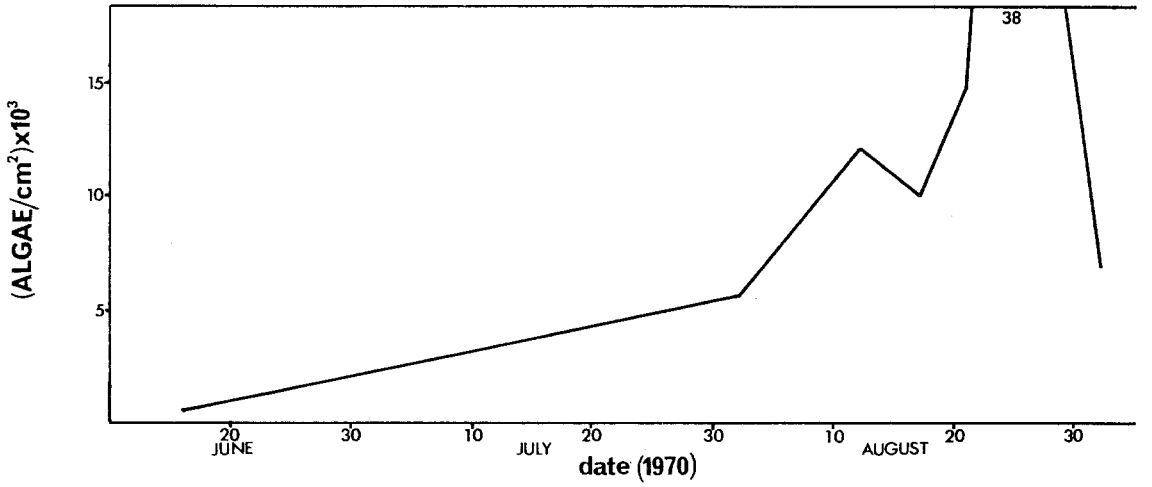

Figure 16. Sedimented Algae, Station N. Graph of the results of analysis for sedimented algae.

Station S, the most westerly station, was also sampled nine times (Fig. 13). The station was first sampled on June 15, 1970 and at that time the algae count was zero. Throughout the study, algae showed a gradual increase to a peak of 5,970 organisms/cm^2 on September 1 with *Tribonema* being dominant for most of this period.

Station M, the most easterly of the five stations, was sampled eight times during the summer with the first sampling on July 17 (Fig. 14) which showed an algal count of 554 organisms/cm^2. The predominant algal forms were coccoid greens. Algal counts increased to 2,001 organisms/cm^2 on August 4, declined then rebounded to a peak on August 24 at 3,618 organisms/cm^2. The last sample on September 2 showed a decreasing tendency. Filamentous algae were the most common type found during the latter part of the study.

Station R, located approximately nine miles southeast of Pointe Aux Pins, Ontario, Canada, was sampled seven times during the study (Fig. 15). The first sampling was on June 16, 1970 and the algae numbered 92 organisms/cm^2 consisting of coccoid green types. After the initial low count, algal numbers rose to a peak of 4,174 organisms/cm^2 on August 3, then quickly slumped to 699 organisms/cm^2 on August 10. Algal populations then steadily rose finishing the study at 3,710 organisms/cm^2 on August 31. *Tribonema* and *Oedogonium* were the most numerous algae from August 3 to August 31.

Station N, near Fairport, Ohio, was sampled six times during the study (Fig. 16). The first sample collected on June 16, 1970 contained coccoid green algae numbering 570 organisms/cm^2. Algal numbers increased rapidly to a peak of 38,271 organisms/cm^2 on August 24, then decreased to 7,182 organisms/cm^2 on September 2. Prevailing algae genera from August 2 to September 2, 1970 were *Tribonema* and *Oedogonium.*

UNDERWATER OBSERVATIONS AND PHOTOGRAPHS

The observations of trained scientific divers and photography are valuable tools for describing and documenting the biological changes occurring on the sediment surface. Changes in sediment color and texture, and hypolimnion visibility can be correlated to algae deposition, production, and decomposition. As an example, photographs and visual observations were used to compile the following changes that occurred at station P, June – September 1970. Similar descriptive documentation is available for each station but is not listed in this report. Dissolved oxygen concentrations in the hypolimnion are given in parentheses.

Station P

month-day

6-16 The sediment had a brown overlay and was loose, light, and fluffy. Algae were not observed on the sediment or in the hypolimnion. (7.3 mg/1)

7-13 The sediment had a brown overlay. Algae were not noticed on the sediment or in the hypolimnion. (5.4 mg/1)

7-18 Installed time sequence camera. Algae were not noticed on bottom or in the hypolimnion. (5.1 mg/1)

7-19 Retrieved time sequence camera. Algae were not noticed on bottom or in the hypolimnion. (5.0 mg/1)

7-21 Reinstalled time sequence camera. Filamentous algae were noticed at the thermocline and appeared to be settling through the hypolimnion onto the sediments. (4.7 mg/1)

7-28 Algae were present on bottom with heavy growths at thermocline that were settling out on sediments (3.6 mg/1)

7-30 Algae were on the bottom with heavier deposits collected in depressions. Algae were probably moved into these depressions by water currents. (3.5 mg/1)

8-2 -3 Algae were covering bottom to a depth of 1 to 1-1/2 inches (3.2 and 2.8 mg/1 respectively). Oligochaeta tubes appeared as a mat or web under algae

8-4 A heavy growth of algae was again noted in the hypolimnion. The sediment was completely covered with algae. Visibility was reduced from 10 feet in epilimnion to 2 feet in hypolimnion. (3.0 mg/1)

8-5 6 Conditions similar to those on 8-4 however, visibility in the hypolimnion had increased to approximately 6 to 10 feet. (2.8 and 2.7 mg/1 respectively)

8-7 Algae were covering the bottom. Visibility in the hypolimnion had increased to approximately 15 feet because of a decrease in the amount of suspended algae. (2.6 and 2.6 mg/1 respectively)

8-11 12 14 Algae were matting down on sediment; visibility was approximately 15 feet. Oligochaeta tubes were noticed protruding through the green layer of algae. (2.2, 2.1 and 2.1 mg/1 respectively)

Plate 1. Photograph of the fluffy green covering of algae in early August at a depth of 25m.

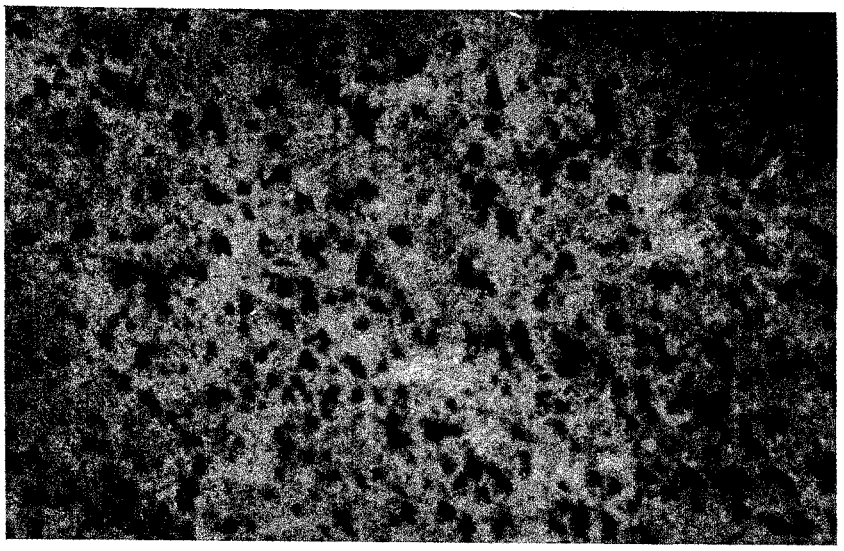

Plate 2. Photograph showing *Oligochaeta* tubes extending approximately one inch above the mat of algae (August 10th).

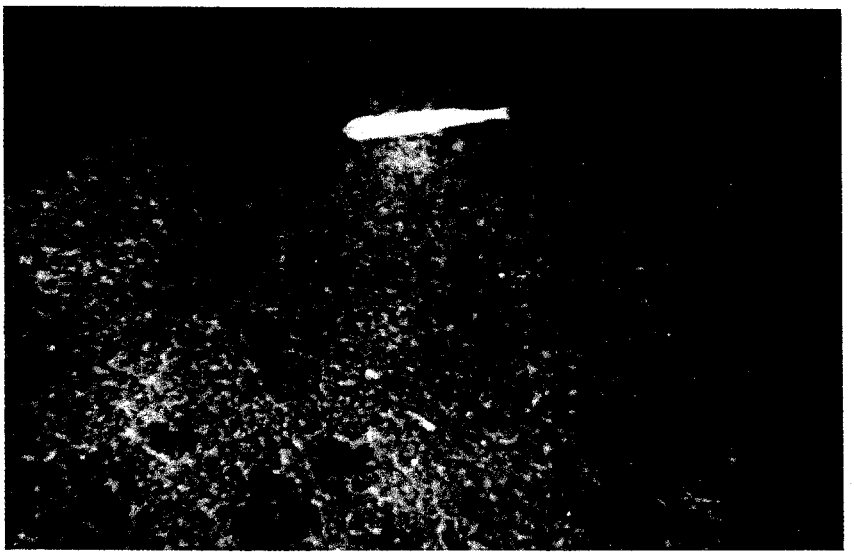

Plate 3. Photograph showing black color of bottom at Station N on September 2, 1970.

8-21 to 23 Algae appeared brown, however photographs still revealed green color. The sediment layer under the algae was black. Visibility in the hypolimnion was about 5 feet, apparently due to the regeneration of minerals from the sediment. (1.3 and 1.1 mg/1 respectively)

8-24 to 25 Black patches began to appear; visibility was 5 to 8 feet. (1.1 and 0.9 mg/1 respectively)

8-27 to 9-1 Black areas were enlarging and visibility was continually increasing. (0.5 to 0.1 mg/1)

In situ Underwater Camera

8-3 Algae began to fall at 3 AM and continued to fall until 6 PM on August 4. At times the "rain" of algae was heavy enough to obscure the lake bottom and the current direction indicator. (3.1 to 2.9 mg/1)

8-5 Algae began falling at 6 AM and ceased falling at 12 AM the same day. (2.8 to 2.9 mg/1)

8-6 A light amount of algae fell from 10 PM to 1 AM on 8-7. (2.6 to 2.6 mg/1)

8-10 Algae fell from 3 to 4 AM. (2.4 to 2.4 mg/1)

8-19 A sparse growth of algae fell from 5 AM to 12 noon, and from 5 to 9 PM (1.1 to 1.7 mg/1 and 1.7 to 1.6 mg/1)

Sufficient natural light was available at all stations to enable divers to perform tasks without artificial lights during much of the intensive study. The shading of the sun by clouds could be detected at the bottom, even at mid-lake stations. Artificial lights, however, were used to more accurately document color changes. The duration and intensity of sunlight reaching the bottom each day decreased throughout the study, as the angle of incidence became progressively larger.

DISCUSSION

Appearance of the sediment surface underwent changes throughout the study. Most changes in the sediment surface and hypolimnion were related to the presence or absence of algae and their physiological condition. The extent of these changes is dramatized by photographs of the bottom showing the extreme conditions noted during the study (Plates 1 to 3).

Observations made in June found the sediment easily disturbed by divers and covered with a light reddish-brown layer, apparently oxidized iron (see Plate 1 on page 103). The first evidence of algae occurring on the bottom was found at station S on June 30 when small wisps of green algae were noted on the brown sediment. Midge pupae were active at the sediment surface on this date. Stations R and M showed light patches of green algae in mid-July while station P appeared to have no algae on the sediment. On July 21 station P was observed to have large amounts of algae at the thermocline and throughout the hypolimnion. Unfortunately station N was not observed during this critical time.

Stations R, S, P and N observed from July 28 to 30 showed significant amounts of algae on the sediments. Station M was the only station where the bottom was not completely covered by algae. The occurrence of algae on the bottom was associated with increased phytoplankton volumes at, and slightly above, the thermocline, consisting predominantly of *Oedogonium*. All five stations had a fluffy green covering of algae on the bottom by August 4 (Plate 1) and additional algal "rains" were noted at some stations. Observations of benthic fauna during the first week of August revealed Oligochaeta (worm) tubes forming a mat under the algae while Chironomidae (midges) and Tricoptera (caddisflies) insects were emerging at the water surface.

From July 21 to August 10, the algae by virtue of their color and appearance, seemed to be at their optimum production levels, and had a net effect of reducing the rate of oxygen depletion in the hypolimnion. This was substantiated by reduced Sediment Oxygen Demand rates as measured by benthic respirometers and minor increases in dissolved oxygen concentration measured near the sediments (Lucas and Thomas, pg 48).

Beginning approximately August 10 the algae layer became matted, losing the previous fluffy appearance. This produced a layer of material with a relatively high surface tension requiring considerable turbulence before the sediments could be disturbed. Oligochaeta tubes also contributed to the mat covering the sediment. These tubes extended approximately 1 inch (Plate 2) above the mat. Apparently the matting down of the algae is related to the cessation of photosynthesis, death and the start of large scale decomposition. Color changes of the algal mass (from green to yellow green to almost brown) occurred during this time.

Black patches appeared on the surface of the sediments from August 5 to 24. The black areas, most likely iron sulfide although not substantiated as such, indicated regions of anaerobiosis since these areas were associated with very low levels of hypolimnetic dissolved oxygen. The black areas continued to increase in size and number until the study was terminated, September 2. At that time the sediment surface at station N was completely black (Plate 3). Dissolved oxygen in the hypolimnion at this station was zero. Bacteria were growing on the algae covering the bottom and strong odors of hydrogen sulfide were detected in the water samples collected. However, analyses of sediment algae at this station, revealed large numbers of apparently viable filaments of *Tribonema.* The low temperature and light requirements together with symbiotic bacterial relationships of this genus may have contributed to its extended viability (Fritsch, 1961).

Averages of phytoplankton volumes from all five stations showed some quantitative trends (Fig. 9). Two major peaks of phytoplankton were generally evident at the upper three sampling levels, while little change occurred in the hypolimnion. The first peak recorded during the background study in mid-July, occurred primarily at the mid-epilimnion depth and was dominated by *Oedogonium.* Nutrient levels in the hypolimnion were not limiting at this time, therefore light and temperature were the major factors affecting the growth rate and the depth at which growth could occur. Lower average volumes during the next three sampling cruises, July 29 to August 6, coincided with decreased *Oedogonium* volumes and nutrient levels in the epilimnion and thermocline. The decline in the green filamentous algal *Oedogonium* also coincided with visual observations of algae settling to the lake bottom as "algal rains" from the thermocline. By this time, soluble nitrogen and temperature apparently had become limiting to filamentous green algae. Because of blue-green algal ability to fix atmospheric nitrogen and also due to reduced ecological competition by the fading non-nitrogen fixing green algae, *Anacystis* became established at the surface. Large volumes of *Ceratium* were concentrated at the thermocline and mid-epilimnion depths on August 11 and 12, probably initiated by limited amounts of nutrients being transferred from the hypolimnion through the thermocline. *Anacystis* also increased to become the dominant algal genus and contributed to the slightly elevated average phytoplankton volumes measured during the second week of August. This may reflect an input of nutrients from the hypolimnion.

The second peak of phytoplankton, August 25 through September 1, was dominated by *Anacystis* and was apparently due to a transfer of even greater amounts of nutrients from the hypolimnion to the thermocline and epilimnion. As dissolved oxygen levels reached zero and diffused nutrients increased in the hypolimnion, sharp increases in phytoplankton in and near the thermocline were noted. Phytoplankton volumes even increased in the hypolimnion as dissolved oxygen reached zero, but soon declined as light most likely became a limiting factor. The following interrelated factors were responsible for hypolimnion limiting light conditions: (1) the shading effect of the increasing phytoplankton populations above, (2) the declination of the angle of the sun resulting in a reduction in the duration and intensity of light striking the water surface, and (3) increased surface turbulence near the end of the study which caused increased reflection of incident light.

The highest total phytoplankton volumes recorded during the study, $1{,}228.9 \times 10^4 \mu^3$/ml,

occurred in the epilimnion at station N on August 25, shortly after the hypolimnion became devoid of dissolved oxygen. Volumes of over $1{,}000 \times 10^4 \mu^3$/ml were measured at stations R and S under similar circumstances on August 27 and September 1, respectively. This indicates that nutrients regenerated from the sediments, because of the absence of dissolved oxygen in the hypolimnion, readily pass through the thermocline and into the epilimnion.

A definite sequence of phytoplankton genera can be identified beginning in June with *Tribonema*, pennate diatoms and centric diatoms. Next, *Oedogonium* appeared in July and continued through the first week in August. During the first two weeks in August there were brief, apparently stratified growths of *Ceratium* which caused it to become dominant at only one or two depths at a particular station, while *Anacystis* became established at the surface. During the last two weeks of the study, coinciding with the mid-August phytoplankton volume increase, *Anacystis* was dominant throughout the water column. The larger size of *Anacystis* was responsible for their dominance over the generally more numerous *Oocystis* during this period. The few occurrences of *Cosmarium* as a dominant form during the last week of the study were also due to its large size and may indicate that a shift in dominant genera was about to occur.

The sedimentation trap analyses show rather large amounts of volatile solids settled between June 23 and July 6 with corresponding low algal count and volume indicating volatile solids in early summer are composed of particulate or detrital material. During mid-summer, filamentous algae became the primary source of volatile solids in the hypolimnion. The concurrent large quantities of sedimented volatile solids and algae from August 1 to August 4, (Figures 10 and 11) related to a filamentous algal bloom in the hypolimnion, as reported by divers' observations and recorded by the *in situ* underwater camera. By late summer, substantial volatile solids were again accompanied by low algal populations and volumes. The relatively low algal populations and volume during this period may have been caused by the change in predominant genera from *Oedogonium* to *Anacystis*. It is more likely, however, that with increased temperatures and bacterial activity, the sedimented algae were quickly decomposed to unidentifiable organic detritus.

From data developed in the sedimentation trap study it was indicated that certain algal genera were capable of growing and reproducing on the lake bottom although their origin was in the overlying waters. Data from station P (Table 3, Appendix IV) show that *Oedogonium* was dominant in the hypolimnion only once, on August 2, and in the thermocline from July 13 to August 6. After this period *Anacystis* was the most dominant genera in the hypolimnion and thermocline until the end of the study, with one exception, August 15, when *Ceratium* became dominant at the thermocline. Furthermore, *Oedogonium* was never among the top three dominant genera at any level in the water column after August 11. On the other hand, the data from the sedimentation traps (2 meters above lake bottom) showed that *Oedogonium* was the dominant sedimented form by volume from July 28 to August 17 (Table 5, Appendix IV). *Anacystis* then became dominant from August 17 to 21. It was indicated from these trap data that *Oedogonium* was reproducing in the hypolimnion two meters above the lake bottom.

The results of the sedimented algae analyses show a large influx of algae to the lake bottom (Fig. 17). Although *Tribonema* was very seldom dominant throughout the water column, it was the most abundant genus on the lake bottom during the study. Numerically it was the first dominant genus 68.4 percent of the time while *Oedogonium* on the other hand was dominant on the bottom only 19.4 percent of the time. The predominance of these genera at the five stations sampled for sedimented algae began between August 3 and August 11. After the latter date, although their importance in the water column progressively decreased, *Tribonema* and *Oedogonium* never relinquished their hold on the first dominant position at any station.

Data from the water column (Table 9, Appendix IV) show *Oedogonium* and *Tribonema* dominate the phytoplankton count only 8.8 percent and 1 percent of the time, respectively. Further, *Oedogonium* is among the top three dominant genera only 7.3 percent and *Tribonema* only 3.2 percent of the time. These two genera are mentioned among the three dominant genera in the water column between July 29 and August 6. After this time they no longer attain a position of importance in the water column.

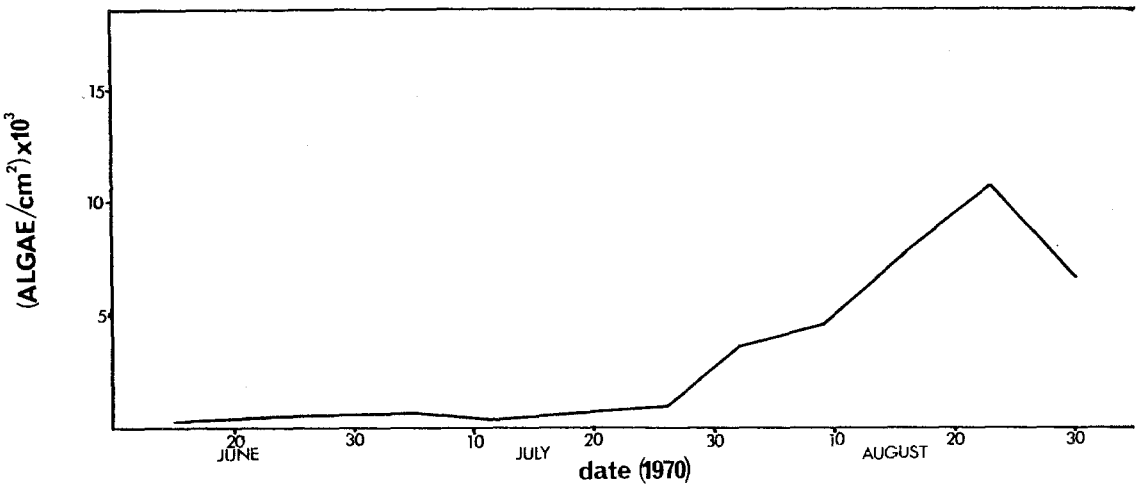

Figure 17. Sedimented Algae, Weekly Averages. Graph of the weekly averages of results from all five stations of analysis for sedimented algae.

By comparing water column and sedimented algae analyses it is apparent that *Tribonema* and *Oedogonium* show increases in numbers on the lake bottom after they have virtually disappeared from the water column. This leads to the conclusion that these algae are able to live and reproduce on the lake bottom.

Horizontal comparison of sedimented algae results show that the numbers of algae are small to moderate to the north and east of the basin (stations R & M). To the west and in the center of the basin (stations P & S) the numbers of algae are moderate to high, while toward the south shore (station N) the values are generally high. This trend correlates with the heavy pollution loads entering the Central Basin from the Western Basin and the south shore (FWPCA, 1968).

SUMMARY AND CONCLUSIONS

Biological studies of "Project Hypo" produced the following findings relating to the processes of oxygen depletion and nutrient regeneration in the Central Basin of Lake Erie.

Algal volumes increased throughout the study in the water column above the hypolimnion. Volumes were generally less than $75x10^4\mu^3$/ml in June as compared to ranges of 100 to $300x10^4\mu^3$/ml in mid-July and 300 to $500x10^4\mu^3$/ml in late August. Maximum peaks over $1{,}000x10^4\mu^3$/ml were noticed after August 24 and occurred at stations which displayed oxygen depletion in the hypolimnion.

Phytoplankton volume increases above the hypolimnion were associated with changes in genera. The low values in June were dominated by the Chrysophyta *Tribonema* and diatom assemblages. The volume increases in July and August were due to the Chlorophyta *Oedogonium* and the Cyanophyta *Anacystis,* respectively. Brief pulses of the Pyrrhophyta *Ceratium* were noticed in early August.

Trends in the phytoplankton were not evident in the hypolimnion; however, algal volumes were considerably less than those in the overlying waters. *Tribonema* and diatoms were dominant through July 29, with *Oedogonium* dominating through August 15 and *Anacystis* through September 1.

Algae of planktonic origin were deposited on the bottom of the Lake Erie Central Basin in July and August. Major depositions as much as $6.33x10^4$ organisms $cm.^{-2}day^{-1}$ dominated by *Oedogonium* and *Tribonema* occurred between July 21 and July 28, and August 1 through August 4. Lesser deposits of $2.84x10^4$ organisms $cm.^{-2}day^{-1}$ dominated by the Chlorophyta genera *Oocystis* and *Staurastrum* were recorded August 19 and 21.

Algae sedimenting to the bottom in late July and early August covered the bottom with a fluffy green layer. This layer of algae on the bottom, mostly *Tribonema* and *Oedogonium*, was associated with small net increases in dissolved oxygen near the bottom and reduced sediment oxygen demand measurements. However, the small net increases in oxygen and reduced sediment oxygen demand measurements did not contribute significantly to the total dissolved oxygen content in the hypolimnion. The matting down of algae, color changes, the occurrence of black patches, August 11-15, and increased sediment oxygen demand rates in September indicated a decline in algal photosynthetic activity.

The dominant genus on the sediment was *Tribonema* which increased in numbers long after declining in dominance in the water column.

The highest counts of sedimented algae 38,271 organisms/cm^2, occurred at the southern nearshore station N. Maximum values of less than 4,275 organisms/cm^2 occurred at the north and easternmost stations R and M.

During most of the study, adequate amounts of light reached the bottom to permit diving operations without artificial light. The duration of light penetrating to the bottom progressively decreased during the study.

The preceding biological findings lead to the following interpretations:

1. Algae, primarily the Chrysophyta *Tribonema* and the Chlorophyta *Oedogonium*, deposited on the bottom were the major source of organic carbon utilized in the consumption of hypolimnetic oxygen as a result of bacterial activity at the water-sediment interface.

2. Algae on the sediments are of planktonic origin; however *Tribonema* and *Oedogonium* maintain growth after light becomes limiting for other sedimenting forms.

3. The mixing of nutrient-rich hypolimnion water into the thermocline and lower epilimnion stimulated algal growth primarily the Cyanophyta *Anacystis* at these levels, particularly at stations where dissolved oxygen depletion in the hypolimnion had been recorded.

4. The period of maximum photosynthetic activity on the bottom was from approximately July 21 to August 10, resulting in a reduced Sediment Oxygen Demand.

5. The decreasing photoperiod and the shading effect of increasing phytoplankton volumes in the overlying waters reduced light on the bottom to biologically limiting levels in mid-August.

6. It is apparent that algae do contribute oxygen to the hypolimnion for a period of time; however, the impact and magnitude of this contribution appears to be masked by stronger oxygen demanding physical and chemical phenomena.

ACKNOWLEDGEMENTS

The authors wish to express their sincere thanks to Mr. Chris Potos, Environmental Protection Agency, Ohio District Office, for his assistance.

The authors also wish to express their sincere thanks to Mr. Charles J. Beier, Jr. for his technical assistance in the construction of sampling instruments, and to Dr. Noel Burns and Mr. Clayton Healy of the Canada Centre for Inland Waters for their valuable assistance in completing the biological studies of Project Hypo.

REFERENCES

FEDERAL WATER POLLUTION CONTROL ADMINISTRATION, 1968. Lake Erie Report, U.S. Dept. of Interior, Gt. Lakes Region.

FRITSCH, F.E. 1961. Structure and Reproduction of the Algae, Vol. 1, University Press, Cambridge.

KLEVENO, C.O., T.E. BRAIDECH, and P.E. GEHRING. 1971. Hypothesis for Dissolved Oxygen Depletion in the Central Basin Hypolimnion of Lake Erie. Proc. 14th Conf. on Great Lakes Research.

POTOS, CHRIS, 1970. Hypolimnetic Oxygen Depletion Mechanisms in Lake Erie. Proc. 13th Conf. on Great Lakes Research. Part 2.

7. *Microbiological Studies Related to Oxygen Depletion and Nutrient Regeneration Processes in the Lake Erie Central Basin*

A.S. Menon
Microbiology Laboratory, Public Health Engineering Division
Department of Fisheries and Forestry
Canada Centre for Inland Waters,
Burlington, Ontario, Canada.

C.V. Marion, Ph.D., and A.N. Miller,
Microbiology Laboratory, U.S. Environmental Protection Agency,
Region V, Fairview Park, Ohio, U.S.A.

The significance of bacterial activity in the overall processes of oxygen depletion and nutrient regeneration in the Central Basin of Lake Erie was assessed. Most intensive bacterial activity occurred at the sediment-water interface. Bacterial decomposition of organic matter accumulating at the interface resulted in the formation of reduced products of low molecular weight and depletion of oxygen in the hypolimnion. These compounds were subsequently oxidized by chemoautotrophic bacteria with further loss of O_2. Reducing conditions on the bottom adversely affected nitrifying bacterial densities. However, actively photosynthesizing algae freshly deposited on the bottom stimulated multiplication of nitrifying bacteria and nitrification.

Large bacterial populations were absent in the thermocline, suggesting that this zone was not a site for intensive bacterial activity. Quantitative analysis indicated that the high bacterial densities in the hypolimnion, especially at the sediment-water interface, respiring at the rate of 2.4×10^{-11} mg O_2 per cell per hour could account for oxygen depletion in the lake.

INTRODUCTION

The effect of bacteria in the overall process of biological productivity in lakes has been studied by many investigators but there is relatively little information on the role played by bacteria as agencies which deplete the oxygen content of the lake. Kusnetzow (1935) and others have shown that the activities of heterotrophic bacteria in the decomposition of organic matter from the sediment and the subsequent oxidation of released methane and hydrogen gases by autotrophic bacteria were the main causes of oxygen depletion in a lake during the period of stratification. Similar conclusions were reached by ZoBell (1940) who investigated the factors which influenced oxygen consumption by bacteria on Lake Mendota. In an effort to understand more fully the mechanisms involved in oxygen depletion and nutrient regeneration in the Central Basin of Lake Erie, a bacteriological study was undertaken during the period July 28 to August 26, 1970.

The aim of the bacteriological study was: (1) to evaluate the distribution of bacterial densities and biotypes at the sediment-water interface and the overlying waters in relation to time, chemical, physical, and biological data, and (2) to try to assess the role they play in the overall processes of oxygen depletion and nutrient regeneration in the hypolimnion.

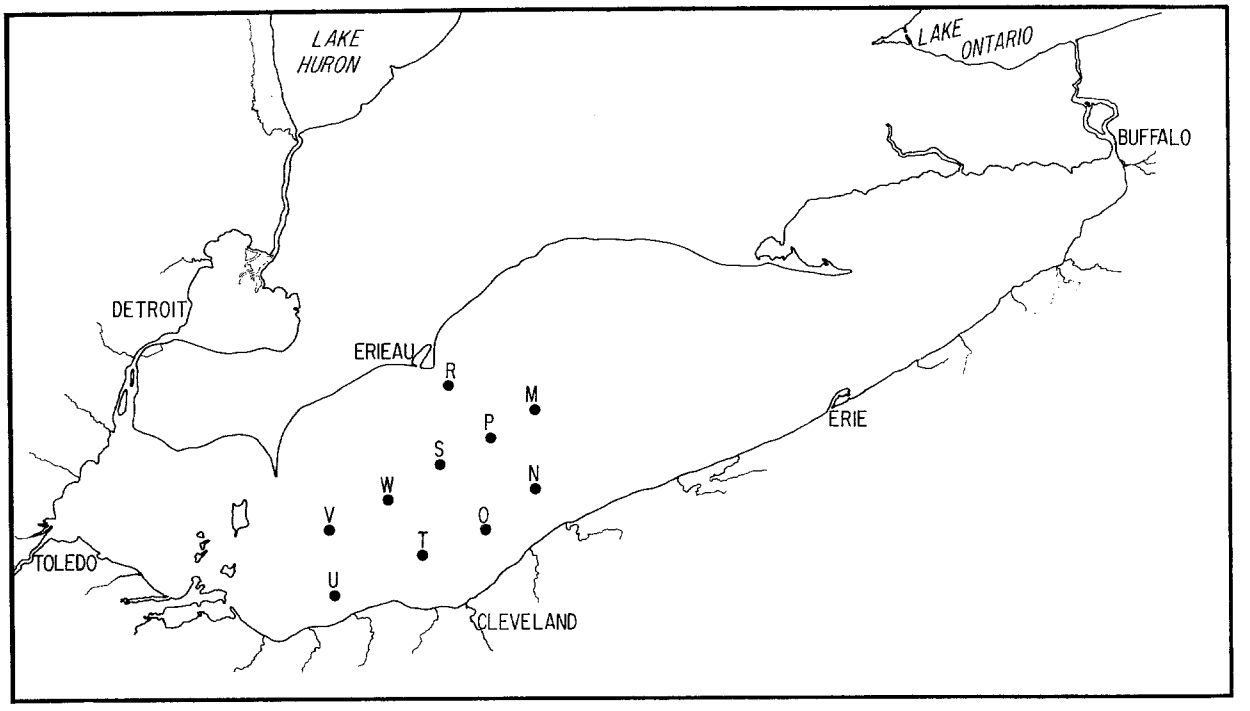

Figure 1. Geographical positions of bacteriological sampling locations within the Central Basin of Lake Erie.

MATERIALS AND METHODS

SAMPLE COLLECTION

Water samples were collected from five major stations (M, N, P, R, and S) with occasional samplings at five additional stations (O, T, U, V, and W) (Figure 1, Table 1 of the Appendix V) at the following depths: A = 2 meters below surface; B = 1 meter above thermocline; C = within thermocline; D = 1 meter below thermocline; E = 2 meters above bottom; F = 3 inches above bottom; G = sediment-water interface; G* = 1 inch above bottom. Water samples from the top five depths (A, B, C, D, and E) were collected by sterilized ZoBell bottles (ZoBell, 1941) and the two bottom depths (F and G) by divers using sterile rubber bulbs. The samples collected were refrigerated and shipped to the laboratory for analysis of the following parameters: aerobic heterotrophic bacteria, anaerobic heterotrophic bacteria, bacterial biomass, nitrifying bacteria (*Nitrosomonas sp.* and *Nitrobacter sp.*), sulfur-oxidizing bacteria (*Thiobacillus sp.*) and sulfate reducing bacteria (*Desulfovibrio sp.*)

LABORATORY PROCEDURES

Aerobic Heterotrophic Bacteria – Aerobic heterotrophic bacterial densities were determined on all samples by the membrane filtration technique using Foot and Taylor medium (Foot and Taylor, 1942, Appendix V) with aerobic incubation at 20°C for 10 days. All dilutions were performed in duplicate and colony counts were read with the aid of a 10-power stereomicroscope. Counts were calculated and recorded in terms of colonies per ml of water.

Anaerobic Heterotrophic Bacteria – Anaerobic heterotrophic bacterial densities were determined on all samples by the membrane filtration technique using a Re-enforced Clostridial Medium (Oxoid-British Drug House) with anaerobic incubation in a anaerobic jar (Gaspak – BBL) at 20°C for 10 days. All dilutions were performed in duplicate and colony counts were read with the aid of a 10-power stereomicroscope. As with aerobic heterotrophs, counts were calculated and recorded in terms of colonies per ml of water.

Bacterial Biomass – Bacterial biomass was determined for the top six depths (A, B, C, D, E, and F) by the coulter counter technique. A fifty ml aliquot water sample was inoculated with one ml of tween 80 (5,000 ppm) and 0.45 gm of sterile NaCl, and shaken mechanically for five minutes. Samples were then prefiltered through a 25-micron stainless steel mesh and the filtrate centrifuged for 10 minutes at 1500 rpm. The supernatant was poured through a Model B coulter counter equipped with 30-micron diameter orifice tube and a J-plotter. The median of three counts was used for all calculations.

The bacterial biomass was calculated by applying the following formula to the size distribution graph which was obtained by the J-plotter (Mulligan and Kingsburg, 1968).

$$\text{Bacterial biomass} = \frac{d}{10^3} \sum_{i=a}^{k} n_i v_i$$

where d = dilution factor, k = upper threshold setting, a = lower threshold setting, n = number of particles at each size interval, and v = average particle volume at each size interval.

Nitrifying Bacteria – Nitrifying bacterial densities were determined by a tube dilution Most Probable Number (MPN) technique (Thompson, 1969) on samples collected from 2 meters below the surface (A), 2 meters above the bottom (E), 3 inches above the bottom (F), and at the sediment-water interface (G). A five test tube series of *Nitrosomonas* Broth Medium (see Appendix V) previously sterilized by autoclaving was inoculated with appropriate aliquots (multiples and submultiples of 1 ml) of each sample. All inoculated tubes were incubated aerobically at 38°C for four weeks. An uninoculated tube of each dilution was included for negative control. At the end of the incubation period, all MPN tubes were checked for the presence of nitrification. A diphenylamine-H_2SO_4 spot test was carried out in the series of *Nitrosomonas* Broth tubes to check for evidence of ammonia oxidation. The development of a deep blue color indicated a positive test for nitrite and nitrate and therefore the presence of nitrifying bacteria. Nitrifying bacterial densities were estimated and recorded in terms of 100 ml of water sample.

Sulfur Oxidizing Bacteria – Sulfur oxidizing bacterial densities (*Thiobacillus thioxidans* and *Thiobacillus thioparus*) were determined by a tube dilution Most Probable Number (MPN) technique (Postgate, 1966) on samples collected from 2 meters below the surface (A), 2 meters above the bottom (E), 3 inches above the bottom (F) and at the sediment-water interface (B). A five test tube series of *Thiobacillus* Broth Medium (see Appendix V) was inoculated with appropriate aliquots of each sample. All inoculated tubes were incubated aerobically at 28°C for three weeks. An uninoculated tube of each dilution was included for negative control. At the end of the incubation period, all MPN tubes were tested for the presence of sulfur oxidation. A positive reaction was indicated by a drop in pH and/or a precipitation of yellow sulfur on the wall of the test tubes when compared to the negative controls. Sulfur-oxidizing bacterial densities were estimated and recorded in terms of 100 ml of water sample.

Sulfate-Reducing Bacteria – Sulfate-reducing bacterial densities (*Desulfovibrio sp.*) were determined on samples by a tube dilution, Most Probable Number (MPN) technique (Starkey, 1948) collected from 2 meters below the surface (A), 1 meter below the thermocline (B), 2 meters above the bottom (E), 3 inches above the bottom (F), and at the sediment-water interface (G). A five test tube series of Starkey's Broth Medium (see Appendix V) was inoculated with appropriate aliquots of each sample. Approximately one inch of sterilized mineral oil was added on top of each inoculated tube to ensure anaerobic conditions. All inoculated tubes were incubated anaerobically at 28°C for two weeks. At the end of the incubation period, all MPN tubes were tested for the presence of sulfide production. A positive reaction was indicated by the presence of a black precipitate (ferrous sulfide) and production of a yellow precipitate (cadmium sulfide) when three drops of cadmium chloride were added to each tube. Sulfate-reducing bacterial densities were estimated and recorded in terms of 100 ml of water sample.

RESULTS AND DISCUSSION

VERTICAL DISTRIBUTION OF BACTERIAL POPULATIONS

The bacteriological data obtained from all sampling stations (M, N, O, P, R, S, T, U, V, and W) are presented in Tables 2 to 9 of Appendix V. The mean vertical distribution of bacterial parameters,

TABLE I. Mean Vertical Distribution of all Bacterial Parameters for the Five Major Stations, – M, N, R, P and S.

Depth	Aerobic Heterotrophs per ml	Anaerobic Heterotrophs per ml	Nitrifying Bacteria per 100 ml	*Thiobacillus sp.* per 100 ml	*Desulfovibrio sp.* per 100 ml	Bacterial Biomass µg/liter
A	490	18	<2	8	<2	217.3
B	600	26	–	–	–	187.3
C	1,000	39	–	–		170.9
D	1,500	58	–	–	30	181.9
E	1,900	83	<2	9	50	183.7
F	3,000	590	<2	12	300	232.6
G	3.6×10^6	8.5×10^5	870	2.0×10^4	3.9×10^5	–

A = 2 meters below surface
B = 1 meter above thermocline
C = Within thermocline
D = 1 meter below thermocline
E = 2 meters above bottom
F = 3 inches above bottom
G = Sediment-water interface

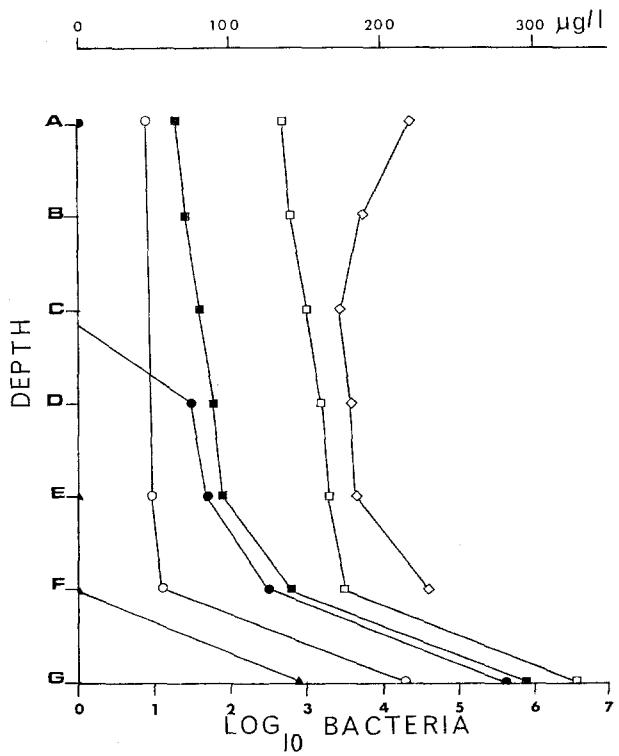

Figure 2. Mean vertical distribution of all bacterial parameters for the five major stations M, N, P, R, and S. Key: ▲ nitrifying bacteria per 100 ml; ● *desulfovibrio sp.* per 100 ml; ○ *thiobacillus sp.* per 100 ml; ■ anaerobic heterotrophs, per ml at 20°C; □ aerobic heterotrophs per ml at 20°C; ◇ bacterial biomass in ug/l.

temperature, and dissolved oxygen at the five major stations is graphically illustrated in Figures 1 to 5 of the Appendix. Nitrifying bacteria, which were found only at the sediment-water interface, are not presented in these figures. A sharp temperature stratification and progressive depletion of oxygen with time and depth in the hypolimnion were observed at all sampling stations during the period of investigation. With the exception of Stations U, V, and W, which became anoxic near the end of the survey, there was still some oxygen left in the hypolimnion at all stations.

All bacterial parameters studied – aerobic heterotrophs, anaerobic heterotrophs, bacterial biomass, nitrifying bacteria, sulfur-oxidizing bacteria, and sulfate-reducing bacteria – indicated significantly higher densities in the hypolimnion than in the epilimnion (Table 1, Figure 2). The large bacterial population observed in the stratified water column near the bottom is apparently the result of a concentration gradient of nutrients and particulate matter which provided a suitable milieu for the growth of bacteria settling downward from the overlying waters and microorganisms moving upwards into this zone from the densely populated sediment layer.

AEROBIC AND ANAEROBIC HETEROTHROPHIC BACTERIA

Aerobic heterotroph densities were consistently higher than anaerobic heterotroph densities in all samples, but nevertheless showed a similar distribution with respect to time (Figures 3 and 4). A statistical analysis of all the samples tested for heterotrophic bacteria showed that 81 percent of the samples contained over 90 percent aerobes (Table 2).

At major station P, aerobic heterotrophic bacterial densities in the epilimnion ranged from 140 to 2,300 per ml; in the thermocline from 340 to 3,100 per ml; in the hypolimnion from 460 to 11,000 per ml; and at the sediment-water interface from 1.2×10^5 to 8.8×10^6 per ml. The anaerobic heterotrophic bacterial densities were generally very low in the water column ($<$ 10 to 6,500 per ml) but were very high at the sediment-water interface (9.8×10^3 to 1.6×10^6 per ml).

The existence of a density gradient of increasing heterotrophic bacterial densities with depth from the epilimnion to the sediment, concomitant with an absence of any large bacterial populations within the thermocline, indicated that the thermocline is not an active site for intensive bacterial activity. The belief that the thermocline acts as a retention zone for plankton and detritus which provide a site for bacterial attachment and multiplication may need re-examination.

The bacterial biomass data indicated two maxima – one at 2 meters below the surface and the other at three inches above the bottom.

A close relationship between heterotrophic bacterial densities and algal rains (camera documented, pg 30) was observed in the hypolimnion at all stations. At station P, heterotrophic bacterial densities sharply increased after August 1 following the first algal rain on July 29; subsequent intermittent algal rains maintained the heterotrophic bacterial densities at a relatively high level for the remainder of the

TABLE II. Percentage of Aerobic Heterotrophic Bacteria from the Total Number of Heterotrophic Bacteria (Aerobes and Anaerobes) at all Stations.

Zone	No. of Samples	Percentages of Aerobes of Total Heterotrophic Population		
		100-95%	95-90%	<90%
Epilimnion	72	.65*	.14*	.21*
Thermocline	35	.57	.26	.17
Hypolimnion	95	.55	.24	.21
Sediment-water Interface	35	.55	.09	.14
TOTAL	237	.62	.19	.19

*These columns denote the fraction of the sampling which fits into the respective aerobic population groups.

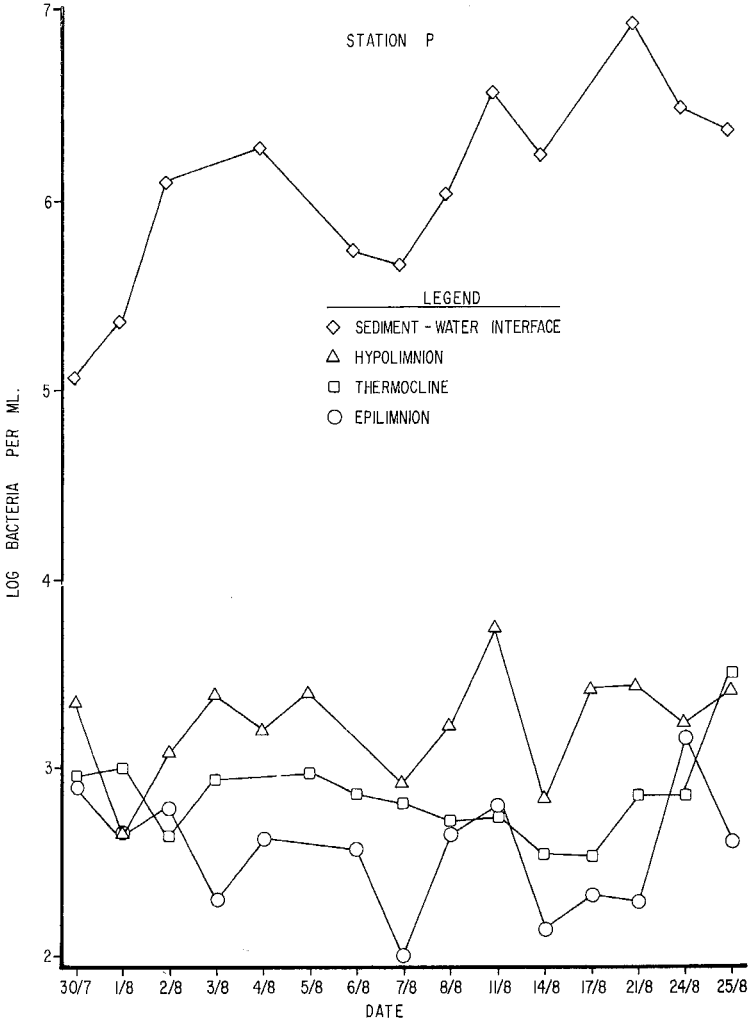

Figure 3. Vertical-time distributions of aerobic heterotrophs per ml at 20°C.

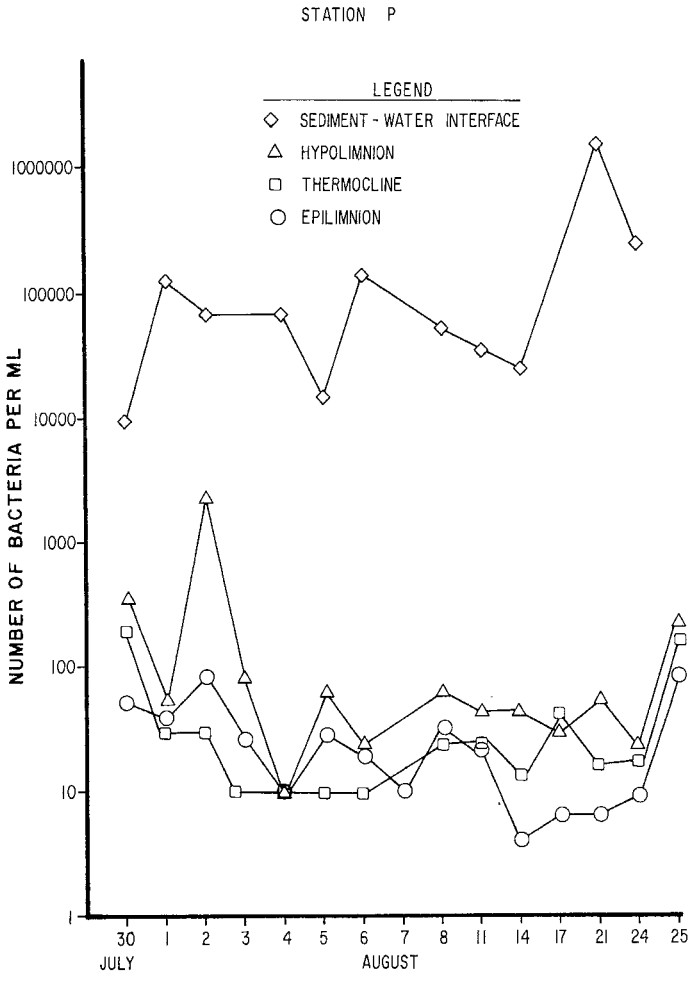

Figure 4. Vertical-time distributions of anaerobic heterotrophs per ml at 20°C.

study (Figure 3). This observation agrees with the theory of Henrici (1938) that . . . "the production of organic matter by plankton organisms is an important factor in determining the number of bacteria in water . . ."

Nitrifying bacteria (23-3500 per 100 ml) were only found at the sediment-water interface, suggesting that bacterial nitrification occurs primarily at this boundary and not in the overlying water. This finding agreed with Quastel's (1954) observation that the adsorption and concentration of nitrifying bacteria and ammonium ions onto clay particles is an important factor in nitrification. The failure to detect any nitrifiers in the water column might be due to the minimal chance of contact between cell and ammonium ion, and also the nitrifier densities were so low that they could not be detected by the MPN analysis of small aliquot samples.

A significant correlation between nitrifying bacterial densities, algal rains, ammonia, and nitrate was observed in the hypolimnion at stations N, R and S (Figure 5-7). A sharp decrease in nitrifying bacterial densities was observed at station S, from 3,500 per 100 ml on August 12 to 70 per 100 ml on August 17 when the black patches of what apparently was ferrous sulfide first appeared on the bottom. A similar phenomenon was observed at station N where the nitrifying bacterial densities dropped from 3,500 per 100 ml on August 12 to less than 200 per 100 ml on August 17 when the black patches appeared.

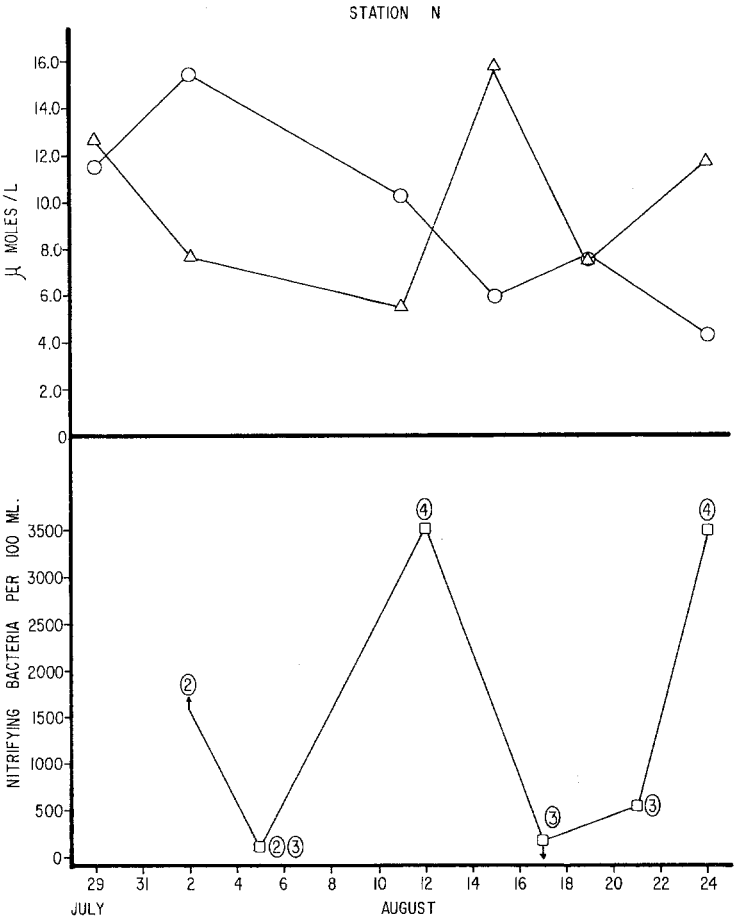

Figure 5. Relationship between nitrifying bacterial densities, nitrate and ammonia concentrations, algal rains, and bottom deposits of algae and/or ferrous sulfide (black patches) at station N. Key: □ nitrifying bacteria per 100 ml; ○ ammonia in μmoles/1; △ nitrate in μmoles/l; 2-algae on bottom; 3-black patches on bottom; 4-thin layer of sediment or algae over black patches; ↑ greater than value indicated; ↓ less than value indicated.

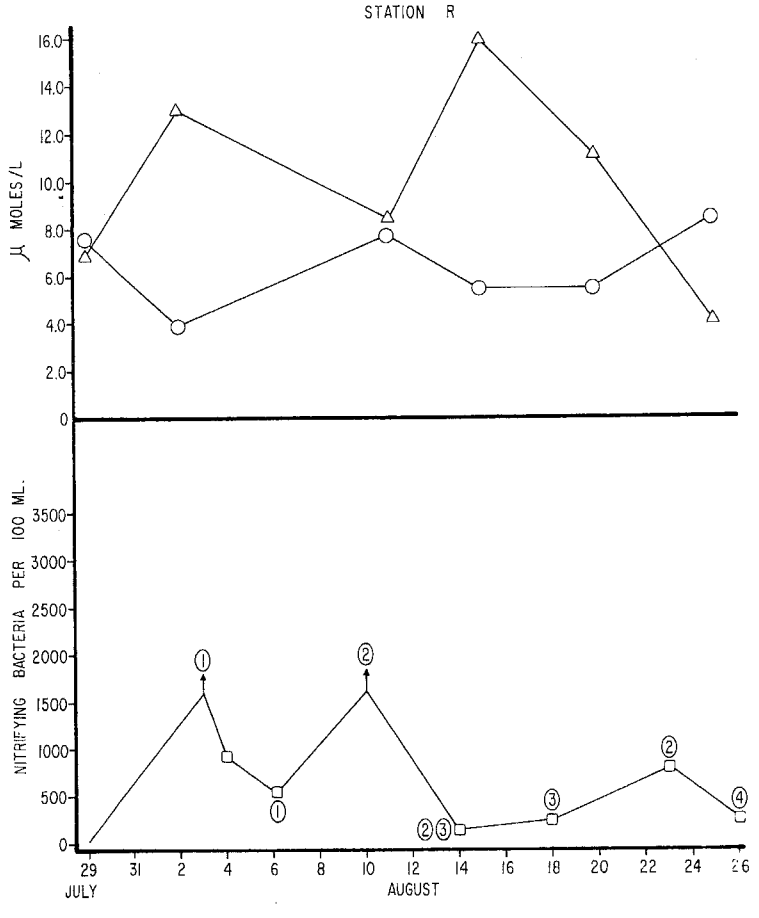

Figure 6. Relationship between nitrifying bacterial densities, nitrate and ammonia concentrations, algal rains, and bottom deposits of algae and/or ferrous sulfide (black patches) at station R. Key: □ nitrifying bacteria per 100 ml; ○ ammonia in μmoles/l; △ nitrate in μmoles/l; 1-algal rain; 2-algae on bottom; 3-black patches on bottom; 4-thin layer of sediment or algae over black patches; ↑ greater than value indicated.

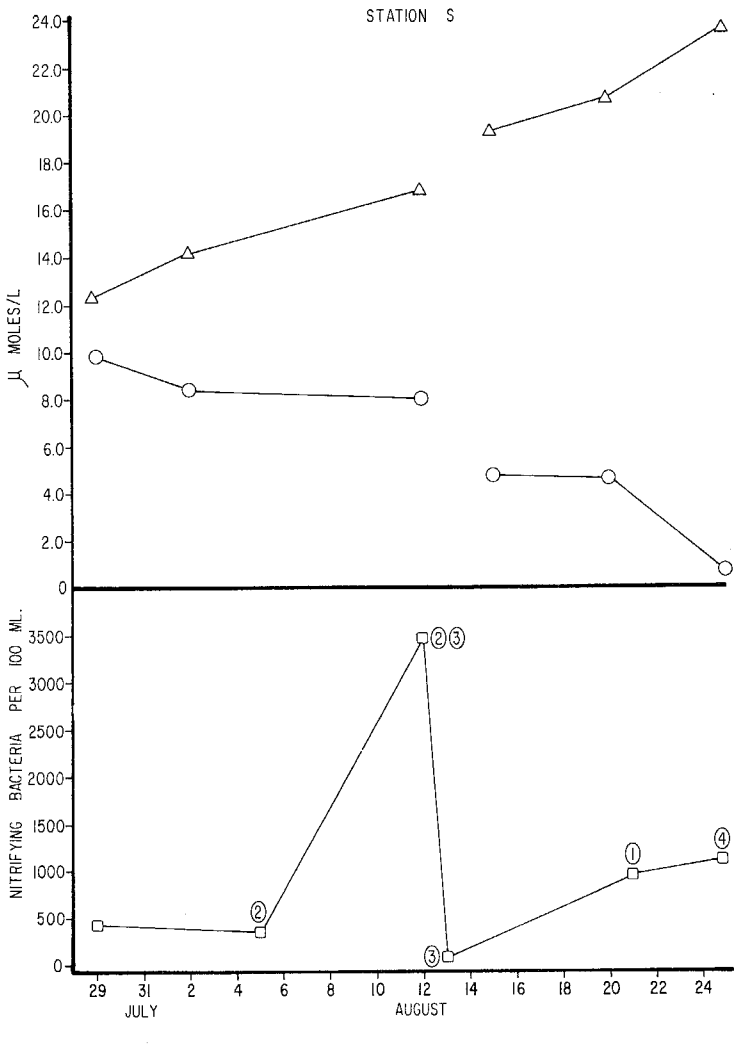

Figure 7. Relationship between nitrifying bacterial densities, nitrate and ammonia concentrations, algal rains, and bottom deposits of algae and/or ferrous sulfide (black patches) at station S. Key: □ nitrifying bacteria per 100 ml; ○ ammonia in μmoles/l; △ nitrate in μmoles/l; 1-algal rain; 2-algae on bottom; 3-black patches on bottom; 4-thin layer of sediment or algae over black patches.

During the same period, nitrate concentrations decreased from 15.8 micromoles/1 to 7.6 micromoles/1 and was followed by an increase of ammonia from 6.0 micromoles/1 to 7.5 micromoles/1 at 20-meter depth at station N. This dramatic decrease in the nitrifying bacterial densities following the appearance of the black patches might have been caused by the development of a reducing condition at the sediment-water interface, and perhaps also to the direct toxic effect of H_2S. The reducing condition was probably caused by heterotrophic bacterial decomposition of accumulated dead algae on the bottom, resulting in oxygen depletion and production of hydrogen sulfide and other low molecular weight reducing products.

Immediately following the next algal rain, the nitrifying bacterial densities at station S increased to 950 per 100 ml accompanied by an increase of nitrate concentration from 16.8 micromoles/1 to 23.6 micromoles/1 and a decrease of ammonia concentration from 8 micromoles/1 to 0.7 micromoles/1 at the 22-meter depth. Concurrently, the nitrifying bacterial densities at station N increased to 3,500 per 100 ml on August 24, followed by an increase in nitrate concentration from 7.6 micromoles/1 to 11.7 micromoles/1 and a concomitant decrease in ammonia concentration from 7.5 micromoles/1 to 4.4 micromoles/1. This suggests the freshly deposited photosynthesizing algae (divers' observation) refurnished the organic supplies and raised the Eh and oxygen tension at the sediment-water interface sufficiently to stimulate the multiplication of nitrifying bacteria and the process of bacterial nitrification.

SULFUR OXIDIZING AND SULFATE REDUCING BACTERIA

Thiobacillus sp. were found throughout the water column with maximum density (10^3 – 10^5 per 100 ml) at the sediment-water interface. *Thiobacillus sp.* densities were generally very low (< 2 to 23 per 100 ml) in the hypolimnion water before August 6, but were comparatively higher (< 2 to 110 per 100 ml) toward the end of the study.

Desulfovibrio sp. were not detected in samples at two meters below the surface where the dissolved oxygen measured 8.2 – 10.6 mg/1, however, comparatively high densities were found in the hypolimnion where the dissolved oxygen fell below 1.5 – 2 mg/1 (Fig. 8). These bacteria were particularly active at the sediment-water interface (10^3 – 10^6 per 100 ml were found) where there were sufficient amounts of readily decomposable organic matter available for bacterial growth. They reduced the sulfate in the sediment to hydrogen sulfide which could either be fixed as ferrous sulfide (black patches observed at the sediment surface) or escape to the overlying waters. The released hydrogen sulfide was then oxidized either abiologically or by sulfur oxidizing bacteria to elemental sulfur and sulfate, resulting in the loss of oxygen from the hypolimnion (Baas-Becking and Wood, 1955). Sorokin (1964) reported that the hydrogen sulfide produced on the bottom of the Black Sea was primarily responsible for the prevailing anaerobic condition in the overlying waters.

A significant trend of time-wise increase in *Desulfovibrio sp.* and *Thiobacillus sp.* densities from the sediment-water interface to one meter below the thermocline was observed as the degree of oxygen depletion became more pronounced (Figs. 9 and 10). The mechanisms involved in this upward migration of sulfur bacteria from the bottom with progressive oxygen depletion might be similar to that discussed by Ruttner (1963). These sulfur bacteria were so high at the sediment-water interface that they might sometimes become visible to the naked eye as a white cover scattered on the bottom sediments. Underwater photographs revealed many white clouds of suspected bacteria in the vicinity of the black patches at the bottom. Microscopic analysis of specimens taken from these white clouds did show them to be bacteria. A similar observation of white clouds of sulfur bacteria on the sediments was reported by Fenchel and Riedl (1970).

FALL OVERTURN

After the fall overturn, all bacterial parameters were fairly evenly distributed throughout the water column at stations M, N, P, R, S, and W (Table 9 of Appendix V). These results suggest that the mixing of the water column caused by the breakdown of thermal stratification was responsible for the uniform re-distribution of bacteria throughout the water column. A similar observation was found in Lake Ontario during the spring overturn (Menon *et al.*, 1970).

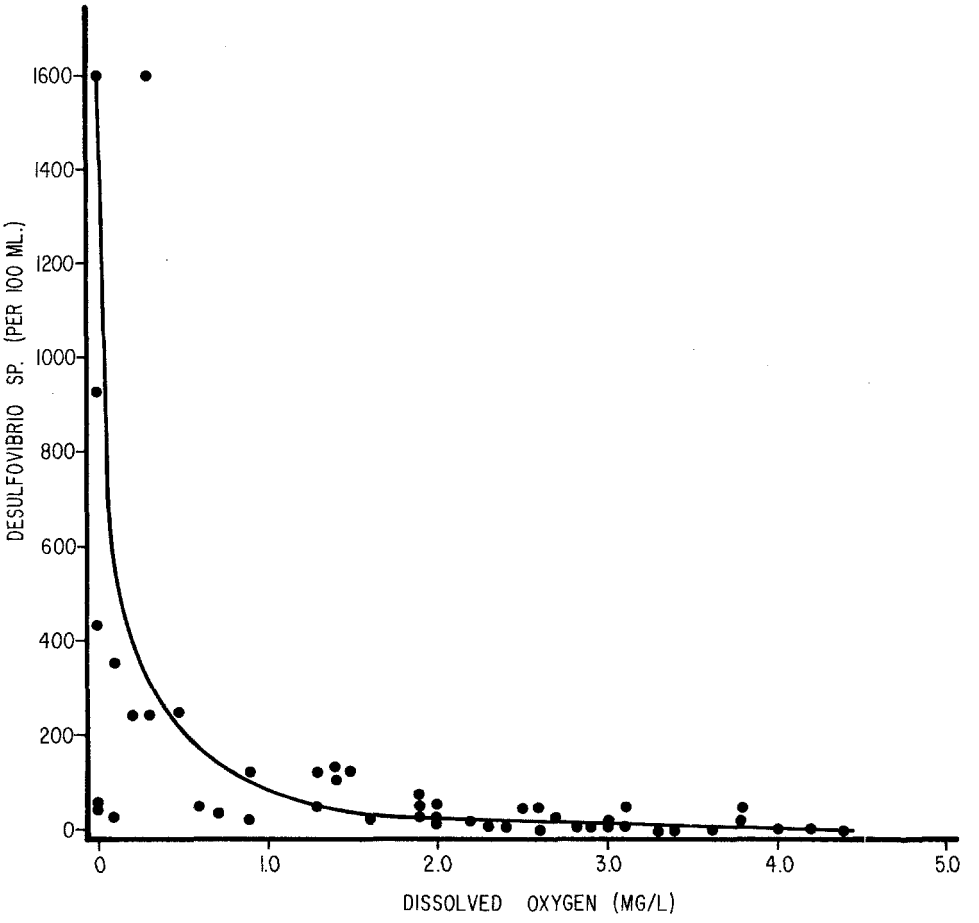

Figure 8. Relationship between *Desulfovibrio sp.* densities and dissolved oxygen.

DEOXYGENATION CALCULATIONS

To determine whether bacterial respiration could account for the observed oxygen loss in the hypolimnion, the following calculations were made. The average hypolimnion volume in the Central Basin was found to be 31.5 km^3, and in this volume, organic decomposition utilized 3.56×10^9 moles of oxygen from July 30 to August 25, 1970 (Burns and Ross, pg 106).

From the laboratory analysis, using ZoBell's method (1940) and applying the formular of Buchanan and Fulmer (1930):

$$m = \frac{2.303\ S \log b/B}{t\ (b\text{-}B)}$$

where m is the oxygen consumed per cell in time t;

S = the total amount of oxygen consumed in time t;
B = the initial bacterial density; and
b = the bacterial density after time t;

it was found that the average rate of oxygen uptake by bacteria at 10°C was 2.4×10^{-11} mg of oxygen per cell per hour (Table 3). Liagina and Kusnetzow (1937) reported that the bacteria from Lake Glubokoje consumed an average of 1.9 to 3.0×10^{-11} mg of oxygen per cell per hour at 10°C and 15°C respectively. While ZoBell (1940) found that the bacteria from Lake Mendota consumed oxygen at the rate of 0.9 to 2.0×10^{-11} mg of oxygen per cell per hour at 8°C and 18°C respectively.

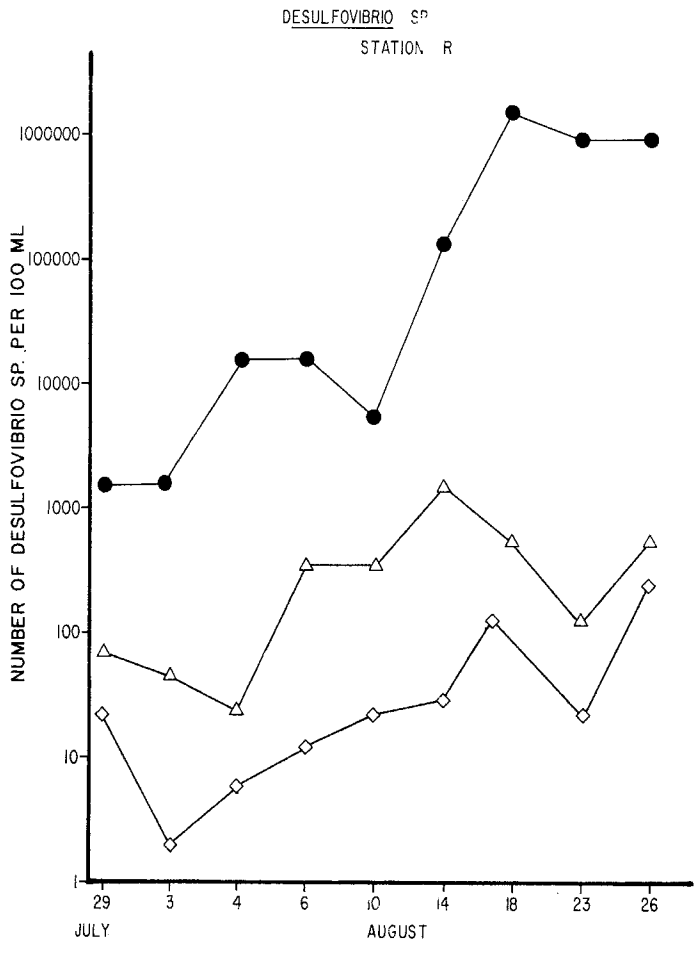

Figure 9. Vertical distribution of *Desulfovibrio sp.* with time at station R. (◇2 meters above bottom, △3 inches above bottom, •sediment-water interface)

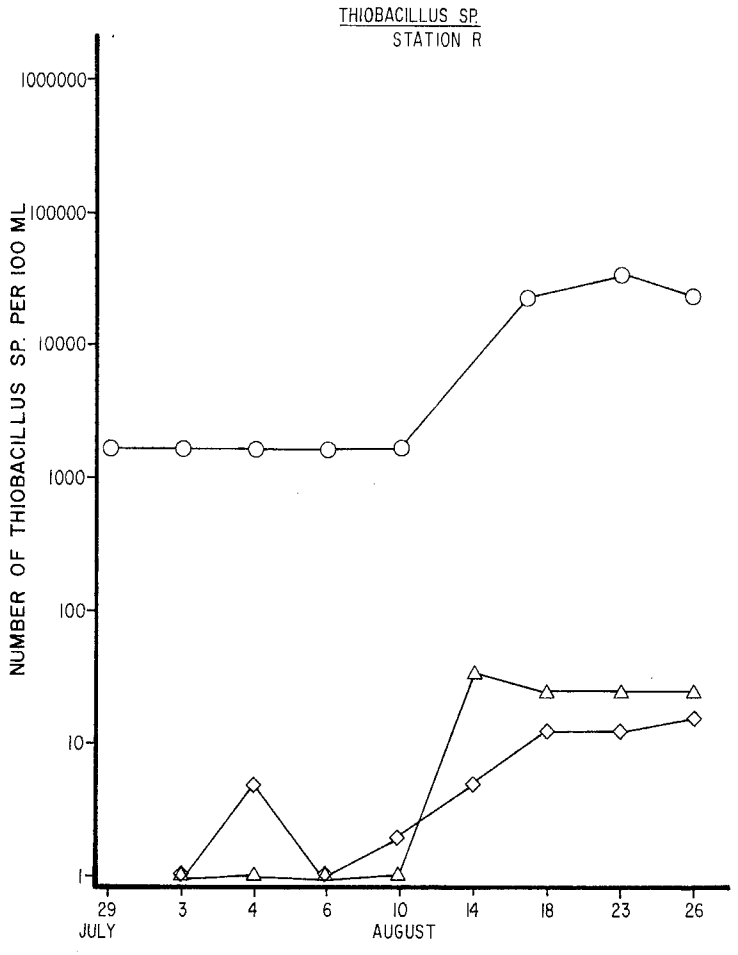

Figure 10. Vertical distribution of *Thiobacillus sp.* with time at station R. (◇2 meters above bottom, △3 inches above bottom, ○sediment-water interface)

TABLE III. Determination of the Rate of Oxygen Uptake by Bacteria in Lake Water at 10°C.

Lake Water	Dissolved Oxygen in mg/1			Bacterial Densities per ml		Rate of Oxygen Uptake in mg per Hour per Bacteria
	Initial	2 Days	Loss	Initial	2 Days	
Sample 1	9.7	9.1	0.6	2.9×10^5	8.7×10^5	2.37×10^{-11}
Sample 2	7.2	6.8	0.4	2.2×10^5	5.1×10^5	2.42×10^{-11}
Sample 3	5.2	5.15	0.05	3.1×10^4	6.1×10^4	2.35×10^{-11}

Since the bacterial densities obtained from the plate counts represent only those viable bacteria able to grow under the provided conditions (medium and temperature) and not the actual population in the lake, assumptions were made to correct the total bacterial densities in the hypolimnion. If the correction factor for plate counts is ten and the dilution factor for the sediment-water interface sample is three (two parts of water to one part of mud was observed in the collected sample), then the bacteria respiring at 2.4×10^{-11} mg of oxygen per cell per hour would utilize 2.8×10^8 moles of oxygen in the hypolimnion and 6.49×10^9 moles of oxygen at the sediment-water interface (Table 4). This was more than the amount of oxygen (3.56×10^{-9} moles) actually lost during the period of study. This indicated that bacteria were not operating at full efficiency, especially at the sediment-water interface where organic matter was more resistant to bacterial oxidation than in the overlying waters and where the oxygen tension often fell below 0.3 mg/1 at which concentration the bacterial respiration rates are decreased (ZoBell, 1940). Nevertheless, calculations do strongly suggest that bacterial respiration in the hypolimnion, especially at the sediment-water interface where high bacterial densities were found (thousands of times higher than that in the overlying waters), could easily account for the oxygen depletion in the Central Basin of Lake Erie.

CONCLUSIONS

The sediment-water interface was found to be the major site of intensive bacterial activity. The organic deposits from the algal rains and other sources which accumulated at the bottom underwent bacterial decomposition resulting in oxygen depletion and the formation of reduced products of low molecular weight. The reduced products were subsequently oxidized by chemoautotrophic bacteria at the sediment-water interface, or in the overlying waters, resulting in additional oxygen depletion. This process repeated itself after each algal rain, causing further loss of oxygen.

The precipitation of particulate matter through the hypolimnion from intermittent algal rains was primarily responsible for the high bacterial densities in the hypolimnion because the

TABLE IV. Amount of Oxygen Consumed by Heterotrophic Bacteria in the Hypolimnion of Lake Erie Central Basin.

Depth	Volume ml.	Corrected Average Aerobic Heterotrophs per ml	Total Aerobic Heterotrophic Bacterial Densities	Amount of Oxygen Possibly Consumed in 26.3 days	Percentage Of Oxygen Loss in The Hypolimnion	Efficiency of Bacterial Respiration
D	6.1×10^{15}	1.5×10^4	9.1×10^{19}	4.4×10^7	1.2%	100%
E	2.3×10^{16}	1.9×10^4	4.4×10^{20}	2.1×10^8	5.9%	100%
F	1.9×10^{15}	3.0×10^4	5.7×10^{19}	2.7×10^7	0.8%	100%
G	1.28×10^{14}	1.08×10^8	1.37×10^{22}	6.49×10^9		100%
				(3.28×10^9)	(92.1%)	50.5%

D = 1 meter below thermocline
E = 2 meters above bottom
F = 3 inches above bottom
G = Sediment-water interface

phytoplankton constituted a locus for bacterial attachment and produced soluble organic substrates for bacterial growth.

The thermocline was not the site of most intensive bacterial activity as indicated by the absence of any large population of heterotrophic bacteria. The belief that the thermocline is a zone of retention of plankton and detritus which provide a site for bacterial attachment and multiplication may require re-examination.

Nitrifying bacterial densities and nitrification decreased sharply when black patches of ferrous sulfide appeared at the sediment-water interface. These results suggest that reducing and toxic conditions produced by organic decomposition and H_2S depressed bacterial nitrification, whereas actively photosynthesizing algae deposited on the bottom stimulated bacterial nitrification.

A significant correlation was obtained between *Desulfovibrio sp.* densities and the degree of oxygen depletion. As the dissolved oxygen content of the hypolimnion was progressively depleted from the sediment upwards, there was a corresponding increase in *Desulfovibrio sp.* densities in the same direction. The increase was more pronounced after the dissolved oxygen content fell below 1.5 to 2 mg/1. The belief that these bacteria are strict anaerobes may require re-examination. Since some of these bacteria were found to tolerate moderate amounts of oxygen as shown in this study, it would appear that they may be either facultative anaerobes or microaerophiles rather than strict anaerobes.

Calculations indicate that high bacterial densities in the hypolimnion, especially at the sediment-water interface, respiring at the rate of 2.4×10^{-11} mg oxygen per cell per hour could easily account for the oxygen depletion in the lake. Furthermore, the oxidation of hydrogen sulfide, ammonia, and methane by chemoautotrophic bacteria also utilizes appreciable amounts of oxygen (ZoBell, 1940). These factors strongly suggest that the activities of heterotrophic and chemoautotrophic bacteria are the principal factors in depleting oxygen in the hypolimnion of the Central Basin of Lake Erie.

ACKNOWLEDGEMENTS

The authors wish to thank the scientific and operational staffs of the bacteriological laboratories, Public Health Engineering Division, Department of National Health and Welfare, Kingston, Ontario, Canada Centre for Inland Waters, Burlington, Ontario and Environmental Protection Agency, Fairview Park, Ohio, for their efforts in making this report possible. Particular appreciation is extended to N.M. Burns and C. Ross, and the Biology Staff, E.P.A., OHDO, for exchanging with the authors their conclusions and findings.

REFERENCES

BAAS-BECKING, L.G.M., and E.J.F. WOOD. 1955. Biological processes in the estuarine environment I and II. Ecology of sulfur cycle. K. Nederlandse akademie van wetenschappen, Amsterdam, Proc. Series B., 58: 160-181.

BUCHANAN, R.E., and E.K. FULMER. 1930. Physiology and Biochemistry of Bacteria. Williams and Wilkins Co., Baltimore, Vol. 3, p. 154.

FENCHEL, T.T., and R.J. RIEDL. 1970. The sulfide system: a new biotic community underneath the oxidized layer of marine sand bottoms. Marine Biology, 7: 255-268.

FOOT, C.H., and C.B. TAYLOR. 1942. The influence of the composition of the medium on the growth of bacteria from water. Proceedings of the Society of Agricultural Bacteriologists, Vol. L: 11-13.

HENRICI, A.T. 1938. Studies of freshwater bacteria. J. Bacteriol., 35: 129.

KUSNETZOW, S.I. 1935. Microbiological researches in the study of the oxygenous regimen of lakes. Verhandl, d. Internat. Vereinigung f. theor. u. angew. Limnologie, 7: 562-582.

LIAGIAN, N.M., and KUSNETZOW, S.I. 1937. The determination of the intensity of respiration of some species of water bacteria at various temperatures under laboratory conditions. Microbiol., 6: 21-27.

MENON, A.S., B.J. DUTKA, and A.A. JURKOVIC. 1970. Preliminary bacteriological investigation of the Lake Ontario thermal bar. Proceedings of 14th Conference on Great Lakes Research, Toronto, Canada, April 19-21, 1971.

MULLIGAN, H.F., and J.M. KINGSBURY. 1968. Application of an electronic particle counter in analyzing natural populations of phytoplankton. Limnol. Oceanog., 13: 499-506.

POSTGATE, J.R. 1966. Media for sulfur bacteria. Journal of Lab. Practice 15: 1239-1244.

QUASTEL, J.H. 1954. Soil Metabolism, Roy. Soc. (London) Proc. B., 143: 159-178.

RUTTNER, F. 1963. Fundamentals of Limnology. (English Translation) 3rd Ed., University of Toronto Press, p. 203.

SOROKIN, YU. I. 1964. On the primary production and bacterial activities in the Black Sea. J. l'Explor. Mer. 29: 41-60.

STARKEY, R.L. 1948. Characteristic and cultivation of sulfate-reducing bacteria. Journal Amer. Water Works Assn., 40: 1291-1298.

THOMPSON, F. 1969. An investigation into the distribution of autotrophic and heterotrophic bacteria in Little Round Lake, with particular emphasis on some bacterial agents of the sulfur cycle. Bacteriological Branch, Division of Laboratories, Ontario Water Resources Commission, p. 32.

ZOBELL, C.E. 1940. Some factors which influence oxygen consumption by bacteria in lake water. Biological Bulletin, 78: 388-402.

ZOBELL, C.E. 1941. Apparatus for collecting water samples from different depths for bacteriological analysis. J. Mar. Res., 4: 173-188.

8. Oxygen-Nutrient Relationships within the Central Basin of Lake Erie

N.M. Burns
Canada Centre for Inland Waters
Burlington, Ontario, Canada

C. Ross
U.S. Environmental Protection Agency, Region V,
Fairview Park, Ohio, U.S.A.

Seven intensive chemical surveys of the Central Basin of Lake Erie were carried out at 4-day intervals during the month of August 1970. Special emphasis was placed on measuring the oxygen and nutrient levels in the hypolimnion. The volume of the hypolimnion was seen to increase during the study and a model has been developed for the calculation of the quantities of materials transferred into the hypolimnion. The complete oxygen depletion pattern was seen to develop first in the western part of the basin and proceed eastwards. The progression was faster in the shallow areas, especially along the south shore. The majority of the oxygen depletion was due to organic decay. Iron, manganese and phosphorus concentrations were seen to increase dramatically when the water became anoxic. A large increase in the chlorophyll content in the epilimnion water was noted when the anoxic hypolimnion water began to mix with the surface water. It appears necessary that oxygenated conditions be maintained in the water as a simple mechanism for ensuring that little of the phosphorus in the sediments returns to the overlying water.

INTRODUCTION

During the planning stages of "Project Hypo", the decision was made to carry out the chemical investigation as quantitatively as possible. It was considered necessary to move beyond the level of the understanding of the system where correlations were observed between simultaneous changes in variables, to the level of trying to establish cause and effect relationships. Thus, efforts were made to plan the sampling and analysis programs such that chemical budget calculations were possible on the components within the hypolimnion. It was decided that knowledge only of changes in the concentrations of the chemical components with time would probably be insufficient to elucidate many of the complex mechanisms which would occur and that further knowledge of the masses of water involved in the various changes was also necessary.

METHODS AND PROCEDURES

It is no simple matter to be quantitative about the Lake Erie Central Basin hypolimnion. It is a thin sheet of cold water having an average thickness of 2.5 meters extending almost 6,000 sq. miles and lying under an average depth of 17.5 meters of thermocline and surface water. However, the implementation of the study was greatly aided by use of an electronic bathythermograph (E.B.T.) which gave a continuous readout of temperature vs depth on an x-y recorder. The instrument had an absolute accuracy of approximately 0.1°C and 0.3 m depth, but relative changes in depth of 0.1 m could be detected. This instrument was strapped to a submersible pump which was used to sample the water. By means of the combination of the two instruments it was possible to have accurate knowledge of the temperature and depth of the water being sampled. By moving the pump up and down it was even possible

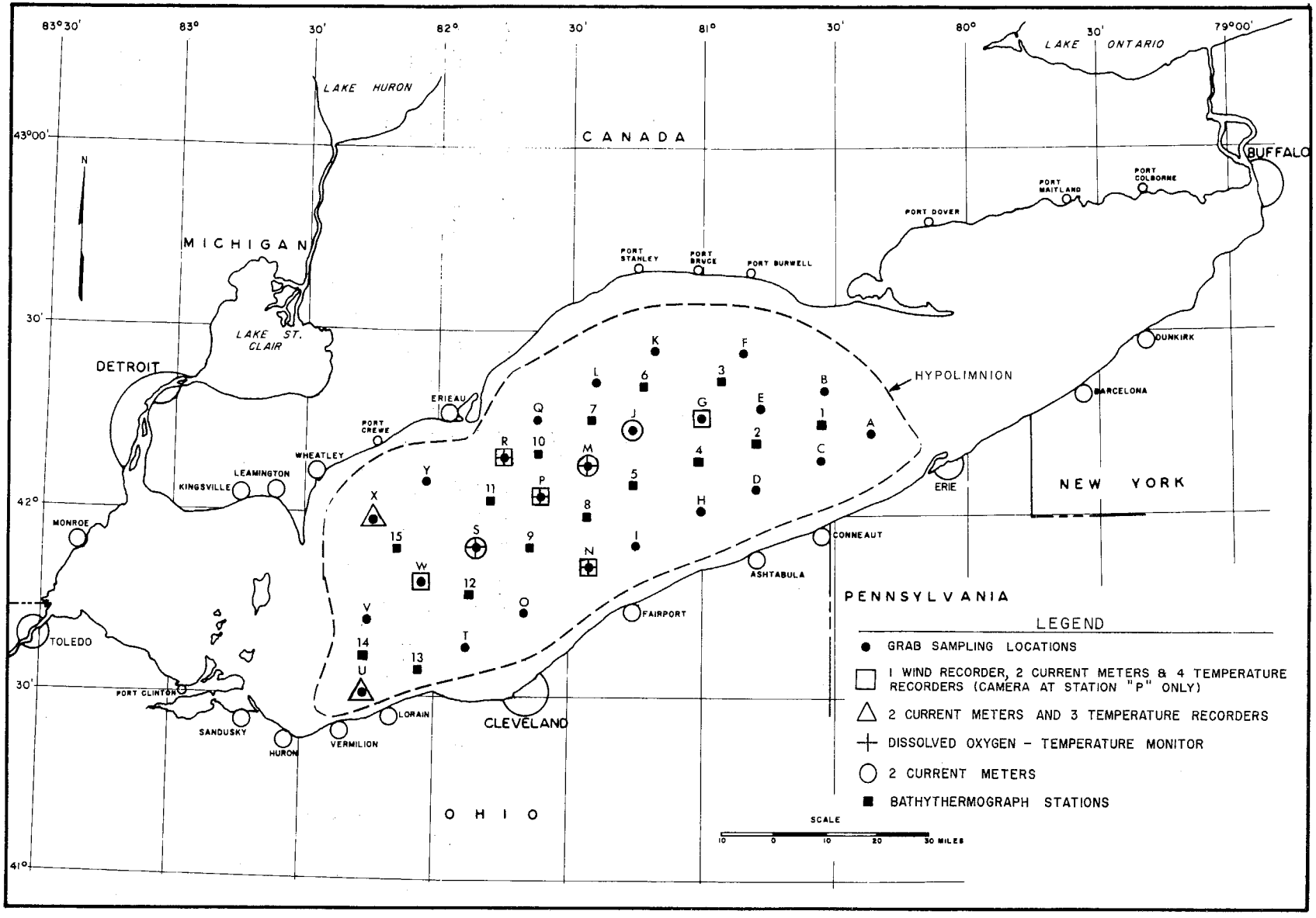

Figure 1. Position of sampling stations and equipment during "Project Hypo".

to sample the middle of the thermocline while it was undergoing internal wave activity. The necessity of the instrument combination in sampling the hypolimnion was only realized after it broke down at the end of Survey 2. The conventional method of oceanographic-type sampling with Van Dorn bottles was used during Survey 3 but it was found to be difficult to obtain hypolimnion samples which were not contaminated with thermocline water. Hence, the results of Survey 3 have not been used in the budget calculations presented here.

Twenty five sampling stations were set up across the Central Basin of Lake Erie and seven surveys of the basin were conducted in the space of 28 days; each survey taking between two and three days and spaced approximately 4 days apart. The positions of the stations are shown in Figure 1.

Water samples were taken from the leeward side of the ship. The E.B.T.-pump was lowered to within 1.0 m of the bottom thereby measuring the thermal structure of the water column. The hypolimnion was then sampled moving upwards, at one meter intervals; the pump was then raised through the thermocline and two surface water samples taken, the first at 1.0 m above the thermocline (mesolimnion) and the second at 1.0 m from the surface. At the five major stations (M, N, P, R, S) mid-thermocline samples were taken when possible.

The list of parameters measured at all the stations was fairly extensive being: dissolved oxygen, pH, Eh, suspended mineral, total CO_2, NH_3, NO_3, NO_2, soluble reactive PO_4, filtered and unfiltered alkalinity, dissolved silica and total hardness. In addition, at the five major stations, samples were also taken for particulate organic carbon and nitrogen, filtered and unfiltered total phosphorus, filtered and unfiltered total nitrogen, calcium hardness, total iron, total manganese and total sulphate.

The ship used for this work was the *CSS Limnos* of the Canada Centre for Inland Waters. The laboratory on the ship was adequate and manned by both Canadian and American scientific workers. Most analyses were done immediately on the ship except for the analyses on the particulate organic materials and those analyses being performed on the total quantities of components. These analyses were done at the shore laboratories in Cleveland and Burlington.

ANALYTICAL PROCEDURES

The water from the pump was passed over two oxygen probes and when these probes gave a steady reading, (approx. 2-5 mins.), water from the pumping system was led into 8.0-litre holding bottles; a second small sample was drawn simultaneously and the pH and Eh measured.

The oxygen probes were calibrated daily by immersing the probes in stirred air-saturated water and the correction made for the barometric pressure; they were then calibrated at the low end of the scale by placing the probes into water which was being vigorously purged with pure nitrogen gas. The % saturation values were converted to μmoles $O_2/1$ from the values in Standard Methods (APHA, 1965). In general the duplicate probes gave values for a sample which agreed to within 1% of an oxygen saturation value.

The suspended mineral values were obtained by filtering water through a precombusted, weighted glass fiber GF/c filter paper and weighing again after combustion had removed the organic materials. This method has a standard deviation of 0.05 mg/l.

The pH was measured on an unstirred sample at approximately the temperature of the pumped sample and values are accurate to 0.1 of a pH unit. Eh was measured simultaneously with pH, using a bright platinum electrode and standard reference electrode. The platinum electrode was cleaned each day and calibrated against a standard solution.

Total CO_2 was determined by purging the CO_2 from an acidified sample and passing the gas mixture through a gas chromatograph. The method had an accuracy of 0.05 millimoles $CO_2/1$.

Filtered and unfiltered alkalinity was measured using an AutoAnalyzer method which has been tested against the normal titration method. Methyl Orange, buffered by a solution of potassium hydrogen phthalate was used an an indicator and standardized against sodium carbonate and bicarbonate solutions. The method has a sensitivity of ±1.0 μmole $CaCO_3$/l for filtered lake water, but appears to undergo significant interference with unfiltered lake water.

At the end of the study, the total CO_2 content and the alkalinity of an anaerobic solution of 1.00 m.molar Na_2CO_3 were measured by the equipment and methods used during the study. The alkalinity method gave values which were 4% higher than those given by the gas chromatograph, where in fact the alkalinity value expressed as m.moles $CaCO_3$ should have been about 1% lower than the total CO_2 value expressed as m.moles CO_2. Since the major use of both the CO_2 and alkalinity values was in the calculation of budgets with the initial quantities of each subtracted from the final quantities, it was decided that any errors introduced were small and no changes were made in the data.

The methods used in the nutrient analyses have already been reported by Chawla and Traversy (1968). The sensitivities of the various methods are listed below:

Phosphorus	– detection limit	0.01 μmoles P/l
Dissolved silica	– detection limit	0.01 μmoles Si/l
Ammonia	– detection limit	0.1 μmoles N/l
Nitrate or nitrite	– detection limit	0.03 μmoles N/l

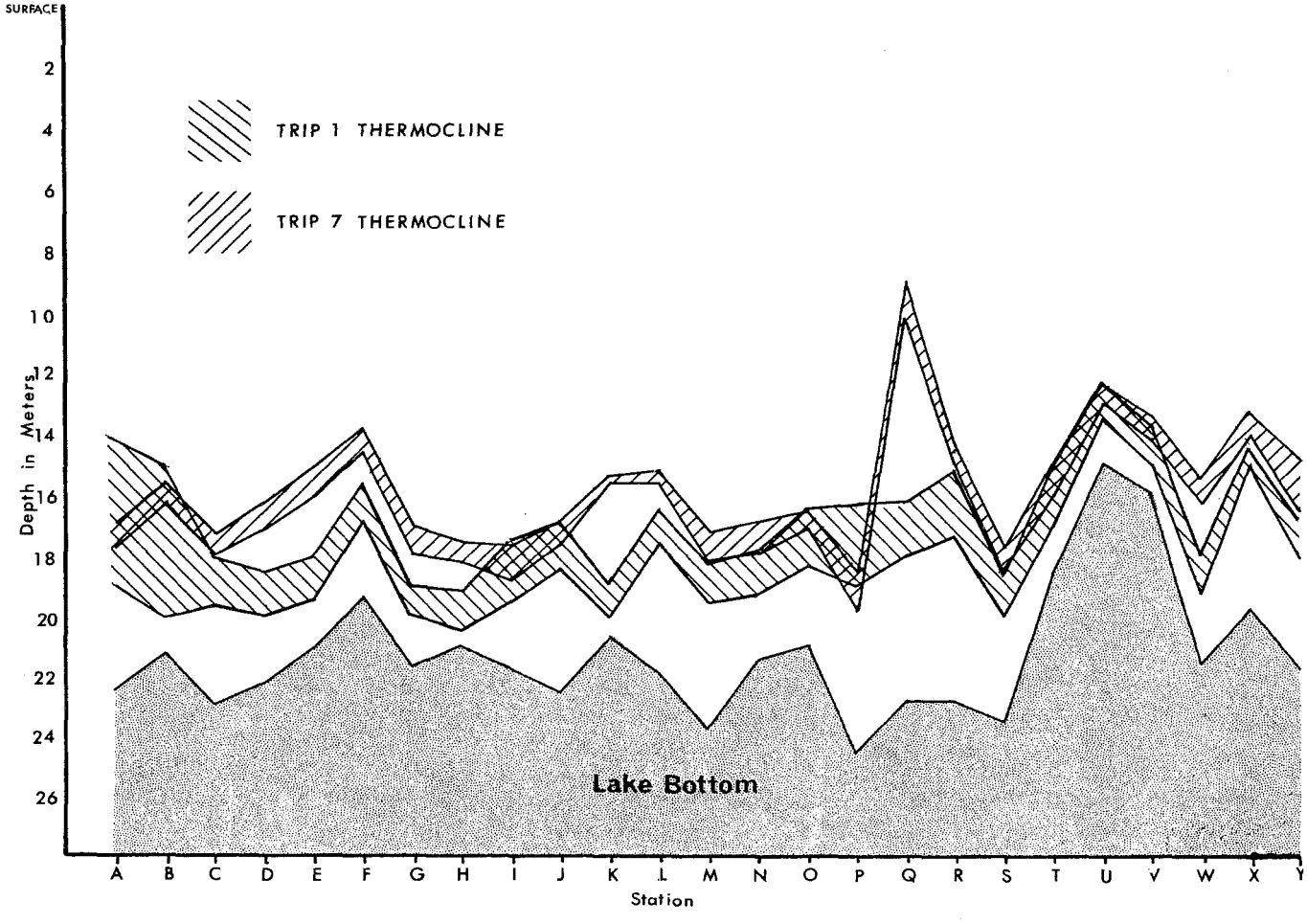

Figure 2. Thermocline depths and thickness at the various stations during Surveys 1 and 7.

Total iron, total manganese and dissolved sulfate were determined according to the Standard Methods for Examination of Water and Wastewater, 12th Edition, with the following sensitivities:

Total iron	– detection limit	0.5 μmoles Fe/l
Total manganese	– detection limit	1.0 μmoles Mn/l
Dissolved sulfate	– detection limit	20 μmoles SO_4/l

The particulate organic carbon and particulate organic nitrogen values were obtained by filtering lake water onto GF/c glass fiber filter papers and after drying in a desiccator, the samples were combusted in a Perkin Elmer CHN Analyser.

RESULTS AND DISCUSSION

GENERAL

The approach in this study has been that a set of five sequential environmental reactions were monitored and that the five reactions were then summed into a net result for the period of observation. The first reaction, labelled R_{12} represents the changes which occurred in the hypolimnion during the period from the end of the first survey to the end of the second survey. The difference then between the dissolved oxygen calculated to be present in the hypolimnion at the end of the first and second surveys represented the dissolved oxygen which had disappeared into other chemical forms during the time interval; its rate of disappearance was also calculated. Also, by noting which other oxygen-containing components increased in quantity during the time interval it was possible to estimate the extent of the various chemical transformations involving oxygen.

The first and most obvious result of the investigation was that the hypolimnion volume increased by almost 100% during the course of the study. This phenomenon is schematically illustrated in Figure 2 and involved thinning and elevation in depth of the thermocline. The hypolimnion volume increase was most unexpected and caused much concern as to the possibility of valid budget calculations. The concentrations of the various materials in the hypolimnion would have remained essentially unchanged with a loss of volume; however, with increasing hypolimnion volumes, water having a quite different concentration of the reactants was introduced into the hypolimnion from the epilimnion.

The validity of the results presented here depends, to a large extent, on the accuracy of the estimates of materials which were added to the hypolimnion, because in many cases the quantities of the materials added during a reaction period were greater than the changes in the quantities which occurred in the hypolimnion due to chemical and biological action.

One method of analysing the situation of increasing hypolimnion volumes is to develop a model of the whole system with the model predicting the behaviour of a certain conservative parameter; a comparison of the calculated levels of this parameter would then be made with the levels which were actually observed. If the model is reasonably accurate in predicting the observed level of the chosen conservative parameter, then the model, with its patterns of mixing can be used to estimate the movement of non-conservative quantities within the water mass. In this study, heat was chosen as the conservative parameter within the hypolimnion and different models were set up to test which was the most reliable in predicting the observed heat budget.

The model which made satisfactory heat budget calculations possible was then used for the calculation of the budgets of the individual chemical components. This information then made it possible to demonstrate the probable chemical pathways which the major components followed.

HEAT BUDGET MODEL

Of the various models which were examined, the one here termed as the "Sequential Mesolimnion Erosion Model" gave values which showed good agreement between estimated and measured hypolimnion heat contents and also between estimated and observed average hypolimnion temperature. In this model, the structure of the thermocline during a particular survey is established. Then if in the next survey, the volume of the hypolimnion is found to have increased by x km^3, the volume of x km^3 of water is taken off the bottom of the mesolimnion, as defined in the first survey, in a slice of constant thickness across the whole basin and added to the hypolimnion as it was observed in the first survey; this mixture now represents the hypolimnion of the second survey and predictions of the hypolimnion heat content and average temperature of the hypolimnion during the second survey can be made. This process can now be applied again with the calculated heat change from Survey 2 to Survey 3 being added onto the calculated heat content of Survey 2, not onto the measured heat content of Survey 2. This procedure is followed whenever there is a volume increase in the hypolimnion and is shown diagrammatically in Figure 3. In the one case where there was a hypolimnion volume decrease, a slice was taken off the top of the hypolimnion and added to the mesolimnion.

The effective heat budget equation for the hypolimnion would be:

$$H_T = H_i + H_m + H_{adv} + H_{cond} - H_{sed}$$

where H_T = total heat within the hypolimnion
H_i = initial heat within hypolimnion
H_m = heat entrained downward from the mesolimnion (thermocline)
H_{adv} = head advected into the hypolimnion by horizontal currents
H_{cond} = heat conducted into the hypolimnion by thermal conduction downward
H_{sed} = heat lost to the sediments

The method of calculating H_m has been explained above. The Western Basin of Lake Erie has no hypolimnion and the Eastern Basin hypolimnion appears to have been effectively cut off from the Central Basin hypolimnion during the study by the ridge separating the two basins (Blanton and Winklhofer, pg 37), thus the assumption was made that $H_{adv} = 0$. The heat conducted down during a period has been calculated by taking the average of the thermocline gradients calculated for surveys before and after the period, using the equation

$$H_{cond} = 0.0014 \frac{\text{cals}}{\text{cm.sec.}^\circ\text{C}} \times \text{gradient } (^\circ\text{C/cm})$$

An estimation of the sediment heat uptake had to be made because the thermal structure of the sediment was not measured during the study; the necessity of this measurement not being realized at the time. Hutchinson (1957, pp. 506) has reported a study by Birge, Juday and March where the sediment heat budget in Lake Mendota at depths varying between 18.0 and 23.5 m was estimated to 1100 cals $cm.^{-2}$ $year^{-1}$. It appears that the bottom water changed in temperature from approximately 1° to 12° in the course of the year. This would indicate that the sediment heat budget of Lake Mendota was 100 cal/cm^2 for each degree change in the bottom water temperature. The deep part of Lake Mendota appears to be similar to the Central Basin of Lake Erie in that both lakes have an average depth of approximately 20.0 m and a bottom water temperature change of about 12°/year. However, they differ quite markedly in their interface characteristics. Lake Mendota has a very ill-defined sediment-water interface (J. Nriagu, G.F. Lee – personal communication) whereas the Lake Erie sediment had a very firm, well-defined sediment-water interface during the study, consisting of approximately a 1 cm thick layer of tightly matted, organic material. The assumption is made here that, because of the smaller amount of sediment-water interaction in Lake Erie as compared to Lake Mendota, the thermal conductivity of the sediment-water interface is lower in Lake Erie and that a value for the sediment heat budget of 70 cals/cm^2 for each degree change in bottom water temperature is assumed. This assumption is borne out to some degree by Hutchinson (1957, pp. 505) who mentions that the thermal conductivity of sediment appears to be lower when measured in the laboratory (presumably under calm water conditions) than the value estimated from field studies. Since the change in the average bottom water temperature during the study was 1.83° and the study duration was 26.28 days, the sediment heat flux was calculated from the equation,

$$H_{sed} = \frac{70 \text{ cals cm.}^{-2}\,^{\circ}C^{-1} \times 1.83^{\circ}C}{26.28 \text{ days}}$$

$$= 4.86 \text{ cals cm.}^{-2} \text{day}^{-1}$$

However, measured volumes have to be used in the calculation of the heat budget and since the measurements of the volumes are themselves subject to error, it is difficult to obtain an objectively correct heat budget. In this regard, the prediction of the average temperature is independent of systematic volume measurement errors since the measurement of temperature depends only on the accuracy of the temperature sensing device.

This can be simply illustrated,

if H_T = total hypolimnion heat
V_i = volume of hypolimnion segment i
t_i = average temperature of segment i
t_T = average temperature of total hypolimnion

then $H_T = \sum_{i=1}^{n} V_i t_i$

and $t_T = \frac{H_T}{\sum_{i=1}^{n} V_i} = \frac{\sum_{i=1}^{n} V_i t_i}{\sum_{i=1}^{n} V_i}$

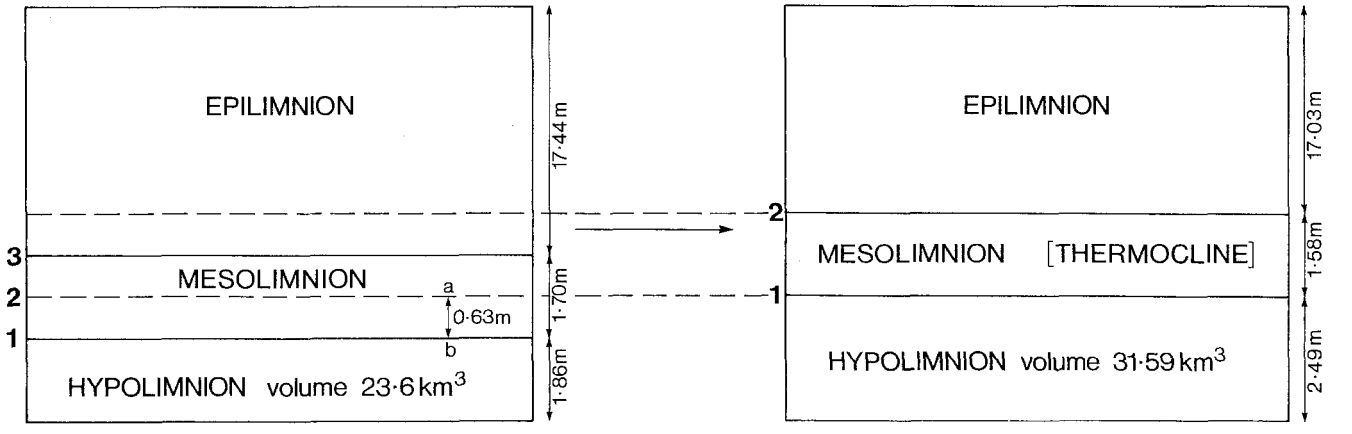

SURVEY 2

THERMAL STRUCTURE

Thermocline gradient = 6·19°/M
1 temperature = 10·15°
2 temperature = 14·04°
3 temperature = 20·65°
average temperature of slice
a - b = 12·09°

SURVEY 4

THERMAL STRUCTURE

Thermocline gradient = 7·51°/M
1 temperature = 10·88°
2 temperature = 22·81°

Heat transferred to hypolimnion during period from Survey 2 to Survey 4 i.e. [Hm] 2→4 = 12·09°× 7·99 km³
= 0·966 × 10^{14} kilocalories

Figure 3. Example of sequential mesolimnion erosion model, showing heat and volume transfers which occurred between Surveys 2 and 4, i.e. during the reaction period R_{24}.

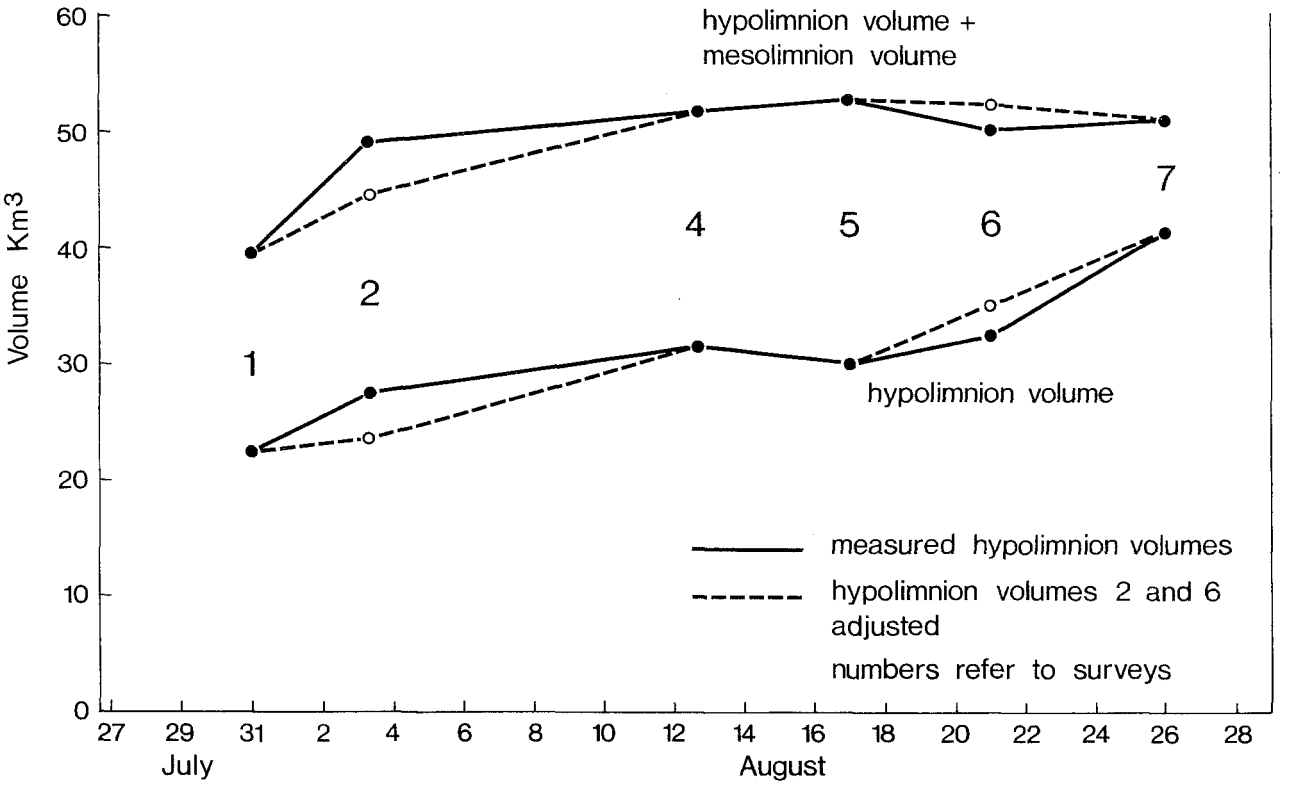

Figure 4. Hypolimnion and mesolimnion volumes measured during "Project Hypo" showing adjusted volumes for Surveys 2 and 6.

A heat budget for the hypolimnion has been calculated and average temperatures estimated according to the methods outlined above (Table 1). The volumes of the hypolimnion which were measured are shown in Figure 4.

However, an examination of Table 1 and Figure 5 shows poor agreement between predicted and observed temperatures for Surveys 2 and 6 (standard deviation of ±0.33°C). During both these cruises a strong wind blew and could have seriously affected any hypolimnion volume measurement. Thus, calculations were done to find the volumes of Surveys 2 and 6 which gave the best agreement between estimated and observed temperatures (standard deviation of ±0.11°C). A second heat budget has been calculated with two of the six survey volumes adjusted. The results of these calculations are shown in Table 2.

Basically, there are two sources of error in a material or energy transfer estimate. The first error is due to incorrect measurement of the hypolimnion volume. This error is difficult to estimate because it is highly variable; the error can be small if the hypolimnion is calm but can be large if the hypolimnion is undergoing extensive seiching activity during measurement. The second error is the result of the inability of the Mesolimnion Erosion Model to reproduce the real situation.

In Table 3 comparisons of the measured transferred heat quantities are made with the estimated quantities. Because the measured quantities are themselves uncertain, the estimated uncertainty in a quantity during a single reaction period is raised from 6.3% to 10.0%. The error in the total transferred quantity, R_{17} is less than the sum of the error in the individual quantities because these errors are self-compensating to some degree. The uncertainty in the net transferred quantity is raised from 2.8% to 5.0% because of volume measurement uncertainties.

The temperature distribution one meter from the bottom is shown in Figure 6. From a comparison of all the bottom temperature maps it appears that appreciably greater downward entrainment of mesolimion water occurred at Stations A, B, G, F, K, T, U, and V. If a weighting factor were applied in

TABLE 1. HYPOLIMNION HEAT BUDGET – MEASURED VOLUMES

Comparison of a theoretical hypolimnion heat budget (calculated by means of sequential mesolimnion erosion model and mesured hypolminion volumes) with the measured hypolimnion heat budget.

Survey #		Estimated Heat Content	Measured Heat Content	Estimated Temperature	Observed Temperature
1	H_i	2.276×10^{14} Kcal	2.276×10^{14} Kcal	10.07°C	10.07°C
	(H_m) 1→2	.605			
	$(H_{cond}-H_{sed})$ 1→2	.018			
2		2.889	2.827	10.40°	10.14°
	(H_m) 2→4	.410			
	$(H_{cond}-H_{sed})$ 2→4	.041			
4		3.350	3.438	10.60°	10.88°
	(H_m) 4→5	-0.152			
	$(H_{cond}-H_{sed})$ 4→5	.018			
5		3.216	3.283	10.66°	10.89°
	(H_m) 5→6	.308			
	$(H_{cond}-H_{sed})$ 5→6	.020			
6		3.544	3.713	10.82°	11.34°
	(H_m) 6→7	1.249			
	$(H_{cond}-H_{sed})$ 6→7	.057			
7	H_T	4.850	4.910	11.74°	11.90°

TABLE 2. HYPOLIMNION HEAT BUDGET – VOLUMES 2 AND 6 ADJUSTED

Comparison of a theoretical heat budget (calculated by means of the sequential mesolimnion erosion model with the hypolimnion volumes of Surveys 2 and 6 adjusted) with the measured hypolimnion heat budget.

Survey #		Estimated Heat Content	Measured Heat Content	Estimated Temperature	Observed Temperature
1	H_i	2.276×10^{14} Kcal	2.276×10^{14} Kcal	10.07°C	10.07°C
	(H_m) 1→2	.103			
	$(H_{cond}-H_{sed})$ 1→2	.018			
2		2.397	2.393	10.16°	10.14°
	(H_m) 2→4	.966			
	$(H_{cond}-H_{sed})$ 2→4	.041			
4		3.404	3.438	10.78°	10.88°
	(H_m) 4→5	-0.152			
	$(H_{cond}-H_{sed})$ 4→5	.018			
5		3.270	3.283	10.88°	10.89°
	(H_m) 5→6	.606			
	$(H_{cond}-H_{sed})$ 5→6	.020			
6		3.896	3.969	11.13°	11.34°
	(H_m) 6→7	.873			
	$(H_{cond}-H_{sed})$ 6→7	.057			
7	H_T	4.826	4.910	11.69°	11.90°

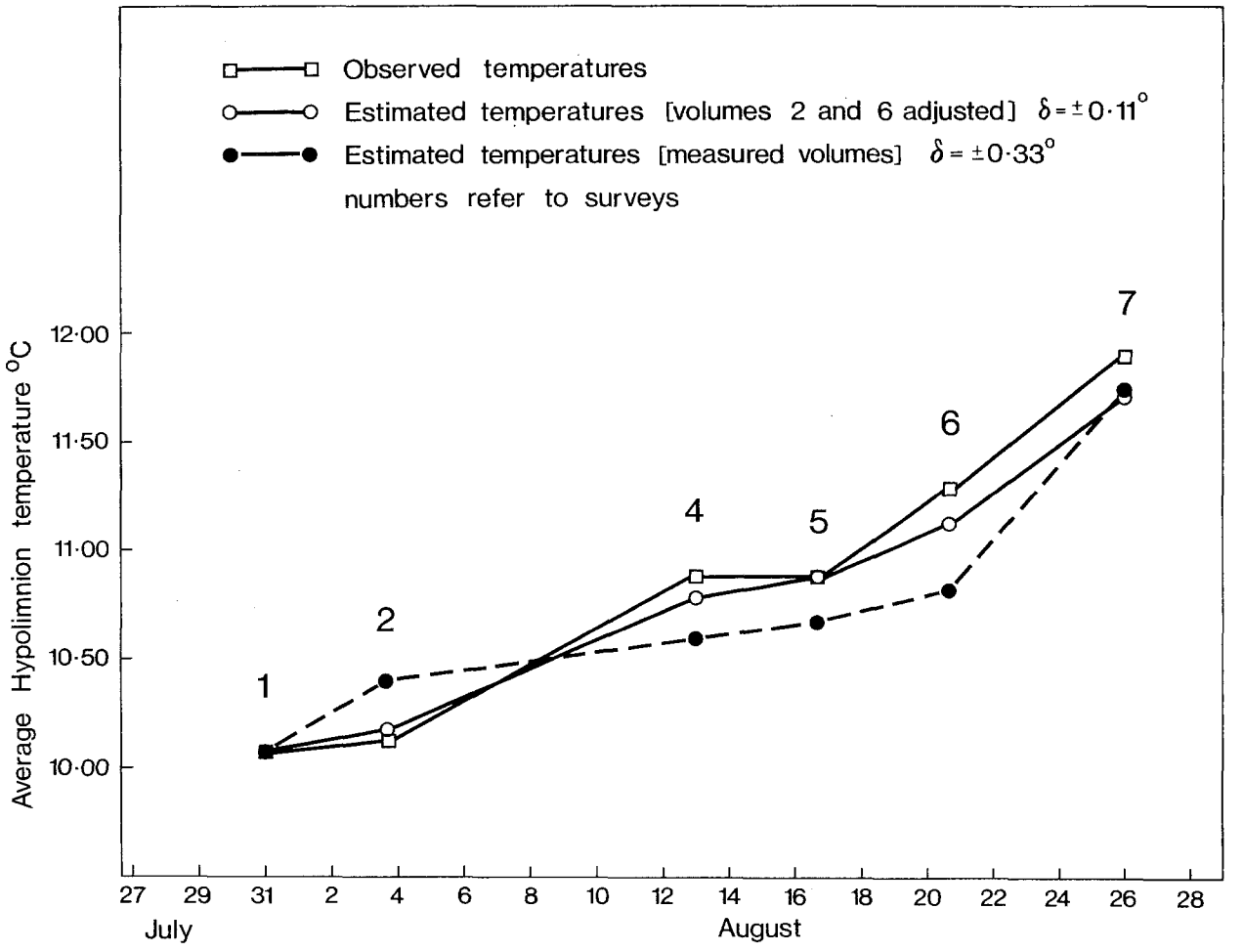

Figure 5. Comparison of observed average temperatures with average temperatures estimated by means of the sequential mesolimnion erosion model

the model calculations so that slightly greater than average entrainment occurred at these stations and slightly less than average entrainment occurred at the other stations, the hypolimnion heat uptake would be estimated to be a little greater and the estimated average temperatures would agree even more closely with the observed average temperatures. While this correction would make the temperature agreement much better, it would only affect the heat budget by approximately 2% and the chemical budgets by approximately 1% of observed change in quantities and is not considered essential.

TABLE 3. COMPARISON OF MEASURED AND ESTIMATED HEAT TRANSFERS

Comparison of measured and estimated heat transfers which occurred between surveys, i.e., during respective reaction periods.

Reaction #	Net Heat Transfer – Measured	Net Heat Transfer – Estimated	Difference	%Difference
R_{12}	$+0.117 \times 10^{14}$ Kcal	$+0.121 \times 10^{14}$ Kcal	$+0.004 \times 10^{14}$ Kcal	+ 3.4%
R_{24}	+ 1.045	- 0.038	- 0.038	- 3.6%
R_{45}	- 0.155	- 0.134	+ 0.021	+13.5%
R_{56}	+ 0.686	+ 0.626	- 0.060	- 9.6%
R_{67}	+ 0.941	+ 0.930	- 0.011	- 1.2%
R_{17}	+ 2.634	+ 2.550	- 0.074	- 2.8%
	Average % Difference $R_{12} \ldots\ldots R_{67} = 6.3\%$			

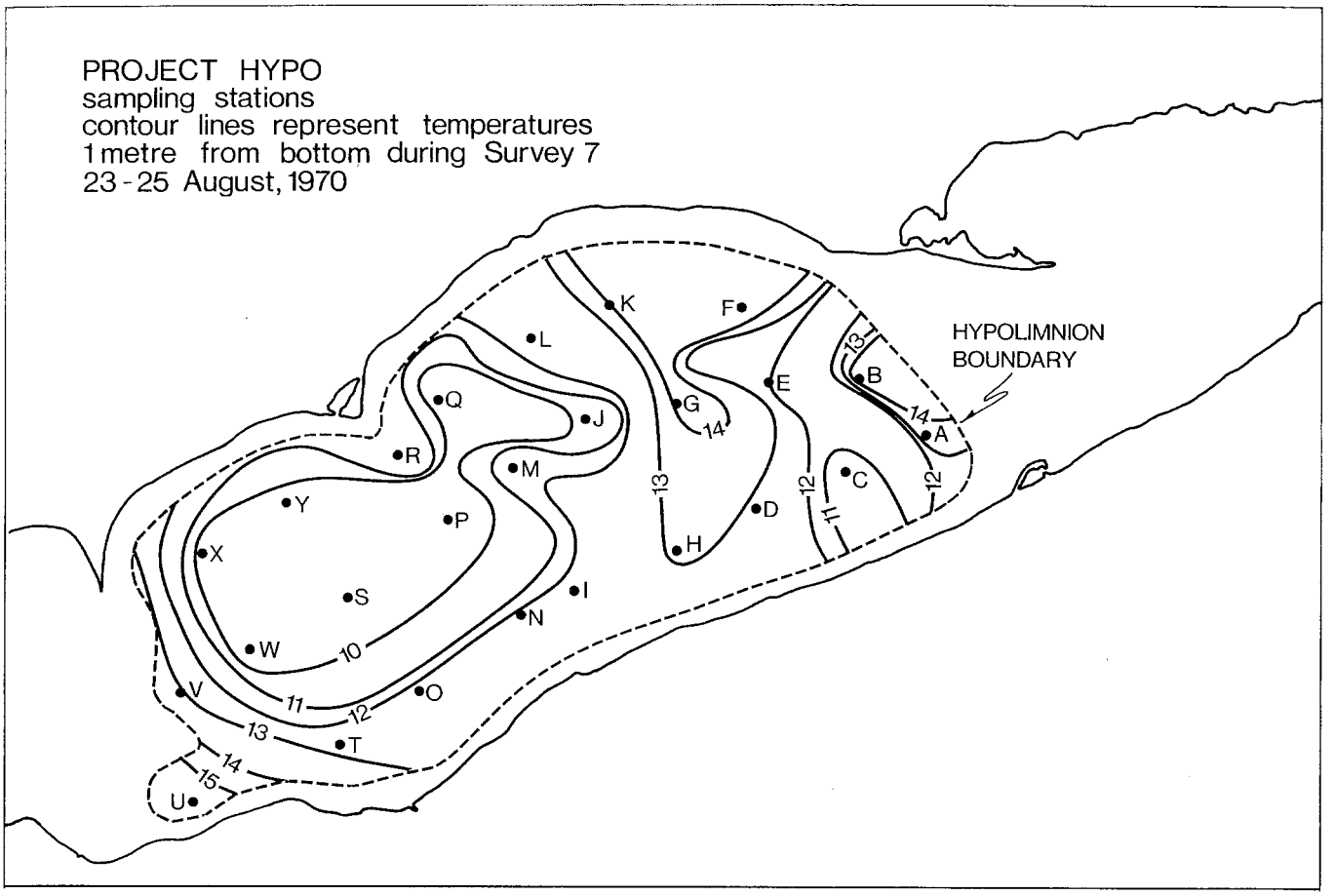

Figure 6. Temperature pattern in °C one meter from the lake bottom in Lake Erie Central Basin.

An interesting aside is that if greater than average hypolimnion volume entrainment occurred at the suggested localities, then hypolimnion currents would be set up away from these localities. A generalized flow pattern can be deduced and this pattern appears to be in agreement with that outlined by Hartley (1968) who used seabed drifters.

When calculating the heat contents of the various hypolimnion segments, the only temperature values which were used were those which corresponded to the water which was sampled for chemical analysis. The information of the full bathythermograph trace was not used. This was done purposely so that the model developed above, together with the error estimates, would be directly applicable to the chemical budget studies.

MESOLIMNION OR THERMOCLINE

Just after a lake has stratified the only real difference between the epilimnion and the hypolimnion is the temperature, but as the stratification persists the differences in the chemical concentrations of the two zones increase. A region of chemical transition between these two zones then comes into existence and is commonly named the thermocline. It is suggested that this zone of transition should preferably be referred to as the mesolimnion, and not the thermocline, since the chemocline gradient may be much more significant than the thermocline gradient. The temperature may change by 10°C or so on passing through the mesolimnion but many of the concentrations of the chemical constituents may change by 1 or 2 orders of magnitude.

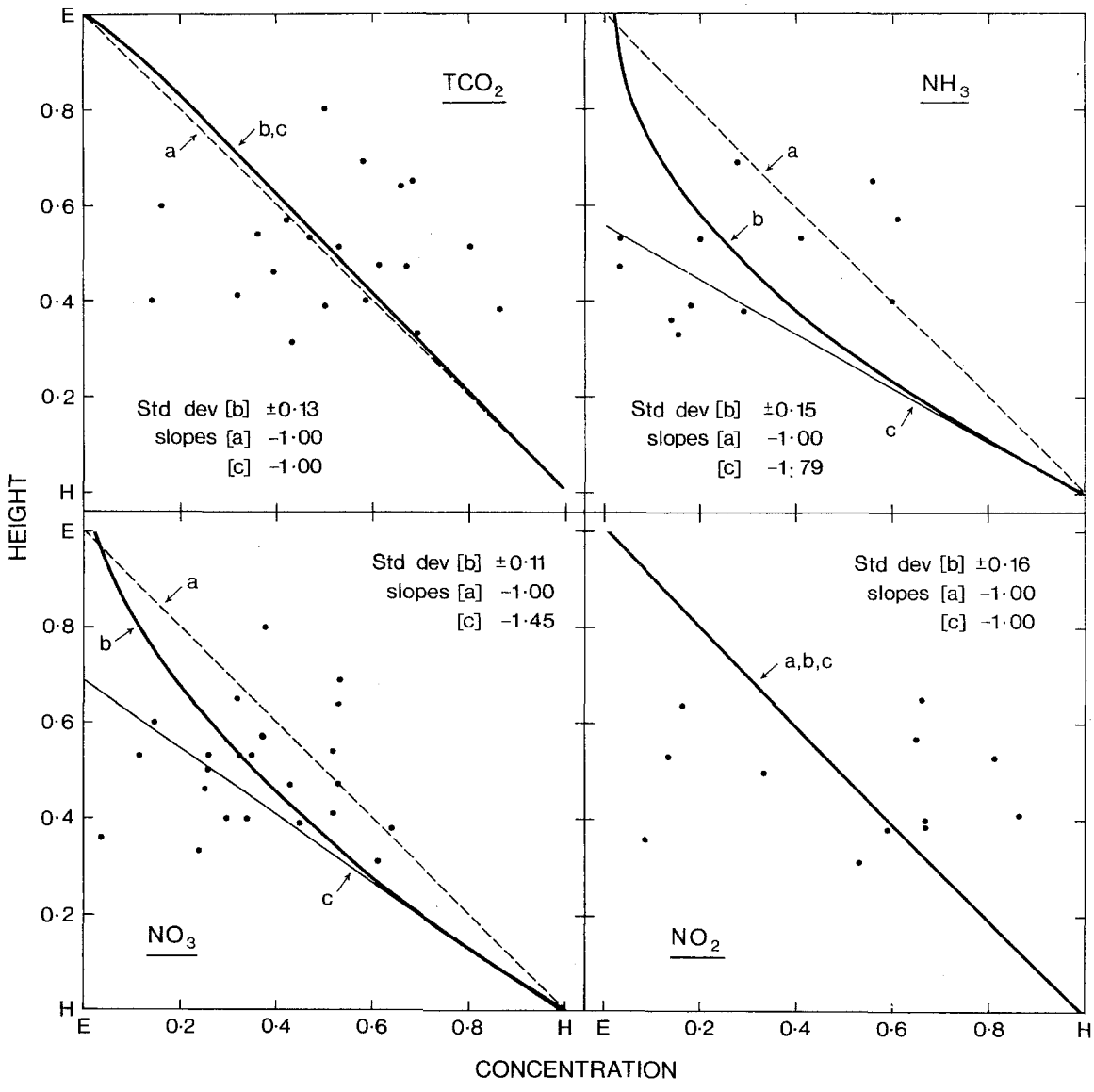

Figure 7. Chemical concentration gradients through the mesolimnion which have been adjusted to a common (i-iv) basis for different mesolimnion thicknesses.

(Concentration values: H = hypolimnion value; E = epilimnion value) (Depth values: H = hypolimnion value = 0; E = epilimnion value = 1.0)

It is known from the bathythermograph traces that the thermocline through the mesolimnion was usually linear with depth, but was the chemocline similarly linear? It was necessary to have some idea of the answer to this question before materials transfer calculations could be done using the Mesolimnion Erosion Model. Mesolimnion data from the five major stations have been processed to obtain some idea of chemical conditions through the mesolimnion. Mesolimnion depth and concentration values have been normalized for comparison because the mesolimnion varied in thickness and concentration gradient. The mesolimnion has been considered to be of unit thickness with the bottom of the epilimnion having a height of 1.0 above the top of the hypolimnion, which had a height of 0.0. Similarly the concentration difference between the top and bottom of the mesolimnion has been taken as 1.0. This is best illustrated with an example:

Depth from surface to top of mesolimnion (bottom of epilimnion)	= 17.4 m; NO_3·conc = 1.2 μmoles/l
Mesolimnion sample depth	= 18.1 m; NO_3·conc = 2.0 μmoles/l

Depth to top of hypolimnion = 18.6 m; NO_3 conc = 5.5 μmoles/l

Relative height of sample above hypolimnion $= \frac{18.6 - 18.1}{18.6 - 17.4} = \frac{0.5}{1.2} = .42$

Relative sample concentration $= \frac{2.0 - 1.2}{5.5 - 1.2} = \frac{0.8}{4.3} = .19$

These values can now be plotted as a point on the graph. The results of the least squares second degree equation were plotted and these results are shown in Figure 7(i)-(viii). It can be seen that CO_2 and NO_2 have a linear chemocline, with O_2, pH, F.Alk, NO_3, NH_3 and SiO_2 having a non-linear relationship. The latter parameters all have lower values than would be expected from a linear chemical gradient (line a) except for O_2 and pH which have higher values. These non-linear features are probably due to the fact that water has been eroded from the bottom of the mesolimnion, tending to bring epilimnion values deeper into the mesolimnion; this was very much the situation in the case of PO_4 where the mesolimnion values were always

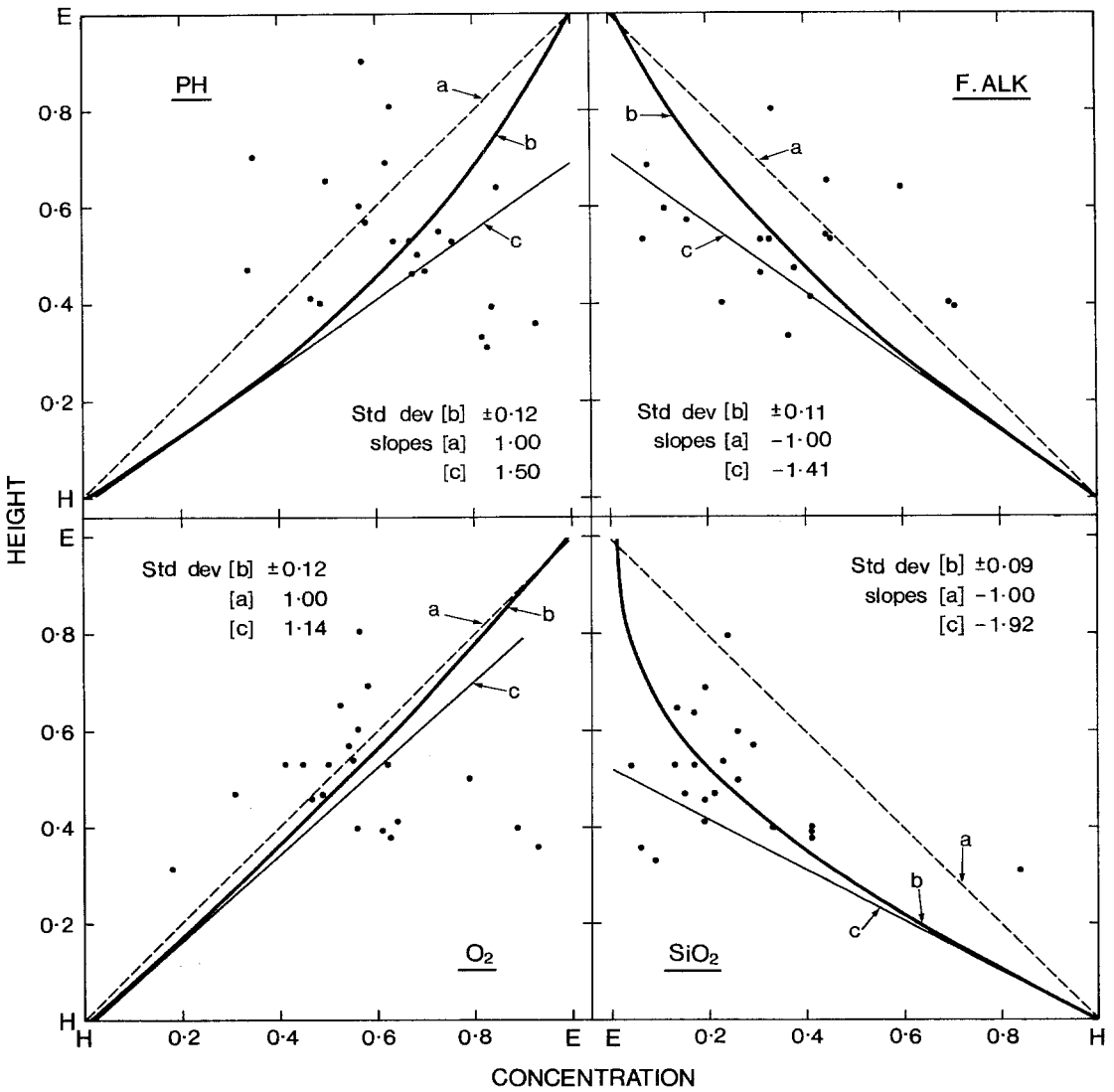

Figure 7. (v-viii) Chemical concentration gradients through the mesolimnion which have been adjusted to a common basis for different mesolimnion thicknesses.

(Concentration values: H = hypolimnion value; E = epilimnion value) (Depth values: H = hypolimnion value = 0; E = epilimnion value = 1.0)

TABLE 4. VOLUMES OF VARIOUS LAKE WATER MASSES

Volumes of various lake water masses observed during "Project Hypo" in Lake Erie Central Basin (Surveys 2 and 6 adjusted; all volumes in km^3).

Survey #	Total Epilimnion Volume	T. Meso. Volume	T. Hypo. Volume	Oxic Hypo. Volume	Anoxic Hypo. Volume
1	229.76	16.84	22.70	22.60	0
2	220.23	21.20	23.60	23.60	0
4	217.65	20.06	31.59	29.03	2.56
5	216.59	22.55	30.16	26.18	3.99
6	219.24	17.32	35.00	28.25	6.76
7	218.32	9.69	41.29	29.08	12.20

TABLE 5. THE VOLUME WEIGHTED AVERAGE CONCENTRATIONS OF THE COMPONENTS MEASURED AT ALL SAMPLING STATIONS

Volume Weighted Average Epilimnion Concentrations

Survey #	Temp.	O_2 μg.at./ℓ	NH_3 μm/ℓ	NO_2 μm/ℓ	NO_3 μm/ℓ	PO_4 μm/ℓ	SiO_2 μm/ℓ	$T.CO_2$[1] m.moles/ℓ	pH	Eh m.volts	F.ALK.[2] μmoles/ℓ	MIN.[3] mg/ℓ
1	21.61	581.5	1.96	0.34	3.08	0.038	2.64	1.67	8.33	–	922	0.28
2	20.63	554.0	2.48	0.42	2.21	0.049	3.03	1.71	8.60	–	929	0.43
4	22.74	539.4	2.53	0.38	1.20	0.059	2.40	1.69	8.68	408	934	0.14
5	23.58	548.5	2.41	0.28	0.81	0.061	2.59	1.71	8.54	384	920	0.13
6	23.64	525.0	2.19	0.66	0.66	0.081	2.38	1.70	8.76	406	917	0.31
7	23.09	530.9	1.85	0.82	0.35	0.105	2.61	1.69	8.71	421	915	0.16

Volume Weighted Average Hypolimnion Concentrations

	Temp.	O_2	NH_3	NO_2	NO_3	PO_4	SiO_2	$T.CO_2$	pH	Eh	F.ALK.	MIN.
1	10.07	265.7	6.53	1.07	11.08	0.054	12.40	1.94	7.38	–	947	0.66
2	10.14	225.7	8.15	1.53	12.09	0.095	15.25	1.99	7.29	–	966	0.77
4	10.88	159.2	8.35	0.63	11.47	0.359	15.93	2.01	7.46	374	974	0.73
5	10.89	85.4	9.08	0.70	11.19	0.349	18.50	2.08	7.39	356	970	0.60
6	11.34	70.3	9.95	1.49	10.44	0.353	16.90	2.06	7.41	424	967	0.66
7	11.90	53.4	4.85	1.68	10.23	0.488	16.38	2.06	7.33	410	972	0.64

Volume Weighted Average Hypolimnion Oxic Concentrations

	Temp.	O_2	NH_3	NO_2	NO_3	PO_4	SiO_2	$T.CO_2$	pH	Eh	F.ALK.	MIN.
1	–	–	6.53	1.07	11.08	0.057	12.40	1.94	7.38	–	947	–
2	–	–	8.15	1.53	12.09	0.095	15.25	1.99	7.29	–	966	–
4	–	–	6.13	0.67	12.46	0.116	14.28	2.01	7.45	400	972	–
5	–	–	5.90	0.67	12.51	0.119	16.45	2.07	7.38	381	967	–
6	–	–	5.68	1.15	13.25	0.140	14.14	2.04	7.41	417	962	–
7	–	–	5.10	1.77	12.05	0.156	14.16	2.04	7.32	470	974	–

Volume Weighted Average Hypolimnion Anoxic Concentrations

	Temp.	O_2	NH_3	NO_2	NO_3	PO_4	SiO_2	$T.CO_2$	pH	Eh	F.ALK.	MIN.
1	–	–	–	–	–	–	–	–	–	–	–	–
2	–	–	–	–	–	–	–	–	–	–	–	–
4	–	–	33.56	0.02	1.43	3.106	34.61	2.11	7.52	71	989	–
5	–	–	30.93	0.09	2.51	1.853	28.91	2.16	7.44	192	993	–
6	–	–	28.91	0.30	2.38	1.194	29.43	2.11	7.40	298	988	–
7	–	–	15.18	0.15	6.42	1.293	21.67	2.10	7.33	267	973	–

(1)Total CO_2 (2)Filtered alkalinity μmoles $CaCO_3$/l (3)Suspended mineral

TABLE 6. AVERAGE CONCENTRATIONS OF COMPONENTS AT MAJOR STATIONS

Unweighted average concentrations of the components sampled at stations M, N, P, R, S only. Anoxic water was sampled at stations O, R, T, U, V, W, X on Survey 7. (Concentrations expressed as μmoles/ l)

Survey #	P.O.N.(1)	SO_4(2)	P.O.C.(3)	P.P.(4)	T.P.(5)	S.O.P.(6)	T.F.P.(7)	S.R.P.(8)	T.Fe(9)	T.Mn(10)
1	3.43	235	30.14	0.21	0.32	.07	0.11	.03	0.13	.10
2	3.65	230	28.36	0.20	0.35	.10	0.15	.06	0.48	.07
4	3.58	232	28.13	0.20	0.37	.11	0.17	.08	0.27	0.00
5	3.53	245	22.06	0.21	0.38	.11	0.17	.08	0.27	0.00
6	2.57	248	20.77	0.21	0.37	.08	0.16	.05	0.48	0.00
7	3.48	234	24.86	0.22	0.39	.07	0.17	.10	0.33	0.00
	Unweighted Average Hypolimnion Oxic Concentrations									
	P.O.N.	SO_4	P.O.C.	P.P.	T.P.	S.O.P.	T.F.P.	S.R.P.	T.Fe	T.Mn
1	3.18	248	29.44	0.21	0.37	.11	0.16	.05	0.42	1.87
2	4.05	243	28.71	0.21	0.40	.13	0.19	.06	1.00	3.59
4	3.81	234	19.72	0.30	0.58	.17	0.28	.11	2.07	4.50
5	3.14	246	17.82	0.39	0.71	.19	0.32	.13	2.83	5.55
6	3.12	248	18.03	0.43	0.73	.14	0.30	.16	3.59	4.58
7	3.92	235	20.67	0.48	0.88	.19	0.36	.17	2.72	4.17
	Unweighted Average Hypolimnion Anoxic Concentrations									
	P.O.N.	SO_4	P.O.C.	P.P.	T.P.	S.O.P.	T.F.P.	S.R.P.	T.Fe	T.Mn
1	–	–	–	–	–	–	–	–	–	–
2	–	–	–	–	–	–	–	–	–	–
4	–	–	–	–	–	–	–	–	–	–
5	–	–	–	–	–	–	–	–	–	–
6	–	–	–	–	–	–	–	–	–	–
7	3.87	211	18.76	0.84	3.07	.92	2.23	1.31	6.21	7.27

(1)Particulate organic nitrogen
(2)Total sulphate
(3)Particulate organic carbon
(4)Particulate phosphorus
(5)Total phosphorus
(6)Soluble organic phosphorus
(7)Total filtered phosphorus
(8)Soluble reactive phosphorus
(9)Total iron
(10)Total manganese

close to the epilimnion value. However, this is not the case with NO_2 and CO_2 and the explanation is not immediately obvious.

In all cases, the thickness of the layer which was eroded from the bottom of the mesolimnion never exceeded 1/3 of the thickness of the mesolimnion, so that a straight line (line c) was approximated to the curve as is shown in Figure 7(i)-(viii) and this correction to an assumed linear gradient was used in calculating the average concentration of materials transferred into the hypolimnion. The transfer of materials downward by molecular diffusion was considered negligible in comparison to the entrainment processes.

BUDGET CALCULATIONS

A highly condensed summary of the chemical data obtained during the study is shown in Tables 4-6. Table 7 shows two budgets worked out in detail, PO_4 (total) and PO_4 (anoxic) with the PO_4 (oxic) being the difference between the other two. The O_2, NO_3, NO_2, NH_3, SiO_2 and $T.CO_2$ total budgets were worked out in the same manner as the total PO_4 budget.

The anoxic budget calculations were made on a different basis to the total budgets because the volumes of specific stations varied markedly from survey-to-survey. When a station changed from the oxic to anoxic condition, the change in the concentration of the parameter under investigation was noted; this value was then multiplied by the volume of the station when it was anoxic to obtain the quantity which was generated by the change. Once a station became anoxic it was then kept in the calculations of anoxic budgets from survey-to-survey. The letters in the center column of Table 7 show which stations were

TABLE 7.

Detailed budget for soluble reactive PO_4, showing the total PO_4 budget for the complete hypolimnion, also shown is the budget calculated for the stations where anoxic water was encountered; finally the oxic PO_4 budget is calculated from the other two budgets. The volumes from Table 4 and the concentrations from Table 5 were used for the total budget. The values for the anoxic calculations are shown in the table.

Survey or Reaction	Total PO_4 Quantity x10^6 moles	Survey or Reaction (Anoxic)	Anoxic PO_4 x10^6 moles	Reaction (Oxic)	Oxic PO_4 x10^6 moles
1	1.225				
1→2 transferred	.052				
2 estimated	1.277				
2 measured	2.243				
R_{12} PO_4 gain	.966 ±.005	R_{12}	0	R_{12} Oxic gain	0.966
		2(U,V) Conc. (μmoles/ℓ)	.0233		
2→4 trans.	.051	4(U,V) Conc. (μmoles/ℓ)	3.105		
4 est.	2.294	(4-2) Conc. Diff.	2.872		
4 meas.	11.340	4(U,V) Anoxic Vol (km^3)	2.559		
R_{24} PO_4 gain	9.05 ±.005	R_{24} [(4-2) Conc.x(4) Vol.]	7.35	R_{24} Oxic gain	1.70
		4(T,U,V) Conc.	2.408		
4→5 trans.	-.168	5(T,U,V) Conc.	1,853		
5 est.	11.172	(5-4) Conc. Diff.	-.555		
5 meas.	10,520	5(T,U,V) Anoxic vol (km^3)	3.786	R_{45} Oxic gain	1.45
R_{45} PO_4 gain	-.652 ±.017	R_{45} [(5-4) Conc.x(5) Vol.]	-2.10		
		5(T,U,V,O,I) Conc.	1.386		
5→6 trans.	.537	6(T,U,V,O,I) Conc.	1.194		
6 est.	11.057	(6-5) Conc. Diff.	-0.192		
6 meas.	12.370	6(T,U,V,O,I) Anoxic Vol. (km^3)	6.752		
R_{56} PO_4 gain	1.31 ±.054	R_{56}[(6-5) Conc. x(6) Vol.]	-1.29	R_{56} Oxic gain	2.60
		6(T,U,V,O,I,W,R,X) Conc.	0.654		
6→7 trans.	.855	7(T,U,V,O,I,W,R,X) Conc.	1.293		
7 est.	13.225	(7-6) Conc. Diff.	0.639		
7 meas.	20.610	7(T,U,V,O,I,W,R,X) Vol. (km^3)	12.204		
R_{67} PO_4 gain	7.39 ±.086	R_{67}[(7-6) Conc.x(7) Vol.]	7.80	R_{67} Oxic loss	-0.41
R_{17} total PO_4 gain	18.06 ±.084	R_{17} Anoxic PO_4 gained	11.76	R_{17} Oxic gain	6.31

found to be anoxic in each survey. The SO_4, Fe and Mn budgets were calculated on a different basis, since these parameters were only sampled at the five major stations which remain oxic throughout the study, except for Station R on Survey 7. However, in addition on Survey 7, all the anoxic stations were sampled as if they were major stations in order to have a better understanding of the chemistry at the anoxic stations. From the 5 major stations it was possible to estimate an oxic budget for the basin for SO_4, Mn and Fe and from the anoxic stations samples, the excess quantities generated by anoxic conditions were calculated. Knowledge of the number of days during which certain stations were anoxic, together with their associated surface areas has made possible the calculation of the anoxic generation rates of various chemical compounds. All these values are summarized in Tables 8, 9 and 10.

EXTERNAL INFLUENCES

The physical cause and effect relationships between wind, hypolimnion currents and mesolimnion entrainment are reported on by Blanton and Winklhofer (pg 38). The wind caused almost complete vertical mixing in the thin hypolimnion (significant chemical gradients were seldom noticed), downward mesolimnion entrainment and was also the partial cause of 'algal rains' into the hypolimnion. The algal conditions during "Project Hypo" were closely followed and are described by Braidech, Gehring, and Kleveno (pg 56). Frequently, high algal concentrations were found in the region of the mesolimnion and these algae would rain down into the hypolimnion periodically because of wind effects on the mesolimnion. These rains were documented by underwater photography (Blanton and Winklhofer, pg 30). One of the more unexpected findings of the whole study was that the sedimented algae would remain alive and photosynthesize for a period after they fell to the lake bottom even at depths of 24 m (80 ft.), Lucas and Thomas (pg 48).

TABLE 8. TOTAL QUANTITY

Changes calculated in the total quantities of the various components in the hypolimnion which were due to chemical and biological action only. Error estimates based on heat budget comparisons are also shown. (units – moles x 10^7 unless specified)

React.	O_2	NO_3	NO_2	NH_3	PO_4	SiO_2	T. Hard	TCO_2	$T.CO_2$-F.ALK.	F.ALK.	ΔEH $x10^{-3}$ Volts	ΔpH	$\Delta MIN.$ mgm/l
R_{12}	-49.1	2.37	1.10	3.88	.097	6.93	-15.8	104.0	56.0	45.4	–	-0.09	0.010
	±1.67	±.11	±.01	±.06	±.0005	±0.11	±13.5	±19.5	±10.0	±9.46			
R_{24}	-138.8	0.93	-2.59	2.53	.905	6.65	14.8	142.0	116.0	30.6	–	0.17	-.041
	±12.43	±.71	±.10	±.44	±.0005	±0.72	±106.3	±154.8	±78.7	±76.5			
R_{45}	-110.8	-0.15	0.21	2.84	-.065	8.21	72.9	117.0	192.0	-9.1	-17.74	-0.07	-0.131
	±1.19	±.17	±.01	±.11	±.0017	±0.23	±19.7	±28.7	±14.8	±13.89			
R_{56}	-43.4	-1.49	2.75	4.35	.131	-2.77	-300.8	-43.0	-40.0	-7.9	67.22	0.02	0.063
	±3.76	±.43	±.04	±.27	±.0054	±0.60	±67.3	±98.9	±52.2	±46.59			
R_{67}	-66.8	1.02	0.69	-7.09	.739	2.11	89.7	47.0	39.0	25.1	-13.57	-0.08	-0.023
	±5.40	±.47	±.10	±.26	±.0086	±0.64	±82.3	±125.3	±64.0	±60.19			
R_{17}	408.9	2.68	2.16	6.52	1.807	21.13	-139.2	427.0	363.0	84.1	35.91	-0.05	-.122
	±12.2	±0.945	±0.13	±0.57	±.0084	±1.15	±144.6	±213.6	±109.9	±103.32			

TABLE 9. OXIC AND ANOXIC QUANTITY

Changes in quantities in the hypolimnion which were calculated to have occurred where oxic and anoxic conditions prevailed in the water. These changes are those due to chemical and biological effexts only. (Units – moles x 10^7)

React. #	TCO_2		NH_3		NO_2		NO_3		F.ALK.	
	Oxic	Anoxic	O.	A.	O.	A.	O.	A.	O.	A.
R_{12}	104.0	0	3.88	0	1.10	0	2.37	0	45.4	0
R_{24}	121.8	20.2	-1.35	3.88	-2.56	-.023	4.11	-3.18	25.32	5.28
R_{45}	144.7	32.3	8.18	-5.34	.18	.022	0.94	-1.09	-15.47	6.37
R_{56}	-20.0	-23.0	0.87	3.48	2.63	.124	0.448	-1.94	-3.19	-4.71
R_{67}	-11.6	58.6	-5.67	-1.42	.74	-.054	4.66	-3.64	21.62	3.48
R_{17}	338.9	88.1	5.92	0.60	2.09	.069	12.53	-9.85	73.68	10.42

React #	PO_4		SiO_2		SO_4		Fe		Mn	
	O.	A.	O.	A.	O.	A.	O.	A.	O.	A.
R_{12}	.097	0	6.93	–	-12.5	–	.57	–	3.59	–
R_{24}	.170	.735	3.20	3.45	-15.0	–	3.82	–	6.80	–
R_{45}	.145	-.210	6.97	1.24	35.6	–	1.89	–	1.13	–
R_{56}	.261	-.129	-4.79	2.02	13.0	–	3.64	–	.21	–
R_{67}	-.041	.780	2.37	-.256	-58.1	–	-2.10	–	2.23	–
R_{17}	.631	1.176	14.68	6.45	-37.0	-26.4	7.84	3.80	13.96	3.79

The sequence of events associated with algal rains is shown schematically in Figure 8 along with dissolved oxygen and NO_3 changes. When the algae first rained down in early August, they formed a fluffy green layer on the bottom 2-3 cm thick (Braidech *et al.* pg 56), but within a week the algae had turned brown and matted down to approximately 1 cm thick. The sedimented algae had obvious effects; (1) they diminished the oxygen demand while they were alive (Fig. 8), (2) the algal rains had a strong stimulating effect on the nitrifying bacteria populations and hence on the nitrate production. Values from Menon, Marion and Miller (App V) included in Table 10 show varying bacteria populations. There is a weak correlation between the nitrate production rate and the concentration of nitrifying bacteria on the bottom (very few nitrifying bacteria were found in the water column). This may have been due to the fact that a very heavy sampling program is needed for quantitative bacteriology because of the high rates of population

TABLE 10. OXIC AND ANOXIC RATES

Rates of change in the quantities of certain materials present in the hypolimnion due to chemical and biological effects. The rates are obtained by dividing the observed change in quantity by the area and time during which the change took place. (Units – millimoles/m^2/day (unless specified))

React #	O_2	TCO_2		NH_3		NO_2		SiO_2		F.ALK.	
	Oxic	Oxic	Anoxic	O.	A.	O.	A.	O.	A.	O.	A.
R_{12}	-9.55	20.23	0	0.75	0	0.21	0	1.35	0	8.83	0
R_{24}	-11.91	11.24	25.0	-0.13	4.81	-0.24	-0.03	0.30	4.28	2.34	6.54
R_{45}	-21.81	31.73	62.6	1.79	-10.35	0.04	0.04	1.53	2.40	-3.39	12.34
R_{56}	-8.95	-5.57	-18.2	.24	2.75	0.73	0.10	-1.33	1.60	-0.89	-3.73
R_{67}	-10.03	-2.48	26.4	-1.28	-0.64	0.17	-0.02	0.54	-0.12	4.88	1.57
R_{17}	-12.23	11.86	18.3	0.21	0.13	0.07	0.014	0.51	1.34	2.58	2.17

React #	PO_4		SO_4		Fe		Mn		Nitrif. Bact.	NO_3	
	Oxic	Anoxic	O.	A.	O.	A.	O.	A.	x10^5/m^2	O.	A.
R_{12}	.019	–	-2.4	–	0.11	–	0.70	–	3.64	0.46	–
R_{24}	.016	.911	-1.3	–	0.33	–	0.58	–	2.94	0.38	-3.94
R_{45}	.032	-.407	7.0	–	0.37	–	0.22	–	0.185	0.18	-2.11
R_{56}	.073	-.102	0.27	–	0.75	–	0.04	–	0.870	0.13	-1.53
R_{67}	-.010	.351	-8.7	–	-0.32	–	0.79	–	3.77	1.05	-1.64
R_{17}	.022	.245	-1.30	-5.5	0.27	0.79	0.49	0.79	2.11	0.44	-2.05

growth and decay. A program of the required size just was not possible. Nevertheless, by using the average nitrate rate value and the average nitrifying bacteria population value found during the study, the estimate is made that the nitrate production rate was 1.9×10^{-9} moles NO_3 per bacterium per day. This value can be extended by including nitrite, giving the combined production rate of 2.1×10^{-9} moles ($NO_3 + NO_2$) per bacterium per day.

The sedimented algae provided an active site for extensive *Desulfovibrio* and *Thiobacillus* bacterial action. During the period 30th July to 12th August (R_{12} and R_{24}) it appears that the *Desulfovibrio* bacteria were fairly actively reducing sulfate. This is evident from the sulfate values shown in Table 9 and Figure 9. Examination of cores which were taken during that period showed that the interface organic mat had an underlying black layer which thickened upward during the period (Plate 2). Presumably this black layer consisted of iron and manganese sulfides resulting from the reaction of the H_2S produced from sulfate reduction, with the Fe^{++} and Mn^{++} ions diffusing out of the sediments.

The reduction of sulfate under these conditions may be represented by the equation, (Stumm and Morgan, pg 432 (1970))

$$SO_4^{--} + 2CH_2O + 2H^+ \rightarrow H_2S + 2CO_2 + 2H_2O \qquad (1)$$

(where CH_2O represents organic matter, i.e., carbohydrate). Some of the H_2S thus produced would then react to form the observed black sulfides. This process is likely since alkalinity increases (removal of protons) were observed with sulfate reduction, together with black sulfides occurring near the mud-organic matter interface. This relationship has been observed previously (Berner *et al.*, 1970).

During the period 13th – 20th August (R_{45} and R_{56}), the metallic sulfides were in contact with the overlying oxygenated water as many black patches (Plate 3) were observed to be at the surface of the organic mat. It is suggested that during this period, especially during R_{45}, the following reaction occurred extensively

$$2FeS + 9/2\ O_2 + 4(OH)^- + H_2O \rightarrow 2Fe(OH)_3 + 2\ SO_4^{--} \qquad (2)$$

This type of process would tend to increase the quantity of iron and manganese in the water as well as

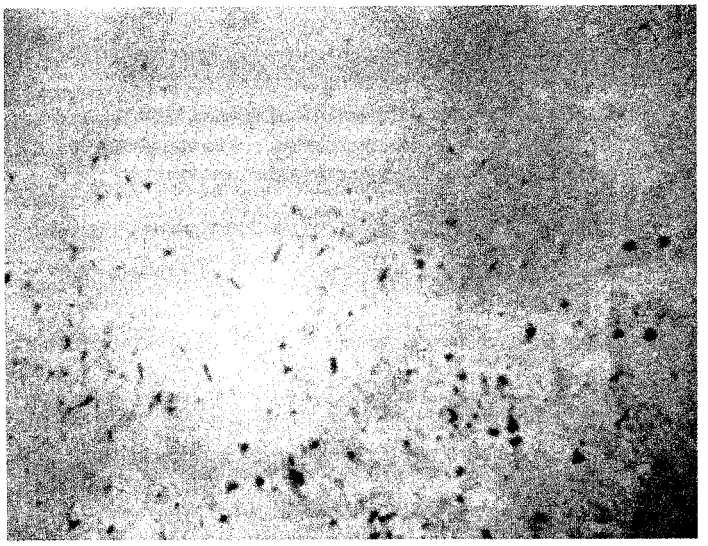

Plate 1. Photograph of sediment in June showing light reddish-brown layer of what presumably was ferric hydroxide.

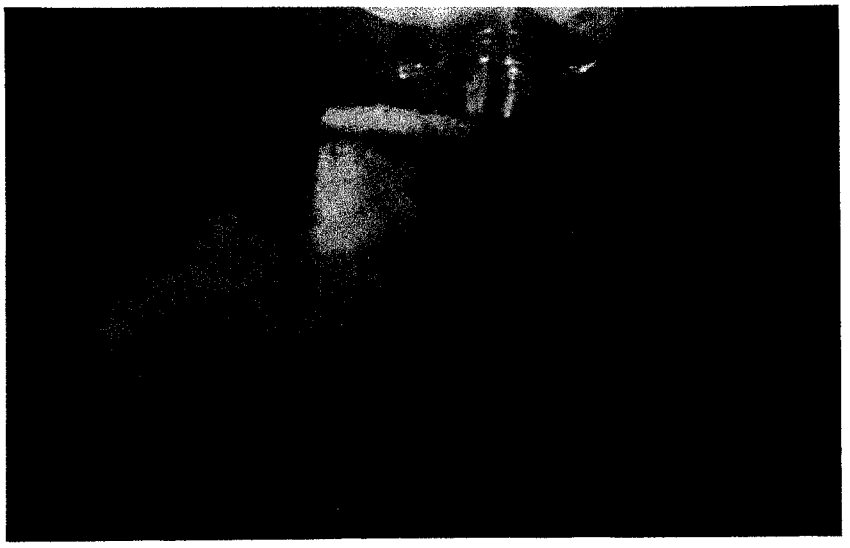

Plate 2. Underwater photograph of a core which has just been pulled from the sediments, showing the grey mud, black reduced organic layer and brown oxidised organic layer.

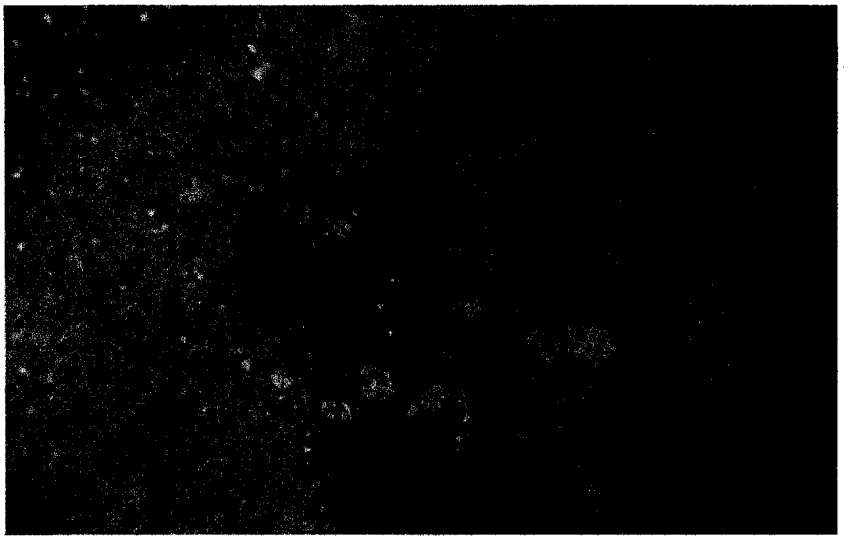

Plate 3. Picture of a "black patch" where the sulphide layer has penetrated up to the surface of the sediment. Part of the organic material in the black patch has decomposed at an accelerated rate, exposing the underlying grey mud.

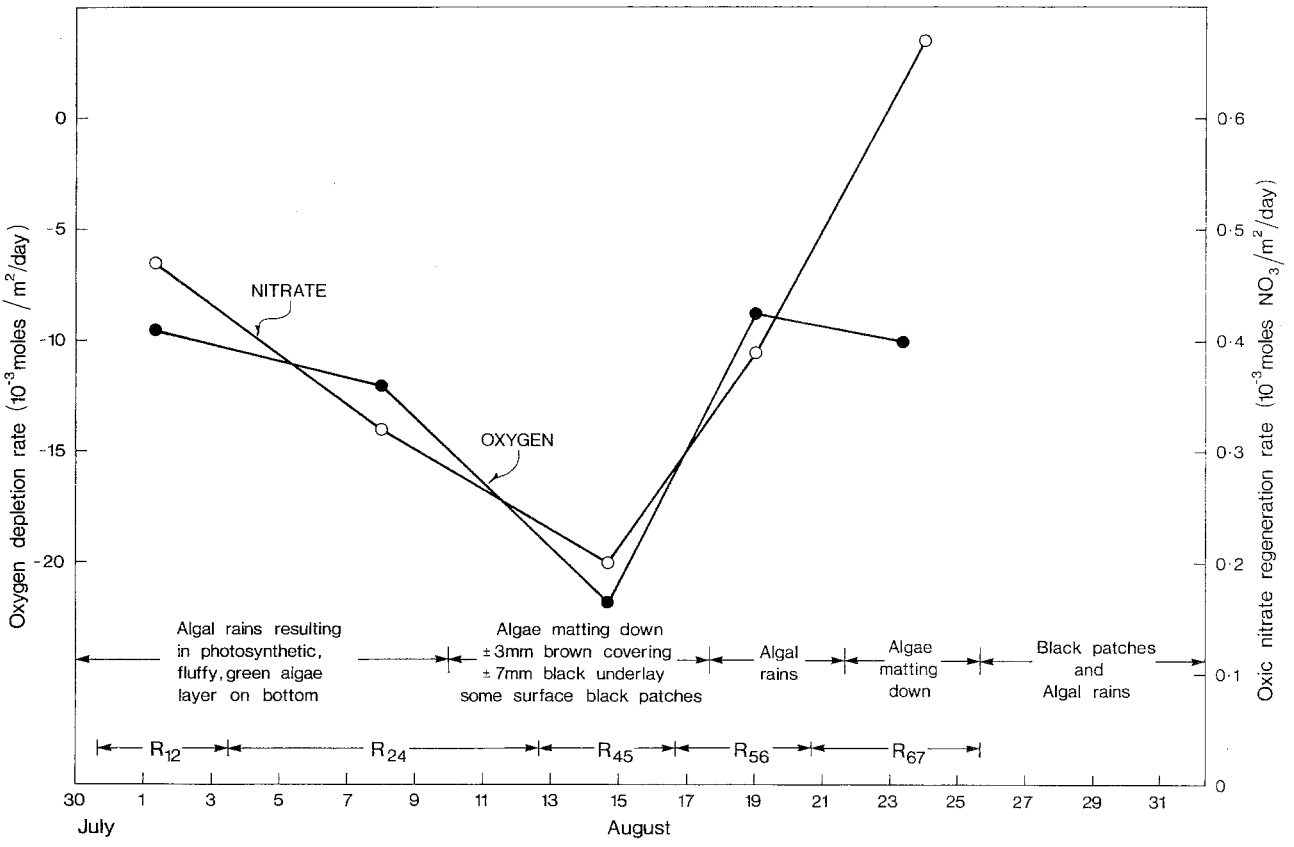

Figure 8. Sequence of events associated with algal rains showing a decreased oxygen demand and increased nitrate production when the algae were photosynthetic and a larger oxygen demand and smaller nitrate production when the algae were dead. The duration of the different reaction periods is shown.

re-establish the brown oxidized layer, produce SO_4 and deplete oxygen at a high rate while reducing the alkalinity; all of which were observed (Fig. 9 and Tables 5, 9). Prior to August 13th the black layers were generally buried fairly deeply down in the organic mat or were non-existent and Figure 9 shows the SO_4 concentrations decreasing with Fe and Mn concentrations increasing during this period. It is probable that during this period, SO_4 reduction was proceeding along with moderate release of Fe and Mn from the sediments; there was probably very little dissolution of FeS. It seems that it is the appearance of the black layers close to the sediment surface which is the controlling mechanism for the reaction of FeS with oxygen.

It is probable that a large part of the oxygen depletion occurred via the sulfate cycle. The oxidation of H_2S can be simply represented by the reaction,

$$H_2S + 2O_2 \rightarrow 2H^+ + SO_4^{--} \qquad (3)$$

If the process represented by reaction (1) occurred in the organic mat and the process represented by reaction (3) occurred in the overlying water, it would not be possible to distinguish the results of this reaction sequence from those obtained from the oxic decay of organic materials. In other words, sulfate can act as a catalyst in the deoxygenation of bottom waters.

It is also likely that there was some elemental sulfur formed from the interaction of SO_4 and H_2S. This possibility is described by Stumm and Morgan (1970, pg. 32). Clouds of white material, which were identified as bacteria (Menon, Marion and Miller, pg 79), were observed on occasion in the water where the black patches were observed.

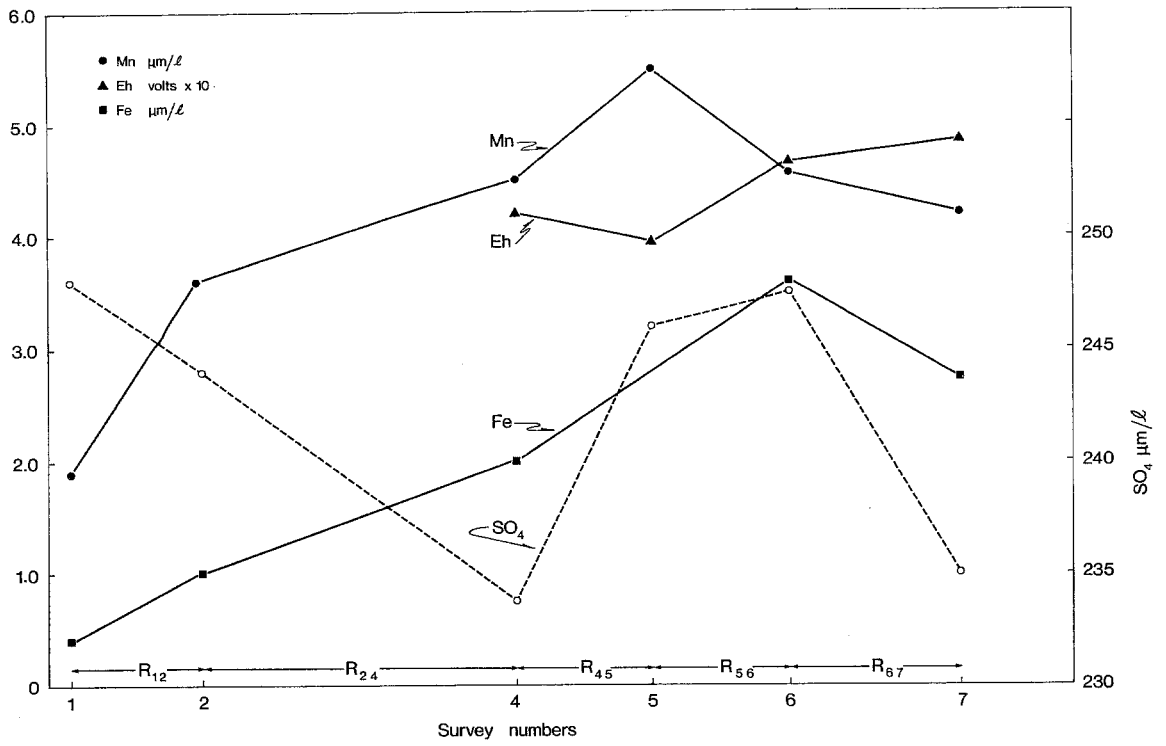

Figure 9. Concentrations of various species at the major stations, showing the interaction of SO_4 with Fe and Mn.

OXYGEN DEPLETION PATTERN

The oxygen areal depletion pattern is shown in Figure 10(i)-(v). The overall oxygen loss was basin-wide during each survey. However, the rate of oxygen depletion is clearly documented by the above figures as being highest in the western end and along the south shoreline while the north shoreline, midlake, and the extreme eastern end of the basin had a lower rate of depletion. This observed pattern is confirmed by the findings from the sediment oxygen uptake studies (Lucas and Thomas pg 48) which indicated that the sediment oxygen uptake rates were higher in the western end and along the south shore than midlake and the north shore. In addition this pattern agrees with the biological findings (Braidech, Gehring, and Kleveno, pg 69) which indicated profuse productivity in the same areas of high rates of oxygen depletion.

The above oxygen depletion pattern resulted in the western stations becoming anoxic first, followed by the south shore stations as demonstrated in Surveys 4, 5 and 6 (Figs. 10(iii), (iv)). Survey 7 indicated anoxic stations in the north shore area while midlake stations became depleted progressively from west to east. This depletion pattern was probably due to the heavy load of nutrients coming into the western end of the lake via the Detroit River, (Report to the I.J.C. 1969). Finally, as shown in the September C.C.I.W. Monitor Cruise Survey (Fig. 10(v)) the total hypolimnion (6600 km^2 or 2500 sq. miles), although diminished in area and volume by this late period in the year, was anoxic.

Two areas were observed to act independently from the pattern discussed above. Station E, although a deep water station and located on the eastern end of the basin, showed a low dissolved oxygen concentration (30 μgram atoms/l) as early as Survey 5 (Fig. 10(iii)). This situation was most likely caused by the valley-like topography of the lake bottom at this station which prevented normal lake circulation of water in and out of the area, creating a stagnant pool.

The extreme eastern stations appeared to be affected by a clockwise rotating current pattern which prevented development of anoxic water in the area of Stations A, B, and C. This situation was probably influenced by a return flow pattern from the north shore and is demonstrated by the intrusion of a shoal

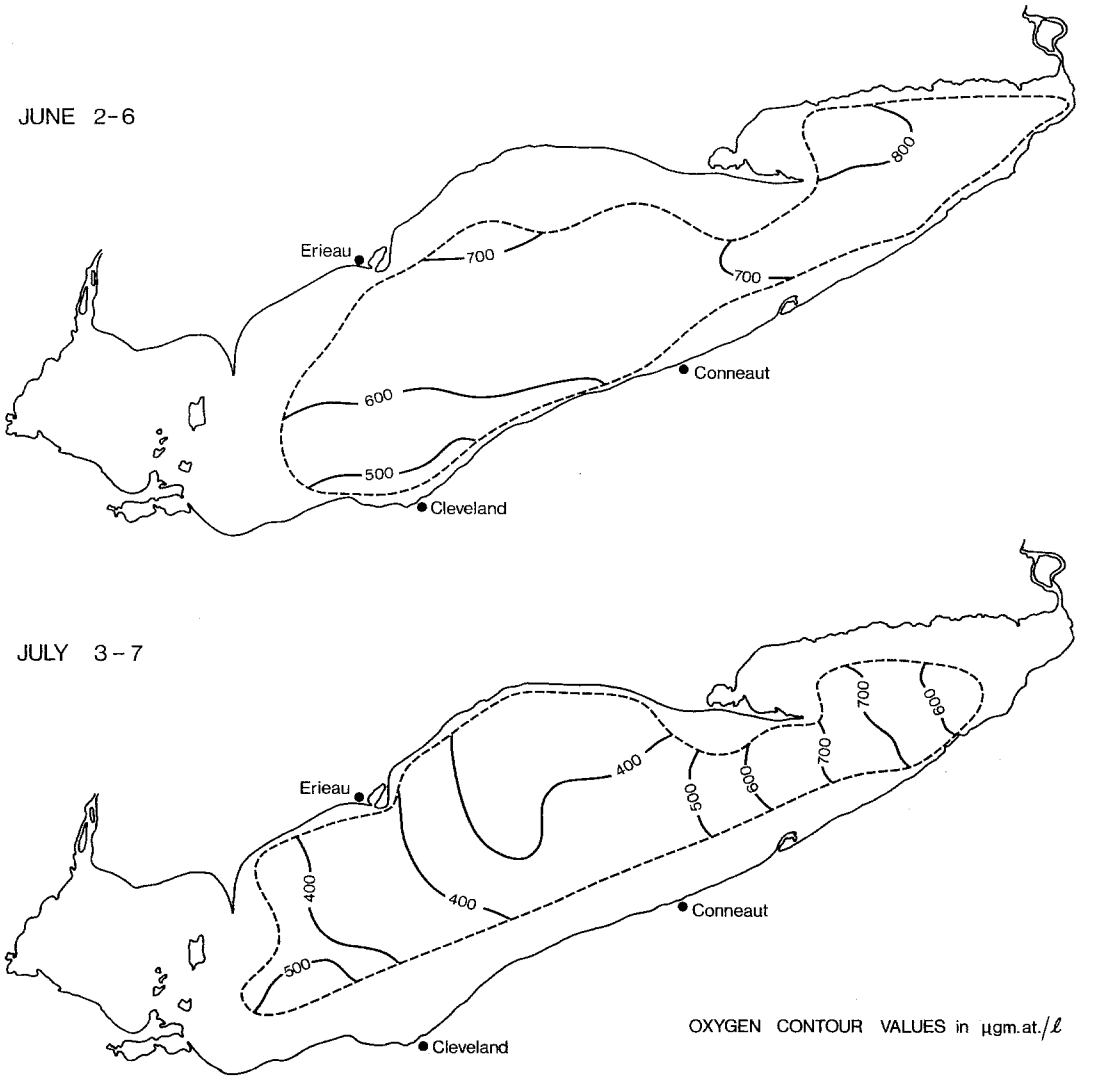

Figure 10. Hypolimnion oxygen concentration patterns, June 2-6; July 3-7, 1970 (C.C.I.W. monitor cruises). (i)

along the lake bottom from Conneaut, Ohio towards Station G. This suggested current pattern agrees with currents at Station G as described by Blanton and Winklhofer (pg 33). However, their projected current patterns throughout the rest of the hypolimnion do not appear to have had a noticeable effect on the dissolved oxygen depletion pattern.

OXYGEN BUDGET

Equation 1 shows one mole of carbonate alkalinity will be gained for each mole of SO_4 reduced. (This relationship is also suggested by Berner *et al.* (1970).) Thus, using the values from Table 8 and 9, the following budget for alkalinity can be calculated:

Alkalinity increase due to SO_4 reduction	= 63.4×10^7 moles
Alkalinity increase due to NH_3 production	= 3.3
Total observed increased alkalinity	= 84.1
∴ Alkalinity increase due to dissolved carbonate species	= 17.4×10^7 moles

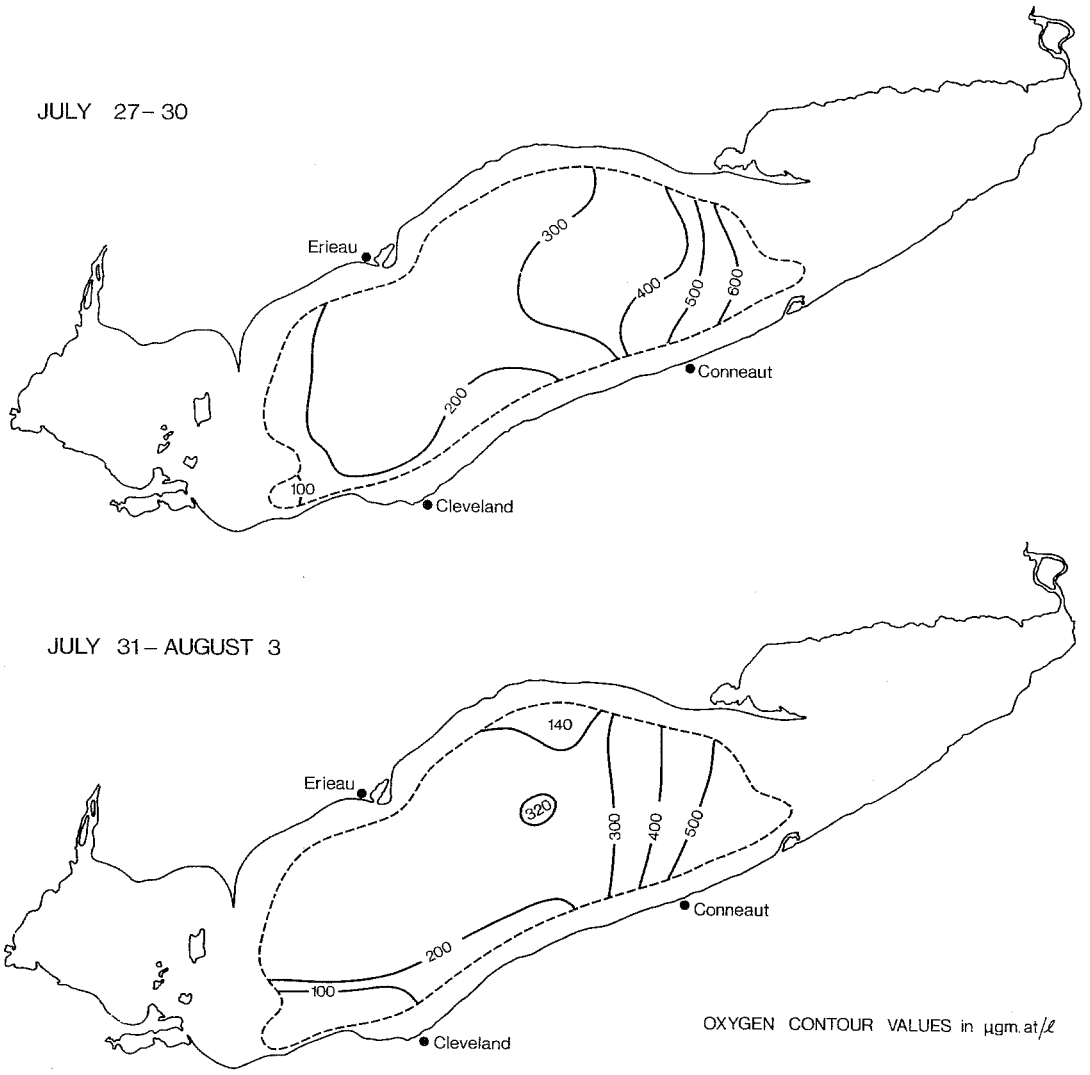

Figure 10. Hypolimnion oxygen concentration patterns, July 27-30 (Survey 1); July 31-August 3, 1970 (ii) (Survey 2).

A fact which should be borne in mind, is that organic compounds, when degrading, produce an appreciable quantity of water from the oxygen taken up; 30% of the oxygen used to oxidize the aliphatic chain of fatty acid will form water and cannot be detected in budget studies. Hutchinson (pp 678) suggests that a realistic value for the Respiratory Quotient is 0.85.

Equation 1 is not entirely correct because the formula for a carbohydrate chain is used. The quantity of CO_2 released per SO_4 ion reduced would be more correctly expressed as 0.85x2 = 1.70 molecules of CO_2. Thus the total CO_2 budget can be estimated as follows:

Total CO_2 produced	$= 427.0 \times 10^7$ moles
CO_2 from precipitated calcite or dissolved carbonates	$= -17.4$
CO_2 from sulphate reduction	$= -107.1$
$\therefore CO_2$ from oxygen depletion	$= 302.5 \times 10^7$ moles
$\therefore$ Total O_2 depleted by decay processes	$= 356.0 \times 10^7$ moles

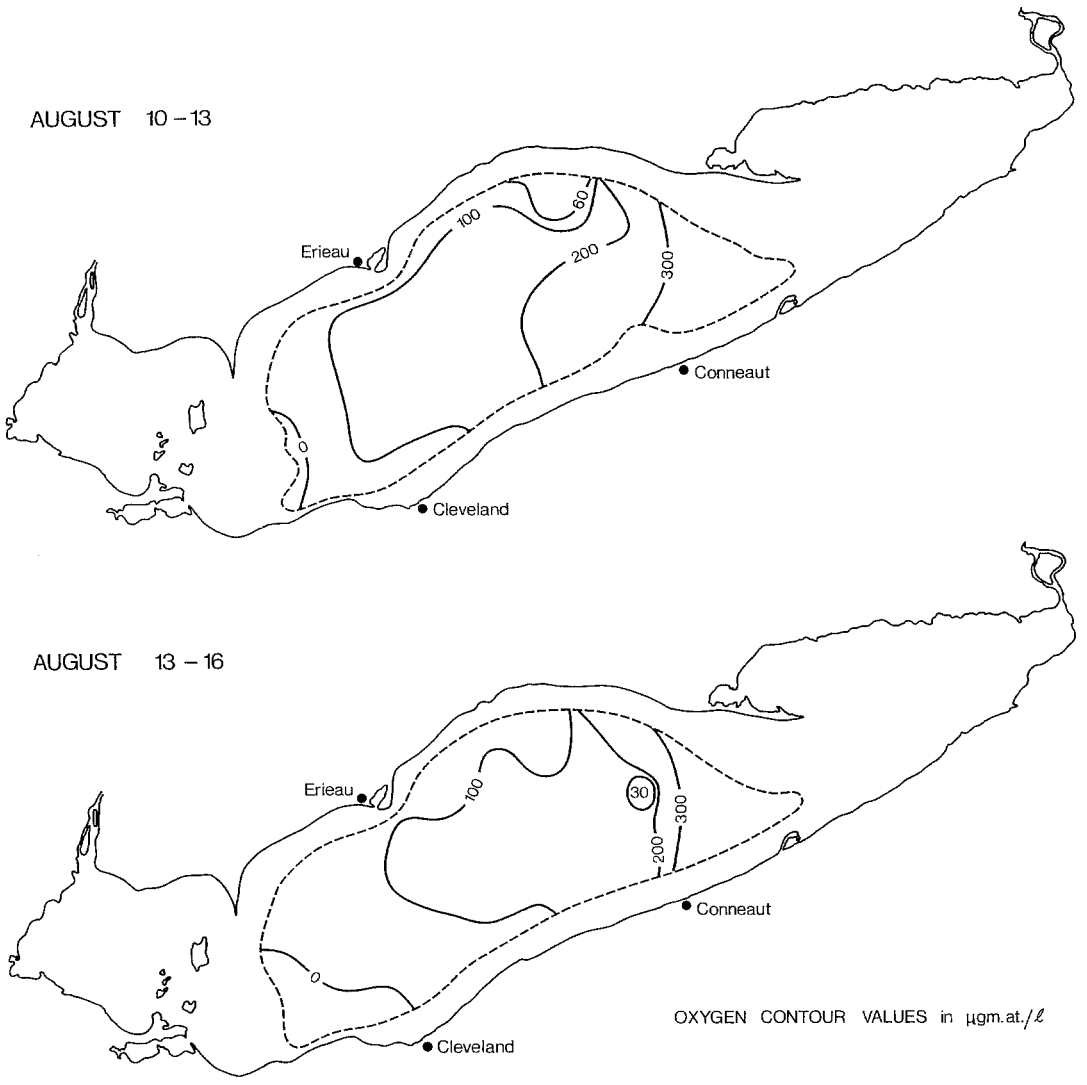

Figure 10. Hypolimnion oxygen concentration patterns, August 10-13 (Survey 4); August 13-16, 1970 (iii) (Survey 5).

It is now possible to calculate a detailed oxygen budget:

Total oxygen depleted from hypolimnion	= 409.00×10^7 moles
O_2 Used in conversion of 2.68 $\times 10^7$ moles NO_2 to NO_3	= -1.34×10^7
O_2 Used in conversion of 2.16 $\times 10^7$ moles NH_3 to NO_2	= -3.78×10^7
O_2 Used in conversion of 0.455×10^7 moles organic P to PO_4	= -0.45×10^7
(assuming 50% of organic phosphorus is in oxidized form in the algae)	

Balance of O_2 depleted	= 403.43×10^7
O_2 used in CO_2 production	= 356.0
$\therefore O_2$ depleted by inorganic processes	= 47.43×10^7 moles
	= 12.2% of total O_2 depletion

From a chemical budget point of view, the conversion of H_2S to sulfate cannot be considered as one of the inorganic oxygen consuming processes because this would result in a net increase of sulfates in the water during the study. Table 9 shows an actual decrease in sulfates during this period and this fact has already been taken into account in the budgets above.

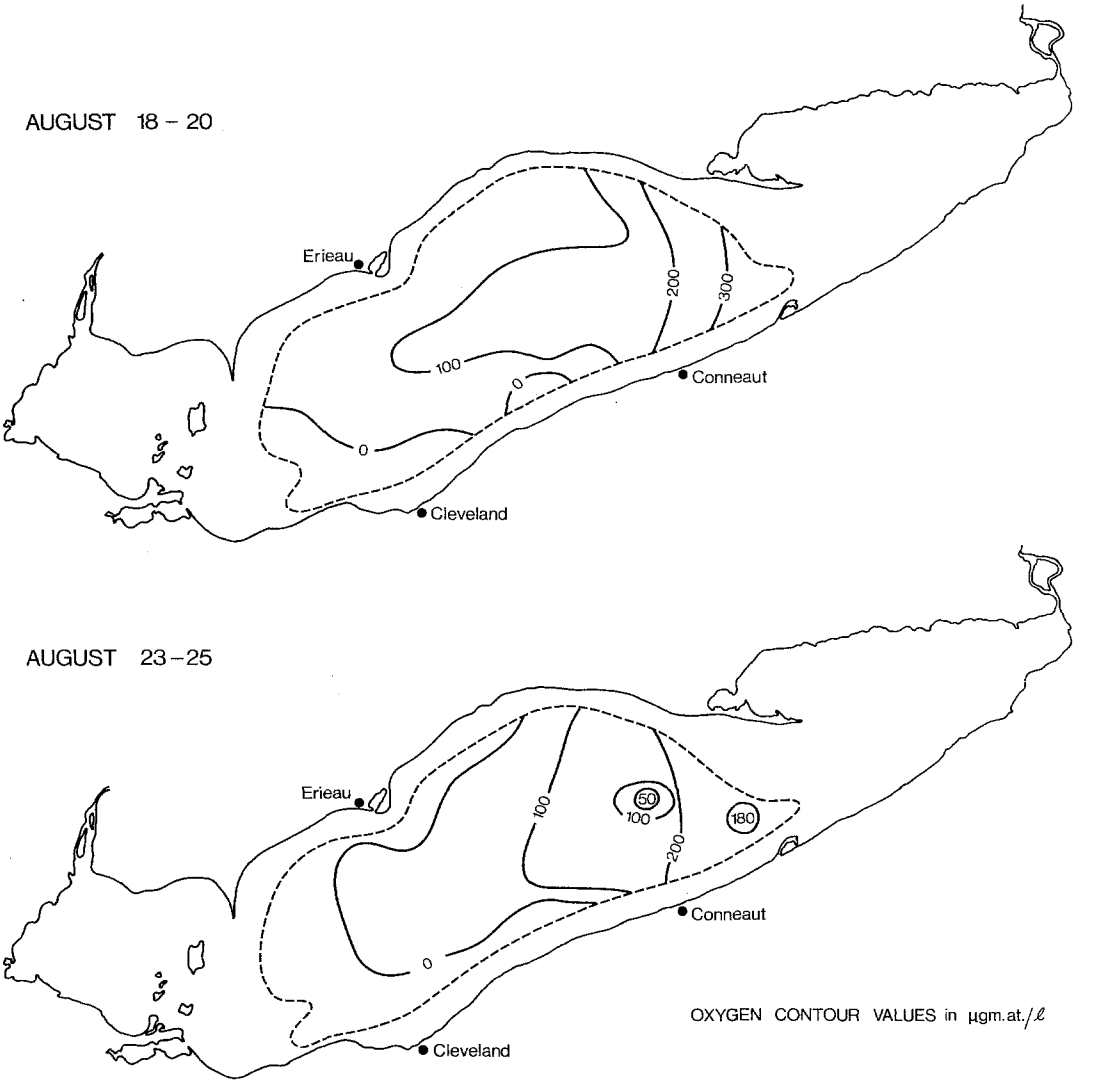

Figure 10. Hypolimnion oxygen concentration patterns, August 18-20 (Survey 6); August 23-25, 1970 (iv) (Survey 7).

It is likely that the 46.0×10^7 moles of oxygen used in inorganic oxidation were consumed in the oxidation of ferrous species. An example of the many possible oxidation processes is:

$$2Fe^{++} + 1/2\ O_2 + 2H^{+} \rightarrow 2Fe^{+++} + H_2O$$

Thus 0.25 moles of O_2 are used for each mole of Fe oxidized. If all the Fe which was oxidized remained in the water this would give the iron an estimated concentration of 45 μmoles/l. The observed final average concentration of iron at the oxic stations was 2.72 μmoles/1 suggesting that in the order of 40 μmoles Fe/1 of iron had been oxidized during the study but that most had settled out of the water. The conditions at the oxic stations, having an Eh between 350 and 500 mv and a pH of approximately 7.4, are likely to keep the iron in the oxidized form and manganese in the reduced form [Stumm and Morgan (1970) pp. 533]. In this discussion, only iron has been mentioned though in reality the reacting species would have been a mixture of iron and manganese ions, however, this will not be discussed further here.

Both Hutchinson and Mortimer (Hutchinson, 1957, pg. 644) have used hypolimnetic oxygen areal depletion rates as a measure of the trophic state of lakes and their suggested criteria are listed as follows:

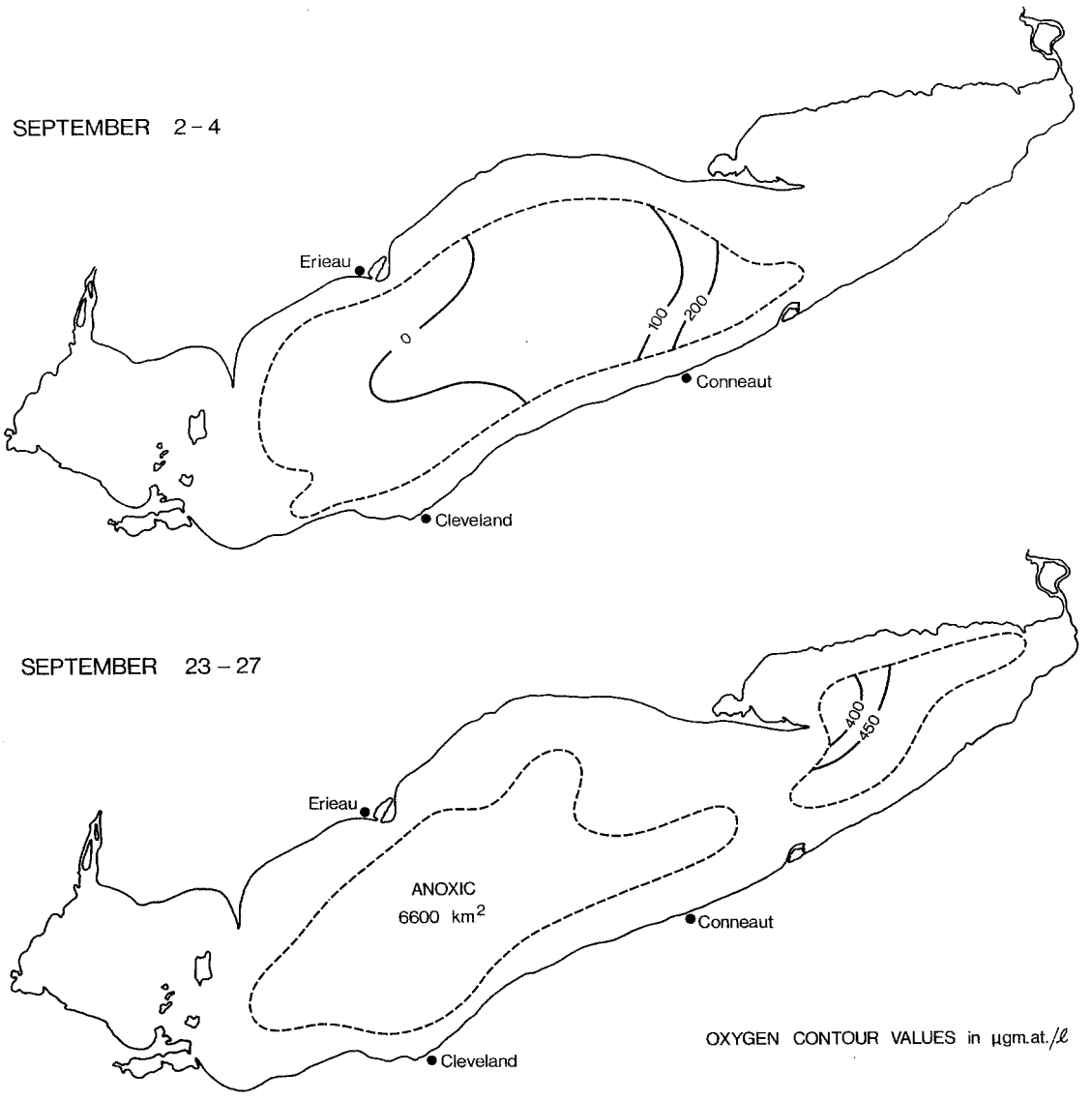

Figure 10. Hypolimnion oxygen concetration patterns, September 2-4; September 23-27, 1970 (C.C.I.W. (v) monitor cruises).

	Hutchinson	Mortimer
	Oxygen Depletion Rates (millimoles $O_2/m.^2/day$)	
Oligotrophic lakes	<-5.3	<-7.7
Mesotrophic lakes	-5.3 to -10.3	-7.7 to -17.2
Eutrophic lakes	>-10.3	>-17.2

The average oxygen depletion rate which was measured during this study was -12.23×10^{-3} moles O_2 $m.^{-2} day^{-1}$. If this value is compared to those listed above, the Central Basin of Lake Erie can be considered as being eutrophic. There has been a marked increase in the oxygen depletion rates in recent years (Dobson and Gilbertson, pg 7).

Since approximately 88% of the hypolimnetic oxygen was consumed in the decay of organic materials, it is probable that the massive algal bloom in the Central Basin during the last week of July 1970 was the major cause of anoxic conditions which subsequently developed in the hypolimnion. The

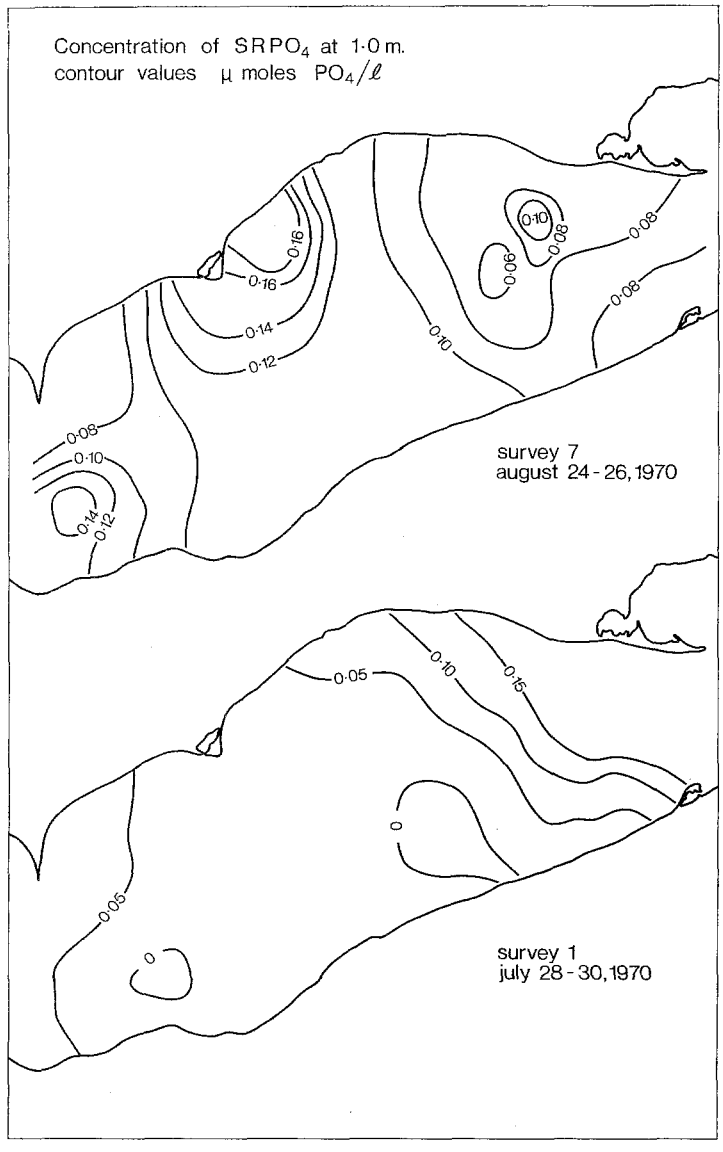

Figure 11. Concentrations of soluble reactive phosphorus at 1.0 m. depth in Central Lake Erie.

magnitude of the initial pulse of this bloom was most likely limited by the supply of soluble reactive phosphorus because the survey completed on the 30th July showed that the phosphorus had been reduced to the barely detectable level in the surface waters of 80% of the basin (Fig. 11). It is probable that the extent of oxygen depletion would have been reduced if the supply of soluble reactive phosphorus had been much less during the last week of July.

OXIC REGENERATION

From the estimate of 17.4×10^7 moles of CO_2 being of inorganic origin, it is possible to calculate that 96% of the CO_2 increase observed in the hypolimnion is of organic origin. Thus from the values shown in Table 9 the following oxic regeneration budget can be drawn up:

$$\begin{aligned} CO_2 \text{(organic origin)} &= 325.3 \times 10^7 \text{ moles} \\ NO_3 + NO_2 + NH_3 &= 20.5 \times 10^7 \text{ moles} \\ PO_4 &= 0.632 \times 10^7 \text{ moles} \end{aligned}$$

TABLE 11. OXIC REGENERATION.

The quantities, rates and proportions of components which returned to the soluble form in oxygenated hypolimnion water.

	Quantity (moles x 10^7)	Rate (moles 10^{-3} $m.^{-2}$ day^{-1})	Ratio
P	= 0.63	.022	1.0
C	= 338.90	11.85	538.6
N	= 20.54	.72	32.6
Si	= 14.68	.51	23.2
Mn	= 13.96	.49	22.2
Fe	= 7.84	.27	12.5
C(org)	= 325.34	11.38	517.3
C(inorg)	= 13.56	0.47	21.4

which gives the following oxic regeneration rates (Table 11):

$$CO_2 = 11.4 \times 10^{-3} \text{ moles } m.^{-2} day^{-1}$$
$$\Sigma N = 0.72 \times 10^{-3} \text{ moles } m.^{-2} day^{-1}$$
$$PO_4 = 0.022 \times 10^{-3} \text{ moles } m.^{-2} day^{-1}$$

and the regeneration ratio is,

$$(C: N: P)_r = 1: 0.063: 0.0019 \qquad (4)$$

The C: N: P ratio in the particulate organic material in the water sampled just above the mesolimnion was found to be:

$$(C: N: P)_p = 122: 18: 1 = 1.0: 0.148: 0.0081 \qquad (5)$$

This is presumably fairly close to the elemental composition of the organic material sedimenting into the hypolimnion.

Dividing (5) into (4) gives the result

$$\frac{(C: N: P)_r}{(C: N: P)_p} = 1: 0.43: 0.235$$

It would appear then, that for every atom of carbon which is mineralized, only 0.43 or 43% of a nitrogen atom is mineralized and 0.235 or 23.5% of a phosphorus atom is mineralized. Thus, it is possible to state that during the study, approximately 45% of the nitrogen and 25% of the phosphorus in the mineralized material returned to the water under oxic conditions: the balance of 55% of the nitrogen and 75% of the phosphorus must have remained complexed in some manner with the material on the bottom or was part of the loss of nitrogen due to denitrification. A possible explanation for the low percentage regeneration of phosphorus is that most of the orthophosphate from the organic decay is produced on the lake bottom in very close proximity to the precipitated ferric hydroxides. Thus at the interface, there is probably a high concentration of orthophosphate in water containing much suspended ferric hydroxide; this would readily lead to the formation of insoluble ferric hydroxy-phosphate complexes. These complexes would most likely dissolve if conditions subsequently became anoxic but would remain insoluble if oxic conditions were maintained. The formation of some soluble organic carbon, nitrogen and phosphorus compounds was probably a step in the mineralization process. The values in Table 6 show that there was a fairly significant increase in the quantity of soluble organic phosphorus. It is assumed that there were corresponding increases in the soluble organic carbon and nitrogen and that these organic components do not seriously affect the ratio argument outlined above.

A comparison of the oxic regeneration rates of phosphate, manganese, iron and silica show that the molecules are regenerated or made soluble in the following ratio (Table 11):

PO_4: Mn: Fe: SiO_2 = 1: 22: 12: 23

This portion is quite different from the anoxic regeneration ratios (Table 12) which are: PO_4: Mn: Fe: SiO_2 = 1: 3.2: 3.2: 5.5

ANOXIC REGENERATION

The anoxic budget for carbon, nitrogen and phosphate was:

$$C = 88.1 \times 10^7 \text{ moles}$$
$$\Sigma N = -9.2 \times 10^7 \text{ moles}$$
$$PO_4 = 1.18 \times 10^7 \text{ moles}$$

The number of $m.^2$ days of anoxic conditions which were observed during the study was 4.82×10^{10} $m.^2$ days; thus the following regeneration rates are observed:

$$C = 18.3 \times 10^{-3} \text{ moles } m.^{-2} \text{ day}^{-1}$$
$$\Sigma N = -1.92 \times 10^{-3} \text{ moles } m.^{-2} \text{ day}^{-1}$$
$$PO_4 = 0.24 \times 10^{-3} \text{ moles } m.^{-2} \text{ day}^{-1}$$

The high rate of CO_2 production could possibly be due in part to the dissolution of carbonates and bicarbonates. The negative value for nitrogen could be explained by suggesting that when anaerobic reduction of NO_3 occurs, significant quantities of N_2 gas are released to the water. If there had been no loss of nitrogen nutrients under anoxic conditions, the total quantity of nitrogen nutrients generated during the study would have been at least 20.54×10^7 moles, however, the quantity was only 11.4×10^7 moles. Thus, the anoxic conditions caused a decrease of about 44% in the quantity of nitrogen nutrients generated. This is presumably part of the natural process of denitrification. Part of the anoxic phosphate regeneration was probably due to organic degradation. If the assumption is made that 96% of the CO_2 is of organic origin (as in the case of the oxic regeneration) i.e., 84.5×10^7 moles, and using the ratios given above, (equation 5) the phosphorus associated with the degraded organic carbon would have been 0.69×10^7 moles of phosphorus. Since 1.176×10^7 moles was actually regenerated, the ratio of the phosphate which was regenerated, to the phosphorus which was contained in the decayed organic material, is 1.7: 1. This means that almost one atom of phosphorus would have been extracted from the sediment for every atom produced by decay assuming 100% return of the phosphorus in the decayed organic material to the water. If however, there was less than 100% return of the phosphorus in the mineralized algae to the water, then the amount of the phosphorus from the sediment which returned to the water would be proportionately greater.

The anoxic regeneration rates for the various components are shown in Table 12. From the values shown in Table 6, it can be seen that there was a significant increase in soluble organic phosphorus as conditions in the hypolimnion water changed from oxic (0.2 μmoles P/1) to anoxic (0.9 μmoles P/1). Thus

TABLE 12. ANOXIC REGENERATION.

The quantities, rates and proportions of components which returned to the soluble form in oxygenated hypolimnion water.

	Quantity (moles $\times 10^7$)	Rate (moles 10^{-3} $m.^{-2}$ day^{-1})	Ratio
PO_4	= 1.18	.245	1.0
C	= 88.1	18.30	74.7
N	= -9.2	-1.91	-7.8
Si	= 6.45	1.34	5.5
Mn	= 3.79	.79	3.2
Fe	= 3.80	.79	3.2
P(org)	= .69	.14	0.6
P(inorg)	= .49	.10	0.4
C(org)	= 84.5	17.6	71.8
C(inorg)	= 3.6	.8	3.3

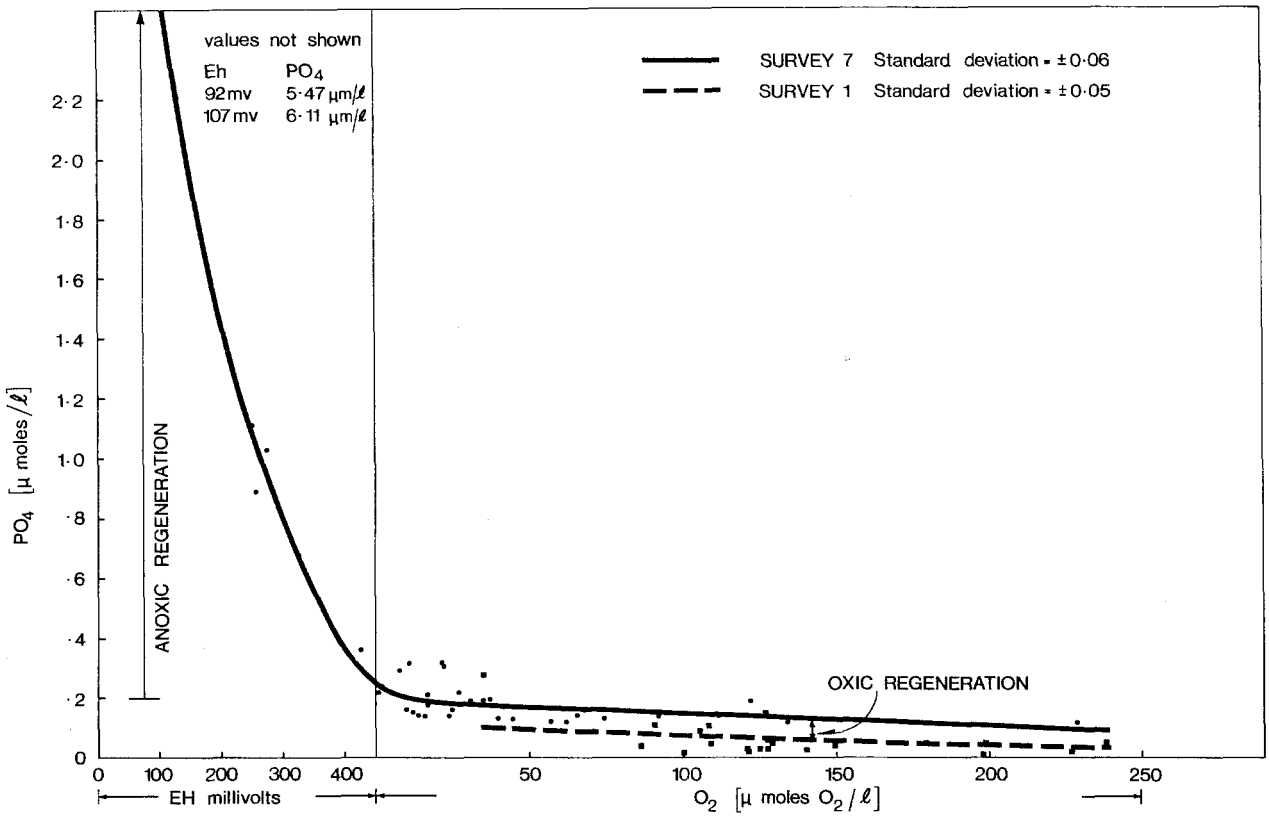

Figure 12. Plot of oxygen-phosphate and Eh-phosphate relationships, Surveys 1 and 7.

the total anoxic phosphorus regeneration was higher than the anoxic inorganic phosphate regeneration. Inorganic phosphate (soluble reactive phosphorus) forms the basis of the following discussion and this means that all phosphorus estimates based on inorganic phosphate regeneration are conservative.

Vollenweider (1968) has made an estimate of the anoxic regeneration rate for phosphate in a lake having two anoxic periods averaging 155 days each and the value obtained was 0.31 m.moles $m.^{-2}\,day^{-1}$ which approximates the values of 0.24 m.moles $m.^{-2}\,day^{-1}$ for Lake Erie. It can be seen that the anoxic phosphate regeneration rate is 11 times greater than the oxic rate.

Kemp *et al.* (1971) has given values for the atomic ratio of organic carbon: nitrogen; phosphorus in the top 3 mm of material from a core taken within 1 mile of Station P in the Central Basin (see (a) below). If one assumes that the C: N: P ratios for the sedimenting algal material (see (b) below) are representative; then, it is possible to calculate what the regeneration ratio of these elements should be (see (c) below). It is of interest to note that the ratio calculated on this basis falls between the values given above for oxic and anoxic regeneration, which suggests that the material remaining on the bottom has undergone decay under both conditions.

(a) Sediment (Kemp *et al.*)	C: N: P = 68: 8.6: 1
(b) Algae	C: N: P = 122: 18: 1
(c) Regeneration (calculated)	C: N: P = 176: 27.4: 1
(d) Regeneration (oxic)	C: N: P = 517: 32.6: 1
(e) Regeneration (anoxic)	C: N: P = 72:-7.8: 1

Figure 12 graphically represents the phosphate-oxygen relationships found on the first and last surveys and gives some idea of the differences which can be caused by oxic and anoxic regeneration. The graph is complex because an attempt has been made to change from an oxygen scale to an Eh scale when

TABLE 13. Phosphorus Quantities in the Central Basin of Lake Erie, September and October 1970.

Month	Volume	Conc.(1) s.r. PO_4	Conc.(2) S.O.P.	Conc. particulate P	Quantity s.r. PO_4	Quantity particulate P	Quantity S.O.P./
September 1970	HYPO – 9.4 km^3	2.00 μm/ℓ	0.394 μm/ℓ	0.81 μm/ℓ	18.8×10^6 moles	7.6×10^6 moles	3.7×10^6 moles
	EPI – 275.7	0.06	0.104	0.30	16.6	82.6	28.6
	TOTAL – 285.7				35.4	90.2	32.3
October 1970	TOTAL – 285.1 km^3	0.112 μm/ℓ	0.007 μm/ℓ	0.256 μm/ℓ	31.9×10^6 moles	73.0×10^6 moles	22.0×10^6 moles

(1) s.r. PO_4 represents soluble reactive phosphorus.

(2) S.O.P. represents soluble organic phosphorus.

the oxygen concentration reached a zero value. The judgement that an Eh of 450 mv was equivalent to 0.0 oxygen content is purely arbitrary. On occasion when a sample had both an oxygen value above 0.0 and a low Eh, the value was plotted according to the oxygen value. It would appear that the phosphates started to increase in concentration in the water when it contained about 20 μmoles O_2/1 (0.64 mg O_2/1). Presumably at this oxygen content in the water 1.0 m from the bottom, the sediment-water interface was already anoxic. This suggestion is largely in agreement with the bacterial findings since the *desulfovibrio* bacterial counts were seen to increase in the water column once the oxygen concentration had decreased to the range of 45-60 μmoles O_2/1 (Menon, Marion and Miller, pg 80). Figure 12 demonstrates quite definitely that if the oxygen content of the hypolimnion water is kept above 30 μmoles O_2/1 (1.0 mg O_2/1), anoxic phosphate regeneration can be averted.

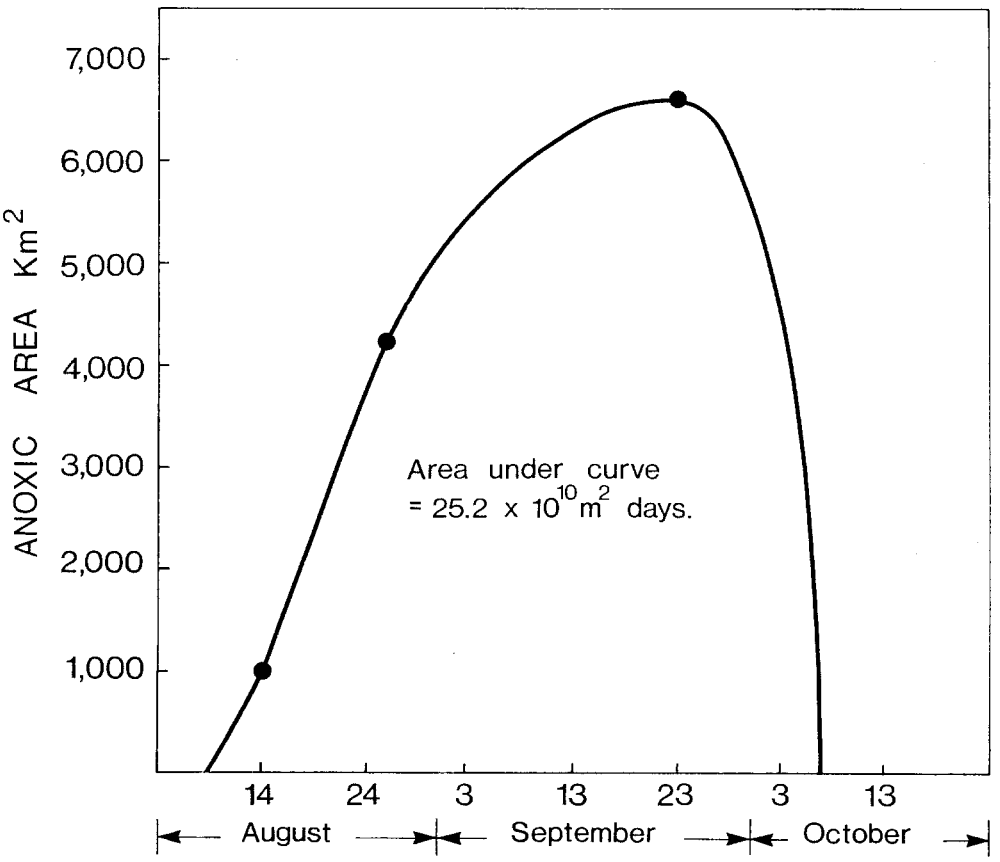

Figure 13. Extent of anoxic conditions during the summer, 1970, Lake Erie Central Basin.

FATE OF REGENERATED QUANTITIES

There is little doubt that the nutrients released under oxic conditions will remain soluble when the hypolimnion water mixes with the surface water during the overturn. During this study a low concentration of iron was always found in the surface water but the manganese was below the detection level in most instances. This may be due to the colloidal form of iron being much less dense than the oxidized manganese form which settled out. It is possible that manganese was a limiting nutrient in the surface waters at times during this study.

Phosphate concentrations of 1.3 μmolar and iron concentrations of 6 μmolar at a pH of 7.4 were about average for the anoxic hypolimnion water found in this study. If this anoxic water were mixed with equal quantities of oxygenated surface water the pH would rise to approximately 8 and it would appear from the equilibria described by Stumm and Morgan [Aquatic Chemistry, Stumm and Morgan, pg. 533], that the iron would precipitate out as the hydroxide and not the phosphate. The ferric hydroxide could then absorb, and exchange with some of the phosphate molecules but it is difficult to estimate the extent of the absorption. In this regard data are available from the C.C.I.W. monitor cruises. The results from two cruises showing the quantities and volume weighted averages of soluble reactive phosphate, particulate phosphorus and soluble organic phosphorus for September 1970 and October 1970 are listed in Table 13. The pertinent information in this case is that there was a small, completely anoxic hypolimnion remaining in the basin in September and that during the time interval between the two cruises, the hypolimnion was eroded away with the result that the lake was completely unstratified and oxygenated in October.

The results shown in Table 13 are that the soluble reactive phosphorus decreased by approximately 10% during the overturn whereas the decrease would have been approximately 53% if all the anoxic soluble reactive phosphorus had converted to the particulate form. In fact the proportion of soluble reactive phosphorus to particulate phosphorus increased rather than decreased with the overturn. These results indicate that a significant part of the soluble phosphorus (both organic and inorganic) regenerated under anoxic conditions re-enters the life cycle of Lake Erie.

Data from the September and October C.C.I.W. monitor cruises together with data from this study have made it possible to estimate the area and duration of anoxic conditions of 25.2×10^{10} m.^{2} days, during the summer of 1970 (Fig. 13). Using the value obtained above for the anoxic regeneration rate for phosphate, it is possible to estimate the quantity of phosphate which was regenerated under anoxic conditions during the summer

$= 25.2 \times 10^{10}$ m.^{2} days x 0.245×10^{-3} moles m.$^{-2}$ day^{-1}
$= 6.3 \times 10^{7}$ moles P
$= 1955$ metric tons of phosphate

The total content of the basin just before the onset of anoxic conditions was 15.5×10^{7} moles of soluble reactive phosphorus (which is taken here as being equivalent to phosphate), thus the anoxic conditions raised the total quantity of available phosphate by 40% between August and October. This was a period of peak algal growth as shown by Figure 14. The values for chlorophyll were corrected for phaeophytin content and represent the viable algae. These data (obtained on various monitor cruises) have been kindly made available by Dr. W.A. Glooschenko (C.C.I.W.). The volumes of the hypolimnion presented here are calculated on the basis of the monitor cruise data and differ somewhat from the volumes calculated using "Project Hypo" data. These differences are largely due to different station patterns and the use of different types of bathythermographs. It can be seen that there is a correlation between hypolimnion volume decrease and chlorophyll increase. The upward entrainment of the anoxic hypolimnion water during September 1970 would have provided a supply of water enriched, by all, or nearly all of the nutrients necessary for algal growth, resulting in the observed large growth pulse. The results of Braidech, Gehring and Kleveno (pg 66) confirm this, for they show that the highest algal concentrations which were encountered in the water during the project, were found just above and in the mesolimnion at stations where the hypolimnion water had recently become anoxic.

INTERNAL LOADING vs. EXTERNAL LOADING

It was demonstrated above that the anoxic conditions added a large amount of phosphate to the lake at a critical period in the annual cycle. The question then arises: how does the internal loading of phosphate compare with the external loading of phosphorus?

The 1970 C.C.I.W. Lake Erie Monitor Cruises made it possible to estimate the loading of phosphorus into the Central Basin. The three monitor cruise stations on the western edge of the Central Basin show a fairly constant value of total phosphorus content in the water of 1.27±0.1 μmole P/1. This fact, together with the information that the annual flow of the Detroit and Maumee Rivers is 160 km^3/yr, means that approximately 6,300 metric tons of phosphorus enter the Central Basin each year from the Western Basin. In addition, the International Joint Commission Report on Lake Erie (1969) estimated the annual input of phosphorus to the basin from external sources to be 3,950 metric tons/yr, giving a total external input to the Central Basin of 10,300 metric tons/yr or 860 metric tons/month.

The period of internal loading due to anoxic conditions lasted a little over two months from August 9th to approximately October 10th, 1970. During this time, the extent of regeneration activity was 89.2×10^{10} $m.^2$ days of which 25.2×10^{10} $m.^2$ days was anoxic and 64.0×10^{10} $m.^2$ days was oxic. Using these values, it is possible to calculate the following quantities for the two-month period prior to the fall overturn:

External phosphorus loading (2-month)	= 1720 m. tons of phosphorus
Internal phosphate loading (2-month) oxic regeneration	= 437 m. tons of phosphorus
Internal phosphate loading (2-month) anoxic regeneration	= 1914 m. tons of phosphorus
Minimum total internal loading (2-month)	= 2351 m. tons of phosphorus
Total loading (2-month)	= 4071 m. tons of phosphorus

These values show that the Central Basin is no longer always acting as a settling basin for phosphorus but instead is becoming a production basin for the element during the period of summer stratification.

Two publications (Prince and Bruce (1971) and the Report to the International Joint Commission on the Pollution of Lakes Erie, Ontario and the St. Lawrence River (1969)) both recommend the reduction of phosphorus inputs to Lake Erie as a means of improving the water quality of the lake. If these assessments of the situation are correct and the phosphorus inputs to the lake are reduced by 80%, which is a preliminary recommendation of the Report to the International Joint Commission, then it is likely that the sediment oxygen demand will be diminished such that anoxic conditions will not occur during the stratified period (Gilbertson, Dobson and Lee, pg 143). It is then possible to make some projections as to the probable phosphorus loading on the Central Basin using the value for the oxic regeneration rate of phosphate:

Estimated external P loading (2-month)	= 342 m. tons of phosphorus
Estimated internal phosphate loading (2-month) oxic conditions prevailing	= 607 m. tons of phosphorus
∴ Estimated total loading (2-month)	= 949 m. tons of phosphorus

This indicates that if the external phosphorus loading on the Central Basin is reduced by 1378 metric tons there will probably be a reduction of the total loading on the basin of at least 3122 metric tons during the two-month late summer period.

SUMMARY

The study can be summarized most simply by following and explaining the observed sequence of events. From the monitor cruise data it is apparent that there was a fairly large erosion of the hypolimnion during the month of July 1970 (43.2 km^3 on July 3rd to 27.6 km^3 on July 27th). This

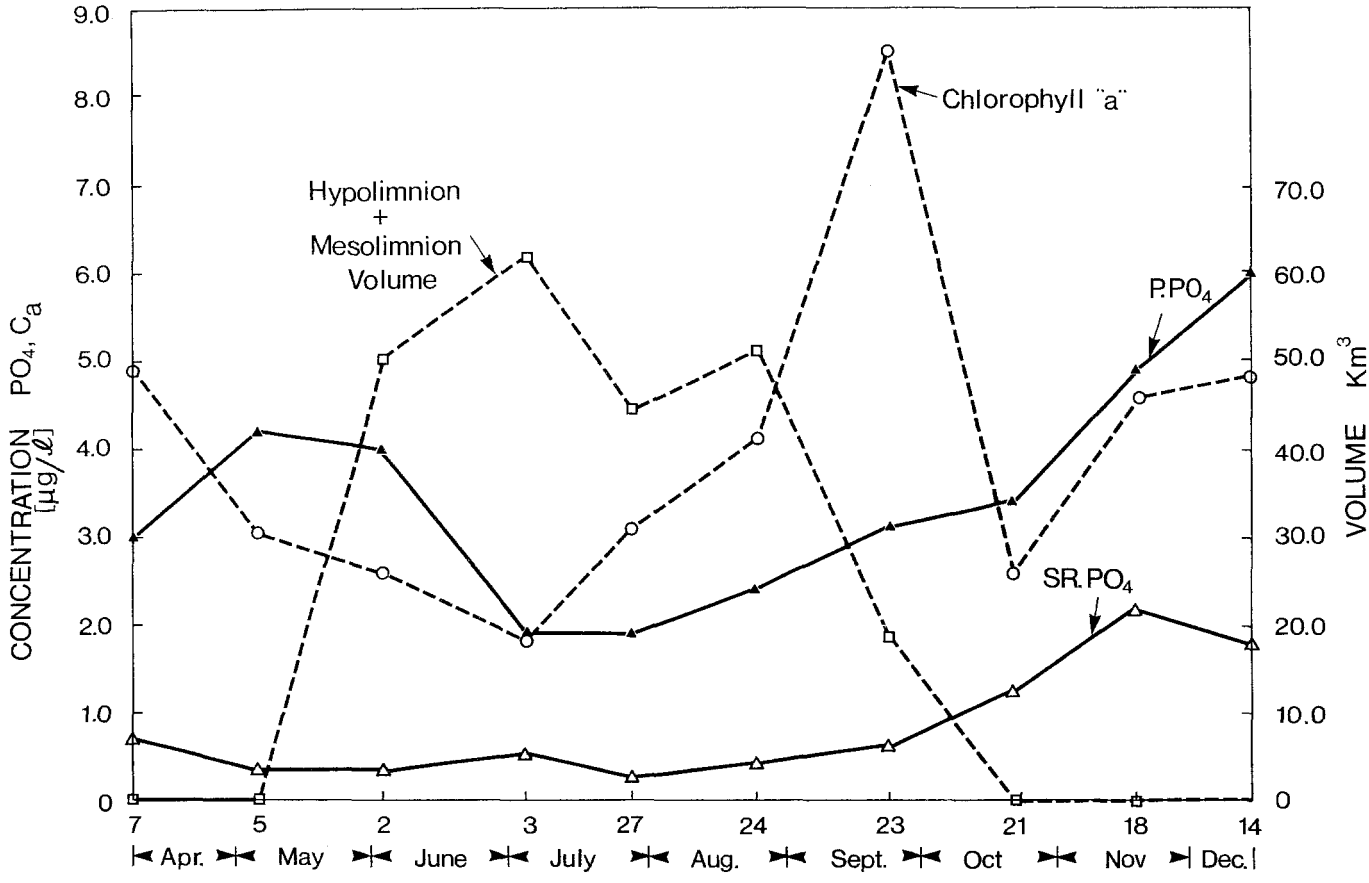

Figure 14. Plots of soluble reactive phosphorus, particulate phosphorus, and Chlorophyll *a* in the Central Basin epilimnion. Also shown is the hypolimnion plus mesolimnion volume.

seemed to be the initial factor in starting the growth period which lasted from the end of July to October 1970. The first bloom was heavy and resulted in a large fall-out of algae onto the lake floor during the last week of July. These sedimented algae were photosynthetic for a while after falling onto the lake bottom. Although the oxygen depletion was ameliorated by the oxygen production of living algae, organic decay continued to cause a net oxygen depletion. The aerobic heterotrophic and sulfate-reducing bacterial populations increased steadily while the living algae on the bottom died and matted down. By approximately the 10th of August most of the sedimented algae seemed to have died. The loss of the oxygen from photosynthesis together with the activity of the large bacterial populations caused a high rate of oxygen depletion from the 10th to 17th August with anoxic conditions being first observed on the 12th of August. The oxygen depletion rate was again diminished on or about the 17th of August by a further period of algal rains which again produced oxygen by photosynthesis. However, the photosynthetic effects of the algae were not sufficient to prevent the spread of anoxis which, by the 25th of August, extended across approximately 4,200 km^2 of the 12,700 km^2 hypolimnion area.

The anoxic conditions caused large scale nutrient regeneration by the dissolution of inorganic forms, and a massive bloom resulted when these nutrients were mixed with surface water during September.

CONCLUSIONS

It is now possible to make a number of conclusions relevant to the initial aims of the study.

1. The massive algal bloom in the Central Basin during the last week of July 1970, caused a 2-3 cm thick layer of algae to be laid down on the floor of the basin and was the major cause of anoxic

conditions which subsequently developed in the hypolimnion.

2. The net oxygen demand was variable being influenced by the photosynthetic oxygen produced by the sedimented algae, but remained negative throughout the study; the average oxygen demand was -12.3×10^{-3} moles O_2 $m.^{-2}$ day^{-1} which is close to the demand expected of a eutrophic lake. The observed change of oxygen concentration in the water was approximately -40 μmoles O_2 $l.^{-1}$ day^{-1} or -3.9 mg O_2 $l.^{-1}$ $month^{-1}$.

3. Approximately 88% of the oxygen uptake was due to bacterial degradation of algal sedimentation, with 12% of the oxygen being taken up in the oxidation of reduced metallic species.

4. Since nutrients cause organic growth, with phosphorus often being the limiting nutrient, and since the oxygen depletion was largely due to organic decay, it can be concluded that a reduction of nutrients, especially phosphorus, would lead to a corresponding decrease in the oxygen depletion rate.

5. Anoxic regeneration of phosphate was observed to commence only when the oxygen concentration in the water fell below 20 μmoles O_2/l (0.6 mg O_2/ l).

6. Since phosphorus deficient growth conditions are often encountered in Lake Erie and the internal loading of phosphate under oxic conditions is *low*, it is possible to make the conclusion that Lake Erie would soon return to an acceptable state if phosphorus inputs to the lake were decreased such that oxygenated conditions were maintained all year in the lake.

7. The oxygen contour maps show that complete oxygen depletion started at the western end of the basin the week of 4th – 10th August and moved eastwards, with the eastward movement being more rapid in the shallow water and along the southern shore. By the 25th of August 1/3 of the hypolimnion was anoxic and on the 23rd September 1970 the complete hypolimnion was found to be anoxic. The extent of observed anoxic conditions during the summer of 1970 was 25.2×10^{10} $m.^2$ days

8. The anoxic regeneration rate of soluble reactive phosphorus was 245.0 μmoles $m.^{-2}$ day^{-1} and was approximately 11 times greater than the oxic rate which was 22.0 μmoles $m.^{-2}$ day^{-1}.

9. The anoxically generated phosphate is largely the result of the solvation of inorganic complexes which were insoluble under oxygenated conditions. In the Central Basin of Lake Erie a large part of the phosphorus regenerated under anoxic conditions apparently re-enters the life cycle of the lake.

10. During the oxic degradation of organic materials only approximately 45% of the nitrogen and 25% of the phosphorus contained in the organic material returned to the water in soluble form.

11. The anoxic conditions caused an internal loading of phosphate to the Central Basin equal to 111% of the external loading of phosphorus during the same period. This quantity together with the oxic regeneration in the complete basin for the same period caused the 2-month internal loading to equal 137% of the external loading. The Central Basin is now changing from being a settlement basin for phosphorus to a production basin for the element during the summer stratification period.

12. Under anoxic conditions there was a considerable loss of inorganic nitrogen nutrients which were presumably converted to nitrogen gas. This loss decreased the quantity of nitrogen nutrients regenerated by 44%.

13. Manganese and iron came out of the sediments in the atomic ratio of Mn : Fe = 2 : 1 under oxic conditions but the ratio under anoxic conditions was Mn : Fe = 1.0 : 1.0.

14. In the mesolimnion, the chemocline gradient varies with the chemical species and is frequently non-linear with depth even when the thermocline gradient is linear.

ACKNOWLEDGEMENTS

We would like to thank the members of the Technical Operations Section and Water Quality Division who were involved in "Project Hypo" and also the Captain and crew of the *Limnos* who worked very steadily during a tiring assignment. The work of the Environmental Protection Agency personnel in providing graphs and figures and almost immediate analysis of shore samples is much appreciated. We would like to thank Dr. Mary Thompson for anticipating both the programming and the ship-time needs of the project as well as ensuring that the necessary number of personnel were available. We would like to thank Dr. Jim Kramer not only for the data processing which was done, but also for suggesting methods for the management of the data.

REFERENCES

AMERICAN PUBLIC HEALTH ASSOCIATION. 1965. Standard methods for the examination of water and wastewater. 21st Ed., A.P.H.A., N.Y.

BERNER, R.A., SCOTT, M.R., and C. THOMLINSON. 1970. Carbonate alkalinity in the pore waters of anoxic marine sediments, Limnol. Oceanogr., 544.

CHAWLA, V.K. and W.J. TRAVERSY. 1968. Methods of analyses on Great Lakes waters. Proc. 11th Conference Great Lakes Res., 524-530.

HARTLEY, R.P. 1968. Bottom currents in Lake Erie. Proc. 11th Conference on Great Lakes Research, Inter. Assoc. Great Lakes Res., p. 398.

HUTCHINSON, G. EVELYN. 1957. A treatise on Limnology. Vol. 1. Wiley Inc., New York.

INTERNATIONAL LAKE ERIE WATER POLLUTION BOARD AND INTERNATIONAL LAKE ONTARIO – St. Lawrence River Water Pollution Board. 1969. Report to the International Joint Commission on the Pollution of Lake Erie, Lake Ontario, and the International Section of the St. Lawrence River. Vol. 1, 150 p.

KEMP, A.L.W., C.B.J. GRAY and A. MURDOCHOVA. Changes in C, N. P and S in the last 140 years in three cores from Lakes Ontario, Erie and Huron, *In* Nutrients in Natural Waters, ed. H. Allen and J.R. Kramer. J. Wyley Inc., New York, N.Y. In Press.

PRINCE, A.T. and J.P. BRUCE (1971). Development of Nutrient Control Policies in Canada. *In* Nutrients in Natural Waters, ed. H. Allen and J.R. Kramer. J. Wyley Inc., New York, N.Y. In Press.

STUMM, W. and J.J. MORGAN. 1970. Aquatic chemistry. An introduction emphasizing chemical equilibria in natural waters, pp. 553. Wiley-Interscience, New York.

VOLLENWEIDER, R.A. 1968. Scientific fundamentals of the eutrophication of lakes and flowing waters, with particular reference to nitrogen and phosphorus as factors in eutrophication. Organization for Economic Co-operation and Development – DAS/CSI/68.27.

9. *Project Hypo - Discussion of Findings*

N.M. Burns, Ph.D.
Canada Centre for Inland Waters
Burlington, Ontario, Canada

C. Ross
U.S. Environmental Protection Agency
Fairview Park, Ohio, U.S.A.

This report discusses some of the interdisciplinary findings of the study together with a few concerns as to future possible changes in the lake. The entire project gives rise to only one recommendation – phosphorus loadings to Lake Erie must be drastically reduced – the immediate implementation of this recommendation is considered to be vital.

EFFECTS OF ALGAE

Algae of planktonic origin were deposited intermittently into the hypolimnion and onto bottom sediments in the Central Basin during July and August. These algae most likely sedimented to the bottom because of hypolimnetic volume increases together with changes in the stages of viability and density of the organisms. The dominant genus on the sediment, *Tribonema,* increased in numbers long after declining in dominance in the water column, indicating cell division on the bottom sediments, (Braidech, Gehring, Kleveno (pg 67)). This was demonstrated by diurnal fluctuations in the sediment oxygen demand which were measured during time intervals after algal rains, indicating photosynthetic activity (Lucas and Thomas (pg 48)). Concurrently, nitrifying bacteria reached maximum peaks at the sediment-water interface. It has been concluded that the large amounts of algae deposited on the bottom of the Central Basin during the study period were the primary source of organic carbon utilized in the consumption of hypolimnetic oxygen by bacteria. A fraction of the sedimented algae did actively photosynthesize, stimulating the nitrification process by supplying oxygen and raising the oxidation potential at times when either parameter would have been limiting to the nitrifying bacteria. Oxygen produced by the algae did not increase the net concentration of dissolved oxygen in the hypolimnion since the overall oxygen uptake rate was so much higher than the input rate, but did temporarily diminish the sediment oxygen demand.

The fact that algae produced oxygen on the bottom sediments needs amplification, because the first implication might be that the algae produced an overall favorable effect in the hypolimnion. Environmental conditions existing at the bottom, i.e., limiting light and less than optimum temperature conditions, caused most algae types to be nonviable with the exception of two genera. Examination of the sediment oxygen uptake rates indicates that the photosynthetic rate rarely exceeded the uptake rate of oxygen at the sediment-water interface. The environmental conditions probably caused the surviving algae to have a respiration rate higher than the photosynthetic rate most of the time. In addition, as the photoperiod progressively decreased during the study, and surface turbidity was increased by increasing phytoplankton volumes, light became biologically limiting to all viable algae.

Analysis of the above facts strongly indicates:

(1) Most algae sedimented to the bottom, died and added to the biological oxygen demand in the hypolimnion almost immediately.

(2) The surviving genera of algae were under great stress due to unfavorable environmental conditions causing the respiration rate to exceed the photosynthetic rate most of the time.

(3) The oxygen produced by the sedimented algae was small in comparison to the oxygen demand created by the expired algae.

Previous claims of the thermocline being a trap or barrier for sinking detrital materials and decaying algae, were not substantiated by the observed bacterial gradient, i.e., no significant build-up of bacteria as related to a region of gross biological decay was found at the thermocline during the period studied (Menon, Marion and Miller, pg 74).

CAUSES AND SITE OF OXYGEN DEPLETION

There were two main oxygen depletion mechanisms operating in the Central Basin. The smaller effect was the oxidation of reduced metallic species and this caused approximately 12% of the observed depletion (Burns and Ross, pg 107).

The larger effect was the oxygen used in the bacterial oxidation of organic materials and constituted 88% of the observed depletion (Burns and Ross, pg 107). The evidence for this statement is chemical and bacteriological. A sufficient quantity of biologically produced CO_2 was observed to be generated in the hypolimnion to account for the oxygen taken up by the biological oxygen demand; the average observed numbers of aerobic heterotrophic bacteria in the hypolimnion was estimated at 14.3×10^{21} cells and at the uptake rate of 24×10^{11} mg/hr would utilize 677×10^7 moles of oxygen during the study, (Menon, Marion, and Miller (pg 82)). Only 356×10^7 moles of oxygen were actually used, that is the bacteria consumed oxygen on the average at only 52.6% of the theoretical maximum and thus could certainly account for the biologically consumed oxygen. An explanation for the apparently low bacterial efficiency rate may be that oxygen could have often been at limiting concentrations within the sediment-water interface and oxygen depletion was to some extent dependent on eddy diffusion of oxygenated water into the organic mat.

It appears that most of the oxygen uptake was occurring at, or very close to the sediment-water interface. The evidence for this is that the two sediment oxygen demand experiments showed that if the rates which were determined, were extended over the study period, then it could be expected that 325×10^7 and 331×10^7 moles of oxygen would be consumed (Blanton and Winklhofer, pg 31). The average of these two numbers, 328×10^7 moles, is 81% of the total quantity consumed, 409×10^7 moles. Secondly, approximately 96% of the total hypolimnion aerobic heterotrophic population was found on the lake bottom.

SEDIMENT OXYGEN DEMAND

Three different methods of measuring the sediment oxygen demand were used during 'Project Hypo'. The measurements of Lucas and Thomas (pg 47) using sediment 'light and dark' boxes demonstrated the viability of the sedimented algae and also gave a mean daily sediment oxygen demand of 12.5 millimoles O_2 $m.^{-2} day^{-1}$ (0.40 gm O_2 $m.^{-2} day^{-1}$) at Station P. Blanton & Winklhofer (pg 31) measured the sediment oxygen demand at this station on two occasions, using a 7-day sediment oxygen demand monitor, and obtained an average value of 9.7 millimoles O_2 $m.^{-2} day^{-1}$ (0.31 gm O_2 $m.^{-2} day^{-1}$). The average oxygen demand for the basin for the month of August calculated by Burns and Ross (pg 102) by means of the *Limnos* cruise data, was 12.2 millimoles O_2 $m.^{-2} day^{-1}$ (0.39 gm O_2 $m.^{-2} day^{-1}$). The value of Burns and Ross must be considered as the most representative since it was calculated on the basis of basin wide surveys. However, the agreement between the three methods is exceptional. It also suggests that Station P is fairly representative of the basin. More important though, is the fact that the agreement indicates that powerful limnological tools have been developed by Lucas and Thomas and by Winklhofer and Beier (pgs 31 and 136).

If stagnant periods in the Western Basin cause anoxic conditions to arise and the nutrients generated under these conditions to subsequently move into the Central Basin, it becomes vitally important to have accurate knowledge of the sediment oxygen demand of the Western Basin. The suggestion is made here that the instruments which have been developed should not go unused, but that a program to measure the sediment oxygen demand of the various parts of Lake Erie at different times of the year should be undertaken.

BUDGET CALCULATIONS

The explanation advanced to explain the variations in the oxygen depletion rates in terms of hypolimnion volume effects as described in the following section would not have been possible if this study had not been carried out on a budget basis but merely on the basis of following changes in concentrations. Many of the values and estimates which have been discussed in this study, were only possible because of the quantitative basis of the investigation. These were:

(a) estimation of aerobic bacterial efficiency;
(b) improved estimate of oxygen demand of the basin;
(c) estimate of inorganic and organic oxygen consumption;
(d) estimate of oxic and anoxic regeneration rates;
(e) estimate of anoxic denitrification;
(f) estimate of internal phosphate loading.

The suggestion is made here that chemical limnology studies should be set on a quantitative basis whenever possible.

HYPOLIMNION VOLUME INCREASE

One of the main features of the hypolimnion volume increases was that significant quantities of oxygen were brought into the depleted hypolimnion without causing large changes in the observed concentrations in the water. This was because the water added to the hypolimnion came from the bottom of the mesolimnion and had an oxygen concentration which was only fractionally higher than that in the water to which it was being added. The observed average rate of depletion was 40 μmoles O_2 $l.^{-1}$ day^{-1} (3.84 mg.$l.^{-1}$ $month^{-1}$). If there had been no volume change in the hypolimnion the oxygen depletion rate would have been 43 μmoles O_2 $l.^{-1}$ day^{-1} (4.13 mg.$l.^{-1}$ $month^{-1}$), that is, approximately 8% higher. If there had been a volume decrease, the depletion rate would have been even higher. Similarly, if there had been no warmer water entrained from above, it is estimated that the warning rate would have been approximately 0.7°C/month, not 1.94°C/month as was observed. Thus by comparing the oxygen depletion rates and warming rates of the Central Basin for different years, an estimate of the frequency of hypolimnion volume increase can be made, since this results in a decreased oxygen depletion rate and an increased warming rate. Dobson and Gilbertson's (pg 7) report shows their 1970 depletion rate (3.3 mg O_2/l/month) as being appreciably lower than their 1962 rate (3.9 mg O_2/l/month). It is possible that the oxygen demand in 1962 was lower than the current one but appeared to be higher because there was a pattern of hypolimnion volume decrease throughout the summer of 1962, resulting in a higher apparent oxygen depletion rate.

A second feature of the hypolimnion volume increase is that this increase may be the cause of the net movements of water in the hypolimnion. The largest observed temperature increases appear to be centered in the northeast and southwest part of the basin. These temperature increases are due largely to the entrainment of warmer surface water into the hypolimnion but a large part of the observed volume increase appears to be manifest in the northwest part of the basin, not where the largest temperature increases were observed. This suggests that the water must travel horizontally to account for the observed entrainment. The hypolimnion currents as outlined by Blanton and Winklhofer (pg 33), for stations N, W, S and R tend to confirm this explanation of hypolimnion currents, especially if a clockwise gyre is considered to exist in the eastern half of the Central Basin as outlined by Hartley (1968).

UPWELLING OF WATER MASSES

There have been observations of regions of colder water at the surface east of Point Pelee (Blanton and Winklhofer, pg 36). This mass of cold water could have originated from a hypolimnion upwelling which has been subsequently warmed or mixed with some warmer surface water. The colder water could also have originated from an upwelling of mesolimnion water. The temperature of the upwelled water is no indication of the origin of the water unless it is very close to the actual temperature of the hypolimnion in that area.

The origin of the upwelled water is very significant in an area where the hypolimnion is anoxic because many of the anoxically generated nutrients appear to have a low diffusivity into the mesolimnion. Phosphate and manganese values in anoxic hypolimnion water are usually one or two orders of magnitude higher than they are in the overlying epilimnion water, also the values of manganese and phosphate in the intervening mesolimnion are very close to those of the overlying epilimnion water. Thus, upwelled water from the mesolimnion would likely only have in the order of 1/50 of the nutrient content of water having the same temperature but being a mixture of hypolimnion and epilimnion water.

PROXIMITY OF A PROCESS OF CONTINUAL SELF-FERTILIZATION

It is not possible, on the basis of this study, to state how close the situation is to that when the lake will recycle large quantities of nutrients from the sediments each winter and summer. The extent of the summer anoxic conditions, with massive nutrient regeneration, is now fairly well known, but because of the many variables, it is not possible to predict the winter conditions on the basis of the summer situation. The winter oxygen and nutrient conditions can only be ascertained from a study of the lake during the winter. If the lake should stratify under ice cover and become anoxic during the winter, then it could be expected that during the following summer, anoxic conditions would be severe, leading to even worse conditions the following winter.

Measurements taken during February and March 1971 from the ice-breaker, *N.B. McLean,* on Lake Erie showed that oxygen was near saturation at all depths at all stations sampled during both cruises. However, the 1971 ice-cover on Lake Erie was light and the situation may not be so favorable in other years. The 1971 winter investigations do indicate, though, that oxygenated conditions are still most likely maintained during the winter and this increases the probability that the lake can be returned to a satisfactory state if immediate action is taken.

Nevertheless, the fact must be kept in mind that it is the summer depleted oxygen conditions which limit the use and enjoyment of the lake for man. The nutrients which are being regenerated *at present* during the summer, together with the continual input, cause the extensive unpleasant surface blooms in the Western and Central Basins as well as making many of the beaches unuseable. Many of the salmonoid types of fish cannot survive in the warm epilimnion temperatures or in the variable temperatures of the mesolimnion. Thus the majority of this type of fish in the Central Basin hypolimnion at the beginning of stratification in June are trapped in this body of water for the summer and must slowly suffocate as the oxygen depletes. Indeed, one of the phenomena immediately obvious to the divers during the project was the number of dead smelt (approximately one per 5-10 m^2) on the bottom where the water had become anoxic.

PHOSPHORUS AND NITROGEN ELIMINATION FROM THE LAKE SYSTEM

The Report to the International Joint Commission by the International Lake Erie Water Pollution Board, Vol. 1, listed the quantity of nitrogen retained in Lake Erie during 1966-67 as being 56%±11% of the quantity loaded into the lake during the same period; the quantity of phosphorus retained as being 84%±11% of that loaded into the lake during the same period. Since the water in Lake Erie has a short residence time with the annual flow through the lake being equal to 1/3 of the volume of the lake, it is not likely that the quantities of nitrogen and phosphorus being retained in the lake are increasing the

TABLE 1. Phosphorus and Nitrogen Elimination Ratios

Method of estimation	% Phosphorus eliminated from water	% Nitrogen eliminated from water
I.J.C. estimated retention	84	56
% retention of sedimented elements	76	57
Average value of elements retained in sediments	80%	56%

concentration of these elements in the waters of the lake, but instead are being consolidated into the sediments.

Evidence is put forward in the report of Burns and Ross (pg 111), which suggests that 76% of the phosphorus and 57% of the nitrogen in algal material which sediments to the lake floor is retained there if oxic conditions are maintained in the overlying water. The above values obtained by the two different methods are summarized in Table 1 giving an average oxic sediment retention value of 80% and 56% of the externally loaded phosphorus and nitrogen to the lake.

MAJOR FINDINGS OF 'PROJECT HYPO'

1. A massive algal bloom occurred in the Central Basin of Lake Erie during the last week of July 1970 and had two obvious effects. The first effect was that the bloom reduced the phosphate concentrations to almost undetectable levels in approximately 80% of the surface waters of the basin. Secondly, the bloom caused a layer of sedimented algae approximately 2.0 cm thick to be laid down across approximately 70% of the basin floor.

2. The organic material from the July bloom and subsequent pulses caused 88% of the oxygen depletion which was observed between July 30th to August 25th, 1970, anoxic conditions were first observed on the 12th August 1970.

3. The phosphate regeneration rate under oxygenated conditions in the Central Basin was found to be 22 μmoles P $m.^{-2} day^{-1}$; while the anoxic regeneration rate was found to be 245 μmoles P $m.^{-2} day^{-1}$; that is, the anoxic regeneration rate was 11 times greater than the oxic rate.

4. From the onset of anoxic conditions on approximately the 9th August, to the estimated date of loss of stratification two months later, the extent of anoxic conditions was 25.2×10^{10} m^2.days; during the same period the extent of oxygenated conditions was 64.0×10^{10} m^2.days.

5. Approximately 80% of the phosphorus and 56% of the nitrogen loaded into Lake Erie from external sources will be removed from the water of the lake if oxygenated conditions are maintained.

ESTIMATES BASED ON FINDINGS

1. It is probable that if the phosphorus inputs to the Central Basin during July 1970 had been considerably smaller, the late July bloom would have been of a much diminished magnitude resulting in the extent of anoxic conditions observed being much less.

2. Since 'Project Hypo' was carried out during 1970 only, any estimates of future conditions must be made in conjunction with studies which have a longer time base. Thus use is made of the estimate of Dobson and Gilbertson (pg 6) that 1960 was the first year when anoxic conditions of significant extent were manifest. Since the extent of anoxic conditions was found 10 years later (1970) to be 25.2×10^{10} m^2.days, the conservative assumption is made that the present increase of anoxic extent will be approximately 2.52×10^{10} m^2.days/year.

3. An estimate of the late summer phosporus budget can now be made. Using the estimates of phosphorus loading to Lake Erie given in the Report to the International Joint Commission (1969) and data from the Canada Centre for Inland Waters 1970 Lake Erie Monitor Cruises, the value for the loading of phosphorus into the Central Basin of Lake Erie during the two-month, late summer period was estimated, (Burns and Ross, pg 106). Further, using the oxic and anoxic regeneration rates and the expected increase of anoxic extent, estimates have been made of (a) the phosphate regeneration if oxygenated conditions had been maintained during the equivalent two-month period; (b) the probable phosphate regeneration which occurred during the two-month anoxic period in the year 1970; (c) the phosphate regeneration which would probably have occurred during the equivalent period in the 1971, given similar weather conditions; and (d) the phosphate regeneration which would probably occur in a two-month period of complete anoxic conditions. These values are:

Estimate of August and September external phosphorus loading on Central Basin	= 1720 metric tons of phosphorus
(a) Estimate of 2 month phosphate regeneration (oxic conditions)	= 607 metric tons of phosphorus
(b) Estimate of 2 month phosphate regeneration (1970 conditions)	= 2351 metric tons of phosphorus
(c) Estimate of 2 month phosphate regeneration (1971 conditions)	= 2524 metric tons of phosphorus
(d) Estimate of 2 month phosphate regeneration (anoxic conditions)	= 6773 metric tons of phosphorus

It can be seen that the Central Basin is now changing from being a settling basin to a production basin for phosporus during the summer. This production of phosphorus, at a critical period in the annual cycle of the lake, occurs just prior to the turnover and fall blooms and is the result of excessive phosphorus loading earlier in the year. A minimum annual increase of 7.4% in the phosphorus available for fall blooms can now be anticipated. It is the personal opinion of the authors that the situation outlined in (d) above will occur in or about the year 1980 if immediate action is not taken to change drastically the present trends of material loadings into Lake Erie.

CONCLUSION FROM 'PROJECT HYPO'

The above findings and estimates lead to one definite conclusion: *Phosphorus input to Lake Erie must be reduced immediately; if this is done, a quick improvement in the condition of the lake can be expected; if it is not done, the rate of deterioration of the lake will be much greater than it has been in recent years.*

ACKNOWLEDGEMENT

As Project Leader, I would like to thank Curtis Ross for his ready co-operation on this project and his willingness to work as the requirements of the project demanded, which requirements were often well beyond his stated duties.

N.M. Burns

We both wish to thank the many people who worked on this project. This long list includes the scientists who undertook the physical, biological and bacteriological investigations and their assistants, the chemical laboratory workers at both Fairview Park and Burlington, the captains and crew of both the C.S.S. Limnos, and the U.S. Coast Guard Ship Bramble, the coxswains of the Agile and Bluewater, the Public Relations Officers of both organizations and the Engineering Support groups at both Burlington, Fairview Park and NASA Lewis, Cleveland. The co-operative manner in which this large group of people discharged their respective duties has had much to do with the success of 'Project Hypo'.

N.M. Burns
C. Ross

REFERENCES

HARTLEY, R.P. Bottom Currents in Lake Erie, Proceedings of 11th Conference on Great Lakes Research (1968), 398.

INTERNATIONAL LAKE ERIE WATER POLLUTION BOARD AND INTERNATIONAL LAKE ONTARIO – ST. LAWRENCE RIVER WATER POLLUTION BOARD. 1969. Report to the International Joint Commission on the Pollution of Lake Erie, Lake Ontario, and the International Section of the St. Lawrence River. Vol. 1. 150 p.

APPENDIX I

An Automatic Underwater Camera System

R.J. Jirberg
Lewis Research Center
National Aeronautics and Space Administration
Cleveland, Ohio, U.S.A.

A special purpose automatic underwater camera system was designed and operated during the summer of 1970 to obtain a time-lapse photographic record of the algae growth and sedimentation at the bottom of mid-Lake Erie. The system was built around a conventional 35 mm camera and electronic flash unit. Automatic control circuitry enabled it to operate unattended at the bottom of the lake for extended periods of time. Details of the system's design and operational characteristics are presented.

INTRODUCTION

To obtain nearly continuous photographic documentation of lake bottom conditions, an automatic underwater camera system was specially designed and built for Project Hypo. This camera, together with an electronic flash unit as a source of illumination, sat just off the bottom in mid-Lake Erie and automatically photographed the bottom at one hour intervals. Up to 10 days of unattended operation was possible while taking up to 250 color photographs, one per hour, before retrieval and reload was required. In this way over 400 color photographs were taken in a time-lapse sequence. Presented here are the details of the construction and operation of the automatic underwater camera system.

SYSTEM DESIGN

THE CAMERA

The camera system was designed and constructed by personnel at the NASA-Lewis Research Center in cooperation with the Water Quality Office, Cleveland, Ohio of the Environmental Protection Agency. As shown in Figure 1, it was basically a two-part system. One water-tight housing contained a 35 mm motor-driven camera along with the timing and control circuitry, while the other contained the flash unit.

The camera is a commercially available 35 mm single lens reflex camera with motorized shutter release and film advance. It was equipped with a moderately wide angle (35 mm focal length) lens. However, due to refraction at the flat air-water interface at the housing, the field of view was more nearly that of a normal (50mm) focal length lens. At a height of 1 meter off the bottom, the field of view encompassed an area of the bottom vertically below the camera measuring approximately 0.6 X 0.9 meters. The actual area photographed could be viewed by the diver through the large pentaprism finder looking directly through the rear panel of the housing.

Although the optics of the system, because of the flat viewing port, were not of the water-corrected variety, the distortions were neither obvious nor objectionable in the resulting photographs. Since the field of view for the purposes of the Project did not need be too large, an extremely short focal length lens was not required. Hence, the flat viewing port was entirely acceptable.

With a maximum load of 250 frames (33-foot length of film), the camera could operate for roughly 10 days (taking one picture per hour) before retrieval and reload was required. After shooting 250

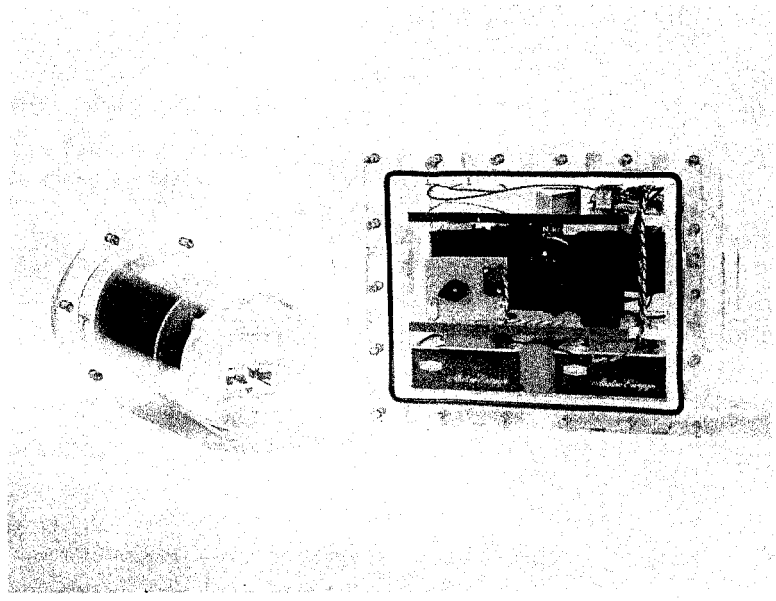

Figure 1. Camera and electronic flash units in their watertight housings.

frames the operation of the camera automatically ceased in the event that the camera was not retrieved in time.

CONTROL CIRCUITRY

Automatic operation of the camera was governed by a small battery-powered clock similar to that found in home wall clocks. Power for the clock was derived from a 1-1/2-volt "C" cell. This resulted in a very efficient timing device both in terms of reliable long term accuracy and low power consumption (one battery could power the unit for over a year).

A cam on the minute-hand shaft of the clock was used to actuate a micro-switch (switch SW-2) as indicated in Figure 2. By appropriately cutting the cam with a multi-lobe pattern, the camera could be triggered as frequently as minutes apart. For this study, a single-lobe cam was selected, giving a one hour picture interval.

As the microswitch was actuated, the silicon-controlled-rectifier SCR-1 was pulsed into conduction, discharging the 3000-μf capacitor through the coil of the relay. The relay was thus momentarily energized, producing a momentary voltage reversal between two of the control leads of the motor drive unit. The nature of the motor drive unit was such that a brief voltage reversal was all that was required to initiate the sequence of (1) tripping the shutter, (2) advancing the film, and (3) recocking the shutter. Thus with each pulse to SCR-1 through the clock-driven microswitch, one frame was exposed and the camera readied for the next frame.

Between exposures the 3000-μf capacitor was recharged through the 100 K-ohm resistor. Within a few seconds after the relay was tripped, the current drain on the 12-volt battery returned to the microamp leakage level of the capacitor. The use of a capacitor discharge system conserved battery energy, and ensured that adequate energy was available to pulse the relay in the event that the battery was degraded by the cold environment of the lake. (The ambient temperature at the lake bottom is typically 6 – 12°C.) Primarily because of the need for extended operation at low temperatures, alkaline-manganese-zinc batteries were chosen in preference to the conventional carbon-zinc (Leclanche) type.

It should be noted that since low-force D.P.D.T. microswitches were not readily available, the SCR-relay-capacitor discharge circuit was a necessary complication. If such D.P.D.T. switches were

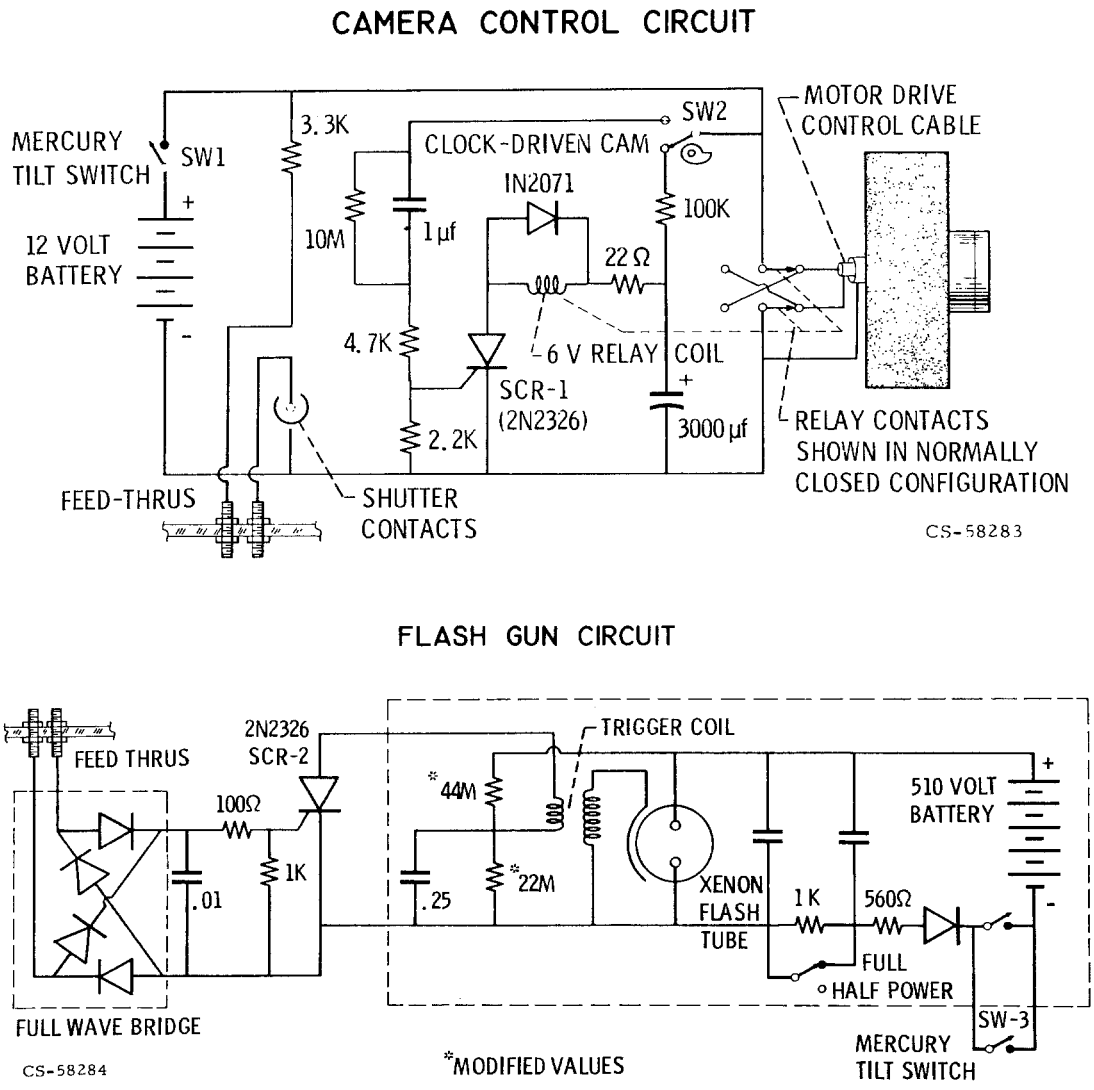

Figure 2. Camera control and electronic flash circuits for underwater camera system.

available, they would have been used to actuate the motor-drive unit directly, and hence reduce the circuit complexity.

FLASH UNIT

The flash unit was contained in a separate water-tight housing. This was done to allow a greater flexibility in positioning the light source in order to minimize the amount of light scattered into the lens by suspended matter, and to bring out texture in the target scene.

The unit is a commercially available item. It was, however, modified slightly to reduce the standby current drain on its battery. The light output of its xenon flash tube is a millisecond duration pulse of 4750 beam-candle power-seconds. Indicated in Figure 2 is the flash gun circuit with the modified trigger section. The unit used capacitor energy storage charged directly from a high voltage (510-volt) battery. Battery life was rated at 1000 flashes. However to ensure battery life for the 10-day time span, the total resistive load imposed by the trigger circuit was increased to 66 megohms. The standby battery current was thereby reduced to somewhat less than 10 microamps.

One additional modification was made to avoid directly cabling the high voltage (170 volt), high impedance trigger circuit between the flash unit and the camera housings. An SCR was added to the circuit to discharge the trigger capacitor through the trigger coil. Thus the interconnecting sync cable needed only to carry a brief current pulse from the 12-volt battery in the camera housing through the shutter contacts, to the gate of the SCR. This also greatly simplified the design of the electrical feed-throughs. A pair of 6-32 screws threaded through the housing wall were adequate for the purpose. The impedance of the gate circuit was low enough that the feed-through terminals could be exposed to the water without being shorted out by conduction through the water.

UNDERWATER HOUSINGS

The water-tight housings were constructed of annealed 1/2-inch thick acrylic plastic with rubber O-ring seals on the cover plates. Each was designed to withstand the hydrostatic pressures of the lake without the use of internal pressurization so as not to stress the camera and electronic components. Two "shelves" were included in the camera housing to support the large front and rear panels against the hydrostatic pressure. By locating the shelves immediately on either side of the lens, distortions due to a deflected viewing port were eliminated.

No attempt was made to determine the ultimate strength of either housing. Both, however, were hydrostatically tested to 65 psi or about 150 percent of the pressure experienced on the lake bottom.

The construction of the housings was also simplified by the fact that no mechanical feed-throughs had to be provided. Gravity sensing (mercury) switches (SW-1 and SW-3) in the battery circuits turned the units on when set in the intended position. The lens aperture and focus were preset before the camera was submerged.

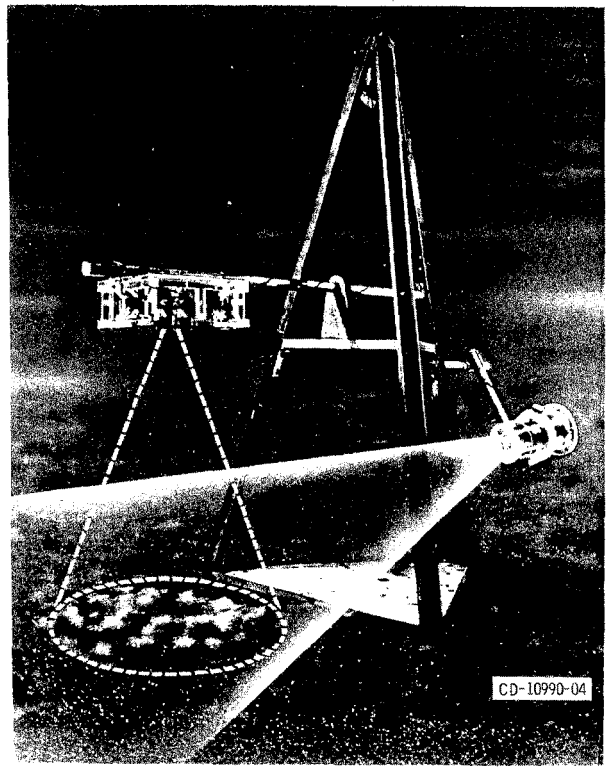

Figure 3. Underwater camera and flash unit on tripod mount as situated on the lake bottom.

IN-SITU MOUNTING

The camera and flash unit were secured to a large angle-iron tripod as shown in Figure 3. When lowered to the bottom of the lake, the legs of the tripod sank into the sediment, and the tripod came to rest with its lower panel essentially floating on the sediment. This located the camera approximately one meter off the bottom looking vertically downward at a 0.6 X 0.9 meter area of the bottom adjacent to the tripod. The flash unit was positioned to one side, nearly 80° off the vertical, to illuminate the bottom at a near glancing angle.

The site selected for the time-lapse study was the central monitoring station for the lake ("Project Hypo," Station P). Instruments at this site included the full complement of meteorological, chemical, and biological monitors. Lines from these as well as the tripod were attached to a central surface marker buoy. Upon returning to the site, divers would retrieve the camera and flash unit, leaving the tripod in position. After reloading the camera and replacing the battery in the flash unit, both were returned to their positions on the tripod to resume the filming of the same area of the bottom.

OPERATIONAL CONSIDERATIONS

In general the camera system performed well and provided valuable information, particularly in regard to the timing of the algae sedimentation, in noting subtle changes occurring on the bottom, and in revealing some unexpected effects of bottom currents on sediment resuspension. For a discussion of these and related topics, consult the several companion papers published herewith. "Project Hypo" is also described in the NASA motion picture film C274 along with some of the photographs taken in the time-lapse sequence. (This film is available upon request by contacting The Lewis Research Center, Cleveland, Ohio.)

During the course of the study, some unforeseen situations did arise in the camera's operation, while on the other hand some situations that were anticipated did not materialize. For example, it was thought that moisture condensing on the inside of the viewing port might present a problem. Initially, in addition to enclosing several silica gel packets in the camera housing, the housing was flushed with dry nitrogen. Later the nitrogen flush was abandoned. No condensation was noted. Indications are that the humidity within the camera housing was quite low since occasional small static electrical discharges were recorded on the film presumably as the film was advanced through the camera.

Condensation was a problem, though, when the camera was brought to the surface. If the housing were immediately opened, moisture from the air would condense heavily on the camera and lens, which of course were at the low temperature of the bottom waters. In the absence of some sort of changing bag on board ship that might be flushed with a dry atmosphere in which to open the housings, the camera was instead returned to shore, warmed and reloaded, and then later returned to the lake.

Also the attenuation of the illumination from the flash unit by the water was more severe than expected. With the flash unit 1-1/2 meters from the center of the field of view, and using Ektachrome type MS5256 film (ASA 64), the lens was set at f/11; a small aperture was desirable to obtain enough margin on the depth of field. Results indicate that f/5.6 would be a better choice for the exposure.

Finally, no problem was experienced with sediment clinging to the viewing port or to the housings in general – a point of initial concern.

CONCLUDING REMARKS

Our experience with this camera system indicates that a camera encased in a simple plastic housing can indeed be submerged to sit on the lake bottom and effectively record imagery data on the physical and biological mechanisms taking place there. Through the use of automatic timing and triggering circuitry, the camera can operate unattended over extended periods of time periodically photographing the

selected scene. This time-lapse photographic record is valuable for documenting both the subtle as well as the long term changes that occur.

In this study the photographs were spaced one hour apart. A review of these photographs shows that changes occurred on the bottom over a time span somewhat shorter than the selected one hour interval. It would therefore be desirable in the future to shorten the picture-taking interval to perhaps every 10 or 15 minutes in order to better trace these changes. Such a timing modification is easily accomplished.

APPENDIX II

A Submersible Automatic Dissolved Oxygen-Temperature Monitoring System

C.J. Beier
U.S. Environmental Protection Agency
Region V, Lake Erie Basin Office
Fairview Park, Ohio, U.S.A.

In July of 1970, five submersible monitors were moored in the Central Basin hypolimnion of Lake Erie. The monitors' function was to measure and record simultaneously both water temperature and dissolved oxygen at each of five Central Basin locations. The monitors proved to be both durable as well as reliable, having provided continuous data for a period of fifty days, during which any changes in either of the parameters were documented as they occurred in the hypolimnion. Preliminary evaluation of these data strongly suggests that they will materially aid limnologists in not only defining depletion rates, but will serve as a guide in explaining the cause and mechanics of deoxygenation in the Central Basin hypolimnion.

INTRODUCTION

Until now, sampling techniques for dissolved oxygen depletion rates were limited to shipboard, manual grab samples or combination dissolved oxygen-temperature profiles, utilizing semi-automatic instrumentation. Surveys of this type were restricted in frequency and duration by prevailing weather conditions. In the summer of 1970, following modifications, five commercially available dissolved oxygen monitors designed to measure and record *in situ* dissolved oxygen and temperature simultaneously and on a continuous basis, were placed at five locations in the Central Basin hypolimnion of Lake Erie, as shown in Figure 1. Here they successfully documented, for the first time, on a continuous basis, the dissolved oxygen depletion rate in the hypolimnion, over a period of fifty days.

DESCRIPTION OF EQUIPMENT

The dissolved oxygen-temperature monitor, was a completely submersible system comprised of three major assemblies; the instrument module, a multi-conductor cable, and the sensor module.

The instrument module housing was rectangular in shape measuring 41.9 cm x 41.9 cm x 54.6 cm and was constructed of welded anodized aluminum. In order to minimize corrosion the entire exterior was coated with epoxy paint. In designing the module, a weight-volume ratio was observed to achieve positive buoyancy, while at the same time maintaining the necessary structural strength required to withstand external pressures at depths down to an including 9 meters.

The interior of the module was divided into two sections. One section was used to restrain the battery packs that constituted the monitor's power supply. The other section served as a cabinet and platform for the dual recorder and analyzer components needed for both the dissolved oxygen and temperature parametric systems. These systems were totally independent of one another except for the common power supply. A mooring bridle was attached to both ends of the instrument module so that it could be moored in an upright position. This was necessary because of the operating characteristics of the strip chart recorders. The instrument module with a full complement of dry cell batteries weighed approximately 39 kilograms.

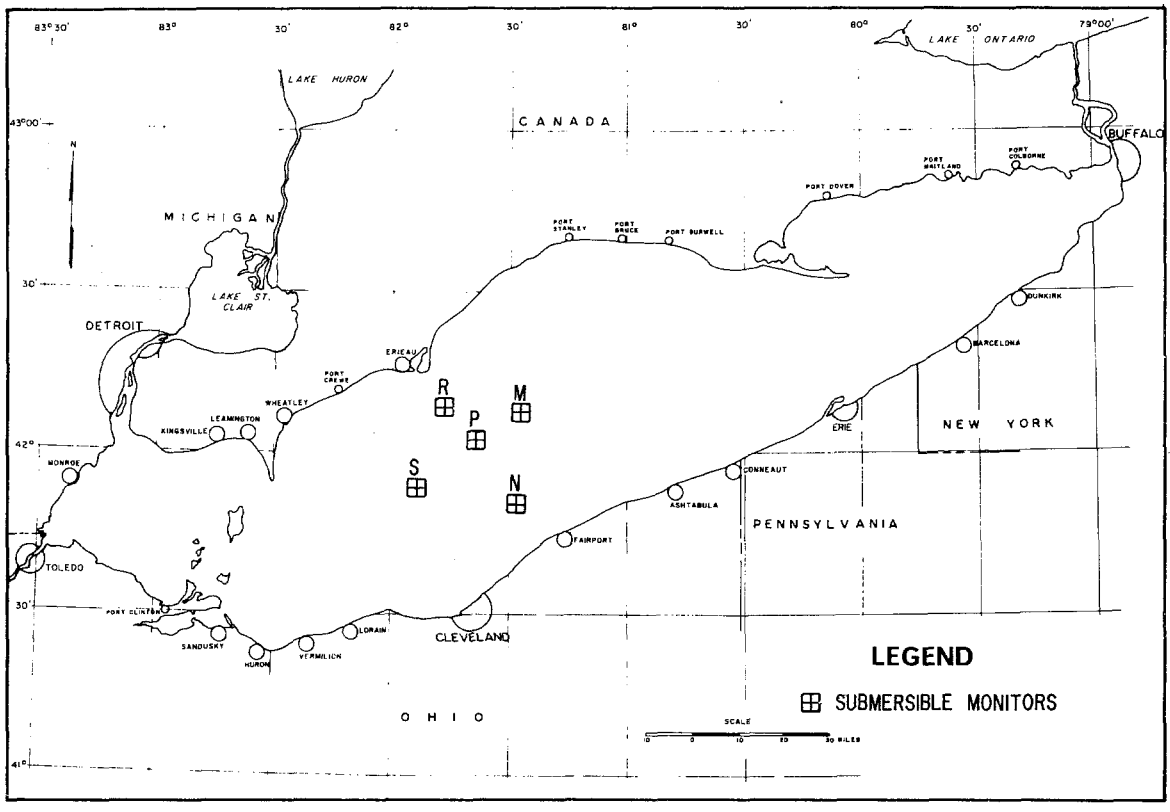

Figure 1. Submersible monitor station locations.

A single multi-conductor cable equipped with waterproof connectors served as a 45 m umbilical between the instrument and sensor modules. The cable transmitted power from the instrument module to the sensor module, and provided a path for transmission of sensor signals to the instrument module. The cable did not aid in mooring the monitor system.

The sensor module, shown in Figure 2, had a maximum depth capability of 76 m and consisted of three sub-assemblies; the probe assembly consisted of the dissolved oxygen sensor, a temperature sensor, and the dissolved oxygen compensating thermistor. A perforated cylinder formed the sampling chamber which also served to protect the sensors and cleaner-agitator impeller. The cleaner-agitator assembly was a motor driven device performing the dual roles of cleaning the dissolved oxygen sensor membrane, and provided a 48.6 cm/sec (1.6 ft/sec) sample flow across the membrane surface.

DISSOLVED OXYGEN PARAMETRIC SYSTEM

The probe assembly housing was cylindrical in shape and constructed of polyvinyl chloride (PVC). The housing contained the anode and 500 ml of electrolyte (Potassium Iodide). The amount of electrolyte coupled with an anode (lead) to cathode (platinum) surface ratio of 250 to 1, produced a long life dissolved oxygen sensor (Polarographic Cell). The versatility of the sensor was increased by the choice of teflon membranes available to suit specific needs or applications. The membranes were precut, teflon discs easily installed and available in thicknesses of 1/2, 1, and 2 millimeters. It should be realized that as the membrane thickness increases, the response time increases. The thermistor for the temperature compensating circuit, was located in close proximity to the dissolved oxygen membrane.

The PVC cleaner-agitator housing was cylindrical in shape and contained a fractional horsepower D.C. motor, drawing approximately 120 milliamps. The motor was magnetically coupled through the housing to the cleaner-agitator impeller. The irregular shape of the impeller enabled it to wipe the sensor membrane while providing the required sampling flow across the membrane surface.

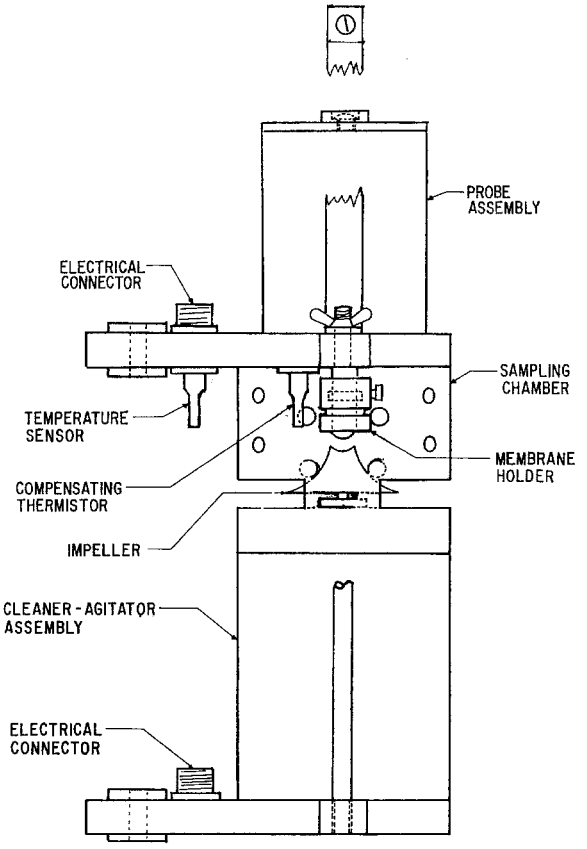

Figure 2. Sensor module.

The dissolved oxygen analyzer was designed to produce a temperature compensated linear input to the analog recorder. The specified accuracy of the system was ± 1% of full scale throughout the entire range. The system's response was dependent on the thickness of the membrane used, but in no case did it exceed 2 min. A dual range, manual switching capability was provided with range options of 0 – 30 mg/1 or, for increased resolution, 0 – 15 mg/1. Zero balance and gain controls were integrated into the circuitry and were readily accessible to facilitate calibration adjustments.

The dissolved oxygen parametric system utilized an analog strip chart recorder with a pressure sensitive carbon backed strip chart. Both the dissolved oxygen and the time scales were linear. Dissolved oxygen was read directly in milligrams per liter, with a zero deflection corresponding to a zero function. The chart advanced at the rate of 2.54 cm/hr, however, for other applications, the rate could be increased or decreased by merely substituting an appropriate gear train. At the rate of 2.54 cm/hr, the chart supply was sufficient for 30 days of continuous recording. The actual trace at this speed appeared as a continuous line since the striker bar recorded once every 2 seconds.

TEMPERATURE PARAMETRIC SYSTEM

The temperature sensor was located on the base of the probe housing, in close proximity to, and on the same plane as the dissolved oxygen membrane. The sensor consisted of two thermistors encased in a metallic waterproof housing. Each thermistor formed one arm of the temperature bridge circuit. To facilitate checking and adjusting the calibration, a test circuit was provided which isolated the sensor from the system. A variable potentiometer was also included for adjusting the span for full-scale deflection.

An analog strip chart recorder, similar to the one used in the dissolved oxygen parametric system, recorded temperature over the range of 0 – 30°C. The specified accuracy was ± 0.5°C with the analyzer producing a linear input to the recorder.

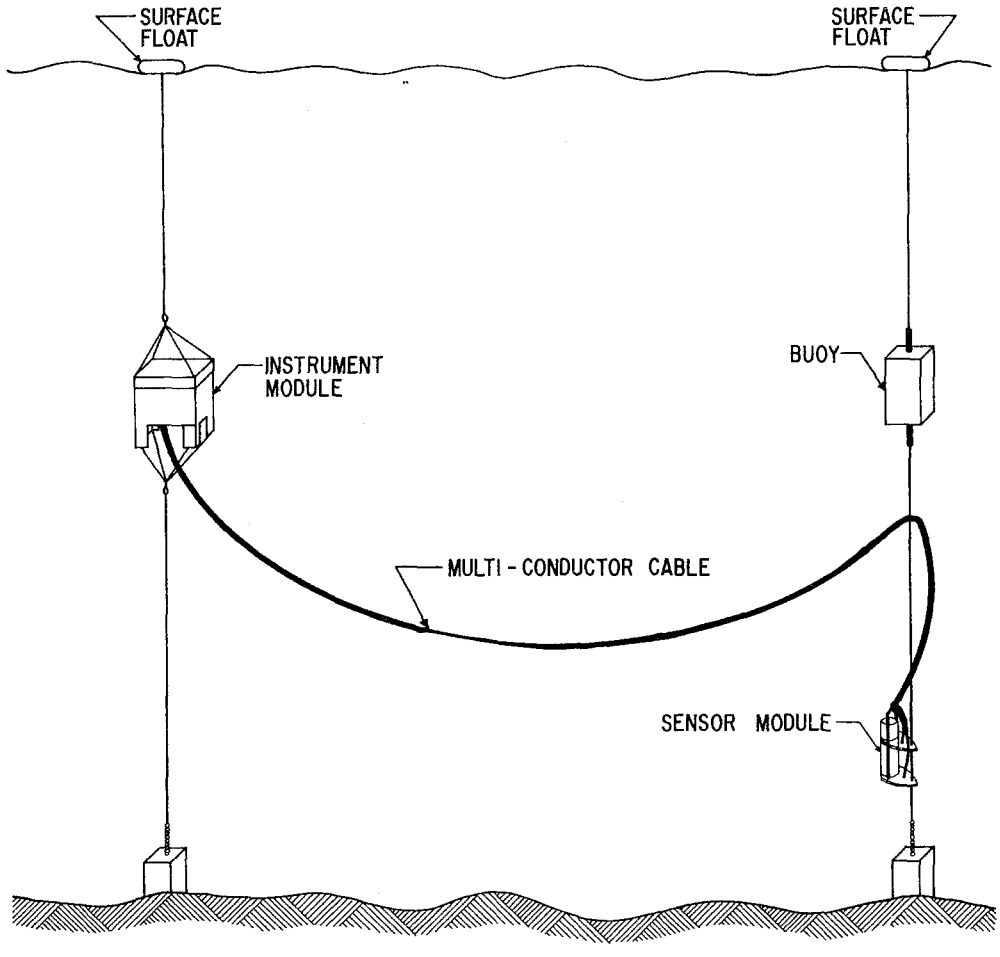

Figure 3. Typical submersible monitor taut-line mooring system.

POWER SUPPLY

The power supply contained four 6v. dry cell batteries wired to produce 12v. This power was fed to a transistorized voltage regulator, which lowered the voltage to a constant 8v. required to operate the cleaner-agitator D.C. motor. A second transistorized voltage regulator was used to provide a constant 2v. to the temperature sensor. The power supply also included two 12v. dry cell batteries that were wired to provide a plus and minus 12v. source for the dissolved oxygen and temperature amplifiers. The power supply was designed to provide ample power for a minimum of eight days of continuous operation.

MOORING

The mooring system was designed so that the instrument module could be retrieved and serviced without disturbing the sensor module. To achieve this, the instrument and sensor modules were moored separately using a taut-line mooring system (Fig. 3) and joined only by the multi-conductor cable.

The instrument module was moored at the maximum service depth capability of 9 m. The positive buoyancy of the module eliminated the need for additional flotation. The mooring was accomplished by attaching a suitable length of line from an anchor to the module bridle. A second line, secured to the module and extending to a small surface float, was used as an aid in both locating and retrieving the instrument module.

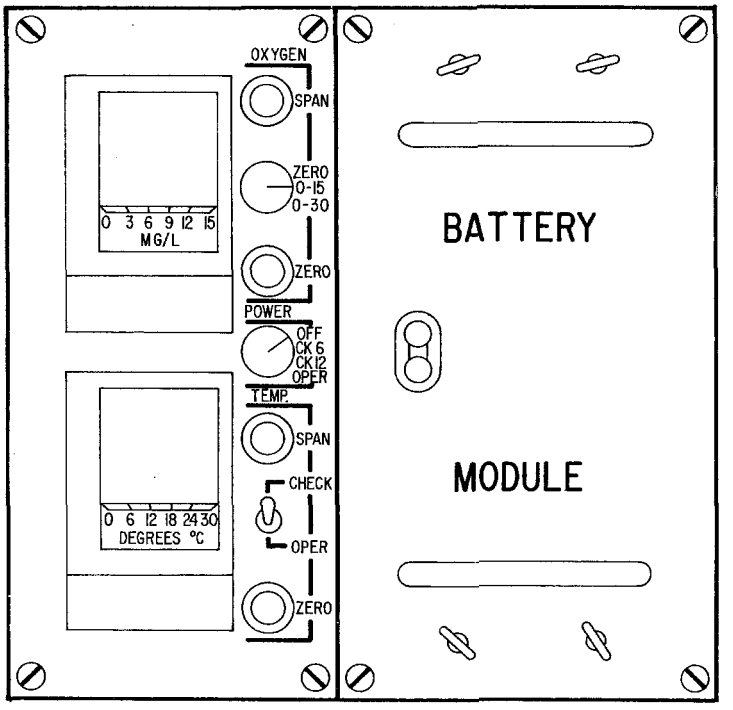

Figure 4. Instrument module control panel.

The sensor module was moored approximately 1.5 m above the lake bottom using a separate taut-line mooring. The module was suspended in the water column using sub-surface flotation. A small float was attached to the sub-surface flotation to identify the mooring.

INSTRUMENT OPERATION

The monitor was serviced at five-day intervals, allowing a three-day grace period in the event that adverse weather prevented the scheduled servicing. The instrument module was relatively easy to handle and service. Upon removing the cover plate, the battery compartment, recorders, and controls required to operate and calibrate the entire system were accessible (Fig. 4). In order to expedite field servicing and calibration, a full complement of test circuitry was provided, including a master switch that could not only activate the system, but also isolate various portions of the system. Electrical test points, for measuring critical voltages and currents, were also incorporated.

CALIBRATION AND SERVICING

The monitor was subjected to a series of control checks in the laboratory prior to attempting any field setting. The checks included determining the accuracy, response, and stability of the temperature and dissolved oxygen systems, as well as checking the recorder performance and monitor power consumption. The multi-conductor cable was checked for insulation damage, broken leads, shorts and leakage in the vicinity of the connectors. The cleaner-agitator assembly was checked for bearing wear, wiper adjustment, and power consumption. The sensor module was assembled, submerged in a container and given 24 hrs. to stabilize. After stabilization the sensor module was joined to the instrument module and calibrated.

The dissolved oxygen system was calibrated against the standard Winkler Method (azide modification). The temperature system was standardized against a laboratory thermometer, having a National Bureau of Standards certified accuracy of ± 0.25°C. Normally, valid readings were realized almost immediately with only minor control adjustments required. Major adjustments were usually an indication of damage to the membrane, or that an air bubble had been entrained in the dissolved oxygen sensor.

During the test period the sensor module was subjected to varying temperature and dissolved oxygen levels to determine the response and stabilization characteristics. A period of three or four days was sufficient to disclose the failures most likely to be encountered. The strip chart recorders were carefully monitored during this test period to assure proper chart advance.

When the monitor met all performance and calibration specifications it was ready for field use. The units were then moved on station in an assembled state to maintain the system integrity that was developed during testing. The dissolved oxygen sensor membrane was immersed in water or wrapped in wet tissue, while in transit.

At the mooring site the water depth was measured and the mooring lines adjusted to suspend the sensor and instrument modules at their assigned depths. After new batteries were installed in the monitor, the sensor module was lowered over the side to a depth of one or two meters. After stabilizing for several minutes, monitor readings were compared with Winkler titrations and thermometer readings of the surface water. When the readings were in agreement, the sensor module was moored at the desired depth. It should be noted that while the sensor module was being moored, the instrument module was still on deck to permit observing the system's reaction to the changing conditions. If during this time, abnormal readings were recorded, it was still possible to initiate corrective measures.

Once in place, monitor readings were again checked either against grab samples, or vertical *in situ* profile measurements obtained using a spare monitor. The latter procedure was preferred particularly when working in thermally stratified water. Following verification of the monitor readings, the strip charts were labeled and the instrument module was sealed and moored on station. This procedure was followed throughout the study for the routine servicing. The only exception was that the sensor module was left in place and only the instrument module was retrieved to exchange batteries and charts and check calibration. With calm to moderate seas, retrieval, servicing, and remooring was accomplished in approximately one hour.

DISCUSSION OF RESULTS

A monitor was moored at each of five Central Basin locations. The monitors were in place for approximately 50 days beginning July 13 and 14, 1970. Complete records were obtained from four monitors. Only a partial record was obtained from one monitor due to leakage of an electrical connector. A monitor record is shown in Fig. 5. The extreme fluctuations were caused by the vertical movement of the thermocline.

PERFORMANCE

Occasionally heavy seas precluded maintaining regular servicing schedules, but in no case did this result in loss of data. Although the power supply was designed for a minimum of eight days continuous operation, uninterrupted operation up to eleven days was realized with no significant loss in calibration.

The designed accuracy of the dissolved oxygen parametric system in the range 0-15 mg/l (range used in the study) was ±0.15 mg/l. Calibration checks (referenced to Winkler Method, Azide Modification) were within this range 89% of the time with an average difference of ±0.11 mg/l. The standard deviation of these data was ±0.2 mg/l.

The temperature parametric system was designed with an accuracy of ±0.5°C. This accuracy was attained in 91% of the calibration checks, with an average difference of ±0.25°C. The standard deviation of these data was ±0.4°C.

During the eight-day operating periods, no significant drift was detected in either the temperature or dissolved oxygen parametric system. The response time of the temperature parametric system was 90% within 20 sec., while the response time of the dissolved oxygen parametric system was 90% within 2 min., using a 2 mm thick membrane.

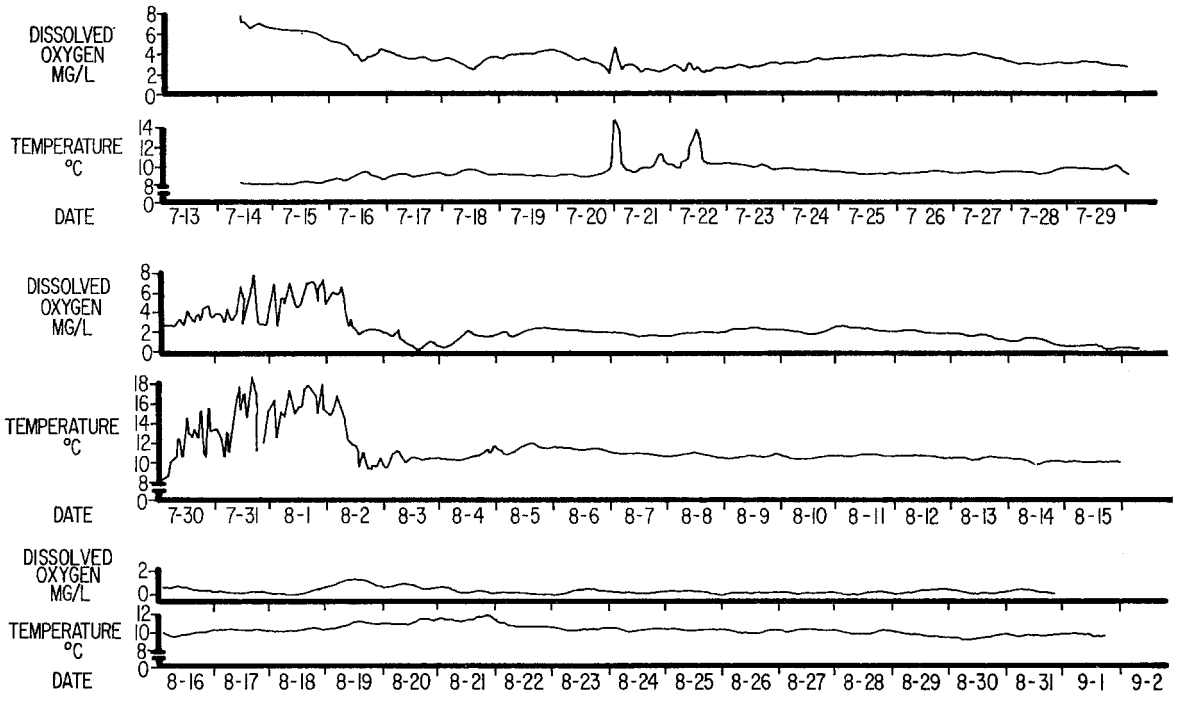

Figure 5. Lake Erie Central Basin hypolimnion temperature and dissolved oxygen data, station N, depth 21.3 m.

Although the monitors were designed for unattended *in situ* operation, their ability to accomplish vertical profiles of depth versus temperature and dissolved oxygen was clearly demonstrated. These measurements confirmed the monitor's response and reproducibility when subjected to rapid temperature and dissolved oxygen changes.

It is important to note that the sensor modules were in place for the entire 50 days. There was no evidence to indicate that aging (reduced sensitivity) had any detrimental effects on the dissolved oxygen system.

Temperature data compared favorably with data obtained from nearby *in situ* temperature recorders. Also monitor data showed good agreement with data obtained during the many basin surveys conducted during "Project Hypo".

GENERAL FINDINGS

The submersible monitors when originally procured were subjected to a detailed evaluation much broader in scope than the calibration and servicing outlined previously. There were a number of minor problems attributed to assembly techniques. The monitors did, however, exhibit two major deficiencies: (1) the power supply was insufficient to sustain eight days of continuous operation, and (2) erroneous dissolved oxygen data were obtained when the sensor module was subjected to radical temperature changes. These deficiencies were corrected before the use of the instruments in "Project Hypo".

Numerous controlled laboratory and field tests were conducted to identify the problems related to erroneous dissolved oxygen measurements associated with rapidly changing temperatures. The sensor module when subjected to a rapid temperature decrease resulted in ballooning of the teflon membrane. The ballooning was found to be the direct result of a buildup of internal pressure caused by the PVC probe housing contracting faster than the electrolyte. In some instances the internal pressure burst the membrane. Once an equilibrated temperature was attained, the ballooning dissipated but the membrane,

after being stretched, appeared wrinkled and still gave erroneous readings. The problem was resolved by placing a small, semi-rigid, rubber bladder in the probe housing that was vented to the outside. This bladder collapsed when the internal pressure increased, and resumed its original shape after the temperature equilibrated.

Servicing was difficult, even in relatively calm seas, because station depths effectively reduced the umbilical by half. This increased the possibility of dragging the sensor module while retrieving and servicing the instrument module. However, with expert seamanship, taking full advantage of wind and sea conditions, and using the surface float, identifying the location of the sensor module, as a guide, disturbance to the sensor module was minimized. A power winch proved useful for retrieving the instrument module, although it could be retrieved manually by two men.

The effects of prolonged exposure to the environment was a major concern at the onset of the study. Algal growths, a major concern, were not observed on the teflon membrane or sensor module. However, algae growths were found on the instrument module and mooring hardware above the thermocline. Another concern was sulfide poisoning the dissolved oxygen sensor. Although several sensors were exposed to sulfide rich environments for a period of several weeks, no detrimental effects were detected. Severe corrosion did occur on the aluminum multi-conductor cable connectors and to a lesser degree on the instrument modules in the vicinity of the cover plate mating surface. This surface was not protected with epoxy paint.

The most serious problem encountered was water leaking into the multi-conductor cable connectors. This was found to be caused by shrinkage of the potting material used to seal the connector to the cable. Almost no data were obtained from one monitor due to this failure.

CONCLUSIONS

1. The submersible monitor is a reliable system capable of automatically recording dissolved oxygen and temperatures *in situ* for extended periods.

2. Although the monitors were designed for a specific application, their versatility in a variety of applications cannot be overemphasized.

RECOMMENDATIONS

The monitors represent a new era in portable automatic monitoring systems. These monitors are considered a prototype for future monitoring systems having greatly expanded capabilities. Although the performance and ability of the monitors were demonstrated, the following recommendations are directed toward perfecting the monitoring system:

1. Improved analog recorders requiring less maintenance and having a more stable chart advance.

2. New multi-conductor cables incorporating non-corrosion and leakproof connectors, and an internal stranded steel cable to prevent stretching.

3. Multi-conductor cables should be constructed so that additional lengths of cable can be added.

4. The power supply should be converted to rechargeable batteries with provisions to accept 110 v. external power.

APPENDIX III

Phosphorus and Hypolimnial Dissolved Oxygen in Lake Erie

M. Gilbertson
Canadian Wildlife Service
Ottawa, Ontario, Canada

H.H. Dobson and T.R. Lee
Canada Centre for Inland Waters
867 Lakeshore Road, Burlington, Ontario, Canada

INTRODUCTION

The International Joint Commission, following investigations of the very marked environmental change in Lake Erie, has recommended that the plant nutrient, phosphorus, should be controlled (I.J.C. 1970). The evidence and information supporting and discussing this recommendation have been extensively reviewed and will not be considered further in this work (Prince and Bruce, in press). Observations on the rapid eutrophication of Lake Erie had been made many times over the last thirty years but little is known of the history of the relationship between phosphorus loadings to the lake and its trophic state.

This present note explores the possible interrelationship between phosphorus contributions to the lake and oxygen depletion in the hypolimnion of the Central Basin of Lake Erie, as an indicator, of the trophic state of the lake. It is hoped that this exercise will be a guide as to the effect of the proposed control measures on the phosphorus loading to Lake Erie and an aid to decision makers in estimating the expected improvement in hypolimnial conditions with various reductions of contributions of phosphorus.

Basically, this paper compares and then discusses the comparison of two sets of information. The information compared is estimates of phosphorus loadings from the human population of the Lake Erie Basin and its use of detergents and estimates of the oyxgen depletion rates in the Central Basin, from 1931 to the present.

PHOSPHORUS CONTRIBUTIONS

The contribution of municipal phosphorus to the lake was estimated as the sum of detergent phosphorus and the phosphorus in human excrement. Crude estimates of the total quantity of detergent phosphorus used in the Lake Erie Basin were calculated from statistics of the annual use of phosphates by the soap and detergent industry supplied by Statistics Canada and the U.S. Bureau of the Census. These totals were converted into per capita figures by dividing each country's total by their populations (Table I). The total consumption of detergent phosphorus in the Lake Erie Basin was then estimated by multiplying this per capita data by the population of the basin in each country for the years taken.

The basin populations estimated for each year used in the comparison (Table II) were calculated upon the basis of the proportion of the census unit within the basin and the known distribution of population. The basic data was obtained from various censuses and the Great Lakes Basin Commission. The population information is therefore subject to estimating error but is probably the more accurate calculation that has yet been made of the population living in the Lake Erie Basin.

Table I: Per capita Use of Detergent Phosphorus (Lbs/Year)						
	1931	1941	1951	1956	1961	1966
Canada	.03	.12	.60	1.10	1.20	1.50
United States	.04	.15	.86	1.50	1.96	2.49

Table II: Population of the Lake Erie Basin $\times 10^{-3}$						
	1931	1941	1951	1956	1961	1966
Canada	759	810	996	1,128	1,245	1,374
United States	5,848	6,254	7,559	8,657	9,312	9,783
Total	6,607	7,064	8,555	9,785	10,557	11,157

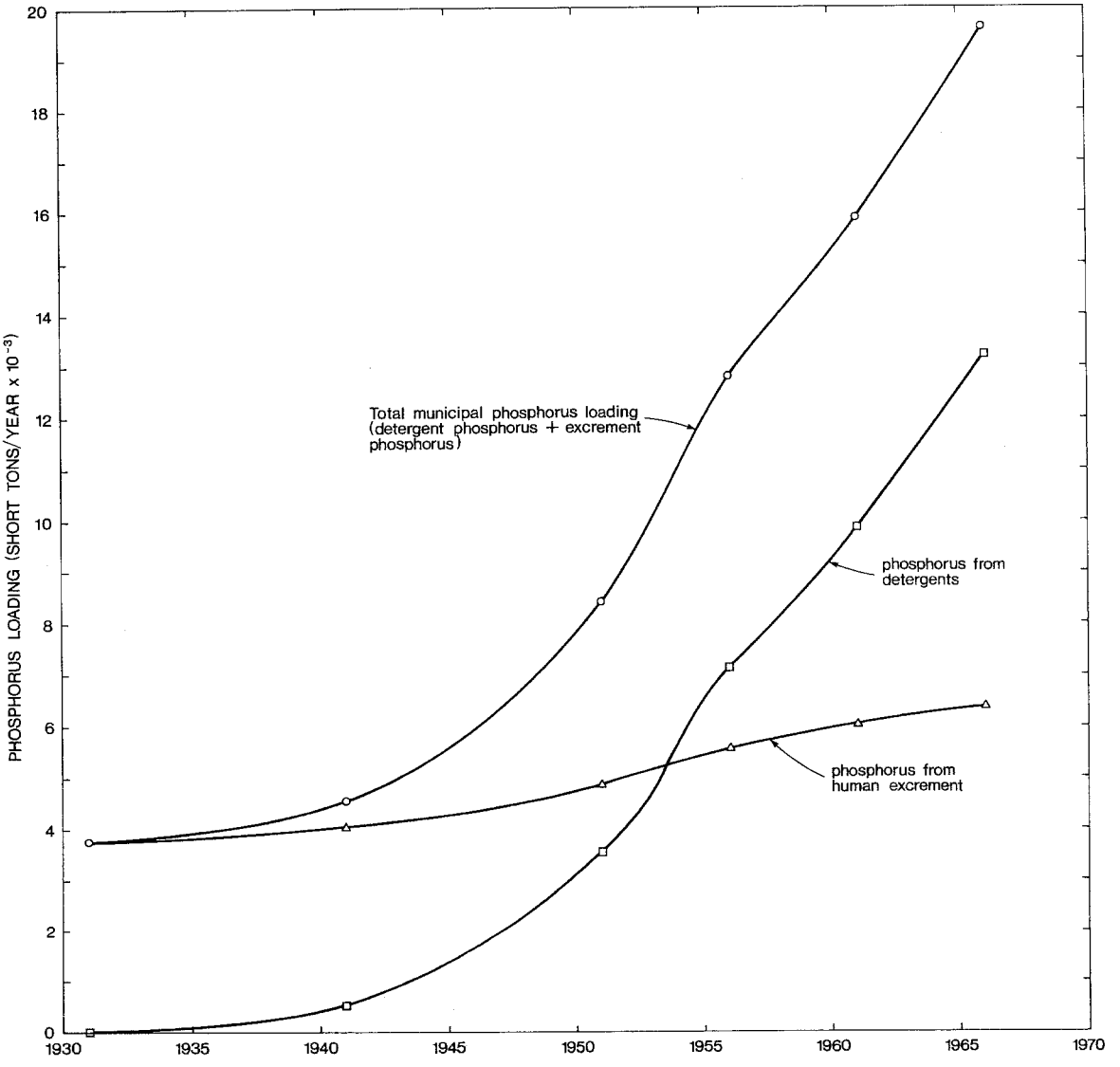

Figure 1. Estimates of the municipal fraction of the phosphorus loading for Lake Erie, versus time.

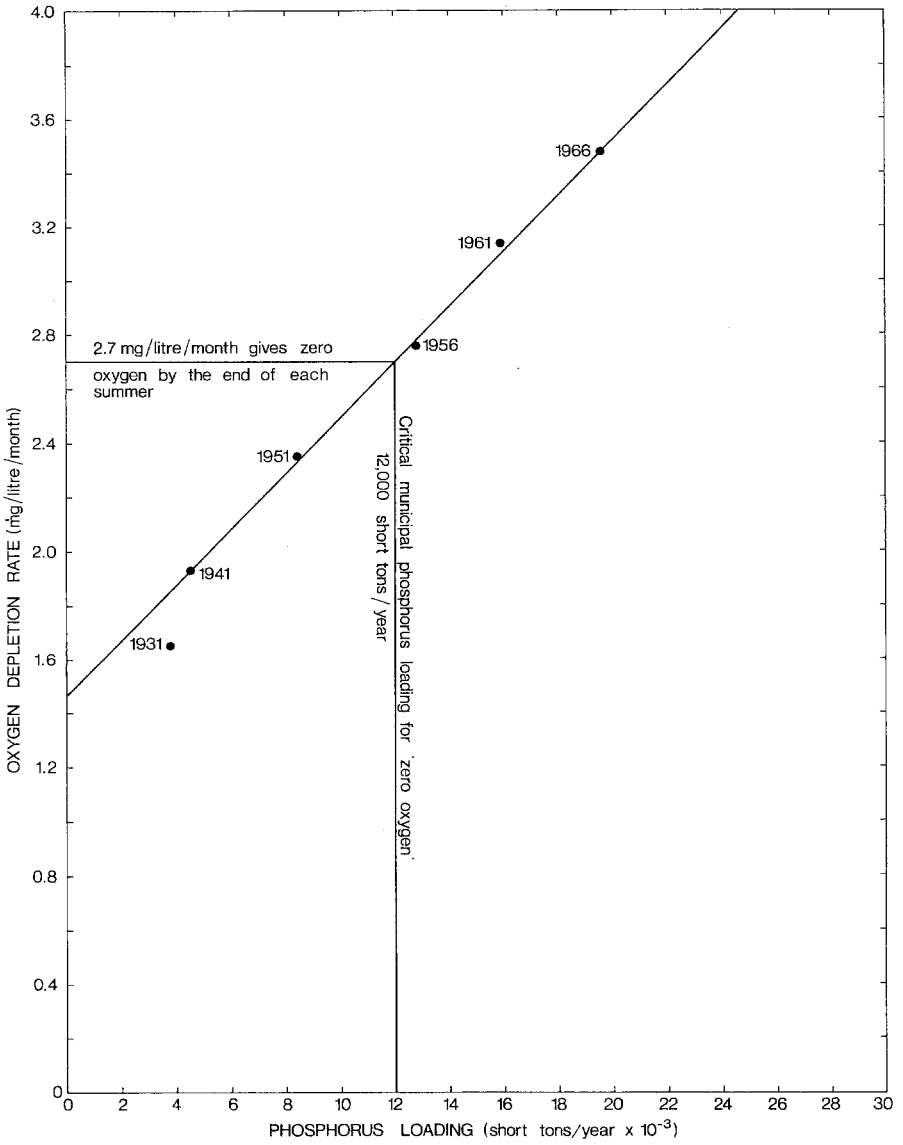

Figure 2. Estimates of the municipal phosphorus loading (sewage and detergents) for the entire Lake Erie basin, versus the oxygen depletion rates observed in the Central Basin hypolimnion of Lake Erie.

Similar estimates were produced for the human excrement phosphorus contribution. In this case, the population estimates were multiplied by an annual per capita contribution of 1.14 pounds. This figure was taken from Vollenweider (1968) on the assumption that there was no major change in dietary phosphorus over the last thirty years. These two estimates, together, are assumed to represent the total municipal loading to Lake Erie from Canadian and United States sources.

Besides the possible population estimate error, the present estimates do not allow for the fact that the total population of the Lake Erie Basin was not sewered for this period or for any non-human or non-detergent phosphorus contribution to the sewered input. It is assumed that these two factors would cancel each other out and that the estimates given are representative of historical municipal phosphorus loadings to Lake Erie. These loadings are shown graphically in total, and by detergent phosphorus and human excrement alone in Figure 1.

Table III: Total Contribution of Municipal Phosphorus (Short Tons/Yr)						
	1931	1941	1951	1956	1961	1966
Canada	444	509	864	1,236	1,463	1,847
United States	3,333	4,034	7,559	11,576	14,434	17,758
Total	3,777	4,543	8,423	12,812	15,897	19,605

Table IV: Rate of Oxygen Depletion in the Central Basin (Mg/l/Month)					
1931	1941	1951	1956	1961	1966
1.65	1.93	2.35	2.76	3.14	3.48

OXYGEN DEPLETION

The estimates of oxygen depletion rates in the Central Basin of Lake Erie (Table IV) were based on the work of Dobson and Gilbertson (pg 7) and represent the figures derived from the long term trend of oxygen depletion.

The estimates of oxygen depletion rates in the hypolimnion of the Central Basin are plotted against the municipal loading estimates for Lake Erie in Figure 2. This graph suggests a possible significant relationship between the two parameters. The rate of oxygen depletion has increased with the increasing municipal loadings.

Minimum oxygen levels attained each year depend not only upon depletion rates but also the duration of stratification. The period of summer stratification is variable from year to year. Thermal stratification commences approximately June 1 when oxygen levels are near 11 mg/1. In their previous work, Dobson and Gilbertson chose 110 days as representing the average period of stratification. With that assumption the critical depletion rate, that is, when zero dissolved oxygen was found at several locations before the end of stratification, was estimated to be 3.0 mg.litre^{-1}month^{-1} and first occurred about 1960. The longest period of stratification is about 125 days. Under these conditions the critical depletion rate is about 2.7 mg.litre^{-1}month^{-1}. This corresponds with conditions in 1955 and with a municipal contribution of 12,000 short tons of phosphorus per year.

Unfortunately, the only year for which estimates based on measurement have been made is 1967 (I.J.C. 1969 and 1970). In that year, it was estimated that municipal phosphorus contribution was 19,100 tons which closely approximates the amounts estimated here, 19,605 tons in 1966. The total quantity of phosphorus entering the lake from all sources in 1967 was 30,100 tons. Even in 1967 almost forty percent of the total loadings came from other sources and this proportion probably increases historically. The absolute size of the non-municipal contribution has probably increased also over the last forty years but the pattern of increase is not yet known.

CONCLUSIONS

The discussion in this note has been based on some assumptions and some estimates of the history of phosphorus loadings to Lake Erie. It does present, however, further evidence of the real relationship between the phosphorus loading to Lake Erie and the degree of deoxygenation in the hypolimnion of the Central Basin of the lake. It does allow the estimation of the required phosphorus input reductions necessary to reach certain water quality standards for the lake.

The International Joint Commission has proposed specific water quality objectives for Lake Erie which would involve the reduction of phosphorus loadings. The contribution of phosphorus to Lake Erie is proposed to be limited to a level which would "prevent nuisance growths, algae, weeds and slime which are or may become injurious to any beneficial water use". This limitation would not be total but would occur in stages. The first requirement would be for an immediate holding action to avoid the occurrence of anoxic conditions and related large scale recycling of nutrients. It would appear that a reduction to at least 12,000 tons in the municipal contribution of phosphorus is required to return oxygen conditions in the lake to a level approximating conditions which prevailed in 1955. Further large scale reductions in loadings would be required if the lake is to return to conditions which are economically and aesthetically satisfactory. It has been estimated that this would mean a reduction in the total phosphorus loading to the lake to a level of some 11,100 tons a year. It might be noted that the non-municipal contribution of phosphate to the lake in 1967 was 11,000 tons (including 2,250 tons from Lake Huron). If this objective is met, and the lake responds in the same way to decreasing phosphorus loads as it appears to have behaved with increasing loads, then the probable depletion rate will drop below 2 $mg.litre^{-1} month^{-1}$ and may approximate hypolimnial conditions prior to 1931. It is the achievement of this situation which is envisaged in the recommendations of the I.J.C. for "maintaining native populations of fish and other aquatic life".

ACKNOWLEDGEMENTS

We thank the following for their contribution to this discussion: Dr. A.R. LeFeuvre, Dr. N.M. Burns, Dr. R.A. Vollenweider and particularly Mr. G.E. Bangay and Mr. J.N. Thomson for supplying the information for Tables I, II and III.

REFERENCES

Census of Canada. 1966. Dominion Bureau of Statistics. Catalogue Number 92-605 (1967).

Census of Canada. 1961. Dominion Bureau of Statistics. Catalogue Number 92-539 (1963).

PRINCE A.T. and J.P. BRUCE. 1971. Development of Nutrient Control Policies in Canada. *In* Nutrients in Natural Waters, ed. H. Allen and J.R. Kramer. J. Wyley Inc., New York, N.Y. In Press.

Report to the International Joint Commission on the Pollution of Lake Erie, Lake Ontario and the International Section of the St. Lawrence River. Vol. 2. 1969.

Report of the International Joint Commission on Pollution of Lake Erie, Lake Ontario and the International Section of the St. Lawrence River, 1970.

VOLLENWEIDER, R.A. 1968. Scientific fundamentals of the eutrophication of lakes and flowing waters, with particular reference to nitrogen and phosphorus as factors in eutrophication. O.E.C.D. Technical Report. DAS/CSI/68.27.

Water Quality Criteria. F.W.P.C.A. Washington, 1968.

Biological Data

TABLE 1

PHYTOPLANKTON VOLUMES

Cruise & Date

	6-16-70 to 6-23-70		7-13-70 to 7-18-70		SURVEY A		B		C	
					1		2		3	
					TIME 7-29-70 (0.)		8-2-70 (4.0)		8-5 & 6-70 (7.0)	
Station	*D	**Vol.	D	Vol.	Depth	Vol.	D	Vol.	D	Vol.
	1	6.0	1	177.8	1	69.8	2	212.0	1	94.9
P	12	9.0	10	421.6	12	212.3	14	301.3	10	84.8
	–	–	–	–	17	288.3	19	240.2	18	100.6
	23	60.6	22	109.9	22	201.7	23	165.0	22	120.2
	1	33.7	1	385.8	1	63.8	1	139.2	1	91.1
	12	39.8	–	–	9	126.6	14	98.9	12	148.2
M	18	70.2	17	388.0	19	92.2	17	125.9	17	282.7
	22	2.3	22	88.4	21	77.1	20	157.3	20	193.4
	–	–	–	–	–	–	22	141.2	–	–
	1	96.7	1	151.5	1	102.1	1	111.7	1	472.7
	–	–	–	–	10	517.7	12	305.7	12	205.5
S	–	–	17	75.3	18	198.3	18	283.3	18	69.5
	21	82.8	21	82.8	21	112.7	21	165.8	21	95.8
	1	17.2	–	–	1	232.2	1	317.4	1	81.8
	10	34.0	–	–	11	163.8	18	104.0	10	184.7
N	18	348.7	–	–	19	171.3	19	133.7	19	64.3
	19	569.4	–	–	20	291.4	21	117.4	21	31.4
	1	13.0	1	247.4	1	123.7	1	119.9	1	107.8
	12	9.0	10	531.4	12	268.1	11	137.8	14	158.6
R	–	–	–	–	16	218.7	15	377.2	15	500.1
	25	65.5	20	169.1	20	134.4	22	267.4	21	117.7
Averages of:										
Surface		33.3		240.6		118.3		180.0		169.7
Mid-epilimnion		23.0		476.5		257.7		189.5		196.4
Thermocline		209.5		231.7		193.8		232.1		203.4
Bottom		156.1		112.6		163.5		169.0		111.7

*D = Depth in meters
**Vol = Cubic microns X 10^4/ml

~ 100 org/ml

org = 10^3 μ^3 ; = 10^5 μ^3/ml

~ 100 x 10^4 μ^3/ml.

∴ 6.0 => 6 x 10^4 μ^3/ml

600 => 6 x 10^6 μ^3/ml.

TABLE 1 (Cont.)

PHYTOPLANKTON VOLUMES

	D		E		F		Cruise & Date G		H		I		J	
	4 8-11 & 12-70 (13.)		5 8-15-70 (17.)		6 8-19 & 20-70 (20.)		7 8-24 & 25-70 (26.)		9 8-25-70 (27.)		10 8-27-70 (29.)		11 9-1 & 2-70 (34.)	
Station	*D	**Vol.	D	Vol.	D	Vol.	D	Vol.	D	Vol.	D	Vol.	D	Vol.
	1	95.1	1	266.9	1	333.3	1	498.3	1	118.0	1	632.7	1	434.9
	12	279.3	14	171.4	10	338.9	12	560.0	15	287.8	12	347.6	12	460.4
P	17	130.4	19	152.1	17	271.4	19	302.9	20	215.4	19	480.3	19	620.8
	21	130.1	22	94.3	21	294.5	22	147.3	23	181.1	23	206.4	23	93.4
	1	190.4	1	192.7	1	241.3	1	515.2	1	520.6	1	406.8	–	–
	11	159.5	12	132.6	2	355.8	16	352.4	11	331.2	12	353.5	–	–
	16	884.4	17	118.5	14	377.8	16	352.4	19	357.6	18	398.3	–	–
M	18	76.5	21	67.6	18	469.7	21	119.0	22	260.8	23	192.0	–	–
	19	99.7	–	–	22	115.9	–	–	–	–	–	–	–	–
	21	104.8	–	–	–	–	–	–	–	–	–	–	–	–
	1	448.4	1	186.6	1	445.6	1	343.0	–	–	1	176.6	1	364.9
	12	353.7	14	208.3	12	228.7	12	282.2	–	–	11	487.0	11	456.2
S	17	145.2	19	126.5	19	178.2	18	311.4	–	–	19	386.5	20	1048.5
	20	80.7	21	92.2	21	193.4	22	345.3	–	–	21	176.0	22	161.8
	1	144.2	1	97.8	1	103.8	1	153.2	1	232.8	1	117.3	–	–
	–	–	11	230.6	11	146.4	12	464.1	12	1228.9	7	463.1	–	–
N	–	–	18	126.4	17	134.6	17	749.8	18	191.0	18	696.2	17	999.8
	20	41.3	20	130.1	20	47.8	19	275.4	12	225.8	21	169.6	–	–
	1	202.3	1	374.7	–	–	1	272.4	1	120.4	–	–	1	310.9
	9	134.4	12	491.5	15	650.3	13	380.1	14	440.3	11	1187.8	12	157.9
R	15	221.1	16	486.1	17	522.3	17	36.1	–	–	15	813.8	18	83.4
	20	81.1	20	41.7	–	–	20	31.8	22	113.2	23	79.2	21	166.8
Averages of:														
Surface		216.1		223.7		296.0		356.4		248.0		333.4		370.2
Mid-epilimnion		231.7		246.9		348.4		407.8		572.1		567.8		358.2
Thermocline		345.3		201.9		371.1		375.7		254.7		555.0		688.1
Bottom		87.7		85.2		162.9		183.8		195.2		164.6		140.7

*D = Depth in meters

**Vol = Cubic microns $\times 10^4$/ml

TABLE 2

PHYTOPLANKTON NUMBERS

Cruise & Date

	6-16-70 to 6-23-70		7-13-70 to 7-18-70		1 7-29-70		2 8-2-70		3 8-5 & 6-70	
Station	*D	**No.	D	No.	D	No.	D	No.	D	No.
	1	9	1	101	1	68	2	137	1	86
P	12	11	10	119	12	86	14	98	10	80
	–	–	–	–	17	89	19	86	18	72
	23	54	22	76	22	113	23	84	22	75
	1	33	1	118	1	66	1	95	1	81
	12	55	–	–	9	155	14	101	12	94
M	18	121	17	146	19	55	17	66	17	117
	24	22	22	64	21	60	20	76	20	79
	–	–	–	–	–	–	22	85	–	–
	1	567	1	82	1	97	1	96	1	116
	–	–	–	–	10	174	12	92	12	84
S	–	–	17	55	18	71	18	83	18	42
	21	360	22	91	21	57	21	70	21	56
	1	45	–	–	1	79	1	95	1	109
	10	45	–	–	11	73	18	57	10	108
N	18	203	–	–	19	78	19	54	19	42
	19	304	–	–	20	68	21	52	21	29
	1	27	1	212	1	78	1	73	1	67
	12	11	10	238	12	106	11	71	14	83
R	–	–	–	–	16	97	15	144	15	143
	25	44	20	100	20	68	22	153	21	60
Averages of:										
Surface		136		128		78		99		92
Mid-epilimnion		31		179		99		84		90
Thermocline		162		101		78		85		83
Bottom		157		83		73		89		60

*D = Depth in meters

**No. = Number of organisms/ml

TABLE 2 (Cont.)

PHYTOPLANKTON NUMBERS

Cruise & Date

	4 8-11 & 12-70		5 8-15-70		6 8-19 & 20-70		7 8-24 & 25-70		9 8-25-70		10 8-27-70		11 9-1 & 2-70	
Station	*D	**No.	D	No.	D	No.	D	No.	D	No.	D	No.	D	No.
	1	96	1	137	1	228	1	281	1	128	1	381	1	310
	12	128	14	109	10	204	12	262	15	196	12	241	12	227
P	17	62	19	83	17	183	19	213	20	168	19	274	19	243
	21	58	22	46	21	152	22	85	23	59	23	88	23	65
	1	94	1	167	1	160	1	237	1	271	1	331	–	–
	11	100	12	91	2	278	16	269	11	321	12	281	–	–
M	16	265	17	64	14	115	17	288	19	267	18	344	–	–
	18	44	21	44	18	116	21	72	22	96	23	96	–	–
	19	38	–	–	21	112	–	–	–	–	–	–	–	–
	21	56	–	–	22	53	–	–	–	–	–	–	–	–
	1	137	1	164	1	226	1	235	–	–	1	217	1	233
	12	118	14	221	12	154	12	197	–	–	11	208	11	267
S	17	58	19	75	19	129	18	198	–	–	19	242	20	275
	20	46	21	54	21	74	22	115	–	–	21	69	22	127
	1	100	1	85	1	118	1	150	1	218	1	173	–	–
	–	–	11	125	11	94	12	169	12	312	7	216	–	–
N	–	–	18	59	17	75	17	207	18	245	18	245	17	232
	20	24	20	48	20	35	19	78	22	93	21	57	–	–
	1	120	1	250	–	–	1	109	1	125	–	–	1	212
	9	79	12	219	15	267	13	134	14	234	11	393	12	194
R	15	70	16	149	17	283	17	41	–	–	15	342	18	66
	20	51	20	37	–	–	20	24	22	40	23	63	21	71
Averages of:														
Surface		109		161		202		202		186		276		252
Mid-epilimnion		106		153		142		206		266		268		229
Thermocline		114		86		176		183		227		289		204
Bottom		45		46		85		75		72		74		88

*D = Depth in meters

**No. = Number of organisms/ml

TABLE 3

PHYTOPLANKTON DOMINANCE BY VOLUME*
STATION P

Date	Depth in meters	1st Dominant	Volume	2nd Dominant	Volume	3rd Dominant	Volume	Total Volume
6-17-70	1	Asterococcus	6.0					6.0
	12.3	Tribonema	9.0					9.0
	23	Tribonema	35.3	Pennate Diatoms	25.3			60.6
7-13-70	1	Oedogonium	123.9	Pennate Diatoms	20.8	Unident. Filamentous Green	14.8	177.8
	10	Oedogonium	327.5	Anacystis	80.2	Oocystis	12.1	421.6
	22	Centric Diatoms	92.3	Tribonema	9.0	Oocystis	7.4	109.9
7-29-70	1	Cosmarium	22.4	Oedogonium	17.7	Oocystis	13.4	69.8
	12	Oedogonium	53.1	Cosmarium	44.7	Ceratium	39.3	212.3
	17	Oedogonium	115.1	Ceratium	19.6	Pennate Diatoms	18.5	288.2
	22	Pennate Diatoms	103.8	Centric Diatoms	38.6	Oedogonium	35.4	201.7
8-2-70	2	Anacystis	107.0	Ceratium	44.6	Cosmarium	22.4	212.0
	14	Ceratium	162.0	Oedogonium	53.1	Cosmarium	37.3	301.3
	19	Oedogonium	106.2	Ceratium	49.1	Pennate Diatoms	25.4	240.2
	23	Oedogonium	62.0	Centric Diatoms	34.3	Pennate Diatoms	32.3	165.0
8-6-70	1	Anacystis	35.7	Oocystis	18.1	Ceratium	14.7	94.9
	10	Oocystis	22.1	Oedogonium	17.7	Sphaerocystis	6.0	84.8
	18	Oedogonium	35.4	Centric Diatoms	21.4	Pennate Diatoms	16.2	100.6
	22	Pennate Diatoms	25.3	Oedogonium	22.1	Centric Diatoms	21.4	120.2
8-11-70	1	Anacystis	35.7	Oocystis	24.1	Oedogonium	8.9	95.1
	12	Anacystis	160.4	Oocystis	30.8	Cosmarium	22.4	279.3
	17	Anacystis	71.3	Oocystis	19.5	Ceratium	14.7	130.4
	21	Anacystis	71.3	Oedogonium	13.3	Oocystis	12.7	130.1
8-15-70	1	Anacystis	178.3	Oocystis	38.9	Gelocystis	10.4	266.9
	14	Ceratium	93.3	Oocystis	29.5	Cosmarium	22.4	171.4
	18.5	Ceratium	58.9	Anacystis	44.6	Oocystis	21.5	152.1
	22	Anacystis	44.6	Centric Diatoms	12.9	Oocystis	10.1	94.3
8-19-70	1	Anacystis	151.5	Oocystis	79.1	Ceratium	29.5	333.3
	10	Anacystis	160.4	Oocystis	67.7	Cosmarium	37.3	338.9
	17	Anacystis	89.1	Oocystis	75.1	Ceratium	44.2	271.4
	21	Anacystis	187.1	Oocystis	57.7	Ceratium	24.5	294.5
8-24-70	1	Anacystis	258.5	Oocystis	76.4	Cosmarium	44.8	498.3
	12	Anacystis	347.6	Oocystis	60.4	Cosmarium	52.2	560.0
	19	Anacystis	115.9	Oocystis	53.6	Cosmarium	44.8	302.9
	24	Anacystis	71.3	Oocystis	31.5	Ceratium	19.6	147.3
8-25-70	1	Anacystis	35.7	Oocystis	34.2	Sphaerocystis	27.6	118.0
	15	Anacystis	115.9	Cosmarium	67.2	Oocystis	54.3	287.8
	20	Anacystis	53.5	Oocystis	51.0	Sphaerocystis	33.6	215.4
	23	Anacystis	151.5	Oocystis	16.1	Pediastrum	3.9	181.1
8-27-70	1	Anacystis	329.8	Cosmarium	67.2	Oocystis	67.1	632.7
	12	Anacystis	115.9	Oocystis	58.3	Cosmarium	52.2	347.6
	19	Anacystis	249.6	Oocystis	93.9	Ceratium	29.5	480.3
	23	Anacystis	151.5	Oocystis	29.5	Pennate Diatoms	6.9	206.4
9-1-70	1	Anacystis	231.8	Staurastrum	44.3	Gomphosphaeria	34.4	434.9
	12	Anacystis	178.3	Aphanizomenon	77.6	Gomphosphaeria	63.8	460.4
	19	Anacystis	347.6	Cosmarium	67.2	Pennate Diatoms	39.2	602.8
	23	Anacystis	26.7	Oocystis	19.5	Pennate Diatoms	18.4	93.4

*Volume = Cubic microns $\times 10^4$/ml

TABLE 3 (Cont.)

PHYTOPLANKTON DOMINANCE BY VOLUME*
STATION R

Date	Depth in meters	1st Dominant	Volume	2nd Dominant	Volume	3rd Dominant	Volume	Total Volume
6-16-70	1	Micratinium	12.1	Unident.	0.9			13.0
	11.8	Unident, Filamentous Green	9.0	Coccoid Green				9.0
	25.0	Pennate Diatoms	50.8	Tribonema	9.0	Staurastrum	5.7	65.5
7-13-70	1	Oedogonium	79.7	Pennate Diatoms	64.6	Ceratium	44.2	247.4
	10	Oedogonium	367.3	Pennate Diatoms	106.1	Oocystis	24.8	531.4
	20	Pennate Diatoms	64.6	Oedogonium	39.8	Centric Diatoms	38.6	169.1
7-29-70	1	Pennate Diatoms	25.4	Ceratium	24.5	Melosira	19.3	123.7
	12	Oedogonium	150.5	Ceratium	44.2	Anacystis	26.7	268.1
	16	Oedogonium	97.4	Centric Diatoms	49.3	Cosmarium	29.9	218.7
	20	Centric Diatoms	36.4	Pennate Diatoms	36.4	Oedogonium	26.6	134.9
8-2-70	1	Pennate Diatoms	53.1	Centric Diatoms	25.7	Oedogonium	17.7	119.9
	11	Centric Diatoms	40.7	Oedogonium	39.8	Pennate Diatoms	36.9	138.8
	15	Ceratium	162.0	Pennate Diatoms	96.9	Cosmarium	44.8	377.2
	21.5	Anacystis	133.7	Pennate Diatoms	32.3	Oedogonium	26.6	267.4
8-6-70	1	Cosmarium	22.4	Oedogonium	22.1	Oocystis	13.4	107.8
	14	Anacystis	44.6	Ceratium	34.4	Oedogonium	26.6	158.6
	15	Ceratium	427.1	Cosmarium	44.8	Oocystis	17.4	500.1
	21	Pennate Diatoms	39.2	Centric Diatoms	34.3	Oedogonium	22.1	117.7
8-11-70	1	Anacystis	107.0	Oocystis	40.2	Ceratium	24.5	202.3
	9	Ceratium	39.3	Anacystis	35.7	Oocystis	18.1	134.4
	15	Anacystis	133.7	Oedogonium	35.4	Ceratium	19.6	221.1
	20	Centric Diatoms	23.6	Anacystis	17.8	Pennate Diatoms	16.2	81.0
8-15-70	1	Anacystis	196.1	Oocystis	53.0	Ceratium	29.5	374.7
	12	Anacystis	356.5	Oocystis	77.8	Cosmarium	29.9	491.5
	15.5	Anacystis	347.6	Ceratium	58.9	Oocystis	42.2	486.1
	20	Centric Diatoms	17.1	Oocystis	9.4	Pennate Diatoms	4.6	41.7
8-20-70	15	Anacystis	508.1	Oocystis	80.5	Sphaerocystis	17.2	650.3
	16.5	Anacystis	249.6	Oocystis	100.6	Cosmarium	67.2	522.3
8-25-70	1	Anacystis	151.5	Ceratium	44.2	Cosmarium	29.9	272.4
A	13	Anacystis	276.3	Ceratium	34.4	Oocystis	16.8	380.1
	16.5	Oocystis	14.1	Anacystis	8.9	Pennate Diatoms	6.9	36.1
	20	Anacystis	8.9	Oocystis	6.7	Ceratium	4.9	31.8
8-25-70	1	Oocystis	34.9	Anacystis	26.7	Cosmarium	14.9	120.4
B	14	Anacystis	213.9	Oocystis	61.0	Pennate Diatoms	55.4	440.3
	22	Anacystis	89.1	Oocystis	10.1	Centric Diatoms	4.3	113.2
8-27-70	11	Anacystis	891.4	Oocystis	54.3	Ceratium	54.0	1187.8
	15	Aacystis	392.2	Ceratium	171.8	Oocystis	69.1	813.8
	23	Ceratium	24.5	Oocystis	18.8	Pennate Diatoms	18.5	79.9
9-1-70	1	Cosmarium	97.0	Anacystis	62.4	Oocystis	34.2	310.9
	12	Oocystis	37.5	Pennate Diatoms	25.4	Anacystis	17.8	157.9
	18	Oocystis	16.1	Cosmarium	14.9	Gomphosphaeria	14.7	83.4
	21	Anacystis	133.7	Oocystis	13.4	Pennate Diatoms	11.5	166.8

*Volume = Cubic Microns $\times 10^4$/ml

TABLE 3 (Cont.)

PHYTOPLANKTON DOMINANCE BY VOLUME*
STATION S

Date	Depth in meters	1st Dominant	Volume	2nd Dominant	Volume	3rd Dominant	Volume	Total Volume
6-23-70	1	Anacystis	80.2	Oocystis	6.0	Schroederia	5.8	96.7
	21	Centric Diatoms	70.7	Staurastrum	5.7	Schroederia	3.0	82.8
7-18-70	1	Oedogonium	123.9	Tribonema	14.8	Oocystis	12.1	151.5
	17	Oedogonium	39.8	Tribonema	23.0	Sphaerocystis	7.8	75.3
	22	Tribonema	45.2	Pennate Diatoms	20.8	Oocystis	12.1	82.8
7-29-70	1	Oedogonium	75.2	Centric Diatoms	6.4	Oocystis	6.0	102.1
	10	Oedogonium	451.4	Uni. Coccoid Gr.	20.1	Ceratium	14.7	517.7
	18	Oedogonium	154.9	Cosmarium	14.9	Tribonema	9.9	198.3
	21	Oedogonium	53.1	Anacystis	26.7	Oocystis	10.1	112.7
8-2-70	1	Oedogonium	53.1	Ceratium	19.6	Cosmarium	7.5	111.7
	12	Anacystis	107.0	Ceratium	78.5	Oedogonium	75.2	305.7
	18	Ceratium	171.8	Oedogonium	88.5	Pennate Diatoms	6.9	293.5
	21	Oedogonium	75.2	Anacystis	44.6	Centric Diatoms	12.9	165.8
8-6-70	1	Anacystis	410.0	Ceratium	19.6	Oocystis	18.1	472.7
	12	Ceratium	103.1	Oedogonium	39.8	Trachelomonas	13.1	189.1
	18	Oedogonium	31.0	Oocystis	9.4	Pennate Diatoms	9.2	69.5
	21	Oedogonium	44.3	Pennate Diatoms	11.5	Cosmarium	7.5	95.8
8-12-70	1	Anacystis	365.5	Oocystis	28.2	Oedogonium	22.1	448.4
	12	Anacystis	231.8	Cosmarium	37.3	Ceratium	29.5	353.7
	17	Ceratium	83.4	Anacystis	17.8	Oedogonium	17.7	145.2
	20	Oedogonium	22.1	Anacystis	17.8	Pennate Diatoms	9.2	80.7
8-15-70	1	Oocystis	66.4	Anacystis	35.7	Cosmarium	29.9	186.6
	15	Oocystis	93.2	Oedogonium	39.8	Anacystis	17.8	208.3
	19	Ceratium	34.4	Oocystis	26.1	Oedogonium	22.1	126.5
	21	Oedogonium	39.8	Pennate Diatoms	25.4	Oocystis	10.7	92.2
8-20-70	1	Anacystis	258.5	Oocystis	87.8	Ceratium	29.5	445.6
	12	Anacystis	107.0	Oocystis	56.3	Cosmarium	22.4	228.7
	18.5	Anacystis	62.4	Oocystis	53.6	Cosmarium	29.9	178.2
	21	Anacystis	89.1	Ceratium	58.9	Oocystis	18.8	193.4
8-25-70	1	Anacystis	133.7	Oocystis	77.8	Cosmarium	67.2	343.0
	12	Anacystis	133.7	Oocystis	66.4	Cosmarium	22.4	282.2
	18	Anacystis	169.4	Oocystis	71.7	Staurastrum	15.6	311.4
	21	Anacystis	276.3	Oocystis	32.2	Ceratium	19.6	345.3
8-27-70	1	Oocystis	74.4	Anacystis	35.7	Staurastrum	14.6	176.6
	11	Anacystis	329.8	Cosmarium	52.2	Oocystis	36.6	487.0
	19	Anacystis	213.9	Oocystis	63.7	Cosmarium	29.9	386.5
	21	Anacystis	115.9	Oocystis	17.4	Ceratium	14.7	176.0
9-1-70	1	Cosmarium	126.9	Anacystis	98.0	Oocystis	43.6	364.3
	11	Anacystis	249.6	Oocystis	75.1	Cosmarium	44.8	456.2
	20	Anacystis	873.5	Oocystis	57.0	Cosmarium	44.8	1048.5
	22	Anacystis	80.2	Oocystis	39.6	Cosmarium	14.9	161.8

*Volume = Cubic Microns $\times 10^4$/ml

TABLE 3 (Cont.)

PHYTOPLANKTON DOMINANCE BY VOLUME*
STATION M

Date	Depth in meters	1st Dominant	Volume	2nd Dominant	Volume	3rd Dominant	Volume	Total Volume
6-16-70	1	Centric Diatoms	23.6	Tribonema	9.0	Unident. Green Flagellates	1.1	33.7
	12.4	Centric Diatoms	23.6	Tribonema	4.0	Staurastrum	5.7	39.8
	18.0	Tribonema	27.1	Pennate Diatoms	25.4	Staurastrum	11.5	70.2
	22.4	Unident. Green Flagellates	2.3					2.3
7-17-70	1	Anacystis	249.6	Oedogonium	79.7	Centric Diatoms	38.6	385.8
	17	Oedogonium	327.5	Pennate Diatoms	20.8	Centric Diatoms	19.3	388.0
	22	Centric Diatoms	38.6	Tribonema	23.0	Pennate Diatoms	20.8	88.4
7-29-70	1	Ceratium	14.7	Oedogonium	8.9	Centric Diatoms	8.6	63.8
	9	Oedogonium	84.1	Cosmarium	14.9	Ceratium	9.8	126.6
	19	Oedogonium	35.4	Pennate Diatoms	18.5	Anacystis	8.9	92.2
	21	Pennate Diatoms	30.0	Oedogonium	13.3	Oocystis	8.0	77.1
8-2-70	1	Pennate Diatoms	43.8	Oedogonium	31.0	Anacystis	17.8	139.2
	14	Oedogonium	44.3	Pennate Diatoms	23.1	Melosira	8.6	98.9
	16.8	Ceratium	49.1	Oedogonium	26.6	Pennate Diatoms	13.9	125.9
	20	Ceratium	83.5	Pennate Diatoms	23.1	Oedogonium	22.1	157.3
	22	Cosmarium	37.3	Ceratium	29.5	Anacystis	26.7	141.2
8-5-70	1	Anacystis	26.7	Oocystis	16.8	Centric Diatoms	12.9	91.1
	12	Ceratium	78.5	Oocystis	18.8	Cosmarium	14.9	148.2
	17	Ceratium	201.3	Cosmarium	22.4	Oocystis	14.1	282.7
	20	Ceratium	73.6	Oedogonium	35.4	Pennate Diatoms	30.0	193.4
8-11-70	1	Anacystis	98.1	Oedogonium	26.6	Oocystis	22.8	190.4
	11	Anacystis	44.6	Ceratium	29.5	Cosmarium	22.4	159.5
	16	Ceratium	800.1	Oocystis	36.2	Cosmarium	14.9	884.4
	18	Oedogonium	39.8	Ceratium	14.8	Oocystis	10.7	76.5
	19	Ceratium	19.6	Pennate Diatoms	18.5	Anacystis	17.8	99.7
	20.9	Pennate Diatoms	34.6	Anacystis	26.7	Centric Diatoms	23.6	104.8
8-15-70	1	Oocystis	65.0	Ceratium	44.1	Oedogonium	26.6	192.7
	12	Anacystis	44.6	Oocystis	24.8	Ceratium	24.5	132.6
	17	Ceratium	78.5	Oocystis	18.1	Cosmarium	7.5	118.5
	21	Pennate Diatoms	18.5	Oocystis	10.7	Centric Diatoms	10.7	67.6
8-19-70	1	Anacystis	107.0	Oocystis	48.9	Ceratium	44.2	241.3
	2	Anacystis	133.7	Oocystis	94.5	Ceratium	34.4	355.8
	13.5	Anacystis	249.6	Oocystis	47.6	Cosmarium	29.9	377.8
	21	Anacystis	285.2	Oocystis	27.5	Centric Diatoms	23.6	381.5
8-24-70	1	Anacystis	356.5	Oocystis	66.4	Cosmarium	52.2	515.2
	16	Cosmarium	97.0	Oocystis	93.2	Anacystis	80.2	352.4
	17	Anacystis	213.9	Oocystis	108.0	Cosmarium	67.2	478.3
	21	Ceratium	54.0	Oocystis	26.1	Anacystis	8.9	119.0
8-25-70	1	Anacystis	347.6	Oocystis	57.7	Sphaerocystis	33.6	520.6
	11	Oocystis	99.2	Oedogonium	39.8	Anacystis	35.7	313.2
	19	Ceratium	152.2	Oocystis	77.1	Anacystis	35.7	375.6
	22	Anacystis	196.1	Oocystis	29.5	Sphaerocystis	7.8	260.8
8-27-70	1	Cosmarium	97.0	Ceratium	73.6	Oocystis	71.1	406.8
	12	Cosmarium	97.0	Anacystis	80.2	Oocystis	53.6	353.5
	18	Oocystis	81.8	Cosmarium	67.2	Gomphosphaeria	63.8	398.3
	23	Anacystis	89.1	Oocystis	32.9	Gomphospharia and Ceratium	19.6	192.0

*Volume = Cubic microns $\times 10^4$/ml

TABLE 3 (Cont.)

PHYTOPLANKTON DOMINANCE BY VOLUME*
STATION N

Date	Depth in meters	1st Dominant	Volume	2nd Dominant	Volume	3rd Dominant	Volume	Total Volume
6-17-70	1	Sphaerocystis	7.8	Tribonema	7.4	Uniden. Coccoid Green	1.9	17.2
	10	Oocystis	12.1	Trachelomonas	9.8	Tribonema	7.4	34.0
	18	Centric Diatoms	177.9	Pennate Diatoms	150.0	Pediastrum	17.7	348.7
	19	Pennate Diatoms	297.7	Centric Diatoms	158.6	Melosira	60.0	569.4
7-29-70	1	Oedogonium	177.0	Ceratium	14.7	Cosmarium	7.5	233.2
	11	Oedogonium	88.5	Anacystis	26.7	Ceratium	14.7	163.8
	18.6	Oedogonium	97.4	Pennate Diatoms	16.2	Tribonema	15.6	171.3
	20	Oedogonium	84.1	Anacystis	71.3	Cosmarium	22.4	219.4
8-2-70	1	Anacystis	133.7	Oedogonium	84.1	Ceratium	29.5	317.4
	18	Oedogonium	66.4	Ceratium	9.8	Cosmarium	7.4	104.0
	19.3	Oedogonium	101.8	Ceratium	9.8	Oocystis	6.0	133.7
	21	Oedogonium	88.5	Pennate Diatoms	6.9	Tribonema & Ceratium	4.9	117.4
8-6-70	1	Anacystis	26.7	Oedogonium	13.3	Oocystis	12.1	81.8
	10	Ceratium	63.8	Oedogonium	53.1	Oocystis	18.8	184.7
	19	Oedogonium	35.4	Ceratium	9.8	Tribonema	7.4	64.3
	21	Oedogonium	13.3	Pennate Diatoms	6.9	Tribonema	5.8	31.4
8-11-70	1	Oedogonium	48.7	Oocystis	24.1	Cosmarium	22.4	144.2
	20	Oedogonium	13.3	Centric Diatoms	8.6	Cosmarium	7.4	41.3
8-15-70	1	Ceratium	24.5	Cosmarium	22.4	Oocystis	22.1	97.8
	11	Anacystis	142.6	Oocystis	29.5	Oedogonium	17.7	230.6
	18	Anacystis	35.7	Ceratium	24.5	Cosmarium	22.4	126.4
	20	Anacystis	53.5	Ceratium	34.4	Oedogonium	17.7	130.1
8-19-70	1	Oocystis	38.9	Anacystis	17.8	Staurastrum	13.6	103.8
	11	Anacystis	71.3	Oocystis	34.9	Cosmarium	22.4	146.4
	17	Anacystis	80.2	Oocystis	26.8	Oedogonium	8.9	134.6
	20	Ceratium	24.5	Oocystis	7.4	Centric Diatoms	4.2	47.8
8-24-70	1	Oocystis	37.5	Anacystis	35.7	Cosmarium	22.4	153.2
	12	Anacystis	329.8	Cosmarium	29.9	Oocystis	28.2	464.1
	17.3	Anacystis	659.6	Oocystis	54.3	Staurastrum	12.5	749.8
	19	Anacystis	196.1	Ceratium	34.4	Oocystis	16.8	275.4
8-25-70	1	Anacystis	80.2	Oocystis	58.3	Oedogonium	31.0	232.8
	12	Anacystis	1123.1	Oocystis	43.2	Sphaerocystis	25.9	1228.9
	18	Oocystis	78.4	Gomphosphaeria	19.6	Sphaerocystis	19.0	191.0
	22	Anacystis	169.4	Oocystis	20.1	Centric Diatoms	12.9	225.8
8-27-70	1	Oocystis	32.2	Sphaerocystis	15.5	Anacystis	15.2	117.3
	7	Anacystis	213.9	Cosmarium	97.0	Centric Diatoms	36.4	463.1
	18	Anacystis	570.5	Oocystis	60.3	Sphaerocystis	26.7	696.2
	21	Anacystis	151.5	Centric Diatoms	12.9	Oocystis	10.7	169.6
9-2-70	17	Anacystis	918.1	Oocystis	49.6	Sphaerocystis	11.2	999.8

*Volume = Cubic microns $\times 10^4$/ml

TABLE 4

SEDIMENTATION TRAP
RESULTS OF VOLATILE SOLIDS AND
PHYTOPLANKTON ANALYSES

Date	Volatile Solids $mg/cm^2/day$	Phytoplankton Count $No/cm^2/day$	Phytoplankton Volume $\mu^3/cm^2/day$
6-13-70 to 7-6-70	0.118	0.96×10^4	1.58×10^7
7-28-70 to 8-1-70	0.061	2.17×10^4	8.76×10^7
8-1-70 to 8-4-70	0.177	6.33×10^4	30.19×10^7
8-4-70 to 8-11-70	0.077	1.63×10^4	4.70×10^7
8-11-70 to 8-17-70	0.045	0.79×10^4	2.05×10^7
8-17-70 to 8-21-70	0.168	2.84×10^4	5.61×10^7

TABLE 5

SEDIMENTATION TRAP
PHYTOPLANKTON DOMINANCE
BY VOLUME

Date	1st Dominant	Volume $\mu^3 x10^7/cm^2/day$	2nd Dominant	Volume $\mu^3 x10^7/cm^2/day$	3rd Dominant	Volume $\mu^3 x10^7/cm^2/day$	Total Volume $\mu^3 x10^7/cm^2/day$
6-23-70 to 7-6-70	Centric diatoms	0.62	Staurastrum	0.34	Tribonema	0.33	1.58
7-28-70 to 8-1-70	Oedogonium	4.81	Pennate Diatoms	1.74	Anacystis	0.84	8.76
8-1-70 to 8-4-70	Oedogonium	23.26	Pennate Diatoms	3.35	Tribonema	1.65	30.19
8-4-70 to 8-11-70	Oedogonium	1.91	Pennate Diatoms	0.87	Tribonema	0.77	4.70
8-11-70 to 8-17-70	Oedogonium	0.97	Pennate Diatoms	0.36	Oocystis	0.21	2.05
8-17-70 to 8-21-70	Anacystis	1.26	Oocystis	1.23	Pennate Diatoms	1.20	5.61

TABLE 6

SEDIMENTED ALGAE

PHYTOPLANKTON COUNTS
(organisms/cm^2)

1970

Station	6/14 to 6/20	6/21 to 6/27	6/28 to 7/4	7/5 to 7/11	7/12 to 7/18	7/19 to 7/25	7/26 to 8/1	8/2 to 8/8	8/9 to 8/15	8/16 to 8/22	8/23 to 8/29	8/30 to 9/5
P	428	No Sample	No Sample	No Sample	184	No Sample	819	876 11,872	3,732	12,708	5,831	13,700
R	92	No Sample	No Sample	No Sample	639	No Sample	No Sample	4,174	699	2,948	3,198	3,710
S	0	460	No Sample	600	No Sample	No Sample	1,920	991	5,550	5,866	3,303	5,970
M	No Sample	No Sample	No Sample	No Sample	554	No Sample	302	2,001	945	1,049	3,618	2,430
N	570	No Sample	No Sample	No Sample	No Sample	No Sample	No Sample	5,797	12,377	10,245 14,985	38,271	7,182
Average	273	460	–	600	459	–	1,014	4,285	4,660	7,967	10,845	6,599

TABLE 7(a)

SEDIMENTED ALGAE DOMINANCE
STATION P

Date	1st Dominant	No./cm^2	2nd Dominant	No./cm^2	3rd Dominant	No./cm^2	Total No./cm^2
6-16-70	Pediastrum	171	Oocystis Staurastrum Tribonema	85 85 85	–	–	428
7-13-70	Oedogonium Tribonema	92 92	–	–	–	–	184
7-30-70	Oedogonium Tribonema Cosmarium	273 273 273	–	–	–	–	819
8-6-70	Cosmarium Pediastrum	438 438	–	–	–	–	876
8-8-70	Oedogonium	8,866	Tribonema	2,030	Oocystis	363	11,872
8-11-70	Tribonema	2,382	Oedogonium	363	Scenedesmus	198	3,732
8-17-70	Tribonema	10,078	Oedogonium	1,602	Tetraedron	438	12,708
8-24-70	Oedogonium	3,237	Tribonema	2,104	Oocystis	326	5,831
9-1-70	Oedogonium	1,955	Tribonema	1,469	Staurastrum	977	13,700

TABLE 7(b)

SEDIMENTED ALGAE DOMINANCE
STATION R

Date	1st Dominant	No./cm^2	2nd Dominant	No./cm^2	3rd Dominant	No./cm^2	Total No./cm^2
6-16-70	Oocystis	91	–	–	–	–	91
7-13-70	Pediastrum	641	–	–	–	–	641
8-3-70	Tribonema	1,388	Pediastrum	694	Oedogonium Oocystis Cosmarium Staurastrum	465 465 465 465	4,170
8-10-70	Tribonema Oedogonium	347 347	–	–	–	–	694
8-18-70	Tribonema	1,474	Oedogonium	924	Staurastrum	368	2,948
8-26-70	Tribonema	1,041	Pediastrum	507	Oedogonium Oocystis	336 336	3,199
8-31-70	Tribonema	1,623	Oedogonium	929	Oocystis	694	3,706

TABLE 7(c)

SEDIMENTED ALGAE DOMINANCE
STATION S

Date	1st Dominant	No./cm^2	2nd Dominant	No/cm^2	3rd Dominant	No./cm^2	Total No./cm^2
6-15-70	–	–	–	–	–	–	0
6-23-70	Staurastrum	368	Scenedesmus	92	–	–	460
7-6-70	Tribonema	465	Scenedesmus Pediastrum	65 65	–	–	600
7-29-70	Tribonema Staurastrum Tetraedron Schizothrix Unident. Blue-Green Filamentous	384 384 384 384 384	–	–	–	–	1,920
8-5-70	Tribonema	827	Pediastrum	164	–	–	991
8-12-70	Tribonema	3,738	Oedogonium	720	Pediastrum	363	5,550
8-21-70	Oedogonium	2,707	Tribonema	2,029	Oocystis Staurastrum	427 427	5,866
8-25-70	Tribonema	2,066	Oedogonium	1,237		–	3,303
9-1-70	Tribonema	3,300	Oedogonium	1,015	Oocystis	635	5,970

TABLE 7(d)

SEDIMENTED ALGAE DOMINANCE
STATION M

Date	1st Dominant	No./cm^2	2nd Dominant	No./cm^2	3rd Dominant	No./cm^2	Total No./cm^2
7-17-70	Pediastrum Staurastrum	277 277	–	–	–	–	554
7-29-70	Tribonema	302	–	–	–	–	302
8-4-70	Tribonema	999	Oedogonium	571	Pediastrum	288	2,001
8-11-70	Tribonema Oocystis Pediastrum	315 315 315	–	–	–	–	945
8-18-70	Tribonema	877	Pediastrum	172	–	–	1,049
8-24-70	Tribonema	1,917	Oedogonium	1,063	Pediastrum	427	3,618
9-2-70	Tribonema	1,143	Sphaerocystis	577	Oedogonium	491	7,182

TABLE 7(e)

SEDIMENTED ALGAE DOMINANCE
STATION N

Date	1st Dominant	No./cm^2	2nd Dominant	No./cm^2	3rd Dominant	No./cm^2	Total No./cm^2
6-16-70	Staurastrum	570	–	–	–	–	570
8-2-70	Tribonema	2,783	Oedogonium Pediastrum	1,159 1,159	Staurastrum	465	5,979
8-12-70	Tribonema	10,420	Oedogonium	1,303	Oocystis	262	12,377
8-17-70	Tribonema	8,556	Staurastrum	604	Oedogonium	481	10,245
8-21-70	Tribonema	12,797	Staurastrum	844	Oedogonium	673	14,985
8-24-70	Tribonema	35,496	Oedogonium	1,901	Oocystis	732	38,271

TABLE 8(a)

PHYTOPLANKTON DOMINANCE BY NUMBER
STATION P

Date Cruise	Depth in meters	1st Dominant	No/ml	2nd Dominant	No/ml	3rd Dominant	No/ml	Total No/ml
7-29-70	1	Oocystis	20	Staurastrum	13	Tribonema	9	68
1	12	Oedogonium	12	Pennate Diatoms	11	Unident. Green Coccoid	10	86
	17	Oedogonium	26	Oocystis	12	Tribonema	12	89
	22	Pennate Diatoms	45	Unident. Green Coccoid	12	Oedogonium	8	113
8-2-70	2	Filament. Blue-Green Unident.	30	Oocystis	22	Unident. Green Coccoid	22	137
2	14	Oocystis	17	Oedogonium	12	Tribonema	7	98
	19	Oedogonium	24	Oocystis	12	Pennate Diatoms	11	86
	23	Centric Diatoms	16	Pennate Diatoms	14	Oedogonium	14	84
8-6-70	1	Oocystis	27	Unident. Filament. Blue-Green	12	Trachelomonas	7	86
3	10	Oocystis	33	Unident. Green Coccoid	9	Staurastrum	8	80
	18	Centric Diatoms	10	Oocystis	10	Unident. Green Coccoid	9	72
	22	Tribonema	13	Pennate Diatoms	11	Centric Diatoms	10	75
8-11-70	1	Oocystis	36	Phacotus	16	Staurastrum	15	96
4	12	Oocystis	46	Anacystis	18	Staurastrum	16	128
	17	Oocystis	29	Anacystis	8	Staurastrum	7	62
	21	Oocystis	19	Anacystis	8	Phacus	6	58
8-15-70	1	Oocystis	58	Anacystis	20	Unident. Green Coccoid	11	137
5	14	Oocystis	44	Ceratium	19	Staurastrum	14	109
	18.5	Oocystis	32	Phacotus	12	Ceratium	12	83
	22	Oocystis	15	Centric Diatoms	6	Anacystis	5	46
8-19-70	1	Oocystis	118	Sphaerocystis	18	Anacystis	17	228
6	10	Oocystis	101	Anacystis	18	Sphaerocystis	17	204
	17	Oocystis	112	Staurastrum	15	Anacystis	10	183
	21	Oocystis	86	Anacystis	21	Sphaerocystis	12	152
8-24-70	1	Oocystis	114	Sphaerocystis	35	Gleocystis	31	281
7	12	Oocystis	90	Sphaerocystis	52	Anacystis	39	262
	19	Oocystis	80	Sphaerocystis	38	Staurastrum	16	213
	22	Oocystis	47	Unident. Green Coccoid	8	Anacystis	8	85
8-25-70	1	Oocystis	51	Sphaerocystis	32	Phacotus	12	128
9	15	Oocystis	81	Sphaerocystis	33	Phacotus	18	196
	20	Oocystis	76	Sphaerocystis	39	Phacotus	15	168
	23	Oocystis	24	Aphanizomenon	17	Crucigenia & Anacystis	3	59
8-27-70	1	Oocystis	100	Phacotus	54	Aphanizomenon	48	381
10	12	Oocystis	87	Staurastrum	41	Sphaerocystis	22	241
	19	Sphaerocystis	33	Staurastrum	28	Pennate Diatoms	9	134
	23	Oocystis	44	Anacystis	17	Sphaerocystis	6	88
9-1-70	1	Staurastrum	85	Phacotus	54	Oocystis	50	310
11	12	Aphanizomenon	52	Oocystis	42	Phacotus	31	227
	19	Oocystis	48	Anacystis	39	Staurastrum	35	243
	23	Oocystis	29	Pennate Diatoms	8	Aphanizomenon	7	65

TABLE 8(b)

PHYTOPLANKTON DOMINANCE BY NUMBER
STATION R

Date Cruise	Depth in meters	1st Dominant	No /ml	2nd Dominant	No /ml	3rd Dominant	No/ml	Total No/ml
7-29-70	1	Oocystis	16	Pennate Diatoms	11	Aphanizomenon	10	78
1	12	Oedogonium	34	Tribonema	15	Oocystis	13	106
	16	Centric Diatoms	23	Oedogonium	22	Oocystis	16	97
	20	Centric Diatoms	17	Pennate Diatoms	15	Unident. Green Coccoid	13	68
8-2-70	1	Pennate Diatoms	23	Centric Diatoms	12	Unident. Green Coccoid	10	73
2	11	Centric Diatoms	19	Pennate Diatoms	16	Tribonema	15	71
	15	Pennate Diatoms	42	Ceratium	33	Oocystis	20	144
	21.5	Oocystis	22	Unident. Green Coccoid	22	Unident. Filament. Blue-Green	18	153
8-6-70	1	Oocystis	20	Staurastrum	6	Nephrocytium	6	67
3	14	Oocystis	29	Ceratium	7	Nephrocytium & Oedogonium	6	83
	15	Ceratium	87	Oocystis	26	Unident. Green Coccoid	13	143
	21	Pennate Diatoms	17	Centric Diatoms	16	Oocystis	8	60
8-11-70	1	Oocystis	60	Phacotus	21	Anacystis	12	120
4	9	Oocystis	27	Ceratium	8	Staurastrum	8	79
	15	Oocystis	17	Anacystis	15	Oedogonium	8	70
	20	Oocystis	13	Centric Diatoms	11	Pennate Diatoms	7	51
8-15-70	1	Oocystis	79	Phacotus	57	Sphaerocystis	33	250
5	12	Oocystis	116	Anacystis	40	Phacotus	24	219
	15.5	Oocystis	63	Anacystis	39	Phacotus	15	149
	20	Oocystis	14	Centric Diatoms	8	Anabaena	6	37
8-20-70	15	Oocystis	120	Anacystis	57	Sphaerocystis	20	267
6	16.5	Oocystis	150	Anacystis	28	Sphaerocystis & Phacotus	20	283
8-25-70	1	Oocystis	28	Phacotus	21	Anacystis	17	109
7	13	Anacystis	31	Oocystis	25	Staurastrum & Phacotus	21	134
	16.5	Oocystis	21	Phacus	6	Unident. Green Coccoid	4	41
	20	Oocystis	10	Staurastrum	3	Phacus	2	24
8-25-70	1	Oocystis	52	Phacotus	22	Aphanizomenon	16	248
9	14	Oocystis	91	Sphaerocystis	28	Anacystis & Pennate Diatoms	24	234
	22	Oocystis	15	Anacystis	10	Phacotus & Centric Diatoms	2	40
8-27-70	11	Anacystis	100	Oocystis	81	Phacotus	59	393
10	15	Oocystis	103	Sphaerocystis	50	Anacystis	44	324
	23	Oocystis	28	Pennate Diatoms	8	Unident. Green Flagellate	6	63
9-1-70	1	Oocystis	51	Staurastrum	36	Aphanizomenon	26	212
11	12	Oocystis	56	Aphanizomenon	39	Staurastrum	28	194
	18	Oocystis	24	Aphanizomenon	14	Pennate Diatoms & Crucigenia	4	71
	21	Oocystis	20	Aphanizomenon	17	Anacystis	15	66

TABLE 8(c)

PHYTOPLANKTON DOMINANCE BY NUMBER
STATION S

Date Cruise	Depth in meters	1st Dominant	No/ml	2nd Dominant	No/ml	3rd Dominant	No/ml	Total No/ml
7-29-70 1	1	Unident. Filament. Blue-Green	56	Oedogonium	17	Oocystis	9	97
	10	Oedogonium	102	Unident. Green Coccoid	20	Schroederia & Tribonema	11	174
	18	Oedogonium	35	Tribonema	12	Oocystis	7	71
	21	Oocystis	15	Oedogonium	12	Tribonema	9	57
8-2-70 2	1	United. Filament. Blue-Green	39	Oedogonium	12	Oocystis	10	96
	12	Oedogonium	17	Ceratium	16	Anacystis	12	92
	18	Ceratium	35	Oedogonium	20	Unident. Green Coccoid	7	83
	21	Oedogonium	17	Oocystis	11	Unident. Green Coccoid	10	70
8-6-70 3	1	Anacystis	46	Oocystis	27	Staurastrum & Unident. Filament. Blue-Green	7	115
	12	Ceratium	21	Oocystis	19	Trachelomonas	12	84
	18	Oocystis	14	Staurastrum	7	Oedogonium	7	42
	21	Oocystis	11	Oedogonium	10	Trachelomonas & Pennate Diatoms	5	56
8-12-70 4	1	Oocystis	42	Anacystis	41	Oedogonium & Unident. Filament. Blue-Green	5	137
	12	Oocystis	41	Anacystis	26	Staurastrum	15	118
	17	Oocystis	22	Ceratium	17	Oedogonium & Tribonema	4	58
	20	Oocystis	13	Tribonema	7	Oedogonium & Phacus	5	46
8-15-70 5	1	Oocystis	99	Staurastrum	15	Trachelomanos	7	164
	14	Oocystis	139	Staurastrum	22	Sphaerocystis & Oedogonium	9	221
	19	Oocystis	39	Ceratium	7	Oedogonium	5	75
	21	Oocystis	16	Pennate Diatoms	11	Oedogonium	9	54
8-20-70 6	1	Oocystis	131	Anacystis	29	Sphaerocystis	15	226
	12	Oocystis	84	Staurastrum	20	Sphaerocystis	13	154
	18.5	Oocystis	80	Staurastrum	17	Anacystis	7	129
	21	Oocystis	28	Staurastrum	12	Ceratium	12	74
8-25-70 7	1	Oocystis	116	Staurastrum	20	Sphaerocystis	18	235
	12	Oocystis	99	Staurastrum	41	Anacystis	15	197
	18	Oocystis	107	Staurastrum	30	Anacystis	19	198
	21	Oocystis	48	Anacystis	31	Staurastrum	10	115
8-27-70 10	1	Oocystis	111	Staurastrum	28	Phacotus & Unident. Green Flagellates	13	217
	11	Oocystis	55	Phacotus	39	Anacystis	37	208
	19	Oocystis	95	Phacotus	30	Anacystis	24	242
	21	Oocystis	26	Anacystis	13	Aphanizomenon	6	69
9-1-70 11	1	Oocystis	65	Phacotus	33	Staurastrum	22	231
	11	Oocystis	112	Sphaerocystis	29	Anacystis	28	267
	20	Anacystis	98	Oocystis	85	Sphaerocystis	29	275
	22	Oocystis	59	Unident. Green Flagellate	17	Unident. Green Coccoid	13	127

TABLE 8(d)

PHYTOPLANKTON DOMINANCE BY NUMBER
STATION M

Date Cruise	Depth in meters	1st Dominant	No/ml	2nd Dominant	No/ml	3rd Dominant	No/ml	Total No/ml
7-29-70 1	1	Unident. Filament. Blue-Green	32	Oocystis	5	Centric Diatoms & Sphaerocystis	4	66
	9	Oedogonium	19	Schroederia	6	Unident. Filament. Blue-Green	6	55
	19	Unident. Green Coccoid	14	Pennate Diatoms	8	Oedogonium	8	55
	21	Unident. Green Coccoid	17	Pennate Diatoms	13	Oocystis	12	60
8-2-70 2	1	Unident. Green Coccoid	24	Pennate Diatoms	19	Oocystis	12	95
	14	Unident. Green Coccoid	43	Pennate Diatoms	10	Oocystis	10	101
	16.8	Oocystis	12	Ceratium	10	Oedogonium	6	66
	20	Oocystis	20	Ceratium	17	Pennate Diatoms	10	76
	22	Oocystis	19	Aphanizomenon	17	Unident. Green Coccoid	14	85
8-5-70 3	1	Oocystis	25	Unident. Green Coccoid	7	Centric Diatoms	6	81
	12	Oocystis	28	Ceratium	16	Staurastrum	11	94
	17	Ceratium	41	Oocystis	21	Phacus	11	117
	20	Ceratium	15	Pennate Diatoms	13	Oocystis	9	79
8-11-70 4	1	Oocystis	34	Unident. Filament. Blue-Green	12	Anacystis	11	94
	11	Oocystis	31	Unident. Filament. Blue-Green	9	Centric Diatoms	6	100
	16	Ceratium	163	Oocystis	54	Staurastrum	20	265
	18	Oocystis	16	Oedogonium	9	Sphaerocystis	3	44
	19	Pennate Diatoms	8	Oocystis	6	Centric Diatoms	5	38
	20.9	Pennate Diatoms	15	Centric Diatoms	11	Oocystis	11	56
8-15-70 5	1	Oocystis	97	Ceratium	10	Staurastrum	9	167
	12	Oocystis	37	Phacotus	11	Staurastrum	10	91
	17	Oocystis	27	Ceratium	16	Phacotus	4	64
	21	Oocystis	16	Pennate Diatoms	8	Centric Diatoms	5	44
8-19-70 6	1	Oocystis	73	Staurastrum	20	Phacotus	15	160
	2	Oocystis	141	Staurastrum	35	Sphaerocystis	24	278
	13.5	Oocystis	71	Anacystis	28	Staurastrum	11	165
	17.5	Oocystis	43	Anacystis	35	Phacotus	10	116
	21	Oocystis	41	Anacystis	32	Centric Diatoms	11	112
	22	Oocystis	16	Ceratium	13	Pennate Diatoms	5	53
8-24-70 7	1	Oocystis	99	Anacystis	40	Sphaerocystis	17	237
	16	Oocystis	139	Staurastrum	28	Sphaerocystis	20	269
	17	Oocystis	161	Staurastrum	24	Anacystis	24	288
	21	Oocystis	39	Ceratium	11	Staurastrum	5	72
8-25-70 9	1	Oocystis	86	Sphaerocystis	39	Anacystis	39	271
	11	Oocystis	148	Sphaerocystis	26	Staurastrum	22	321
	19	Oocystis	115	Sphaerocystis	31	Ceratium	31	267
	22	Oocystis	44	Anacystis	22	Sphaerocystis	9	96
8-27-70 10	1	Oocystis	106	Staurastrum	59	Sphaerocystis	37	331
	12	Oocystis	80	Staurastrum	67	Sphaerocystis	33	281
	18	Oocystis	122	Sphaerocystis	67	Unident. Green Coccoid	30	344
	23	Oocystis	49	Anacystis	10	Aphanizomenon	9	96

TABLE 8(e)

PHYTOPLANKTON DOMINANCE BY NUMBER
STATION N

Date Cruise	Depth in meters	1st Dominant	No/ml	2nd Dominant	No/ml	3rd Dominant	No/ml	Total No/ml
7-29-70 1	1	Oedogonium	40	Tribonema	8	Oocystis	7	79
	11	Oedogonium	20	Oocystis	16	Unident. Green Coccoid	8	73
	18.6	Oedogonium	22	Tribonema	19	Oocystis	11	78
	20	Oedogonium	19	Oocystis	9	Anacystis	8	68
8-2-70 2	1	Oocystis	20	Oedogonium	19	Anacystis	15	95
	18	Oedogonium	15	Oocystis	10	Tribonema	6	57
	19.3	Oedogonium	23	Oocystis	9	Tribonema	7	54
	21	Oedogonium	20	Oocystis	6	Tribonema	6	52
8-6-70 3	1	Phacotus	29	Oocystis	18	Unident. Green Coccoid	16	109
	10	Oocystis	28	Green 15 Coccoid	15	Staurastrum	13	108
	19	Tribonema	9	Oocystis	8	Oedogonium	8	42
	21	Unident. Green Coccoid	7	Tribonema	7	Oocystis	6	29
8-11-70 4	1	Oocystis	36	Staurastrum	24	Oedogonium	11	100
	20	Oocystis	6	Centric Diatoms	4	Oedogonium & Phacotus	3	24
8-15-70 5	1	Oocystis	33	Staurastrum	16	Sphaerocystis	9	85
	11	Oocystis	44	Staurastrum	25	Anacystis	16	125
	18	Oocystis	19	Ceratium	5	Oedogonium & Anacystis	4	59
	20	Oocystis	17	Ceratium	9	Anacystis	6	48
8-19-70 6	1	Oocystis	58	Staurastrum	26	Phacotus	8	118
	11	Oocystis	52	Staurastrum	14	Anacystis	8	94
	17	Oocystis	11	Ceratium	5	Quadrigula	4	35
	20	Oocystis	40	Anacystis	9	Staurastrum & Phacotus	5	75
8-24-70 7	1	Oocystis	56	Phacotus	12	Staurastrum & Trachelomonas	9	150
	12	Oocystis	42	Anacystis	37	Staurastrum	27	169
	17.3	Oocystis	81	Anacystis	74	Staurastrum	24	207
	19	Oocystis	25	Anacystis	22	Ceratium	7	78
8-25-70 9	1	Oocystis	87	Anabaena	20	Staurastrum	15	218
	12	Anacystis	126	Oocystis	63	Staurastrum & Sphaerocystis	30	312
	18	Oocystis	117	Staurastrum	33	Sphaerocystis	22	245
	22	Oocystis	30	Anacystis	19	Aphanizomenon	18	93
8-27-70 10	1	Oocystis	48	Sphaerocystis	18	Unident. Filament. Blue-Green	17	156
	7	Oocystis	52	Phacotus	29	Anacystis	24	216
	18	Oocystis	90	Anacystis	64	Sphaerocystis	31	246
	21	Anacystis	17	Oocystis	16	Centric Diatoms & Aphanizomenon	6	57
9-2-70 11	17	Anacystis	103	Oocystis	74	Sphaerocystis	13	232

APPENDIX V

Bacteriological Data

TEST

The procedure for the spot test for nitrite plus nitrate was as follows: 1 drop test solution was placed in a depression of a spot plate, then 1 drop diphenylamine reagent was added and mixed, followed by 2 drops concentrated H_2SO_4.

MEDIA

Nitrosomonas Broth Medium: $(NH_4)_2SO_4$ – 2.0 g; K_2HPO_4 – 2.0 g; NaCl – 1.0 g; $MgSO_4.7H_2O$ – 1.0 g; $CaCl_2$ – 0.2 g; Trace element solution – 1.0 ml; Distilled Water – 1 liter; adjust pH to 7.4. Media was dispensed into tubes and sterilized by autoclaving for 10 minutes at 10 pounds pressure.

Diphenylamine Reagent: Dissolve 0.7 g diphenylamine in a mixture of 60 ml conc. H_2SO_4 and 28.8 ml distilled water. Cool the mixture and slowly add 11.3 ml conc. HCl and let stand overnight before using.

Trace Element Solution: $MgCl_2$ – 0.2 g; $ZnSO_4.7H_2O$ – 0.42 g; $CuSO_4.5H_2O$ – 0.11 g; $FeSO_4.7H_2O$ – 2.0 g; molybdic acid – 0.03 g; $CaCl_4.6H_2O$ – 0.09 g; Distilled Water – 1 liter; adjust pH to 2.5 with conc. H_2SO_4; sterilize by filtration.

Starkey's Broth Medium: Sodium lactate – 3.5 g; NH_4Cl – 1.0 g; K_2HPO_4 – 0.5 g; $MgSO_4.7H_2O$ – 2.0 g; $NaSO_4$ – 0.5 g; $CaCl_2.2H_2O$ – 0.1 g; Mohr's salt – trace; Distilled Water – 1 liter. The prepared media was dispensed into screw capped tubes and sterilized by autoclaving for 10 minutes at 10 pounds pressure.

Foot and Taylor Medium: Peptone – 3.0 g; K_2HPO_4 – 0.2 g; $MgSO_4$ – 0.05 g; $FeCl_3$ – trace; agar – 20 g; Distilled Water – 1 litre. Adjust pH to 7.2 and sterilize by autoclaving for 10 minutes at 15 pounds pressure.

Table I. Geographical Positions of Bacteriological Sampling Locations in "Project Hypo"

Station No.	Depth in feet	Latitude	Longitude
M	79	42° 08.3′ N.	81° 26.2′ W
N	75	41° 51.2′	81° 26.0′
O	66	41° 42.7′	81° 41.8′
P	83	42° 02.6′	81° 37.5′
R	79	42° 09.9′	81° 45.1′
S	74	41° 53.3′	81° 52.2′
T	66	41° 36.8′	81° 54.5′
U	47	41° 30.5′	82° 17.0′
V	60	41° 42.0′	82° 18.0′
W	74	41° 47.5′	82° 04.7′

Table II. Bacteriological and Physical Parameters at Station M.

Parameter	Depth	July	August					
		29	4	6	11	14	18	24
20 °C Aerobic Heterotrophs per ml	A	60	180	500	890	250		
	B	940	320	510	1100	400		600
	C	200	320	360	1000	510		300
	D		1400	1700	1900	930		750
	E	680	5000		2400	1000		1200
	F	8300	1100		1200	730		$1.0x10^4$
	G	$1.4x10^6$	$2.4x10^6$	$1.1x10^6$	$3.2x10^4$*	$7.9x10^5$		$6.7x10^6$
20°C Anaerobic Heterotrophs per ml	A	10	<10	<10	6	1		13
	B	25	<10	<10	34	22		11
	C	25	<10	100	39	4		17
	D		80	70	51	79		40
	E		<10	40	110	140		96
	F		10	30	210	40		85
	G	$3.5x10^4$	$3.3x10^4$	$1.1x10^4$	2000*	$2.5x10^4$		$4.0x10^4$
Bacterial Biomass (ug/litre)	A	195.3	155.6	171.8	468.1	234.9	129.5	250.4
	B	166.5	118.7	199.3	328.3	115.3	208.1	292.5
	C	135.0	118.8		248.7	115.7	234.3	157.4
	D		120.7	136.9	197.2	170.7	318.8	269.0
	E	100.8	112.8	138.1	168.9	158.8	153.3	196.4
	F	145.9	152.1	184.9			228.1	489.1
Nitrifying Bacteria per 100 ml	A	<2	<2	<2	<2	<2	<2	<2
	E	<2	<2	<2	<2	<2	<2	<2
	F	<2	<2	<2	<2	<2	<2	<2
	G	130	140	23	23*	350	70	3500
Thiobacillus sp. per 100 ml	A	<2	<2	2	13	23	<2	13
	E	<2	<2	<2	<2	23	23	23
	F	<2	<2	2	22	2	2	13
	G	1600	>1600	>1600	49*	$>1.6x10^4$	$1.3x10^4$	$2.3x10^4$
Desulfovibrio sp. per 100 ml	A	<2	<2	<2	<2	<2	<2	<2
	D							23
	E	5	<2	8	2	5	49	110
	F	23	13	23	350	49	49	130
	G	>1600	$<1.6x10^4$	$>1.6x10^4$	1400*	$3.5 x10^5$	$1.3x10^5$	$4.9x10^4$
Temperature (°C)	A	24.5	23.5	24.0	22.8	24.3	23.9	23.9
	B	21.2	23.0	21.5	21.8	19.0	18.8	23.3
	C	16.0	17.5	18.0	16.5	13.7	10.0	18.5
	D		11.2	12.0	14.2	9.2	9.4	12.0
	E	11.0	11.2	11.6	13.9	9.1	9.3	11.9
Dissolved Oxygen (mg/liter)	A	10.1	8.5	8.9	8.7	9.0	8.5	8.6
	B	7.8	8.0	7.3	7.8	5.9	5.5	8.2
	C	6.1	6.4	6.2	4.0	4.3	2.3	7.3
	D		3.6	4.1	3.0	2.5	1.8	1.4
	E	4.2	3.3	3.0	2.6	2.4	1.8	1.4

A = 2 meters below surface
B = 1 meter above thermocline
C = Within thermocline
D = 1 meter below thermocline
E = 2 meters above bottom
F = 3 inches above bottom
G = Sediment-water interface
G*= 1 inch above bottom

Table III. Bacteriological and Physical Parameters at Station N.

Parameter	Depth	August 2	5	12	17	21	24
20°C Aerobic	A	250	320		70	550	
Heterotrophs	B	370			110	460	880
per ml	C	520			460	1500	850
	D				280		1600
	E	3300			60	3500	2000
	F	6000	300		2500	1700	640
	G	7.1×10^5	8.4×10^6		2.4×10^5	2.1×10^6	2.6×10^6
20°C Anaerobic	A	10	<10		16	2	17
Heterotrophs	B	30	10		31	19	9
per ml	C	40	20		61	22	13
	D				42		21
	E	250			27	33	7
	F	240	30		87	45	47
	G	3.0×10^4	1.9×10^4		5.7×10^4	6.6×10^4	1.1×10^5
Bacterial Biomass	A	179.1	218.9	177.2	123.0	128.6	350.0
(ug/litre)	B	189.3	97.0	150.8	101.5	127.5	184.3
	C	103.7	130.9	209.1	164.8	197.0	261.7
	D				159.3		224.7
	E	122.1	154.7	190.6	199.8	255.3	247.8
	F	144.6	178.3	491.3	225.8		191.6
Nitrifying	A	<2	<2	<2	<2	<2	<2
Bacteria per	E	<2	<2	<2	<2	<2	<2
100 ml	F	<2	<2	<2	<2	<2	<2
	G	>1600	120	3500	<200	790	3500
Thiobacillus sp.	A	<2	33	5	<2	13	23
per 100 ml	E	2	8	23	8	8	23
	F	8	12	40	17	5	13
	G	>1600	>1600	$>1.6 \times 10^4$	7.9×10^4	7.9×10^4	1.4×10^5
Desulfovibrio sp.	A	<2	<2	<2	<2	<2	<2
per 100 ml	D					2	70
	E	8	49	56	350	240	240
	F	33	49	1600	920	240	540
	G	>1600	$>1.6 \times 10^4$	$>1.6 \times 10^6$	9.2×10^5	1.6×10^6	5.4×10^5
Temperature	A	24.3	24.0	24.0	24.2	23.2	24.6
(°C)	B	20.6	22.3	19.9	21.5	22.0	24.2
	C	18.0	14.8	12.8	19.0	14.6	19.9
	D				15.5		14.0
	E	11.3	13.5	10.5	10.6	11.4	14.0
Dissolved Oxygen	A	8.8	8.9	8.7	8.6	8.2	8.2
(mg/litre)	B	7.7	7.9	6.6	6.8	7.4	8.2
	C	7.5	5.4	4.0	6.3	3.0	6.3
	D				3.9		1.0
	E	2.0	2.5	2.0	0.1	0.5	0.3

A = 2 meters below surface
B = 1 meter above thermocline
C = Within thermocline
D = 1 meter below thermocline
E = 2 meters above bottom
F = 3 inches above bottom
G = Sediment-water interface

Table IV (a). Bacteriological and Physical Parameters at Station P.

Parameter	Depth	July		August					
		28	30	1	2	3	4	5	6
20°C Aerobic Heterotrophs per ml	A		1700	660	710	200	150		470
	B		2800	260	540		690		270
	C		820	1000	430	870		930	710
	D			450	2400		1600	2600	
	E		980	650	1200	2400	8500	720	
	F		800	270				2500	
	G		$1.2x10^5$	$2.3x10^5$	$1.3x10^6$		$1.9x10^6$		$5.5x10^5$
20°C Anaerobic Heterotrophs per ml	A		55	<10	80	30	<10		<10
	B		45	60	90	20	10	30	30
	C		195	30	30	10	10	<10	<10
	D			80	20	130	10	20	10
	E		390	<10	130	30	20	30	40
	F		140	60	6500		10	140	20
	G		9800	$1.2x10^5$	$6.7x10^4$		$6.1x10^4$	$1.4x10^4$	$1.3x10^5$
Bacterial Biomass (ug/litre)	A	147.4	130.8	237.9	195.6	170.6	130.1	107.0	109.5
	B	138.4	178.0	206.2	145.3	217.0	76.6	64.8	85.5
	C	193.8	98.8	163.6	139.6	195.9	103.5	98.2	83.7
	D			108.2	88.9	96.7	104.0	79.6	103.3
	E	124.1	99.0	88.7	245.9	129.2	106.1	174.6	117.6
	F	115.9	138.9	212.1		97.3	140.5		131.5
Nitrifying Bacteria per 100 ml	A	<2	<2	<2	<2	<2	<2	<2	<2
	E	<2	<2	<2	<2	<2	<2	<2	<2
	F	<2	<2	<2	<2	<2	<2	<2	<2
	G	>1600	350	>1600	920	350	>1600	>1600	920
Thiobacillus sp. per 100 ml	A	<2	<2	<2	<2	<2	<2	<2	<2
	E	<2	<2	<2	<2	<2	<2	<2	<2
	F	<2	<2	<2	23	<2	4	2	2
	G	>1600	>1600	1600	>1600	1600	>1600	>1600	>1600
Desulfovibrio sp. per 100 ml	A	<2	<2	<2	<2	<2	<2	<2	<2
	D								
	E	<2	7	2	49	20	9	9	7
	F	5	33	79	210	110	40	49	23
	G	>1600	>1600	>1600	$1.6x10^4$	$>1.6x10^4$	$>1.6x10^4$	$>1.6x10^4$	$>1.6x10^4$
Temperature (°C)	A	22.6	23.5	24.8	24.2	23.8	23.8	24.0	23.6
	B	20.2	21.0	21.0	20.8	21.3	21.4	21.2	21.0
	C	13.0	14.6	17.7	16.5	17.0	17.0	13.5	17.0
	D			10.5	10.0	11.2	11.4	11.0	11.0
	E	8.3	10.0	10.0	10.0	11.0	11.0		10.8
Dissolved Oxygen (mg/litre)	A	9.8	9.6	9.2	8.9	8.7	7.9	8.9	9.0
	B	8.5	8.0	7.6	7.6	7.6	8.1	7.4	7.5
	C	7.0	5.1	6.8	6.7	7.8		6.5	5.4
	D			3.8	4.3	4.2		3.6	3.5
	E	4.4	3.6	3.6	3.8	3.8	3.1		3.3

A = 2 meters below surface
B = 1 meter above thermocline
C = Within thermocline
D = 1 meter below thermocline
E = 2 meters above bottom
F = 3 inches above bottom
G = Sediment-water interface

Table IV (b). Bacteriological and Physical Parameters at Station P.

Parameter	Depth	August						
		7	8	11	12	13	14	17
20°C Aerobic	A		450	490			100	190
Heterotrophs	B	70	410	740			170	230
per ml	C	650	510	550			340	340
	D	320	600	5700			830	2600
	E	1300	1600	1500			270	4500
	F		4000	5800			680	770
	G	4.7×10^5	1.1×10^6	3.8×10^6			1.8×10^6	
20°C Anaerobic	A	10	36	28			5	5
Heterotrophs	B	10	27	14			4	8
per ml	C		24	22			12	40
	D		80	44			28	17
	E		75	69			82	20
	F	200	38	25			13	52
	G		5.0×10^4	3.4×10^4			2.4×10^4	2.9×10^4
Bacterial Biomass	A	156.1	195.9	416.4	589.0	447.8	473.2	242.7
(ug/litre)	B	189.9	169.1	311.5	234.4	326.1	146.6	256.5
	C	352.6	172.4	164.8	137.3	154.4	104.7	134.4
	D	420.2	227.6	126.0	159.1	226.9	154.7	161.9
	E	308.2	155.2	143.2	213.4	298.4	170.0	215.9
	F	368.6	246.4	226.3	421.4	304.8	216.9	402.4
Nitrifying	A	<2	<2	<2	<2	<2	<2	<2
Bacteria per	E	<2	<2	<2	<2	<2	<2	<2
100 ml	F	<2	<2	<2	<2	<2	<2	<2
	G	240	280	280	49	23	23	<200
Thiobacillus sp.	A	2	<2	17	2	2	5	2
per 100 ml	E	8	<2	5	2	33	5	5
	F	49	7	<2	11	11	5	5
	G	>1600	>1600	>1600	1.6×10^4	9200	1.6×10^4	1.7×10^4
Desulfovibrio sp.	A	<2	<2	<2	<2	<2	<2	<2
per 100 ml	D							
	E	49	49	7	15	17	17	21
	F	220	170	350	>1600	350	350	170
	G	$>1.6\times10^4$	$>1.6\times10^4$	$>1.6\times10^4$	3.5×10^4	$>1.6\times10^5$	$>1.6\times10^5$	2.2×10^5
Temperature	A	23.5	22.8	22.9	23.4	24.0	24.2	23.9
(°C)	B	21.3	21.0	21.1	21.0	20.8	21.0	20.3
	C	14.8	17.0	11.5	16.0	19.0	14.2	18.0
	D	10.8	13.8	9.0	10.0	9.4	10.5	10.0
	E	10.7	13.5	8.9	9.0	9.0	9.0	9.3
Dissolved Oxygen	A	8.9	9.0	9.0	8.8	9.0	9.3	9.0
(mg/litre)	B	7.6	7.6	8.3	7.7	7.2	7.3	6.4
	C	6.5	4.5	4.5	6.3	6.6	5.5	5.5
	D	3.4	3.0	3.3	3.8	2.6	3.1	2.1
	E	3.1	2.6	3.0	3.0	2.2	2.2	1.6

A = 2 meters below surface
B = 1 meter above thermocline
C = Within thermocline
D = 1 meter below thermocline
E = 2 meters above bottom
F = 3 inches above bottom
G = Sediment-water interface

Table IV (c). Bacteriological and Physical Parameters at Station P.

Parameter	Depth	August				
		18	21	23	24	25
20°C Aerobic Heterotrophs per ml	A		360	290	2100	340
	B		20		710	460
	C		700		720	3100
	D		2600		1700	1600
	E				2500	2500
	F		2800	450	940	2500
	G		8.8×10^6	8.6×10^6	3.2×10^6	2.5×10^6
20°C Anaerobic Heterotrophs per ml	A		7	6	10	90
	B		6		8	80
	C		17		17	170
	D		59		10	210
	E				26	220
	F		45	21	28	210
	G		1.6×10^6	4.5×10^4	2.2×10^5	
Bacterial Biomass (ug/litre)	A	126.6	320.7		291.7	278.4
	B	85.3	213.9		242.9	210.0
	C	85.4	279.6		250.3	145.7
	D	149.2	325.5		241.9	152.7
	E	262.8			233.5	191.3
	F	204.4				224.9
Nitrifying Bacteria per 100 ml	A	<2	<2	<2	<2	<2
	E	<2	<2		<2	<2
	F	<2	<2	<2	<2	<2
	G	540	490	790	1800	790
Thiobacillus sp. per 100 ml	A	<2	17	<2	13	8
	E	13	13		23	13
	F	8	33	8	23	2
	G	1.7×10^4	3.3×10^4	2.2×10^5	4.9×10^4	4.9×10^4
Desulfovibrio sp. per 100 ml	A	<2	<2	<2	<2	<2
	D				79	17
	E	130	49		130	17
	F	540	240	240	240	920
	G	1.6×10^6	1.6×10^6	9.2×10^5	2.2×10^5	9.2×10^5
Temperature (°C)	A	23.9	23.5		24.2	21.5
	B	19.8	23.3		24.0	21.2
	C	11.4	11.2		16.2	13.0
	D	9.5			12.0	9.9
	E	9.4	10.1		12.0	9.1
Dissolved Oxygen (mg/litre)	A	8.7	8.0		8.2	8.2
	B	6.2	7.8		8.1	8.1
	C	2.4	1.6		3.3	2.8
	D	1.5			2.2	1.0
	E	1.5	1.3		0.9	0.9

A = 2 meters below surface
B = 1 meter above thermocline
C = Within thermocline
D = 1 meter below thermocline
E = 2 meters above bottom
F = 3 inches above bottom
G = Sediment-water interface

Table V. Bacteriological and Physical Parameters at Station R.

Parameter	Depth	July	August						
		29	3	4	6	10	14	18	23	26
20°C Aerobic Heterotrophs per ml	A	250		410	900	360	140		470	600
	B	350		60	170	2000	260		750	430
	C	180		1300	2600	370	600		860	280
	D			380	120	740	250		990	1100
	E	110		1400	500	2900	1000		1300	2600
	F	1900		2500		5000	1.9×10^4		2000	1000
	G	1.2×10^5		1.1×10^6	2.8×10^7	4.2×10^6	3.6×10^6		1.7×10^6	8.0×10^5
20°C Anaerobic Heterotrophs per ml	A	20		50	10	16	4		18	9
	B	15		30	70	22	8		10	15
	C	15		10		6	63		4	15
	D			20	<10	250	71		75	5
	E	40		50	60	210	60		84	180
	F	45		200	350	200	940		47	19
	G	4.4×10^4		2.0×10^4	2.1×10^5	1.0×10^5	4.6×10^4		4.2×10^4	2.1×10^4
Bacterial Biomass (ug/litre)	A	153.0	119.7	127.0	136.0	273.7	157.8	172.4	272.9	219.5
	B	134.6	133.1	169.8	167.5	424.1	224.3	374.3	184.5	204.4
	C	101.5	122.8	207.8	169.2	360.2	118.9	174.3	160.1	153.6
	D		102.8	99.3	140.3	301.7	136.1	370.7	187.8	144.6
	E	153.0	106.2	123.2	166.7	213.1	176.6	224.8	198.2	286.0
	F	212.9	192.8	114.0	188.3	434.4	269.9	270.6	235.3	207.1
Nitrifying Bacteria per 100 ml	A	<2	<2	<2	<2	<2	<2	<2	<2	<2
	E	<2	<2	<2	<2	<2	<2	<2	<2	<2
	F	<2	<2	<2	<2	<2	<2	<2	<2	<2
	G	27	>1600	920	540	>1600	130	220	790	490
Thiobacillus sp. per 100 ml	A	<2	<2	<2	13	8	49	8	8	8
	E	<2	<2	5	<2	2	5	13	13	17
	F	<2	<2	<2	2	<2	33	23	23	23
	G	>1600	>1600	>1600	>1600	>1600	1600	2.2×10^4	3.3×10^4	2.2×10^4
Desulfovibrio sp. per 100 ml	A	<2	<2	<2	<2	<2	<2	<2	<2	<2
	D								9	24
	E	22	2	6	13	22	29	130	22	240
	F	70	46	34	350	350	1600	540	130	540
	G	>1600	>1600	$>1.6\times10^4$	$>1.6\times10^4$	5400	$>1.6\times10^5$	1.6×10^6	9.2×10^5	9.2×10^5
Temperature (°C)	A	24.0	24.0	22.5	23.8	22.8	24.5	23.9	23.6	23.0
	B	24.0	22.2	21.9	21.9	21.9	23.0	21.0	23.3	23.0
	C	13.0	17.0	16.0	13.0	16.0	14.8	12.5	15.8	17.0
	D		11.5	11.5	12.0	14.0	9.5	9.5	11.9	12.0
	E	11.5	10.9	10.5	11.9	13.7	9.3	9.4	11.9	11.8
Dissolved Oxygen (mg/litre)	A	10.6	8.9	8.4	9.0	9.2	9.1	8.5	8.2	8.5
	B	10.7	8.5	8.3	8.3	8.2	7.7	6.2	8.3	8.5
	C	4.2	7.3	7.9	3.5	3.2	3.8	1.8	5.8	8.3
	D		4.9	4.1	2.8	2.0	1.9	1.4	0.1	0.3
	E	3.8	3.4	3.3	2.8	2.0	1.9	1.3	0.1	0.2

A = 2 meters below surface
B = 1 meter above thermocline
C = Within thermocline
D = 1 meter below thermocline
E = 2 meters above bottom
F = 3 inches above bottom
G = Sediment-water interface

Table VI. Bacteriological and Physical Parameters at Station S.

Parameter	Depth	July	August				
		29	5	12	13	21	25
20°C Aerobic Heterotrophs per ml	A	95	340		620	350	1200
	B	270	1300		700	900	840
	C	130	590		6600	1100	4300
	D				4000		170
	E	210	360		2600		1000
	F	760	1100		2800		2900
	G	9.0×10^5	4.1×10^5		1.9×10^7		1.5×10^6
20°C Anaerobic Heterotrophs per ml	A		20		30	7	3
	B	65	30		19	34	5
	C	15	10			17	260
	D		20		60		70
	E	85	120		34	47	19
	F	250	40		25	56	10
	G	4.3×10^4	2.0×10^4		8.0×10^4	4.4×10^4	3.0×10^4
Bacterial Biomass (ug/litre)	A	191.9	115.9	228.6	137.0	177.6	181.4
	B	126.9	176.1		221.4	161.6	136.8
	C	110.1	135.5	192.4	358.4	148.2	213.1
	D		124.7	191.9	163.6		244.9
	E	93.0	96.4	265.0	434.7	240.9	196.6
	F	111.8	118.0		425.3	220.5	186.1
Nitrifying Bacteria per 100 ml	A	<2	<2	<2	<2	<2	<2
	E	<2	<2	<2	<2	<2	<2
	F	<2	<2	<2	<2	<2	<2
	G	430	350	3500	70	950	1100
Thiobacillus sp. per 100 ml	A	<2	<2	<2	8	13	23
	E	<2	<2	5	8	23	23
	F	<2	<2	110	8	8	13
	G	>1600	>1600	1.6×10^4	9300	4.9×10^4	7900
Desulfovibrio sp. per 100 ml	A	<2	<2	<2	<2	<2	<2
	D						17
	E	<2	8	7	79	23	34
	F	33	49	70	130	280	170
	G	>1600	>1600	$>1.6 \times 10^5$	$>1.6 \times 10^5$	$>1.6 \times 10^6$	1.6×10^6
Temperature (°C)	A	23.5	23.8	25.0	24.9	23.7	24.0
	B	20.0	21.1	23.1	20.0	22.4	23.7
	C	15.5	13.0	18.0	15.0	11.5	
	D		11.1	9.0	9.3		10.9
	E	6.9	11.0	9.0	9.0	9.3	10.9
Dissolved Oxygen (mg/litre)	A	9.7	8.7	8.8	8.9	8.3	8.5
	B	7.9	7.0	8.4	6.9	6.9	8.2
	C	6.6	6.4	6.4	4.5	1.3	
	D		3.5	2.5	2.0		0.8
	E	4.0	2.9	2.3	1.9	0.0	0.7

A = 2 meters below surface
B = 1 meter above thermocline
C = Within thermocline
D = 1 meter below thermocline
E = 2 meters above bottom
F = 3 inches above bottom
G = Sediment-water interface

Table VII. Bacteriological and Physical Parameters at Station W.

Parameter	Depth	August			
		13	17	20	25
20°C Aerobic Heterotrophs per ml	A	420			1200
	B	7400			860
	C	3800			1200
	D	570			3500
	E	2.3×10^4	8600	3400	5000
	F	1100			2400
	G	6.5×10^5			2.9×10^6
20°C Anaerobic Heterotrophs per ml	A	12			12
	B	400			
	C	210			24
	D	58			17
	E	1500	130	180	
	F	19			200
	G	2.2×10^4			2.7×10^4
Bacterial Biomass (ug/litre)	A	335.8			197.0
	B	579.8			188.5
	C	181.4			155.6
	D	314.6			187.5
	E	286.5			214.9
	F	379.9			235.7
Nitrifying Bacteria per 100 ml	A	<2			<2
	E	<2	<2	<2	<2
	F	<2			<2
	G	1300			3500
Thiobacillus sp. per 100 ml	A	<2			13
	E	23	2	8	33
	F	33			13
	G	1.6×10^4			1.7×10^4
Desulfovibrio sp. per 100 ml	A	<2			<2
	D				130
	E	49	27	350	32
	F	240			540
	G	$>1.6 \times 10^5$			4.0×10^4
Temperature (°C)	A	25.0			24.0
	B	23.0			23.3
	C	18.6			23.0
	D	9.0			10.1
	F	8.1		10.1	10.1
Dissolved Oxygen (mg/litre)	A	8.8			9.8
	B	7.5			8.1
	C	4.3			7.2
	D	0.6			0.1
	E	0.6	2.7	3.5	0.0

A = 2 meters below surface
B = 1 meter above thermocline
C = Within thermocline
D = 1 meter below thermocline
E = 2 meters above bottom
F = 3 inches above bottom
G = Sediment-water interface

Table VIII. Bacteriological and Physical Parameters, 2 Meters above Bottom (E) at Stations O, T, U, and V.

Parameter	Station O	Station T	Station U		Station V
	August	August	August		August
	17	20	17	20	20
20°C Aerobic Heterotrophs per ml	80	1900		7900	5000
20°C Anaerobic Heterotrophs per ml	18	1900	650	76	110
Nitrifying Bacteria per 100 ml	<2	<2	<2	<2	<2
Thiobacillus sp. per 100 ml	46	23	130	23	23
Desulfovibrio sp. per 100 ml	130	1600	920	430	>1600
Temperature (°C)		12.0		17.3	11.1
Dissolved Oxygen (mg/litre	1.4	0.3	0.0	0.0	0.0

Table IX. Bacteriological Data After Fall Overturn at Stations M, N, P, R, S, and W.

Sta.	Date 1970	Depth in Meters	Aerobic Heterotrophs per ml	Anaerobic Heterotrophs Per ml	Nitrifying Bacteria Per 100 ml	*Desulfovibrio* SP. Per 100 ml	*Thiobacillus* SP. Per 100 ml
P	Nov. 27	1	120	65	<2	4	9
		2		130	2	9	2
		7	90	10	<2	9	8
		14		33	<2	13	4
		21	400	43	<2	17	<2
		22	190	46	<2	2	7
		23	270	26	<2	8	5
		24	370	78	<2	2	14
R	Nov. 27	1	80	37	<2	4	5
		7	77	36	<2	9	<2
		18	96	33	2	9	2
W	Nov. 28	2	1800	8	<2	14	49
		7		13	<2	13	17
		12		26	<2	8	240
		16	850	25	<2	27	130
		18	1200	26	<2	33	14
		19				27	7
M	Nov. 29	2	100	6	<2	2	8
		7	80	35	<2	5	<2
		13	80	10	<2	2	2
		20	110	28	<2	<2	2
		22	90	24	<2	5	<2
		23	340	47	<2	<2	<2
S	Nov. 29	2	660	28	<2	8	110
		7	750	41	<2	17	79
		13	750	60	<2	49	170
		19	620	59	13	22	33
		22	810	37	<2	34	180
		23	280	27	<2	22	39
N	Nov. 29	2	350	35	<2	27	2
		7	450	33	<2	79	<2
		13	400	18	<2	33	2
		19		40	<2	22	<2
		21		32	<2	7	2
		22		15	<2	17	4

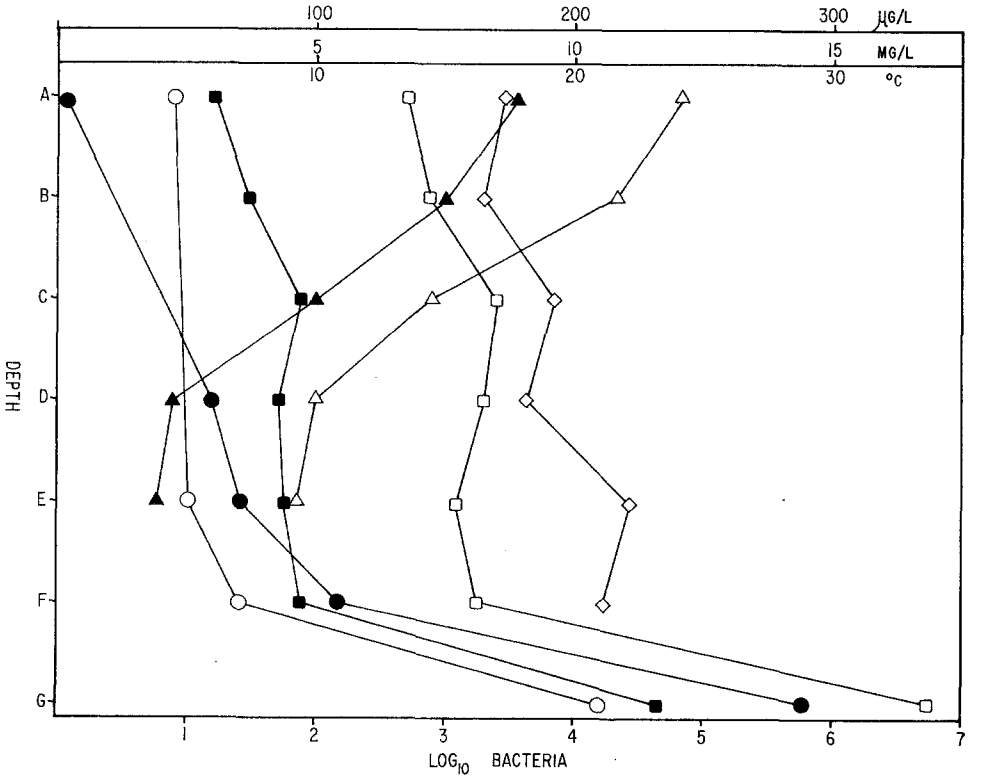

A = 2 meters below surface
B = 1 meter above thermocline
C = Within thermocline
D = 1 meter below thermocline
E = 2 meters above bottom
F = 3 inches above bottom
G = Sediment-water interface
G* = 1 inch above bottom

● = *Desulfovibrio sp.* per 100 ml
○ = *Thiobacillus sp.* per 100 ml
■ = Anaerobic heterotrophs per ml at 25°C
□ = Aerobic heterotrophs per ml at 20°C
▲ = Dissolved oxygen in mg/1
△ = Temperature in °C
◇ = Bacterial biomass in µg/1

Figure 1. Mean Vertical Distributions of Bacteriological and Physical Data at Station M.

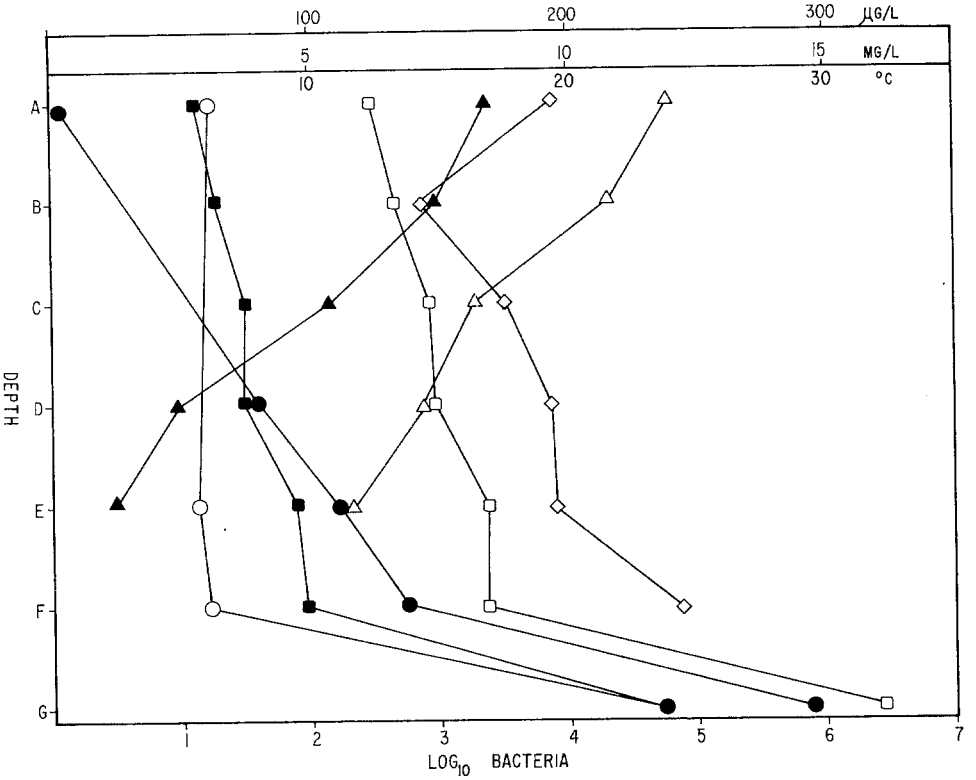

Figure 2. Mean Vertical Distributions of Bacteriological and Physical Data at Station N.

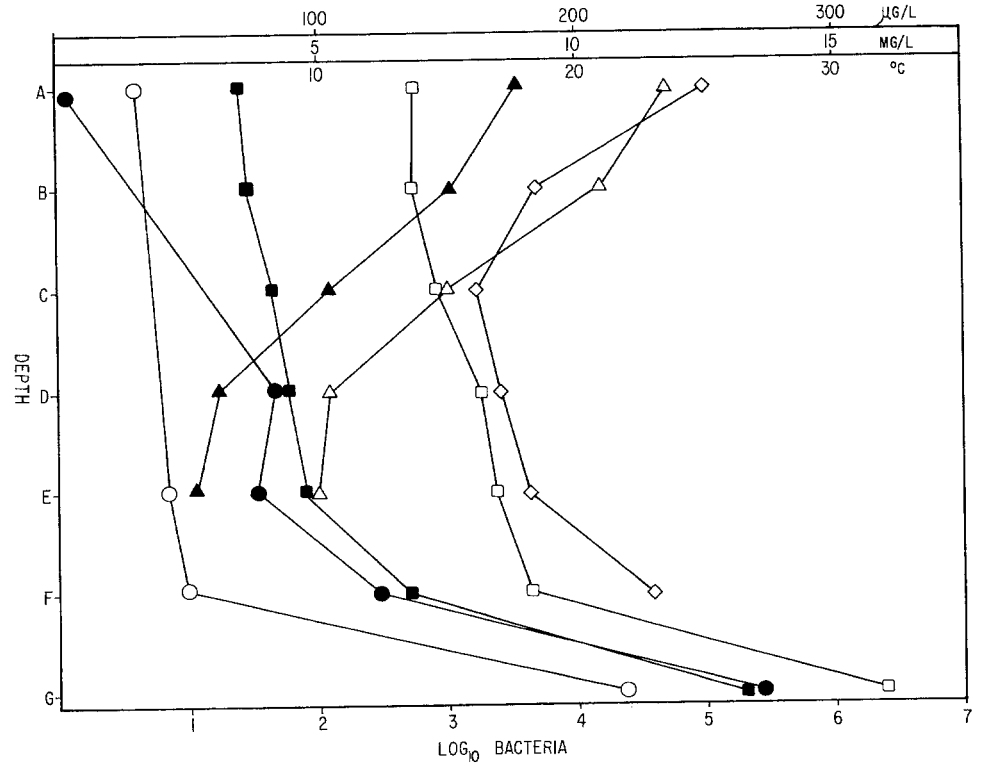

Figure 3. Mean Vertical Distributions of Bacteriological and Physical Data at Station P.

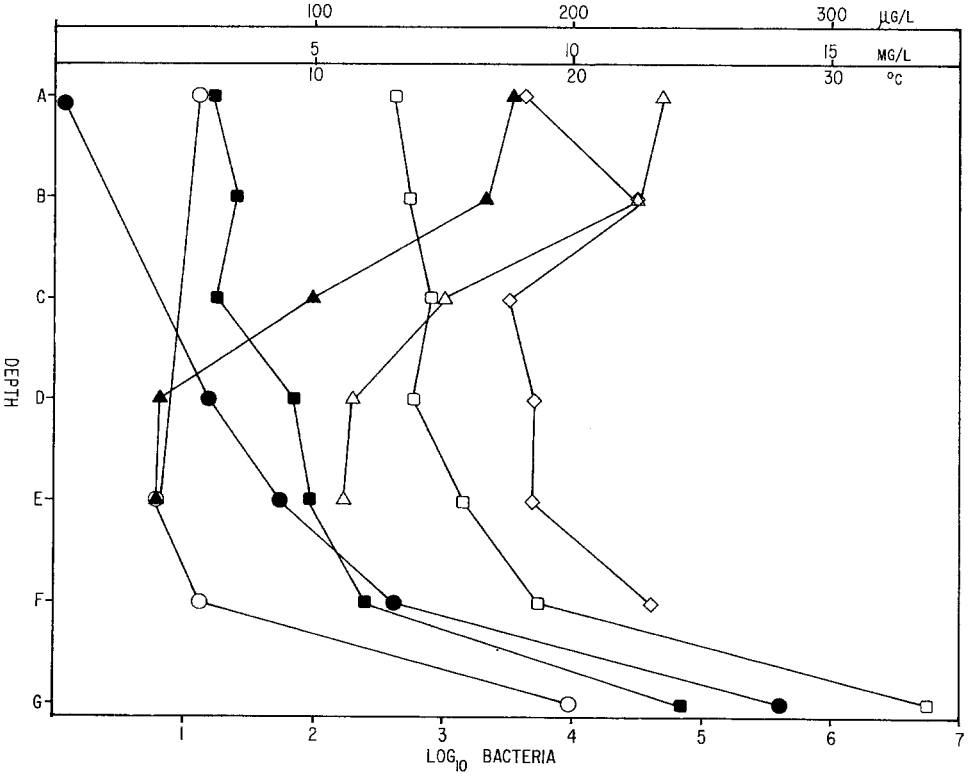

Figure 4. Mean Vertical Distributions of Bacteriological and Physical Data at Station R.

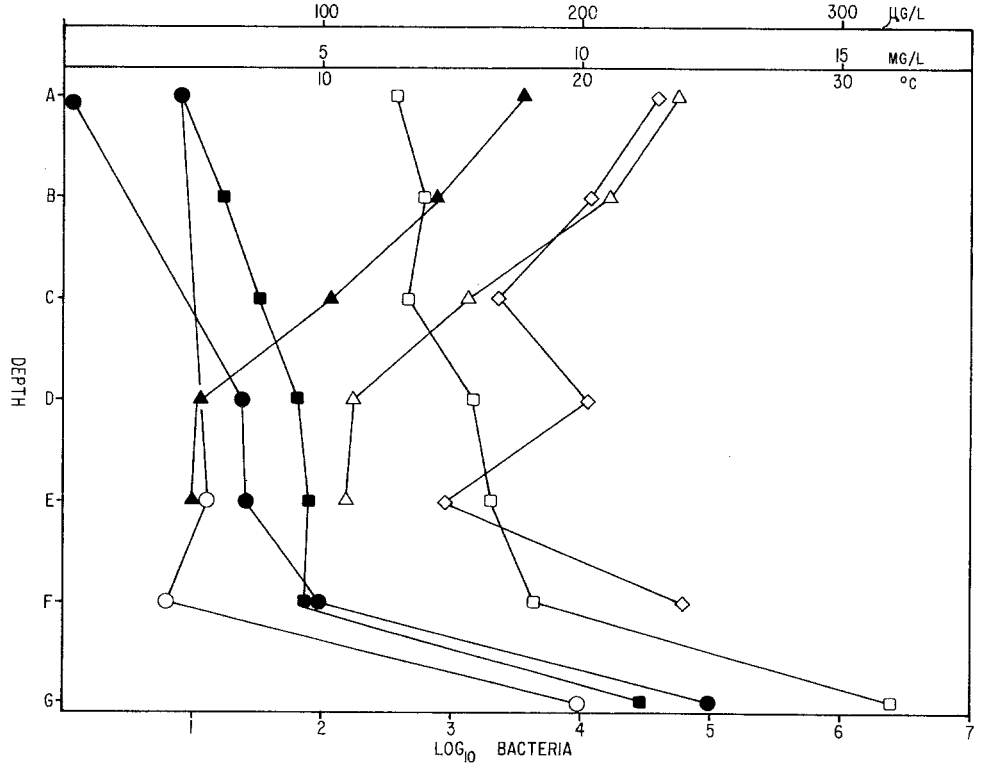

Figure 5. Mean Vertical Distributions of Bacteriological and Physical Data at Station S.

APPENDIX VI

Data and Publication Information

DATA

The biological data and the bateriological data which were obtained during "Project Hypo" are listed in Appendices IV and V respectively.

The physical data on winds, water temperatures and currents are extremely voluminous. Any persons desirous of working with this data should contact either Dr. J.O. Blanton, Canada Centre for Inland Waters, Box 5050, Burlington, Ontario (Tel. 416-637-4233) or Mr. R.A. Winklhofer, U.S. Environmental Protection Agency, Region V, 21929 Lorain Rd., Fairview Park, Ohio (Tel. 216-333-7000).

The chemical data is not as bulky as the physical data but nevertheless constitutes approximately 300 pages of computer printout. Any persons desirous of working further with this data should contact Dr. N.M. Burns, Canada Centre for Inland Waters, Box 5050, Burlington, Ontario (Tel. 416-637-4246), or Mr. C. Ross, U.S. Environmental Protection Agency, Region V, 21929 Lorain Rd., Fairview Park, Ohio (Tel. 216-333-7000).

PUBLICATIONS

Parts of the complete report have been published elsewhere or are currently in press. A listing of the publication history of each report follows:

1. Project Hypo – An Introduction
   N.M. Burns and Curtis Ross

   First publication: Proceedings of the 14th Conference on Great Lakes Research, Toronto, 1971. (In Press).

   Second publication: This report.

2. Oxygen Depletion in the Hypolimnion of the Central Basin of Lake Erie, 1929 to 1970.
   H.H. Dobson and M. Gilbertson

   First publication: Proceedings of the 14th Conference on Great Lakes Research, Toronto, 1971. (In Press).

   Second publication: This report.

3. Physical Processes Affecting the Hypolimnion of the Central Basin of Lake Erie.
   J.O. Blanton, and R.A. Winklhofer

   First Publication: This Report

   Part of the above paper under the title of "Circulation of Hypolimnion Water in the Central Basin of Lake Erie" has been accepted for publication in the Proceedings of the 14th Conference on Great Lakes Research, Toronto, 1971.

4. An Investigation of Diffusion Characteristics of the Hypolimnion of Lake Erie.
   C.R. Murthy.

First Publication: Proceedings of the 14th Conference on Great Lakes Research, Toronto, 1971. (In Press).

Second publication: This report.

5. Sediment Oxygen Demand in Lake Erie's Central Basin, 1970.
A.M. Lucas and N.A. Thomas

First Publication: Proceedings of the 14th Conference on Great Lakes Research, Toronto, 1971. (In Press).

Second publication: This report.

6. Biological Studies Related to Oxygen Depletion and Nutrient Regeneration Processes in the Lake Erie Central Basin.
T. Braidech, P. Gehring, and C. Kleveno.

First Publication: Proceedings of the 14th Conference on Great Lakes Research, Toronto, 1971. (In Press).

Second publication: This report.

7. Microbiological Studies Related to Oxygen Depletion and Nutrient Regeneration Processes in the Lake Erie Central Basin.
A.S. Menon, C.V. Marion, and A.N. Miller.

First publication: Proceedings of the 14th Conference on Great Lakes Research, Toronto, 1971. (In Press).

Second Publication: This report.

8. Oxygen-Nutrient Relationships within the Central Basin of Lake Erie.
N.M. Burns, and C. Ross.

First publication (in summary form): Proceedings of the 14th Conference on Great Lakes Research, Toronto, 1971. (In Press).

Second publication: This report.

Third publication: *In* "Nutrients in Natural Waters", ed. H. Allen and J.R. Kramer, J. Wylie Inc., New York, N.Y. (In Press).

9. Project Hypo – Discussion of Findings.
N.M. Burns and C. Ross.

First Publication: Proceedings of the 14th Conference on Great Lakes Research, Toronto, 1971. (In Press).

Second Publication: This report.

Appendix I An Automatic Underwater Camera System
R.J. Jirberg.

First publication: NASA Technical Memorandum, NASA TMX-67807.

Second publication: This report.

Appendix II A Submersible Automatic Dissolved Oxygen-Temperature Monitoring System.
C.J. Beier.

First publication: This report.

Appendix III Phosphorus and Hypolimnial Dissolved Oxygen in Lake Erie.
M. Gilbertson and H.H. Dobson.

First publication: This report.

This paper is currently being expanded in an attempt to predict the effect of the proposed control measures and to aid decision-makers in estimating the expected improvement of hypolimnial conditions with various reductions of contributions of phosphorus to Lake Erie.

Index

Aerobic heterotrophic bacteria, 72

Algal rains (suspended algae), 28, 30 65, 77, 103, 120

Alkalinity, 88, 98, 101, 102, 105

Ammonia, 88, 98, 101, 102

Anacystis, 59, 61, 66, 68

Anaerobic heterotrophic bacteria, 72, 75

Anoxic conditions, 24, 67, 107, 108, 109, 114, 125

Bacteria –
- analytical methods, 72, 73
- oxygen uptake, 82, 121
- sampling, 72
- vertical distribution, 74, 76

Bathymetry, Lake Erie, 4, 13, 15

Black patches, 64, 65, 66, 77, 78, 103

Benthic respirometers, 23, 31, 47, 121

Biomass, bacterial, 73, 75

Camera, underwater time-lapse –
- electronic flash unit for, 129
- operational characteristics of, 129
- system design of, 127
- timing circuitry for, 128
- water-tight housings for, 128

Carbon, particulate organic, 88, 99, 111

Carbon dioxide (total) 87, 98, 101, 102

Ceratium, 59, 66, 68

Chemoclines, 96, 97

Cosmarium, 59, 68

Currents, 27, 31, 33

Dentrification, 112, 124

Desulfovibrio, 73, 79, 80, 83, 102

Dye –
- release, 41
- sampling, 42

Eddy diffusion, 44

Electronic bathythermograph, 85, 87

Iron 89, 101, 102, 108, 112

Manganese, 89, 101, 102, 112

Nitrifying bacteria, 73, 77

Nitrate and nitrite, 88, 98, 101, 102

Nitrification, 77, 81

Oedogonium, 51, 59, 61, 63, 66, 68

Oocystis, 57

Oxygen –
- causes of depletion, 48, 82, 107, 121
- concentration values, 64, 87
- depletion of, 1, 64, 65, 80, 103 121
- depletion rate, 2, 6, 25, 103, 109, 121

Oxygen meters, in situ, 23, 31, 47, 133

pH, 87, 98, 115

Phosphorus –
- concentration, 98, 101, 102
- detection limits, 88
- elimination, 111, 124
- external loading, 116, 125
- internal loading, 115, 116, 125
- regeneration, 110-113

Phytoplankton –
- quantities, 53, 55-58, 62
- methods, 53
- sampling, 53
- sedimentation, 60, 61, 103, 121

Physical characteristics, Lake Erie, 4, 13, 15

Redox potential, 98

Sulfate, 89, 101, 102

Sulfur oxidizing bacteria, 73, 79

Sulfate reducing bacteria, 73, 79

Station positions, 11, 41, 46, 52, 72, 86, 134

Sediment oxygen demand (SOD), 28, 29, 45-49, 121

Sedimentation traps, 54

Silica, 88, 98, 102, 103, 112

Suspended mineral, 87, 98

Temperature structure, 4, 5, 17, 20, 21, 93, 94, 95

Temperature recorders, 11, 24, 25, 139

Thermocline depths, 20, 22, 139

Thiobacillus, 73, 102

Underwater observations, 55, 64, 65, 103

Upwellings, 44, 123 (see physical paper)

Winds, 16-19, 100

Volumes –
hypolimnion, 35, 98
thermocline, 35, 98

Tribonema utriculosum, 51, 59, 61, 63, 66, 68, 120